CONTRACTOR REPORT

SAND80-8192
UC-62d
Unlimited Release

Volume II—Molten Salt Thermal Energy Storage Subsystem Research Experiment

Martin Marietta Corporation

Prepared by Sandia National Laboratories, Albuquerque, New Mexico 87185 and Livermore, California 94550 for the United States Department of Energy under Contract DE-AC04-76DP00789.

Printed May 1985

FOREWORD

The research and development described in this report was conducted within the U.S. Department of Energy's (DOE) Solar Thermal Technology Program. The Solar Thermal Technology Program directs efforts to advance solar thermal technologies through research and development of solar thermal materials, components, and subsystems, and through testing and evaluation of solar thermal systems. These efforts are carried out through DOE and its network of national laboratories who work with private industry. Together they have established a goal-directed program for providing technically proven and economically competitive options for incorporation into the Nation's energy supply.

There are two primary solar thermal technologies: central receivers and distributed receivers. These two technologies use various point and line-focus optics to concentrate sunlight onto receivers where the solar energy is absorbed as heat and converted to electricity or used as process heat. In central receiver systems, which this report considers, fields of heliostats (two-axis tracking mirrors) focus sunlight onto a single receiver mounted on a tower. The radiant energy is absorbed by a working fluid circulating within the receiver and is transformed into high temperature thermal energy. Temperatures in central receivers may exceed 1500°C.

Contract 20-2988
Report No. MCR-82-1722

Volume 2

Final
Technical
Report

September 1982

MOLTEN SALT THERMAL ENERGY STORAGE SUBSYSTEM RESEARCH EXPERIMENT

Sponsored By:

Sandia National Laboratories
Livermore, California

ABSTRACT

This report documents work sponsored by the U. S. Department of Energy to design, build, and test a thermal storage subsystem research experiment using molten nitrate salt as the working fluid. The project is part of a continuing program to develop molten salt components and subsystems for central receiver systems. The work was performed by Martin Marietta Aerospace in association with American Technigaz Inc., Arizona Public Service Company, and Stearns-Roger under DOE Contract 20-2988. The design is based on a two tank system, one tank to hold cold (550 deg F) salt and one to hold hot (1050 deg F) salt. The cold tank is a conventional design with a carbon steel wall and external insulation. The hot tank employs new technology: it has firebrick insulation internal to a structural shell, with a corrugated liner inside the insulation to contain the salt. The liner is similar to those used in transportation and storage of liquid natural gas. The testing showed that this concept of thermal storage is technically feasible and potentially cost effective. The contract began in November 1980 and testing was completed in August 1982.

This report is in two volumes: Volume I is an Executive Summary which gives highlights of the project. Volume II is the full technical report covering the same information in greater detail.

MARTIN MARIETTA AEROSPACE
DENVER AEROSPACE
P.O. Box 179
Denver, Colorado 80201

FOREWORD

This report is submitted by Martin Marietta Aerospace to the Department of Energy in accordance with the provisions of Contract 20-2988. This final report summarizes the work related to fabrication testing and performance of a prototype molten salt thermal energy storage subsystem. The final technical report is submitted in two volumes:

Volume I - Executive Summary
Volume II - Final Technical Report

Mr. William Peila of Sandia National Laboratories, Livermore, CA was the Technical Manager.

Work on this contract was performed by the following companies:

- Martin Marietta Aerospace
- Stearns-Roger
- Arizona Public Service
- American Technigaz, Inc.

This document was written, edited, and reproduced by Martin Marietta Aerospace.

CONTENTS

CONTENTS

CONTENTS

CONTENTS

CONTENTS

1.0 Introduction

1.0 INTRODUCTION

A wide variety of energy storage subsystems are currently being examined for use with large Solar Thermal Central Receiver (STCR) plants. One of the most attractive of such concepts is the use of a molten nitrate salt (60% $NaNO_3$, 40% KNO_3 by weight) as a sensible heat storage medium. This salt has high heat capacity per unit volume, low vapor pressure, good heat transfer properties and is low in cost. Because the salt can also be used as the working fluid in the solar receiver, its use can considerably simplify the solar side of a plant; this enhances reliability and efficiency. The molten salt working temperature limits of approximately 288°C (550°F) to 566°C (1050°F) are ideally suited to the generation and use of high-pressure, superheated steam for either electrical power generation or industrial process heat applications. Of course, this storage concept can also be used with nonsolar heat sources, such as fossil-fired salt heaters, with the same type of advantages.

1.1 OBJECTIVES

Under the sponsorship of the Department of Energy and Sandia National Laboratories Livermore, we have conducted a Molten Salt Thermal Energy Storage Subsystem Research Experiment (SRE) program. The objectives of this program were to advance the state of the art in the high temperature containment of molten salt, to reduce the costs of thermal energy storage, and to resolve all uncertainties in this storage concept. Our approach was to contain the high temperature salt (566°C/1050°F) in a lined and internally insulated hot tank, and to contain the cold salt (288°C/550°F) in a separate tank made of carbon steel. The use of internal insulation allows the use of low-cost carbon steel as the shell material for the hot tank. The internal insulation is protected from the salt by a metal liner. The liner is a unique design employing a liquid-tight, waffled membrane of the type used extensively in liquid natural gas (LNG) storage applications. The internal insulation is a low-density insulating firebrick. The hot and cold tanks are also externally insulated to minimize heat losses. The remainder of the system consists of a cold tank (carbon steel with external insulation) and the necessary pumps, sumps, pipes, valves, and controls.

This program consisted of the following key elements:

- Preliminary design and cost analysis of a 1200 MWht, commercial-size Thermal Energy Storage (TES) subsystem.

- A critical component development program for the liner and internal insulation; this included numerous fatigue tests of both the liner and the brick, and culminated in the construction and fatigue testing of a laboratory prototype tank of one cubic meter volume with hot salt.

- Design, construction, and testing of a small-scale TES (7 MWht), termed a Subsystem Research Experiment (SRE). The SRE consists of a hot tank, a cold tank, a fossil-fired heater to simulate a solar receiver, an air cooler to simulate a steam generator, and all pumps, sumps, controls, etc necessary to simulate a complete system. (see Fig. 1.1-1).

Figure 1.1-1 Thermal Storage System

1.2 BACKGROUND

1.2.1 Martin Marietta Aerospace Molten Salt Solar Programs

Several molten salt programs in which Martin Marietta Aerospace has participated in which the results are applicable to molten salt storage technology are presented in Table 1.2.1-1. These programs have resulted in a valuable data base upon which to design and develop a thermal energy storage subsystem. During the CRSTPS program we designed, built and tested a 1.6 MWht thermal storage subsystem research experiment which used Hitec heat transfer salt (40% $NaNO_2$, 7% $NaNO_3$, 53% KNO_3 by weight) as a sensible heat storage medium. Figure 1.2.1-1 is a photograph of the experimental system in operation. The Alternate Central Receiver (ACR) Power System program provided opportunity for extensive material compatibility testing. The receiver SRE is shown being assembled on the CRTF tower elevator module in Figure 1.2.1-2.

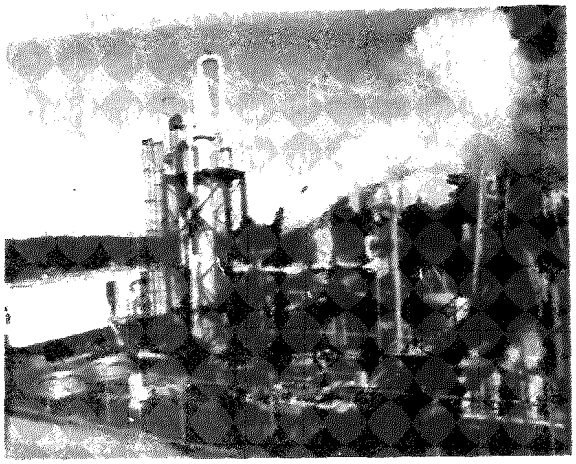

Figure 1.2.1-1
CRSTPS Molten Salt/Oil Storage SRE

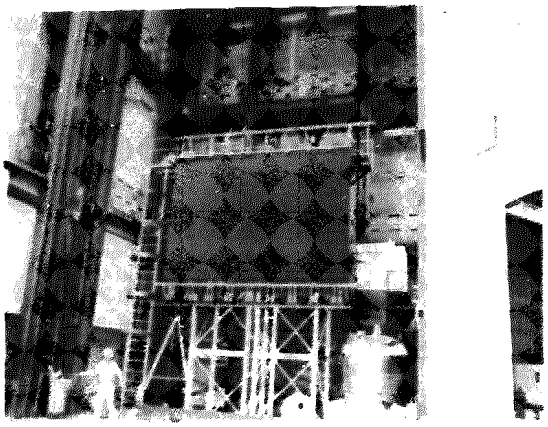

Figure 1.2.1-2
5-MWt Receiver SRE at CRTF, Albuquerque

1.2.2 Other Experience

The Technigaz thermal expansion liner design is used primarily for cryogenic storage of liquified natural gas (LNG) in ships and in land based tanks. It has also been used in high-temperature chemical and nuclear reactor applications. More LNG has been transported in ships using the Technigaz membrane tanks than in any other containment system. Table 1.2.2-1 lists the tanks using the patented Technigaz membrane, all of which are still in operation. Molten salt storage tanks would typically be from 6880 m^3 (223,000 ft^3) in volume for the TES system described in this proposal to 21,000 m^3 (750,000 ft^3) for a large commercial system.

Figure 1.2.2-1 is a photograph of the inside of a Technigaz-lined LNG tank. The liner is a metal membrane with a series of uniquely folded orthogonal corrugations to allow for thermal expansion and contraction of the liner. The liner provides the necessary liquid tightness and transfers the hydrostatic load to the insulating brick and the tank shell. Thus the Technigaz system is ideally suited to contain the molten salt for a solar thermal storage subsystem.

Table 1.2.1-1 Previous Martin Marietta Aerospace Molten Salt Solar Programs

Program	Results
Central Receiver Solar Thermal Power System (CRSTPS)	Demonstrated thermal storage capability of Hitec salt for sensible heat and hydrocarbon oil for latent heat and condensate sensible heat
Alternate Central Receiver (ACR) Power System Phase I	Generated a conceptual design for a 300 MWe solar standalone plant using molten salt for both working and storage fluids
Alternate Central Receiver (ACR) Power System Phase II	Demonstrated Incoloy 800 suitable for design temperatures up to 593°C (1100°F) and carbon steel up to 399°C (750°F).
Solar Central Receiver Hybrid Power System Study	Use of molten salt storage lowers cost of electricity as plant size increases. Recommends use of separate hot and cold salt storage tanks.
Saguaro Power Plant Solar Repowering Project Phase I	Produced a preliminary design of the solar subsystems to be used to repower the Saguaro Power Plant (100 MWe).
Internally Insulated Thermal Storage System Development Program (IITSSD)	No available fibrous or block insulation will survive molten salt environment for 30 years. Recommends thermal expansion liner to protect inner insulation.
Saguaro Power Plant Solar Repowering Project Phase II	Produced a preliminary design of the solar subsystem to be used to repower the Saguaro Power Plant (60MWe).
Conceptual Design of A Solar Cogeneration Facility	Produced a conceptual design to provide process heat for enhanced oil recovery operations and electricity for distribution by a utility.
Solar Desalinization Pilot Plant	Produced a design to provide desalinated water through a multiple effects distillation process or indirectly by generating electrical power for a reverse osmosis process.

Table 1.2.2-1 Tanks Now Lined with Technigaz Membrane

Capacity, m^3	(ft^3)	Temperature, K	(°F)	Service, year
Ship Tanks				
630	(22,250)	111	(-260)	1964
50,000	(1,766,000)	↓	↓	1971
75,000	(2,649,000)			1972
40,000	(1,413,000)			1973
75,000	(2,649,000)			1973
75,000	(2,649,000)			1973
75,000	(2,649,000)			1974
120,000	(4,238,000)			1975
75,000	(2,649,000)			1975
125,000	(4,414,000)			1976
125,000	(4,414,000)			1977
125,000	(4,414,000)			1978
125,000	(4,414,000)			1978
Land Storage*				
--	--	700 at 4 MPa	(800 at 580 psi)	1964
8,000	(283,000)	III	(-260)	1972
14,000	(494,000)	III	(-260)	1972

*There are also several high-temperature land-based applications that are classified and cannot be cited here.

Figure 1.2.2-1
Technigaz Liner in Liquid Natural Gas Tank

1.2.3 Molten Salt Storage Tank and Storage System

The purpose of this study was to determine the most cost effective storage tank and thermal storage system using a parametric analysis of design and economic factors. The results of this study are given in Table 1.2.3-1 for storage tanks and Table 1.2.3-2 for storage systems.

Table 1.2.3-1 General Conclusions from Storage Tank Optimization

1. Cylindrical tanks are more economical than spherical tanks. 2. The mechanical constraints on the tank (maximum soil bearing load, maximum tank hoop stress) tend to limit the optimum tank geometry.

Table 1.2.3-2 General Conclusions from Storage System Optimization

1. The optimum tank configuration for each system is the smallest number of large tanks possible within the mechanical constraints (soil bearing load, tank hoop stress). 2. For small storage systems where all the salt can be stored in one tank (4000 MWht), the dual-tank system is the most economical. 3. For intermediate storage systems (10,000 MWht), the dual-tank system is recommended because the cost advantages of the thermocline and cascade systems do not warrant the added technical risk. 4. For large storage systems (15,000 MWht), the cost advantage of the cascade system is attractive enough to encourage a solution to the thermal cycling problem. In light of the current information, though, a dual-tank system is still recommended.
Note: A dual tank system uses one or more tanks for cold salt storage and one (or more) other tank(s) for hot salt. In a thermocline system, the hot and cold salt is stored in the same tank by using density stratification to separate the different-temperature salts. A cascade system has three or more tanks, which are alternately used for hot and cold salt storage, depending on their respective quantities.

1.2.4 Tank Foundation Design

For the IITSSD program, we recommended a water-cooled slab as the tank foundation for both the hot and cold tanks. This prevents moisture in the underlying soil from reaching the boiling point and eliminates the need for a stainless steel bottom. An extensive literature search and talks with several engineering consulting firms shows that there is little available data on soil properties at high temperatures. The boiling of ground water has the potential of lifting and cracking of foundations. The industry practice is to either cool the foundation or support the tank off the ground.

1.2.5 Salt Chemistry Tests and Material Compatibility

During Phase I of the ACR program we performed tests on salt chemistry, material compatibility and a molten salt flow loop. The results of those tests are presented in Table 1.2.5-1.

Table 1.2.5-1 ACR Phase 1 Test Results

Salt Chemistry - The stability of molten salt is adequate for long-term solar use with carbonate and hydroxide control (by either scrubbing or salt regeneration). - Preliminary economic estimates of atmospheric scrubbing and salt regeneration favor the scrubbing method of carbonate and hydroxide control.
Materials Tests - I800 and RA 330 are acceptable materials for long-term high-temperature [up to 580°C (1076°F)] service. 316 and 316L may also be suitable, pending further investigations. - Control of the carbon content of I-800 and RA330 may be necessary to minimize possible long-term structural degradation of these alloys. (Particularly if sensitization is found to be detrimental to long-term service behavior). - There were no salt-related detrimental effects on either the oxidation behavior or the structural integrity of I-800 and RA330. - The carbon steels are suitable low-temperature molten salt containment materials, up to 399°C (750°F). - The low alloy steel A387 (1 1/4 Cr - 1/2 Mo) appears to be a suitable candidate for low-temperature service (up to 399°C) provided chloride (Cl^-) impurity levels in the molten salt are controlled. - Carbon steels appear to be a suitable intermediate-temperature containment material if proper design allowances can be made for material loss.
Molten Salt Flow Loop - There is no evidence of material transport in a molten salt flow loop. - I-800 coupons exposed to flowing salt in the loop exhibited similar weight gains at 566°C (1050°F) as those in the trace contaminants tests. Coupons at 329°C (625°F) and 482°C (900°F) exhibited minor weight changes. The largest changes occurred at 440°C (825°F), and accelerated with time, but are well within acceptable limits.

1.2.6 Molten Salt Safety Report

Extensive data were gathered through both a literature search and personal contact with industrial producers and users of molten salt to determine the safety hazards, precautions, and procedures to be considered in operating a molten salt solar central receiver power system. The report was evaluated by Arizona Public Service Company and Public Service Company of Colorado. Both utilities concluded that using molten salt in a solar central receiver power plant is acceptable to them, that no major problems exist, that the report gives an adequate safety definition for molten salt use, and that it forms the basis for preparing utility operating procedures.

1.3 STUDY SCOPE

The scope of work for this study included the following eight tasks:

Task 1 - Review TES Subsystem Specification
Task 2 - Critical-Component Development
Task 3 - TES Subsystem Preliminary Design
Task 4 - Subsystem Research Experiment
Task 5 - Evaluation of SRE Results and Assessment of TES Subsystem
Task 6 - Program Plan
Task 7 - Reports and Data
Task 8 - Program Management

Task 1 was completed prior to the Program Kickoff meeting, with a primary recommendation of increasing the Thermal Energy Storage (TES) subsystem size to 1200 MWht. This recommendation was subsequently adopted into the TES subsystem specification.

In Task 2, the following development testing was done;

1) Liner formability using Incoloy 800.
2) Liner element fatigue tests at ambient and 566°C (1050°F).
3) Hydrostatic test of a liner element.
4) Internal insulation testing including:
   a) Compatibility with molten salt at use temperature under load.
   b) Load tests at use temperature.
5) Design, build and test of a 1 m^3 tank using the selected liner configurations, internal insulation and method of liner of attachment. The tank was loaded with molten salt at 566°C (1050°F) and pressure cycled to simulate 30-year operating period.

Task 3 was done early in the program to assure that the development work done in Tasks 2 and 4 addressed the problems expected in a commercial system as realistically as possible. Task 3 included a preliminary design and optimization of a commercial system. This included the selection of the hot tank liner configuration, internal insulation material and thickness, method of attachment of the liner, external insulation material and thickness and the cold tank external insulation material and thickness.

The results of Tasks 2 and 3 were used in Task 4. For example, the SRE tanks used the same liner (material, thickness, corrugations, etc) method of attachment, internal and external insulation and thickness as proposed for the commercial system. The SRE was tested under realistic commercial conditions including operating temperatures, charge, discharge, emergency shutdown and extended periods of no charge or discharge.

In Task 5, we evaluated the SRE test results with emphasis on determining the impact on the commercial design. We also completed a detailed assessment of the TES including a cost estimate and recommendations for future designs.

Tasks 6, 7 & 8 were accomplished in the performance of the above mentioned tasks.

2.0 Thermal Energy Subsystem

2.0 TES PRELIMINARY DESIGN AND ASSESSMENT

A thermal energy storage (TES) subsystem consists of the following major components:

- Hot tank
- Hot sump and pump
- Cold tank
- Salt melter and reprocessor
- Associated piping and valves (heat-traced and insulated)
- Instrumentation and controls

The TES shown schematically in Figure 2.0-1 is a dual tank system. The hot tank is for storing the hot 566°C (1050°F) molten salt from the receiver. The cold tank stores the cold salt 288°C (550°F) from the steam generator. A single working fluid, molten salt, is used for the receiver, storage, and up to the steam generator. The solar receiver control strategy is based on maintaining the hot salt outlet temperature by varying the flow rate through the receiver. This flow rate will generally be different from the flow through the steam generator thus the tanks will act as buffers in addition to storage. The salt from the receiver can flow to either the hot or cold storage tanks. This allows cold salt from receiver startup transients to be returned to the cold tank.

The gas fired melter is used for initial filling the system, salt make-up, and adding energy to the tanks to prevent salt freezing in periods of extended tanks to prevent salt freezing in periods of extended nonsolar days. Residual levels of the tanks allows weeks of heat capacity prior to salt freezing. The reprocessor in the storage system is included to recondition the salt by removing impurities.

This storage system advantages include

- Low cost due to use of molten nitrate salt and internally insulated hot tank with carbon steel shell.

- Decoupling of steam generating rate from short-term fluctuation in solar insulation.

When compared to other storage system, cascade and thermocline (defined Table 1.2.3-2) the dual tank system has the following advantages.

- Simplified overall plant flow control with a minimum of components.

- Minimum thermal cycling on a specific tank, pump, pipe, etc

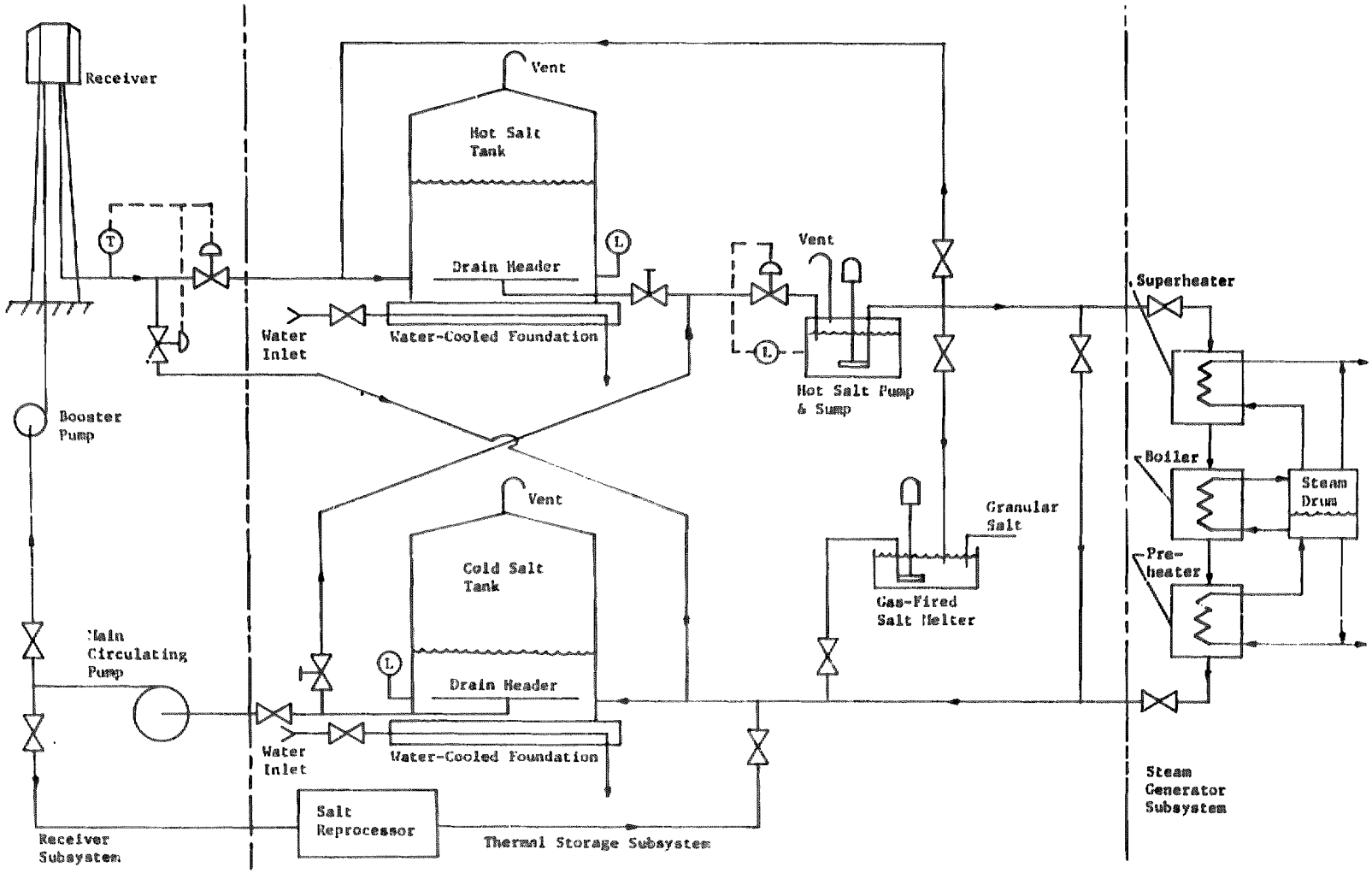

Figure 2.0-1 TES Subsystem Schematic

2.1 TRADE STUDIES

Critical to the commercial acceptance of the TES subsystem is the economic development of the hot salt and cold salt storage tanks. Many preliminary trade studies were performed on critical tank factors to maximize TES cost effectiveness. As a result of the Thermal Storage Tank Optimization study (see paragraph 1.2.3) a cylindrical tank was chosen as the baseline configuration.

Trade studies were performed for the following factors:

- Insulation materials
- Tank height
- TES subsystem cost

2.1.1 Insulation Materials

Heat lost through storage tank external surfaces must be compensated for by adding heliostats to the collector field. Since the cost of heat loss is taken as $1,536,000/MWt ($0.45 Btu/h) based on a heliostat cost of $235/m^2, it is extremely important that the tanks insulation be optimized.

Four separate types of insulation are used in the hot tank. The internal hot tank wall insulation is an insulating firebrick. The internal insulation used on top of the hot tank is a common fibrous insulation. The hot tank also has external insulation consisting of board or block type in the top, fibrous on the sides and a castable on the bottom.

2.1.1.1 Internal Insulation - The most important conclusion of the IITSSD program (see paragraph 1.2.1) is that no commercially produced fibrous or block insulation material will survive the molten salt environment for the 30-year life expected of the system. Consequently, a thermal expansion liner used to protect the internal insulation is used in the storage system. Analysis has shown that the cost of the liner is more than compensated for by increased efficiency due to lower thermal conductivity of dry insulating bricks as opposed to salt saturated bricks. A goal of this program is to use carbon steel as the primary load carrying shell of the tank. A nominal design temperature of 288°C (550°F) was selected for the steel shell to prevent any structural degradation. The shell temperatures are achieved by balancing the internal and external insulation materials and thicknesses. This parameter is the determining factor for internal insulation thickness in the hot tank. The size of the storage tank has no impact on the thickness or type of insulation material.

The desired characteristics of the internal insulation material are as follows:

- Low Installed Cost
- Low Thermal Conductivity
- High Load Bearing Capability
- 30-Year Service Life
- Existing Commercially Available Product
- Compatible with Molten Salt if Liner Leaks
- Nonabrasive to Liner and Shell

Of the four types of insulating materials investigated, only insulating firebrick was found to have adequate load bearing capability for internal use. Ten commercial varieties of insulting firebrick were investigated. Table 2.1.1-1 lists the candidates and their critical parameters. The cost per unit thermal resistance (R) is a ratio of material cost and thermal resistance at 399°C (750°F). Material costs are based on quotes or costs adjusted from previous studies.

Table 2.1.1-1 Properties of Insulating Brick Candidates

Material	Maximum Service Temperature, °C (°F)	Installed Brick Cost, $/R	Cold Crush Strength MPa, psi
Krilite 30	- -	2.880	- -
Krilite 55	1427 (2600)	15.120	≈17 (≈2500)
JM 20SL	1097 (2000)	2.269	0.793 (115)
JM 23SL	1257 (2300)	2.571	0.931 (135)
JM C22ZSL	1097 (2000)	2.899	2.28 (330)
JM 25	1367 (2500)	3.569	1.24 (180)
JM 28	1527 (2800)	5.694	2.07 (300)

Board type insulation was briefly considered. This insulation has adequate compressive strength when dry, but testing indicates that when the material is saturated with molten salt it loses all its compressive strength. Any leakage in the tanks liner would lead to localized insulation collapse and potential liner rupture.

In addition, candidate bricks were subjected to strength tests at elevated temperatures and tests in molten salt.

Cost tradeoffs were performed for each candidate brick. An example is illustrated in Figure 2.1.1-1. Johns Manville C22ZSL insulating firebrick was chosen based on lowest cost per unit area of tank wall insulation.

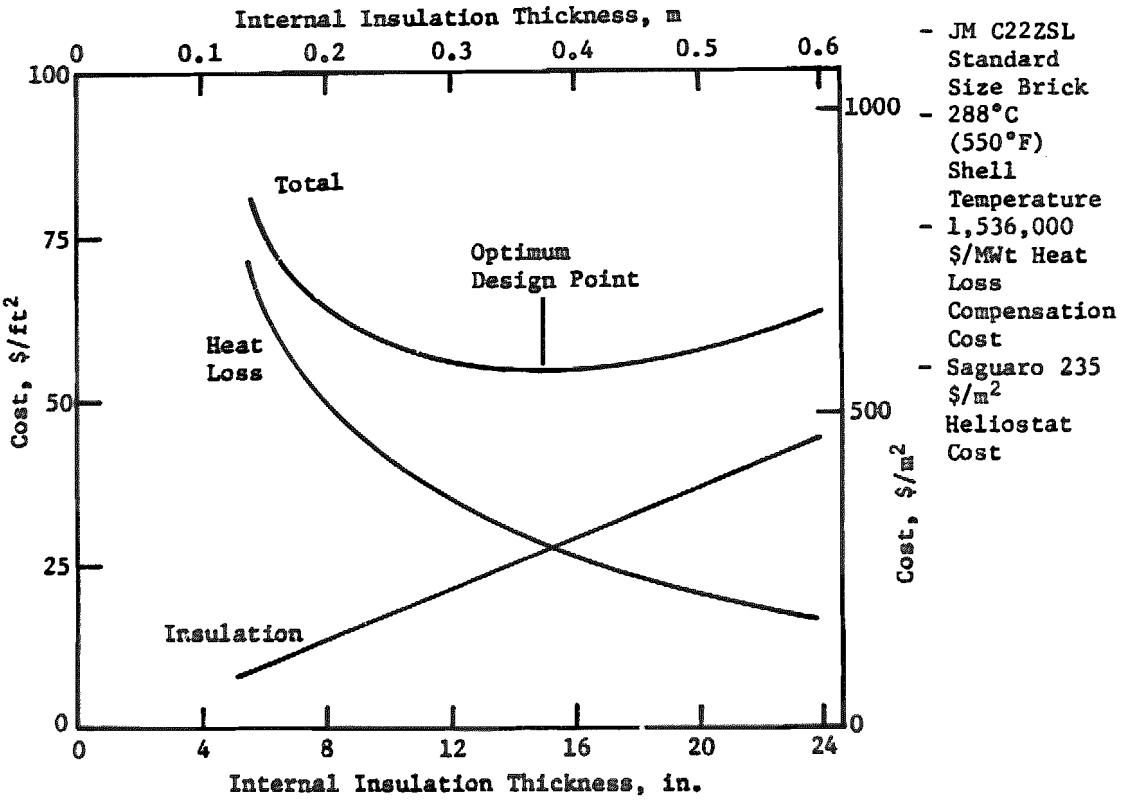

Figure 2.1.1-1 Optimized Insulation Design Methodology

The greater the brick thickness, the less the heat loss from the tank and, therefore, the less the cost of the solar collector system (principally heliostats) required to make up for the lost energy. Our shell temperature design criteria is 288°C (550°F). This design temperature was selected because it is below both the API and ASME maximum code values, and because it results in a thermal expansion of the hot tank shell less than (or equal to) that of the cold tank shell. The API code derates the shell material strength at temperatures exceeding 343°C (650°F). The shell temperature limit allows a margin of 56°C (100°F) using the full strength of the material. A liner leak will increase the shell temperature but at a slow enough rate that external insulation may be removed to maintain the tank shell below 343°C (650°F).

It can be seen from Figure 2.1.1-1 that the brick thickness for minimum total cost is 0.389 m (15.3 in.). In view of the fact that brick only comes in discrete thicknesses, and that the total cost curve is so flat, we selected a design thickness of 0.343 m (13-1/2 in.). This allows the use of two layers of standard 22.9cm x 11.4cm x 6.35cm (9 x 4-1/2 x 2-1/2 in.) size brick. This brick has undergone extensive testing during this program, including over 4000 hours in molten salt,

crush strength tests, creep tests, and fatigue tests, all conducted at 566°C (1050°F). All of these test results indicate that this particular brick will be entirely satisfactory for this application. The brick will be installed using mortar and thermal expansion joints every few feet in both directions. Metal shelves will be used to support the brick on the vertical walls. On both the walls and the floor, the liner is attached to the steel shell with rods (called anchor pieces) which penetrate the brick. Thus, the liner, brick, and shell are intimately coupled both mechanically and thermally.

The mortaring of the bricks is desirable because it results in a stable surface which can be smoothed. A wobbly uneven surface is detrimental to the liner. A slurry mortar in which the bricks can be dipped was selected. A compatibility test of mortars in molten salt resulted in the selection of Zelie mortar manufactured by Johns Manville. The bondline eventually cracked when in the molten salt but no swelling occurred. The mortar will survive a salt leak for months without disastrous results.

The use of larger brick sizes for the tank internal insulation was also investigated. Johns Manville Zelie Jumbo insulating firebrick, the same composition as JM C22ZSL is available in 11, 12, 13-1/2 and 18 inch sizes. Economic evaluation of these candidates indicates an installed cost increase of 24% to 30% compared to the standard 9 inch brick size and was subsequently eliminated from consideration.

The only other internal insulation required for the hot tank is installed at the top where there is no opportunity for degradation by molten salts. Consequently, an inexpensive, commercially available, fibrous insulating material was chosen. The three candidates considered are shown in Table 2.1.1-2. The thermal conductivity (K) of these materials all fall within a rather narrow range. Therefore, Flexwhite 1260 was chosen based on slightly lower K and lower material costs. No significant installation cost differences occur for any of the candidate fibrous insulating materials.

Table 2.1.1-2 Fibrous Insulating Material Candidates

Material (MFG)	K in. W/m-°C	(Btu/h-ft-°F)
Duraback (Carborundum)	0.073	(0.042)
Cerawool (Johns Manville)	0.059	(0.034)
Flexwhite 1260 (Holmes)	0.055	(0.032)

2.1.1.2 External Insulation - In order to minimize heat loss from the tank and retain a 288°C (550°F) temperature of the external steel shell, the external surfaces of the tank are insulated. The top of the tank was insulated with a rigid block type insulation to permit access of test and maintenance personnel. Two primary candidates emerged on the search for block type external insulation.

Duraboard is an alumina-silica composition board with a thermal conductivity of 0.087W/m-h-°C (0.05 Btu/h-ft-°F) at 288°C (550°F). The other block insulation candidate was Holmes 1212 with a thermal conductivity of 0.049 W/m-h-°C (0.028 Btu/ft-h-°F). Based on thermal conductivity and insulation material costs, Holmes 1212 was selected as the tank top insulation.

A castable insulating material is used on the tank bottom to minimize heat loss into the water cooled foundations. The three castable materials investigated are vermiculite concrete and two Johns Manville castable insulations; JM 2100 and JM 2800.

Vermiculite concrete was eliminated from consideration due to the amount of testing and quality control of vermiculite/concrete ratio required to maintain consistent thermal conductivity values. Of the two JM materials, JM 2100 was selected as the most cost effective candidate, when considering thermal conductivity, material cost and dimensional stability at high temperature. Thermal conductivity of the JM 2100 is 0.25 W/m-h-°C (0.143 Btu/ft-h-°F) at 316°C (600°F). No measurable shrinkage of the material at 243°C (550°F) could be detected and it's cold crush strength is 3.45 MPa (500 psi).

2.1.2 Height of Molten Storage Tank

In general, large storage tanks are more cost effective per unit energy stored than smaller ones due to the reduced area to volume ratio. There are, of course, practical limits to how large a single tank can be. Maximum tank height is generally limited by the allowable soil-bearing strength, unless special foundations are used. We have used a typical value of 0.24 MPa (5000 psf) for this study. Tank height can also be limited by the ability of the liner to withstand the salt pressure; this is currently assessed at 0.3 MPa (43.5 psi) which corresponds to a salt height of 17.7 m (58.1 ft). Maximum tank diameter is generally limited by the maximum permissible shell thickness. Large diameter tanks which exceed 3.8 cm (1.5 in) wall thickness are required under API code to have post weld heat treatment, which is prohibitively expensive.

This limits tank diameter to 40-46 m (130-150 ft). Cost optimization studies on the hot tank configuration (i.e., height-to-diameter ratio) show that for 1200 MWh_t capacity, the tank height for precisely minimum cost is 24.5 m (80.3 ft) (see Fig. 2.1.2-1). However, these same studies also show that the cost curve is rather flat, and so the cost penalty for 13.4 m (44 ft) height limitations imposed by the soil bearing stress allowable is only about 3% of the total TES cost.

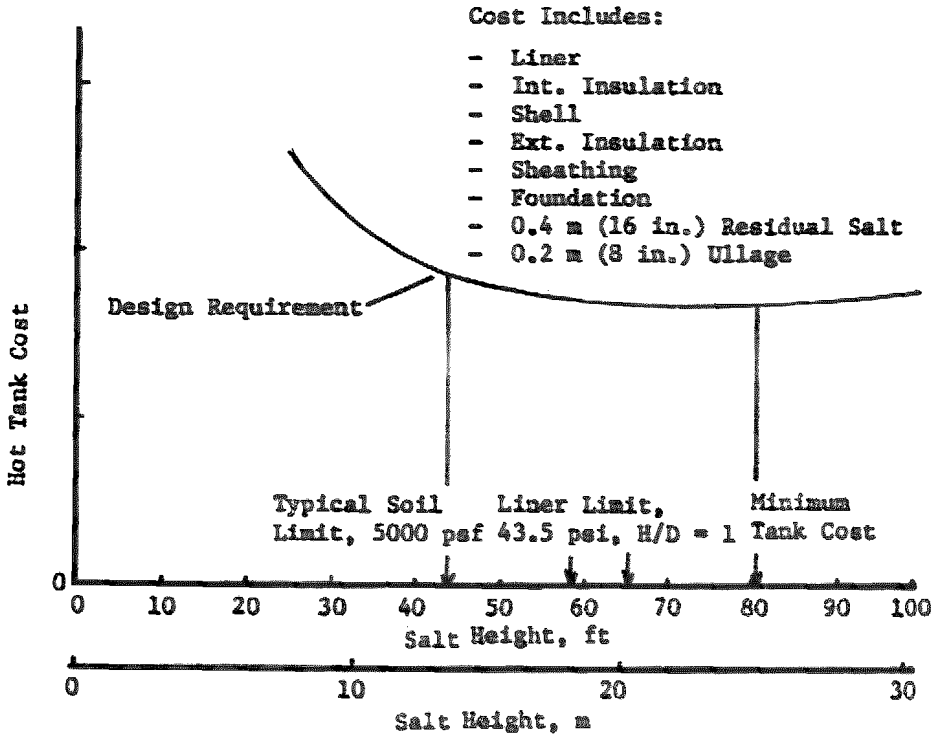

Figure 2.1.2-1 Hot Tank Height Optimization For 1200 MWht Storage Capacity

2.1.3 Thermal Energy Subsystem Cost Trades

Early in the program a parametric study was performed on Thermal Energy Storage subsystem cost and performance. The preliminary TES specification set thermal storage capacity of the subsystem at 375 MWht and this value was used in the cost trades. The study was later increased to 1200 MWht of storage as it was considered a more realistic size system.

Variables in the study included the type of internal insulation material and the rate of heat loss from the tank. Insulation types investigated were Krilite 30 and Krilite 55 insulating firebrick which have thermal conductivities of 0.73 W/m-°C (0.42 Btu/ft-h-°F) and 0.87 W/m-°C (0.50 Btu/ft-h-°F) respectively. Heat loss ratios of 2.8°C/day (5°F/day), 5.6°C/day (10°F/day) and 8.3°C/day (15°F/day) were studied.

The ground rules used to perform the trade study were as follows:

a) Allowable soil bearing strength = 0.24 MPa (5000 psf)
b) Internal insulation prices as of June 1980
c) Minimum salt height is 0.3 m (1 ft)
d) Minimum ullage gas height is 0.3 m (1 ft)

Analysis of TES costs for varying thermal storage capacities was performed for both types of internal insulating firebrick. The results which are shown in Figure 2.1.3-1 clearly indicate that Krilite 30 is the most cost effective of the two insulating firebricks, regardless of which heat loss rate is chosen.

To estimate the thermal performance of the molten salt storage tanks, various operational scenarios are used, the most common being the "normal day" with six hours of charging and discharging, the "good day" with 14 hours, and the solar outage where the system is charged to a certain level and held there for several weeks.

Based on the salt bulk temperatures analytically predicted for days of poor and good solar insulation shown in Figure 2.1.3-2, an overall thermal storage efficiency can be determined (see Fig. 2.1.3-4). In the solar insulation scenario depicted in Figure 2.1.3-2, the solar plant provides salt into the tanks at a variable flow rate but constant temperature (566°C/1050°F) until the tank is full. The tank is then discharged at a constant rate until it is "empty". Figure 2.1.3-3 shows the charge and discharge of the storage tank consistent with the temperature profiles shown in Figure 2.1.3-2. The tank is never completely empty in our design approach, since a small amount of molten salt is left in the tank at all times to reduce thermal cycling, avoid air entrapment in the pipes and preclude freezing of the salt during long periods of low solar insulation. It can be seen that thermal storage efficiency is maintained at a high percentage even under a poor solar day scenario. Since the heat loss was based on a given temperature drop (a percentage of the total heat capacity) the results apply to systems of any size.

2.2 TES REQUIREMENTS

The requirements of the TES subsystem were set forth in the TES Technical Specification prepared by Sandia National Laboratories Livermore. The primary elements of the specification are listed in Table 2.2-1.

In addition the following TES parameters were specified which were considered typical for a standard solar application.

- Earthquake: UBC Zone 2
- Max Wind: 40 m/s (90 mph) at 10m (32.8 ft) height
- Ambient Temperature: -29°C to 36°C (-20°F to +96°F)
- Peak Solar Flux: 978 W/m^2 (310 Btu/ft^2h) horizontal surface
  552 W/m^2 (175 Btu/ft^2h) vertical surface
- Allowable Soil Bearing Strength: .24 MPa (5000 lb/ft^2)

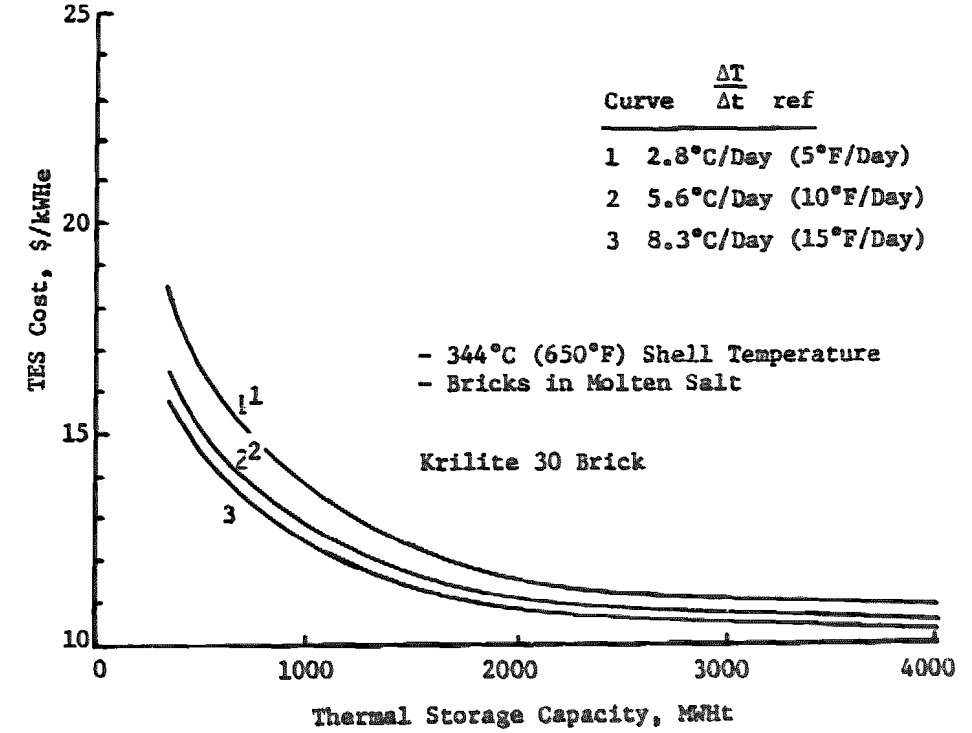

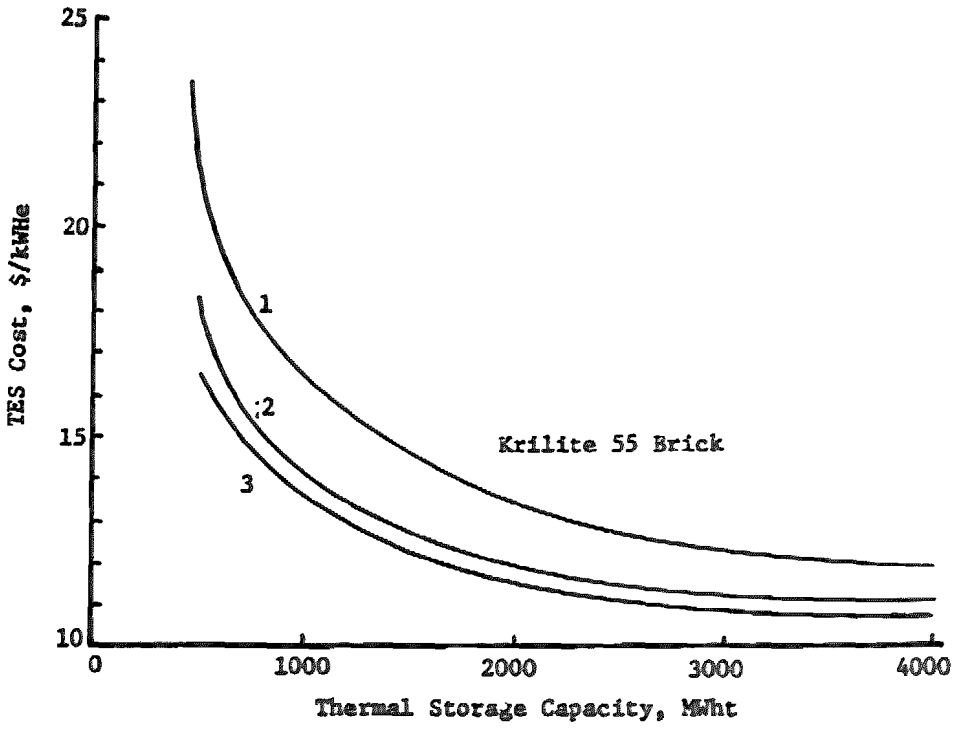

Figure 2.1.3-1 TES Cost vs Capacity for Parametric Designs

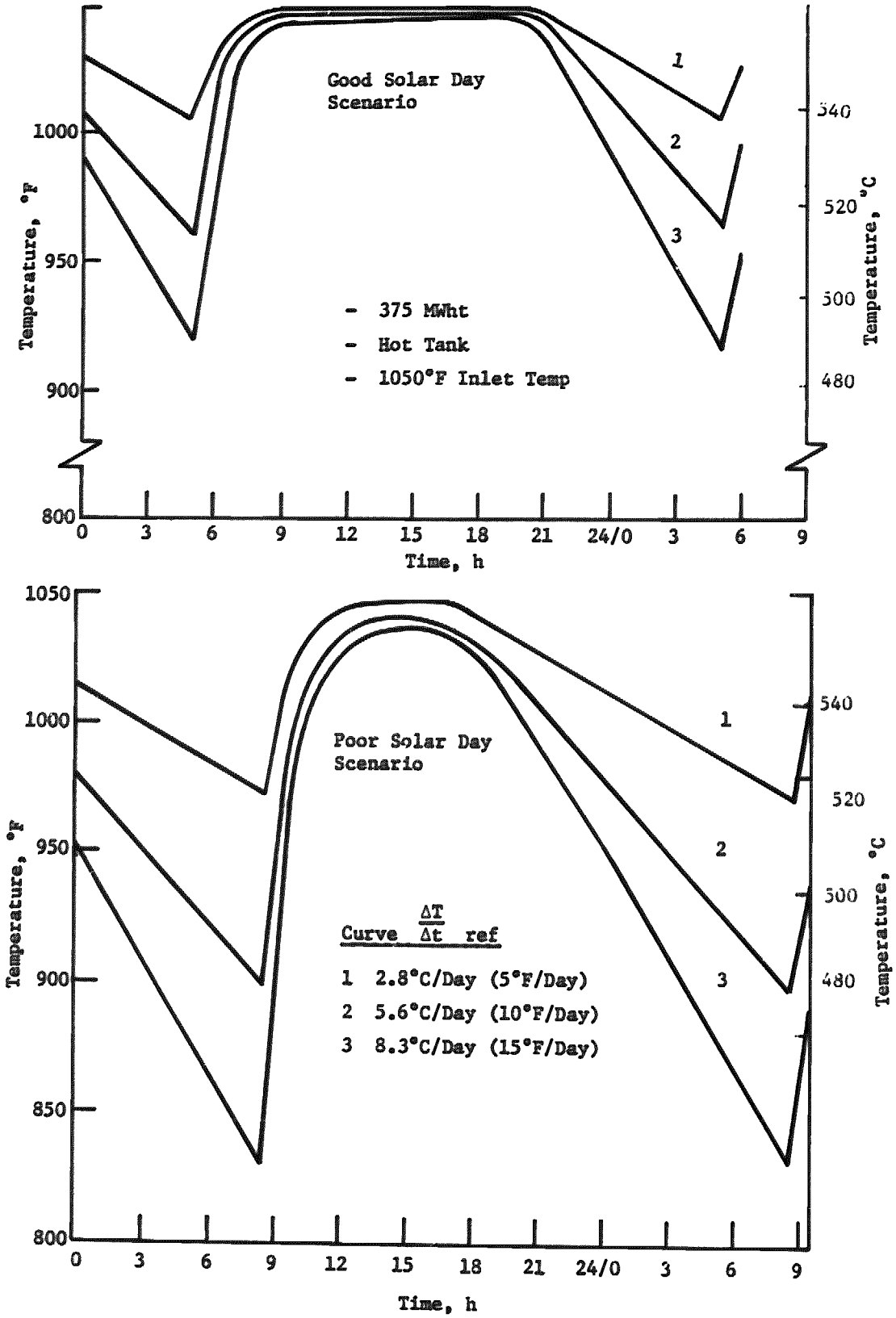

Figure 2.1.3-2 Salt Bulk Temperature Histories for Parametric Designs

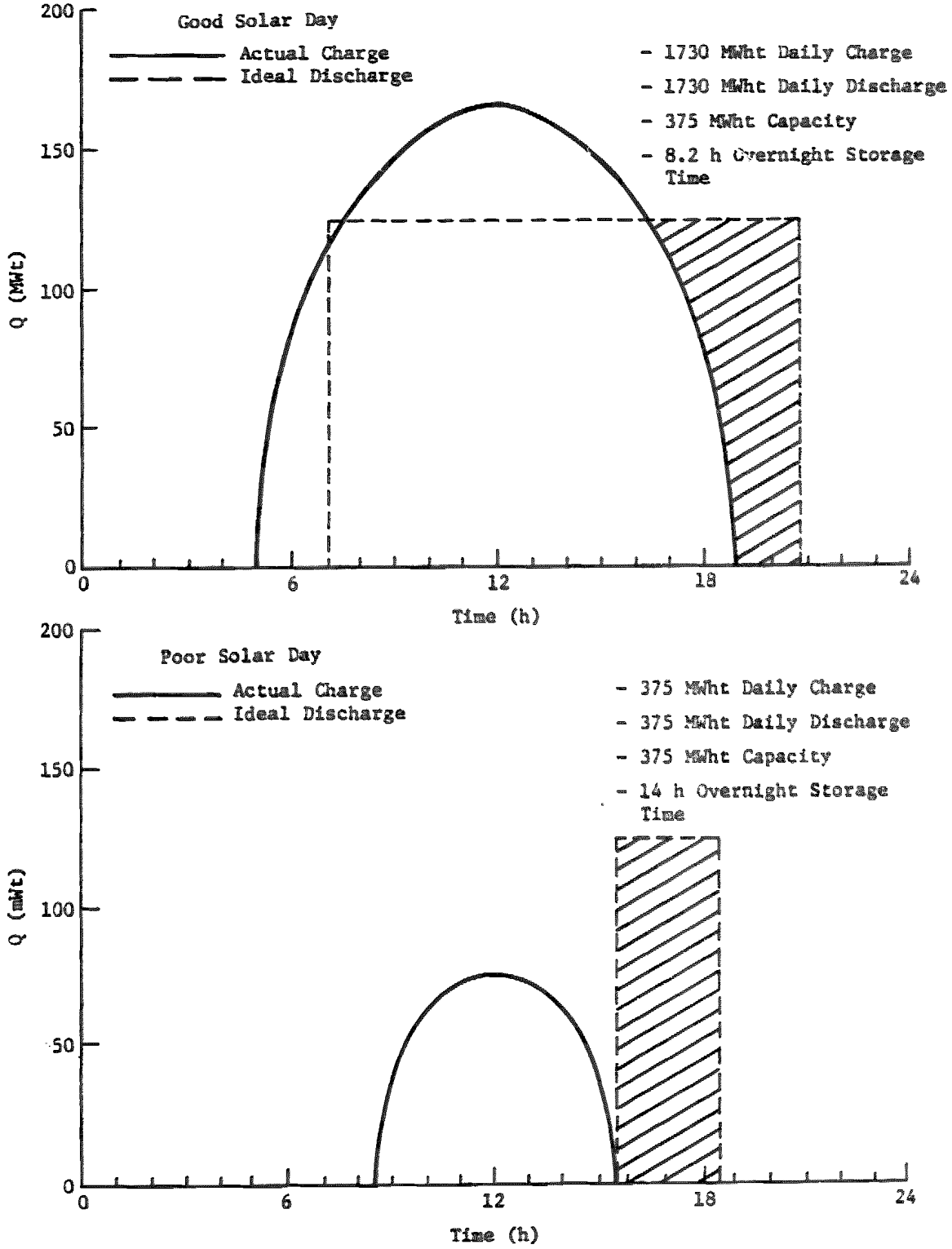

Figure 2.1.3-3 Charge/Discharge Histories for Parametic Designs

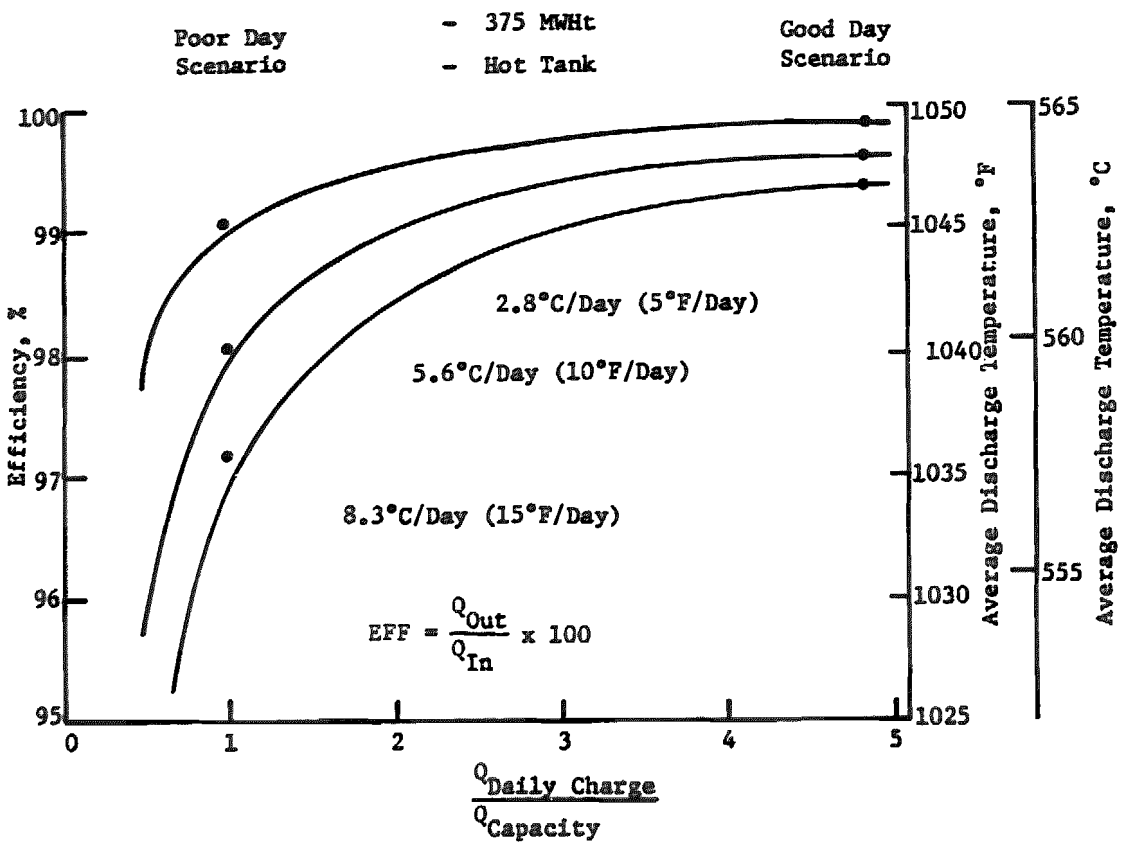

Figure 2.1.3-4 Thermal Storage Efficiency for Parametric Designs

For liner design purposes, values of the maximum salt pressure and temperature variations are required. These were specified as:

- Salt Pressure: 0-0.3 mpa (0-43.5 psig) daily for 30 years (10,950 cycles)

- Salt Temperature: 427-566°C (800-1050°F) daily for 30 years (10,950 cycles)
  Ambient-566°C (1050°F) five times per year for 30 years (150 cycles)

These variations are somewhat larger than the normal expected operating environment, and therefore are conservative.

The entire TES specification is included in Appendix A.

2.3 TES DESIGN

Under Task 3 of this contract, a preliminary design of a commercial size TES was developed. The design was developed in sufficient detail to clearly show the concept and to allow reliable cost estimates to be obtained.

Table 2.2-1 TES Subsystem Technical Specification

Description	Specification
Storage Media	Molten Salt (60 Percent $NaNO_3$/40% KNO_3 by Weight), C_p = 0.366 Calorie/Gr-°C (Btu/lb-°F)
Tankage Configuration	Dual Tanks (Hot and Cold)
Hot Tank Insulation	Internal and External
Cold Tank Insulation	External
Power Plant Rating, Gross	120 MWe
Electrical Power Generation Subsystem Efficiency	40%
Storage Capacity	4 Hours at 120 MWhe (1200 MWht)
Maximum Charge Rate	480 MWt
Minimum Charge Rate	48 MWt
Maximum Discharge Rate	300 MWt
Minimum Discharge Rate	30 MWt
Maximum Heat Loss Rate Hot Tank	1.50 MWt
Maximum Heat Loss Rate Cold Tank	1.50 MWt
Maximum Temperature Drop for Full Hot Tank	8.3°C/day (15°F/day)
Maximum Temperature Drop for Full Cold Tank	8.3°C/day (15°F/day)

2.3.1 System Schematic

A schematic of a commercial size TES is shown in Figure 2.3.1-1. This figure also shows how the TES interfaces with the rest of a solar thermal central receiver (STCR) plant. Note, however, that such items as the steam generator subsystem and the receiver subsystem are not a part of the TES subsystem, even though they are intimately coupled with it. Normal operation is as follows. Cold salt at 288°C (550°F) is pumped up the tower and through the receiver where it is heated to 566°C (1050°C) by solar energy. The hot salt then flows into the hot tank where it is stored for subsequent use. When steam is required, salt is pumped from the hot tank through the steam generator. The salt exits the steam generator at 288°C (550°F) and flows into the cold tank. This approach

is somewhat different than other approaches which charge the storage system only with "excess" solar energy from the receiver subsystem (i.e., most of the receiver output goes directly to the steam generator, and only the "excess" goes to storage to be used later in the day when the receiver output is low). Advantages of this TES subsystem are:

a) Dynamic separation of the steam generator and the receiver to eliminate steam generator input variation due to solar insulation variation.

b) Minimize temperature decrease due to heat loss in the hot and cold tanks.

Our approach has the advantage of minimizing control, piping and valving complexities and thus increasing reliability and reducing cost. This approach does require that each tank have the capability not only for charge alone and discharge alone, but also simultaneous charge and discharge (and generally at different rates).

The major components of the TES are:

1) Hot and cold storage tanks

2) Insulation

3) Storage related salt pumps

4) Piping in storage area

5) Tank foundations and diking

6) Cooling systems

7) Trace heating

8) Storage instrumentation and control

9) Salt mixing and meltdown equipment

10) Molten salt inventory

    a) Working salt

    b) Hot tank residual salt

    c) Cold tank residual salt

    d) Storage area piping salt

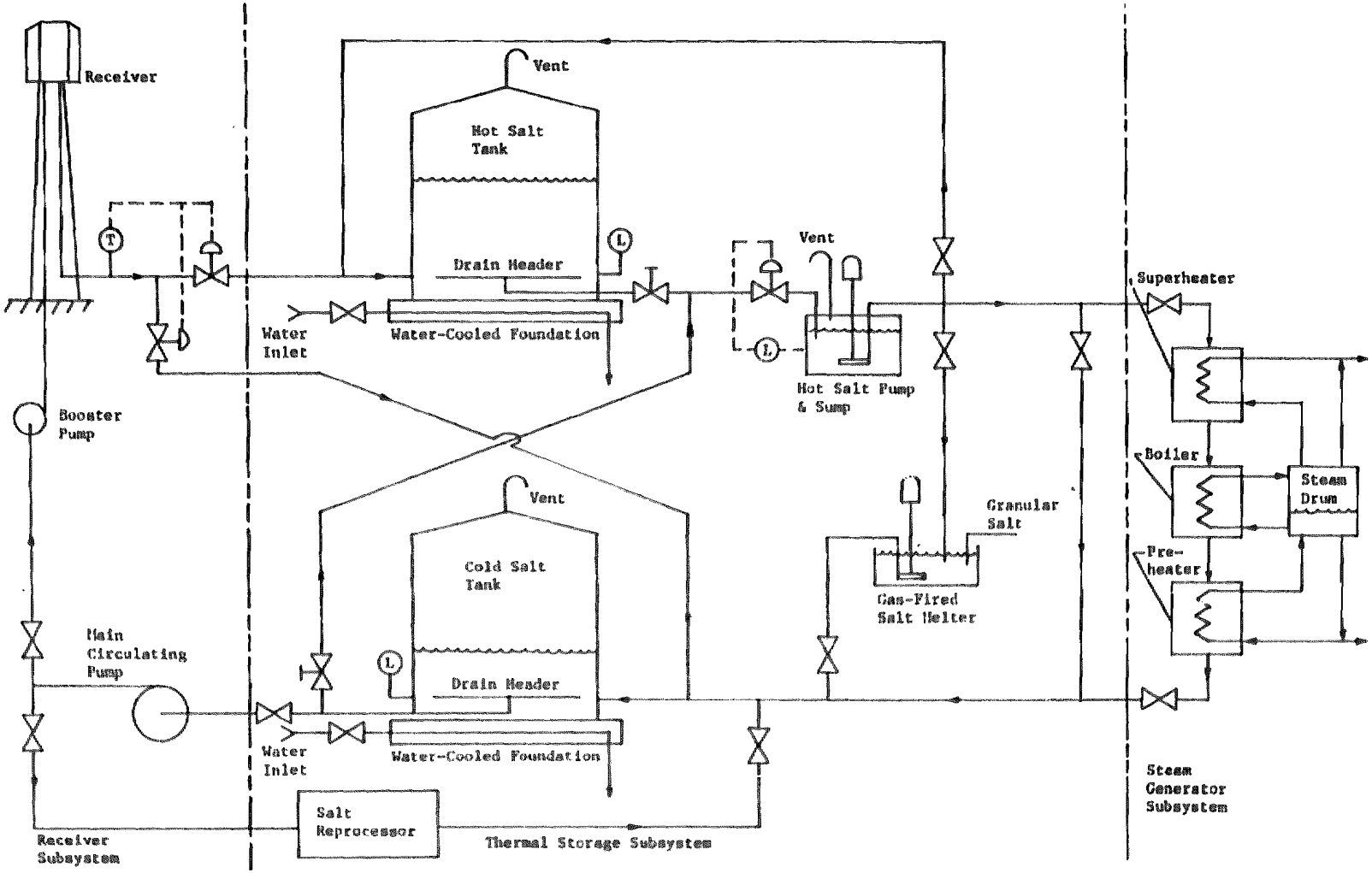

Figure 2.3.1-1 Simplified TES Subsystem Schematic

The level of salt in each tank can vary from full to empty each day. Thus, there is a time varying pressure load on the walls and bottom of each tank. There is also a daily variation on salt temperature. In order to reduce this variation, and to avoid lines going dry, a small amount of salt is always left in the tank--this is called residual salt. The term "working salt" denotes that salt (over and beyond the residual salt) which is used for energy storage.

2.3.2 Salt

The salt used for this system is a mixture of 60% $NaNO_3$ and 40% KNO_3 by weight. This salt has a freezing point of approximately 221°C (430°F). In order to be able to store a nominal 1200 MWh_t of energy using sensible heat between the limits of 288°C (550°F) and 566°C (1050°F), the weight of the working salt must be:

$$W_{ws} = \frac{Q}{C_p \Delta T} = \frac{1200 \times 3.413 \times 10^6}{0.366 \times 500}$$

or W_{ws} = 10,151,500 Kg (22,380,000 lb).

Residual salt height in each tank is currently taken as 41cm (16 in.) as this gives an acceptable daily temperature variation and is adequate to avoid dry lines. This results in 331,000 Kg (729,000 lb) for the hot tank and 387,400 Kg (854,000 lb) for the cold tank based on the tank IDs given in subsequent sections. The tank volumes are sized so that all the salt can be stored in either tank to allow repair upon the other tank.

Thus, the total amount of salt required for the tanks is 10,869,000 Kg (23,963,000 lb). The amount of salt required for the piping and sumps within the TES subsystem has not been determined, but it should be very small compared to the amount required for the tanks.

A specification of the salt purity which was prepared for the SRE is listed below:

	Separate	Mixed
Pure KNO_3	98.1% min	39.2 $\pm$ 5%
Pure $NaNO_3$	99.3% min	59.6 $\pm$ 5%

Maximum allowable trace elements by percent weight are as follows:

Cl	0.30
SO_4	0.23
CO_3	0.11
Alkali	0.10
OH	0.21
H_2O	0.50
Al_2O_3	0.03
Ca	0.03
SiO_2	0.02
Fe	0.01
Insoluble	0.10

The salts may be premixed at the suppliers factory, or they may be mixed at the TES site prior to loading the system with molten salt.

2.3.3 Hot Tank

Figure 2.3.3-1 shows the TES hot tank concept. The tank is a cylinder with a domed top and a flat suspended liner ceiling. The tank volume was 6,220 m^3 (219,600 ft^3). Preliminary cost optimization studies show an optimum salt height of slightly over 22.9 m (75 ft) but this would result in a soil bearing pressure in excess of the allowable. The maximum salt height (working plus residual) which is compatible with the assumed 0.24MPa (5000 lb/ft^2) soil strength is 13.2 m (43 ft 4 in.) (based on a hot salt density of 1728. Kg/m^3 (107.9 lb/ft^3) and including the weight of the tank.

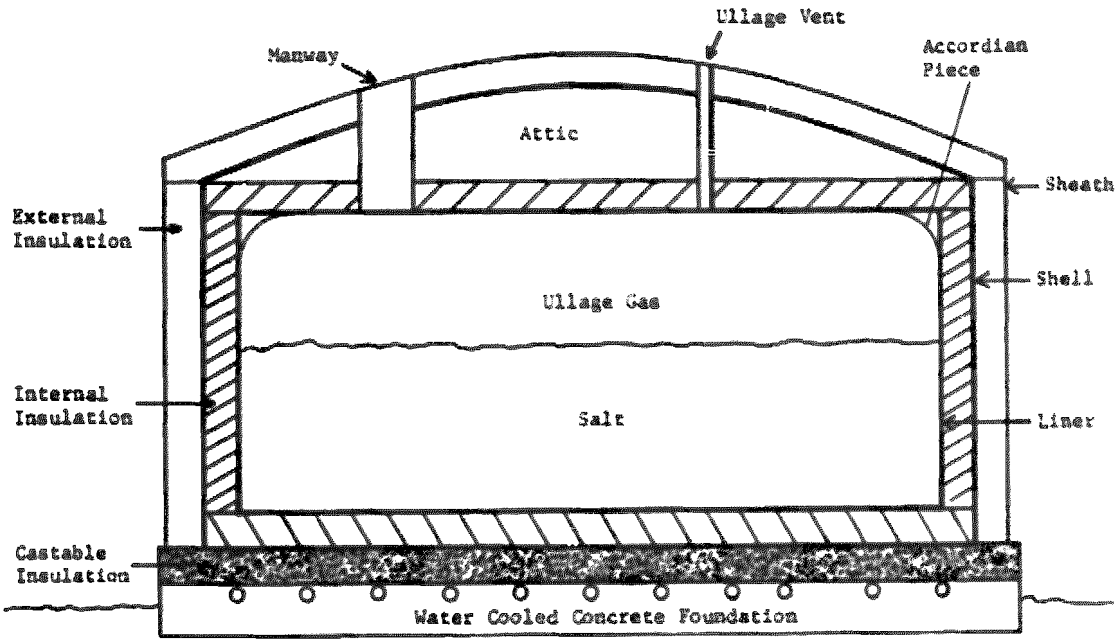

Figure 2.3.3-1 TES Hot Tank Concept

The liner inside diameter is 24.5 m (80 ft 4 in.). The liner inside height from the bottom to the flat deck is 14.6 m (47 ft 11 in.). This allows for 0.4 m (16 in.) residual salt height, 12.8 m (42 ft 0 in.) working salt height and 1.4 m (4 ft 7 in.) ullage space. The ullage space is large to allow for the accordion piece which joins the liner side wall to the flat deck (or suspended deck) ceiling in a gentle curve. The maximum salt height will remain below the welded joint of the accordion piece to the liner.

The shell ID is 25.2 m (82 ft 7 in.) (liner ID plus twice the brick thickness). The shell inside wall height is 15.8 m (51 ft 10 in.); 14.6 m (47 ft 11 in.) inside liner height plus 0.33 m (13-1/2 in.) bottom brick plus 0.5 m (20 in.) top internal insulation plus "attic" space.

The key hot tank dimensions are summarized below:

Liner

Inside diameter	24.5 m (80 ft 4 in.)
Inside height	14.6 m (47 ft 11 in.)

Shell

Inside diameter	25.2 m (82 ft 7 in.)
Inside height	15.8 m (51 ft 10 in.)

Salt

Max working salt height	12.8 m (42 ft 0 in.)
Residual salt height	0.4 m (16 in.)
Max salt height	13.2 m (43 ft 7 in.)

Ullage Space

Min ullage height	1.4 m (4 ft 7 in.)

The hot tank is big enough that if the cold tank had to be shut down for repair, the hot tank could safely hold all of the salt for a reasonable period of time.

Incoloy 800 has good corrosion resistance and strength at elevated temperature and is formable into the liner shape. JM C22ZSL brick has low thermal conductivity, high strength, low cost and is compatible with molten salt if the liner should develop a leak. The foil keeps the brick from scratching the inside of the liner which could reduce fatigue life. The external insulation is sized to keep the shell at 288°C (550°F) under the design "hot day" conditions (tank full of 566°C (1050°F) salt, 36°C (96°F) ambient temperature, no wind, full solar). The sheathing serves to weather-proof the insulation and prevent air infiltration and the white coating minimizes shell temperature variations due to diurnal solar flux variations.

The liner corrugation shape is of the standard Technigaz shape used in LNG applications. The liner pitch (i.e., distance between adjacent corrugations) is 34.0 cm (13.4 in.) between large corrugations, and 24.0 cm (9.45 in.) between small corrugations. On the side wall, the large corrugations run circumferentially in parallel horizontal planes

and the small corrugations run vertically. On the floor, the large corrugations run radially, and the small corrugations run circumferentially. The liner "angle pieces" (i.e., the small right angle pieces that go in the corner of the tank) are fabricated to account for the change in liner corrugation size coming vertically down the wall into radial lines on the bottom.

The liner for the sidewall and bottom is made of Incoloy 800 and is 1.27 mm (0.050 in.) thick. This is the nearest U.S. gauge to the 1.20 mm (0.047 in.) gauge customarily used by Technigaz in previous LNG applications. To reduce cost, the liner ceiling will be a flat, suspended deck with accordion pieces at the tank walls. Also to reduce cost, the liner ceiling is 304 stainless steel since its corrosion and strength properties are adequate for this part of the liner. Each liner sheet on the side walls and bottom will be anchored to the shell via "anchor pieces", and "heavy angles" will be used on the bottom corner.

The bricks are installed using standard techniques including mortar and vertical and horizontal expansion joints (stuffed with refractory fiber). The bricks are supported on the sidewall using carbon steel shelves 22.9 cm (9 in.) wide located every 1.94 m (6.36 ft) in height. The sidewall has two layers of brick, the outer layer consisting of straights and arches running vertically with a 11.4 cm (4-1/2 in.) thickness. The inner layer consists of keys and straights laying flat with 22.9 cm (9 in.) thickness. The floor also has two layers, 22.9 cm (9 in.) vertical brick over 11.4 cm (4-1/2 in.) brick on edge (all straights). The mortaring of the bricks is done by dipping which results in a very thin bond line. This is more economical and is more compatible with molten salt should a leak occur.

The external insulation on the sidewall consists of fibrous batts and is installed using 3.8 cm (1-1/2 in.) insulation rings around the outside of the shell and bands. The roof uses block insulation and bonding. The top and sides are protected with weatherproof aluminum sheathing. The external insulation on the bottom is castable poured over the concrete foundation (the latter has a lip around its outer edges to contain the castable).

The foundation is a standard concrete type compatible with both the weight of the tank and salt and the 0.3 mpa (5000 psf) soil bearing strength. The foundation will be water cooled using 25.4 mm (1 in.) pipe located on 30.5 cm (1 ft) centers, with the tops of the pipe being 38 mm (1-1/2 in.) below the upper surfaces of the concrete. A mixture of 40% ethylene glycol, 60% water will be used to prevent freezing during construction or any shutdown period. The coolant temperature will be maintained slightly less than the boiling point of water.

The dimensional tolerances, welding requirements and all other quality parameters have not been defined in detail specifically for a TES size tank, but the SRE experience will provide all the guidelines necessary for obtaining TSE cost estimates.

The salt inlet to the hot tank will consist of a single pipe coming over the roof into the center, and vertically downwards. It will terminate some distance above the bottom in a "tee". The outlet is located in the center of the bottom. An anti-vortex device is located above the outlet. The outlet pipe will be carried vertically downwards through the brick, shell, castable and into the concrete where there will be a 90° elbow. The outlet pipe will be carried out of the foundation through a tunnel large enough to allow for maintenance and repair. These center located inlets and outlets minimize any tank problems associated with thermal expansions near the outer edges of the tank. All liner penetrations must be sealed by welding to the liner so that no salt can leak out and degrade the insulation.

The selected control for the tank ullage gases is the use of air with the water vapor and carbon dioxide removed. A sieve material which can be regenerated is selected as the method of scrubbing the water and carbon dioxide from the incoming air. The selected system requires a low pressure drop across the scrubber with added safety overpressure devices to achieve a very small pressure across the tank shell.

The key materials and thicknesses for the hot tank are listed in Table 2.3.3-1.

Table 2.3.3-1 Hot Tank Materials and Thicknesses

Component	Tank Side	Tank Top	Tank Bottom
Liner	Incoloy 800 1.27 mm (0.050 in.)	304 Stainless 1.27 mm (0.050 in.)	Incoloy 800 1.27 mm (0.050 in.)
Foil	304 Stainless 0.25 mm (0.010 in.)	N/A	304 Stainless 0.25 mm (0.010 in.)
Internal Insulation	JM C22ZSL Brick 34.3 cm (13-1/2 in.) with Zelie Mortar	Holmes Flexwhite 1260 50.8 cm (10 in.)	JM C22ZSL Brick 34.3 cm (13-1/2 in.) with Zelie Mortar
Shell	A516 Grade 70 Carbon Steel	A516 Grade 70 Carbon Steel	A516 Grade 70 Carbon Steel
External Insulation	Holmes Flexwhite 1260 5.1 cm (2 in.)	Holmes 1212 Block 15.2 cm (6 in.)	JM 2100 Castable 25.4 cm (10 in.)
Sheathing Insulation	Aluminum with White Coating	Aluminum with White Coating	N/A

These materials and thicknesses were selected based upon minimum cost and compatibility with the hot salt environment.

2.3.4 Cold Tank

The cold tank is a carbon steel shell with external insulation (see Fig. 2.3.4-1). It uses the same material as the hot tank, but with differences in dimensions. The shell ID is kept the same as the hot tank to reduce shell fabrication costs. However, the cold tank shell is shorter than the hot tank shell due to a lack of internal insulation, higher salt density 1914. Kg/m^3 (119.5 lb/ft^3), no attic and reduced ullage space (since there are no liner accordion pieces in the cold tank).

A summary of the key tank dimensions is given below:

Shell

Inside diameter	25.2 m (82 ft 7 in.)
Inside height	12.2 m (40 ft 0 in.)

Salt

Max working salt height	10.9 m (35 ft 11 in.)
Residual salt height	0.4 m (16 in.)
Max salt height	11.4 m (37 ft 3 in.)

Ullage Space

Min ullage height	0.84 m (2 ft 9 in.)

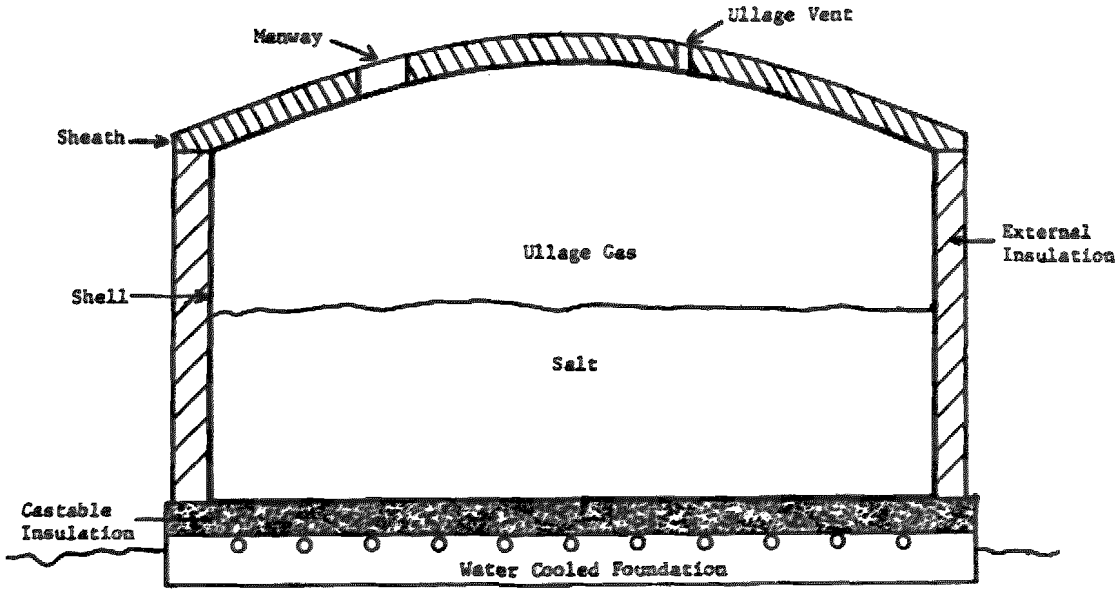

Figure 2.3.4-1 TES Cold Tank Concept

The cold tank is big enough to hold all of the salt from both the hot and cold tanks in the event the hot tank must be shut down for repair.

The key materials used in the cold tank are the same as their counterparts in the hot tank, but the insulation thicknesses are greater because external insulation is much cheaper than internal insulation, so the cold tank cost optimization tradeoff results in relatively more insulation and less heat loss. This has the added advantage of increased freeze protection in the cold tank (relative to the hot tanks) where this could be more of a problem. The materials and thicknesses are summarized in Table 2.3.4-1.

Table 2.3.4-1 Cold Tank Materials and Thicknesses

Component	Tank Side	Tank Top	Tank Bottom
Shell	A516 Grade 70 Carbon Steel	A516 Grade 70 Carbon Steel	A516 Grade 70 Carbon Steel
External Insulation	Holmes Flexwhite 1260 38 cm (15 in.)	Holmes 1212 Block 38 cm (15 in.)	JM 2100 Castable 38 cm (15 in.)
Sheathing	Aluminum with White Coating	Aluminum with White Coating	N/A

The insulation attachments and the water cooled foundation are the same as for the hot tank (except for the already noted dimensional differ- ences).

2.3.5 Control System

The control system for the thermal storage system is relatively simple; as shown in Figure 2.3.5-1, six automatic control loops are required in addition to on-off functions for pumps, valves, trace heaters and the salt melter.

During steady state operations, salt is supplied to the receiver from the cold salt sump (valve #08) and to the steam generation subsystem from the hot salt sump (valve #07). Salt returning from the tower is steered into either the hot or cold salt tanks depending on its temperature. These valves are also used to maintain the salt level in the hot salt collection tank at the outlet of the receiver.

The salt level in each sump is controlled using valve #03, for hot salt and valve #04 for cold salt. In each case, valves #03, #04 rely on gravity head to feed each sump.

In an integrated solar thermal plant using a distributed digital control system, control of the thermal storage system will be integrated with the control of the receiver, steam generator and the rest of the plant. The integrated control system will include operator control stations (CRT Terminals) in the control room, microprocessor-based controllers, printers, loggers, data storage equipment and interconnecting data highways and wiring. This digital control equipment will interface electrically with the transducers, valves and pumps of the thermal storage system and other subsystem in the plant.

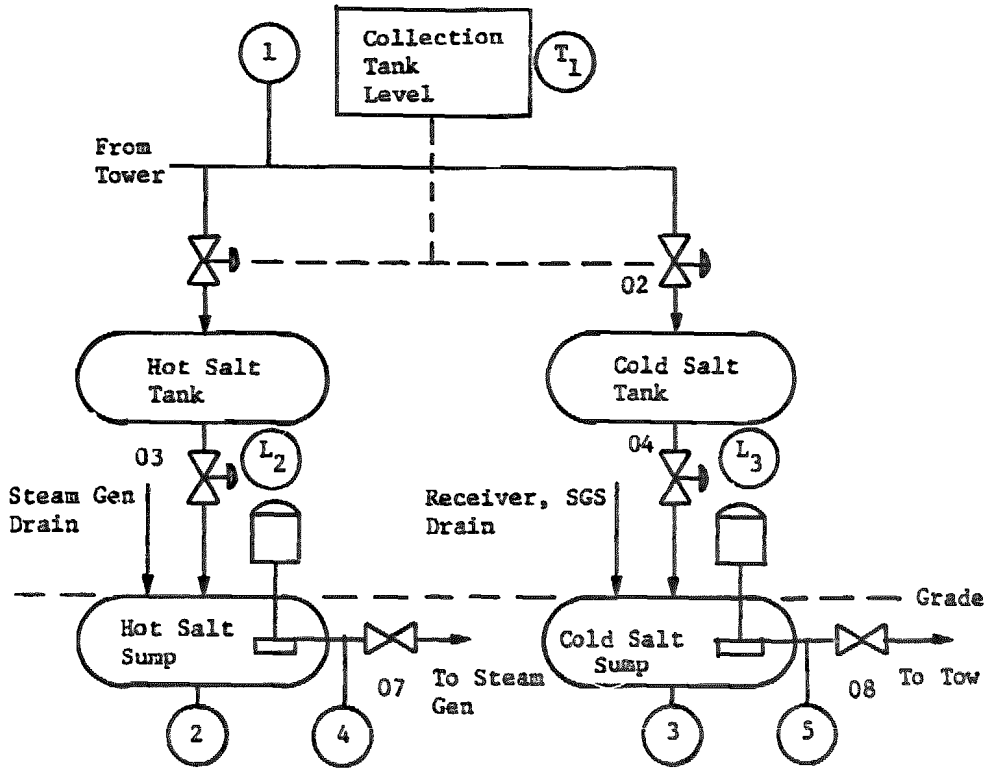

Figure 2.3.5-1 Thermal Storage Control System

The microprocessor-based controllers will be installed in equipment racks that may be located in the control building or in the vicinity of the equipment being controlled. In either case, the controllers for the thermal storage system will probably be located in a rack that includes controllers for other subsystems, such as the steam generation system.

Depending on the supplier of the digital control system hardware, a single microprocessor-based controller may be used to control both the steam generation subsystem and the thermal storage subsystem, or dedicated controllers may be used for each of the individual control loops.

Assuming that a distributed digital control system is included in the plant for controlling the receiver and the steam generator (both of which require more complex controls than the thermal storage subsystem), the cost of the additional input/output cards and controllers for the storage system is estimated to be no more than $20,000.

2.3.6 Other Equipment

Reference to the TES subsystem schematic (Fig. 2.0-1) shows that in a typical application the following components are also required:

a) Piping*
b) Valves*
c) Pumps
d) Sumps*
e. Salt melter
f. Salt reprocessor
g. Instrumentation

*Including trace heating and insulation.

2.4 TES COST ANALYSES

The objective of this study was to develop a cost estimate for the commercial size Thermal Energy Storage System described in Section 2.3 of this report. The ground rules for the estimate are given below:

a) This is an estimate, not a firm fixed price bid. While vendor quotes were highly desirable for the major cost items (e.g. tank shells) they are not mandatory for all items. Judgement and experience (including the SRE) was used where appropriate.

b) Tucson, Arizona was assumed as the site.

c) Current dollars (1982 $) were used i.e., cost if plant were to be built today.

d) It was assumed this is the first plant.

e) The SRE data was used carefully, as much of it should be an upper bound for a big tank (e.g., manhours to install 1000 brick).

The major components of the TES which were costed separately are listed below.

Hot Tank
Cold Tank
Site Preparation
Supporting Equipment
Salt
Operations and Maintenance

For each item, the following cost factors were considered:

Raw material
Shop fabrication (if required)
Shipping
Construction labor to erect

All overhead, G&A, profit, engineering costs, and construction management costs were included in the estimates so that the bottom line represents the estimated price that a solar plant prime contractor would have to pay for a complete TES subsystem.For each major component, a cost breakdown by the subcomponents itemized below was used.

Hot Tank

a) Foundation (including water cooling, tunnel, castable insulation)

b) Shell (including brick shelves, anchor nuts, insulation rings, top, leak testing)

c) Brick (including mortar, hole drilling, etc)

d) Liner (including anchor pieces, foil, flat deck supports, ammonia leak testing)

e) External Insulation (including bands, sheathing)

f) Miscellaneous (including inlet and outlet pipes, ullage gas management, instrumentation, ladders, etc)

Cold Tank

a) Foundation (including water cooling, castable insulation)

b) Shell (including insulation rings, top, leak testing)

c) External Insulation (including bands, sheathing)

d) Miscellaneous (including inlet and outlet pipes ullage gas management, instrumentation, ladders, etc)

Site Preparation

a) Survey

b) Excavation for foundations

c) Construction, electric, water, air

d) Dike

Other Equipment

a) Piping (including trace heating, insulation)

b) Valves

c) Pumps

d) Sumps

e) Controls

f) Salt Melter

g) Salt Reprocessor

h) Instrumentation

Salt

a) Working Salt

b) Residual Salt

c) Salt in pipes and sumps

Operation and Maintenance

a) Maintenance and repair work

b) Operating power costs

2.4.1 Material Costs

The cost of the insulation materials to build the system was obtained by quotes from suppliers based on the types and amount of materials required by the preliminary drawings. The data are presented on Table 2.4.1-1.

2.4.2 Tank Costs

A request for a budgetary estimate along with a tank specification was prepared and sent to Pittsburgh - Des Moines Corporation and Glitch Field Services Company. Both estimates considered the tank shells, external insulation, and the foundations. The estimate from Glitch Field Service included the bricking, anchor, shelves, and liner. The cost listed in Table 2.4.5-1 are considered the most realistic values from the two estimates and experience gained from this program.

2.4.3 Salt and Processing Cost

The TES specifications were sent to Olin Chemical Company along with a request for a budgetary cost estimate. Olin's response of May 1982 is as follows:

I. The cost of 25.0 M pounds of Olin Solar Nitrate Salt inventory, delivered, charged and pumped into the warm storage tank of the 120MWe power plant, Tucson, AZ, at 550°F is included below. Depending upon the number of days desired to charge the material, either a 1MW or 3MW natural gas/oil fired melter is required. It is understood that the natural gas fossil fuel required for the melter will not be provided by Olin.

Table 2.4.1-1 Material for the Hot & Cold Tank

Component & Material	Supplier	Service	Date Estimate Given	Cost Baseline
1. Liner Incoloy 800	Huntington	Membrane	2/5/81	338,243
2. Foil Stainless 304	Teledyne-Rodney Metals	Between Membrane & Brick	12/21/81	16,766
3. Insulation JM C22Z Brick & Zelie Mortar	Johns-Manville	Between Membrane & Shell	2/2/82	333,166
4. Insulation JM Cerawool Millboard	Johns-Manville	Hot Tank Vertical Expansion Joints in Brick	Price Unchanged From SRE 1/18/82	10,717
5. Insulation J-M Cerafiber Bulk	Johns-Manville	Hot Tank Void Filler in Brick	Price Unchanged From SRE 1/18/82	600
6. Insulation JM Cera-blanket (no binder)	Johns-Manville	Hot Tank Horizontal Expansion	Price Unchanged From SRE 1/18/82	900
7. Insulation Holmes Flexwhite	Holmes Insulation Inc.	Suspended Deck Tank Sides Exterior (Hot & Cold)	1/27/82	59,333
8. Insulation Holmes 1212 Block	Holmes Insulation Inc.	Tank Roof Exterior (Hot & Cold)	1/27/82	38,130
		TOTAL ESTIMATE PRICE		797,855

*All prices include freight

II. Item	Cost ($/lb)	Contingency ($/lb)	Total ($/lb)
- Salt (F.O.B. Manufacturing Plant)	$.15		$.15
- Transportation costs including freight from plant to end of railhead and railhead to utility site.	$.041		$.041
- Equipment and labor services for blending and melting operations including portable storage facilities.	$.060		$.060
- Miscellaneous including product loss, rail car demurrage, etc.		$.005	$.005
TOTAL	$.251	$.005	$.256

2.4.4 Other Equipment

The following item prices were required to provide a complete TES cost.

The pipe lines required were identified from the TES schematic, Figure 2.0-1. A flow of 480 MWt requires lines of 0.3m (12 in) diameter. Schedule 10, 316 SS pipe was used for the high temperature salt and carbon steel pipe was used for the low temperature salt. The storage layout used locates the hot sump and reprocessor close to both tanks. Cross tie lines between tanks were laid out for minimum distances. Line costs considered heat tracing insulation and lagging. Cost of electrical equipment for the heat tracing was also included.

Valves were assumed to be .3m (12 in) with below seals, High temperature valves will be stainless construction ($37,000) and low termperatures valves will be mild steel bodies ($27,000).

The hot salt pump selected is a vertical cantilever type with no bearings or seals in the salt. The requirements are:

Flow 0.11	m^3/s	(1700 gpm)
Heat Rise	21.6m	(80 ft)
Salt Temp	566°C	(1050°F)
Motor	74,6 kW	(100hp)

The pump and motor prices were estimated by Lawrence Pump Company at $26,000. Added to this value was the cost of associated electrical equipment.

The sump was sized for line drain back and liquid interface velocity that is compatible with automatic controls. The sump size was 2.4 m 8 ft) diameter and 3.0 m (10 ft) in height and the material was 316 stainless steel.

The following items were included in the instrumentation.

3 - Liquid level
4 - Temperature valves
30 - Thermocouplers

2.4.5 System Cost

The TES cost is detailed in Table 2.4.5-1 . The total cost of 13 million dollars relates to 10.8 $/kWht and 27.1 $/kWe for the 480 MWhe (1200 MWht) storage subsystem. Comparison of the cost was made with the results of a study made in 1979 (Internally Insulated Thermal Storage System Program). This study was for larger sized systems but extrapolating the system cost down to a 1200 MWht size resulted in a predicted storage cost of 6.0 $/kWht and 14.9 $/kWhe. Over the three intervening years inflation has been approximately 25 percent. This present study has a higher estimated cost due to better definition of each aspect of the storage system. It should be noted that the salt storage system is significantly cheaper than other types of storage.

Evaluation shows that operation and maintenance costs for the storage system is small. The operational cost is approximately 0.0003$/kWhe. The personnel and cost to maintain the storage system are considered as a portion of the total system. The pump, motor, trace heating, coolant heat rejection, and instrumentation are the only portions of the system which require maintenance.

Table 2.4.5-1 TES Storage Subsystem Cost

Hot Tank	
Foundation	115,000
Shell	800,000
Brick	795,400
Liner	2,225,000
Fibrous Insulation to Sheathing	135,750
Ullage gas control	25,000
Management	400,000
	$ 4,486,150
Cold Tank	
Foundation	80,000
Shell	685,000
Exterior Insulation	162,000
	$ 927,000
Salt	
Working	5,880,200
Tank Residuals	384,000
Sumps & pumps	12,500
Fuel to melt	30,600
	$ 6,307,300
Site Preparation	
Survey, excavation, dike	130,000
	$ 130,000
Other Equipment	
Piping	285,000
Valves	293,000
Pump	31,000
Sump	52,000
Controls	20,000
Reprocessor	35,000
Instrumentation	18,000
Coolant rejection	12,000
	$ 746,020
Management & design	
	400,000
	$ 400,000
Total Cost	$ 13,006,450

3.0 Critical Component Development

3.0 CRITICAL-COMPONENT DEVELOPMENT

The general objective of this task was to perform all of the development work required to bring any critical component up to a state of readiness for subsequent TES and SRE design and fabrication. Based on our previous molten salt and liquefied natural gas (LNG) experience, the only critical components in the dual-tank molten salt storage concept are the Incoloy 800 flexible corrugated membrane (i.e., the liner) and the internal insulation used in the hot tank. Therefore, the purpose of this development program was to define the specific details of liner and internal insulation design (including fabrication techniques) that could withstand the hot salt thermal, corrosion and pressure cycling environments over a 30-year service life without failing or leaking, and then to verify that design (and its service life) by performing internally insulated subassembly tests with hot salt. This was accomplished by performing cyclic life tests of the liner element for pressure and fatigue.

3.0.1 Rationale and Need for Critical-Component Development

By definition, the term "critical component" means a component whose proper function is essential to operation of the entire system. The term "development" implies that this component has not previously been used in the specific circumstances of this application (i.e., molten salt) and thus requires some development work before it can be used. Each of the various components (or subcomponents) in our TES (and SRE) subsystem design concept have been in industrial use for many years. In fact, most of them have been used in molten salt applications (Table 3.0.1-1) and thus need no further development.

Table 3.0.1-1 Molten Salt Component Applications

Component	Application
Salt	Draw salt has been used for heat treatment of metal since the turn of the century. It (and HITEC) is also commonly used as a heat transfer fluid in industry. Molten salt is used in our flow loop and in our solar receiver SRE.
Cold Tank	Carbon steel tanks are routinely used to hold draw salt for heat-treating applications at temperatures up to 320 to 370°C (600 to 700°F).
Water-Cooled Concrete Foundations	Have been used to support tanks holding hot 210°C (400°F) oil.
Pumps, Valves, Piping, Controls	Routinely used in industry for salt (note the use of cantilever pumps for the hot and cold salt to avoid seal and bearing problems.)

The internally insulated hot salt tank has not been previously used and therefore it (and its components) are the only development issues. The principal concerns about the hot tank revolve about the central issue of leak-free performance for up to 30 years in a cyclic charge/discharge hot molten salt environment. One item that is not a major concern for this development program is the hot tank heat loss. The materials and heat transfer paths are reasonably well known and predictable (to within the usual engineering accuracy) by computer modeling.

The purpose of the liner is to keep the molten salt from coming in contact with any other part of the tank, and since it has never been used in a molten salt application before, it qualifies as a critical component in need of development. The Technigaz liner has, however, been used extensively by the liquefied natural gas (LNG) industry in LNG storage tanks for ships and land depots. This liner has also been used on several applications at elevated temperatures up to 450°C (840°F). A closeup picture of the liner is shown in Figure 3.0.1-1. Although the internal insulation has also not been used in a molten salt application, refractory brick of this general type has been used for years in other high-temperature applications (e.g. furnaces) and in this application it will be protected from the salt by the liner. The hot tank steel shell and external insulation are basically the same as for the cold tank.

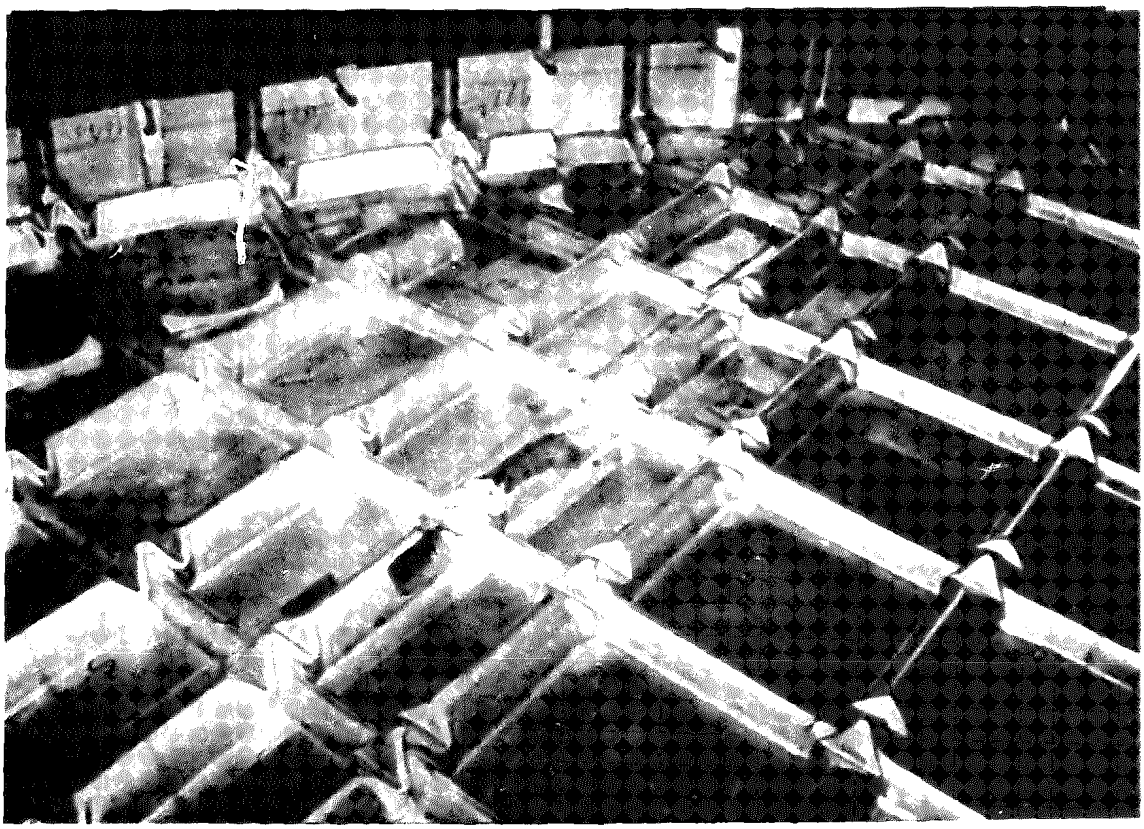

Figure 3.0-1 Waffled Membrane Liner Showing Orthogonal Corrugations

In view of these considerations, the liner and the internal insulation have been identified as the only critical components in the TES (or SRE) system in need of development. The liner identification is fairly obvious. Because the liner is designed to be flexible and transmit the thermal and pressure loads to the shell through the internal insulation, the insulation performance under loading affects liner performance, so the internal insulation is also identified as critical.

It must be emphasized that the fundamental reason the liner and internal insulation have been selected as critical is that they have not previously been used, either separately or together, in a molten salt application. Based on 16 years of Technigaz experience with LNG liners and the thousands of hours of Martin Marietta materials test data in hot salt environments, we are confident this approach is technically sound.

The development programs described in the following subsections were used to resolve all uncertainties associated with using a liner and internal insulation in a hot salt environment. This program closely parallels the LNG liner development program successfully used by Technigaz. This program consisted of three main elements--liner development (Section 3.1), insulation development (3.2), and internally insulated subassembly tests (4.0).

3.1 Liner Development

The development program began with this subtask. The objective was to determine a minimum-cost liner design with a 30-year service life in the TES. There are three possible failure modes for the liner--stress (through overpressurization or overexpansion) causing cracking or corrugation collapse, fatigue (through overexposure to cyclic pressure loadings) causing cracks, and corrosion (through overexposure to hot salt) causing weakness, cracks or holes.

By design, the only liner areas that are stressed are the corrugations and their intersections (knots). Crack propagation in the liner is essentially limited to these areas. Corrosion can, however, occur anywhere, including the welded joints between liner panels, and can be accelerated in the presence of stress.

Any one (or combination) of these failure modes may ultimately lead to a leak in the liner; thus the conditions under which these failures may occur must be determined in the development program. The liner is designed to stay well away from these failure levels. The critical environmental factors that affect these conditions and that therefore drive the liner design are (1) chemical composition of storage fluid and its corrosion potential, (2) temperature of storage fluid, (3) maximum pressure of storage fluid, (4) number of loading/unloading cycles and service life requirements, (5) temperature difference between liner and steel shell, (6) thermal expansion and structural resistance of the internal insulation and pressure vessel, and (7) abrasion of liner against internal insulation.

One of these factors, number of loading/unloading cycles, is substantially less in the TES application than in an LNG application (approximately 50,000 for the former versus up to 60,000,000 for the latter). Another factor, maximum pressure, is similar for the two applications. The remaining factors are generally more severe in the TES application than in the LNG application.

Incoloy 800 was selected as the liner material because of its good strength, corrosion, and fatigue properties in this molten salt environment. This decision was based upon thousands of hours of material test data at 566°C (1050°F) in molten salt generated under another solar energy program at Martin Marietta. The liner thickness will be 1.27 mm (0.050 in.), as Incoloy 800 sheets of this thickness can be readily formed with corrugations, the predicted peak stress levels in service are acceptable, and it is close to the customary LNG value of 1.20 mm (0.047 in.) where there is a wealth of liner experience. It is important that the liner be liquid-tight over its service life. A leak would cause salt to flow into the internal insulation and ultimately to the steel shell. If uncorrected, this would obviously cause many problems, such as high-temperature of the shell, shell corrosion, increased tank heat loss, permanent damage to the internal insulation, etc. The risk of potential leaks in the liner is reduced to the lowest possible level by leak testing every inch of every weld using an ammonia leak test method, and by extensive fatigue testing at (and above) realistic load levels. In addition, active leak detection methods will be used during solar plant operation so that if a leak should develop, the tank can be shut down and repaired. Personnel safety is provided by a dike around the tank.

3.1.1 Liner Formability

Tank liners used for LNG applications are customarily made of 304 stainless steel, which is unsuitable for use at elevated temperatures in a salt environment. Incoloy 800 has a higher yield stress, [310 MPa (45 ksi) than 304 250 MPa (36 ksi)], is available in slightly thicker sheets [1.27mm (0.050 in.) versus].20mm (0.047 in.)] and has lower elongation 45 percent versus 55 percent. Because of these dissimilarities, formability tests were conducted by Techniqaz.

The elongation of the specific batch of Incoloy 800 used on this program was 44 percent in the transverse direction and 35 percent in the longitudinal rolled direction. The coil from which the sheets were taken had been solution annealed at 1205°C (2200°F) rather than the normal 1038°C (1900°F) used for 1.3mm (0.050 in.) thick material. The higher annealing temperature generally increases elongation and decreases tensile strength. This receipt of Incoloy 800 with the higher annealing temperature was coincidence. Forming knots and angles with this material was acceptable; however, the minimum allowable elongation values are not known. Future usage of Incoloy 800 for a liner should assure that the above elongation values are met or repeat formability test when elongation values are less.

Sample knots and angle pieces (see Fig. 3.1.1-1) were formed of both Incoloy 800 and 304 stainless steel.

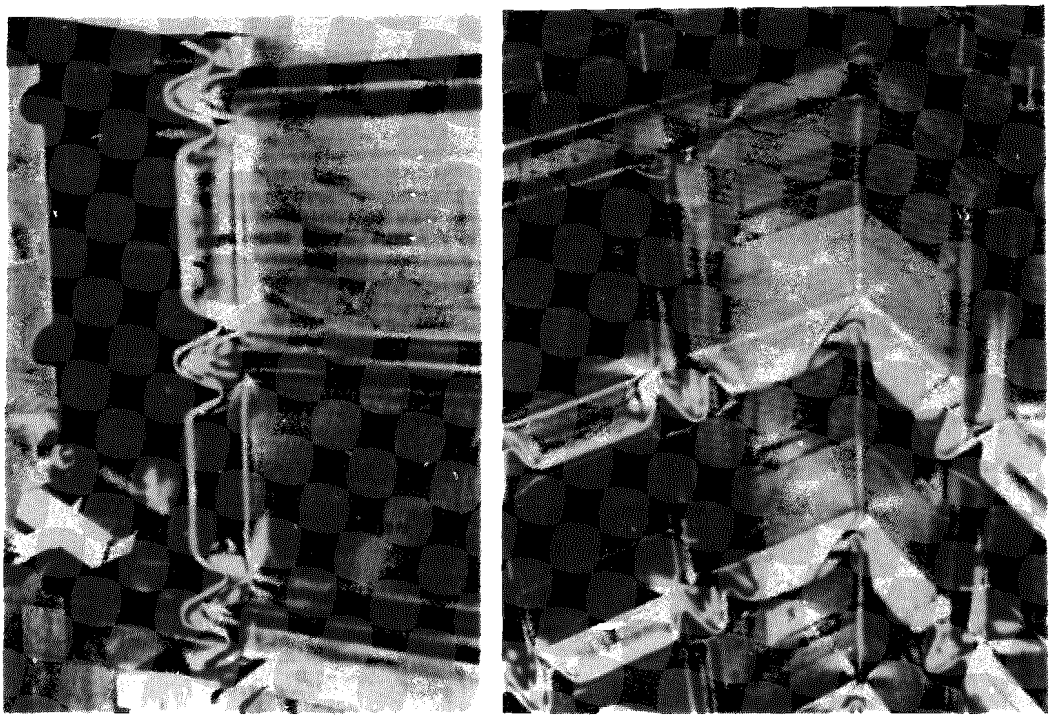

Knot Corner Piece

Figure 3.1.1-1 Liner Forming Configurations

Comparison of the profiles of the corrugations of both materials indicated very close correlation, with both showing slight variation from the theoretical profile. Measurement did show a springback condition in the Incoloy 800 as shown in Figure 3.1.1-2.

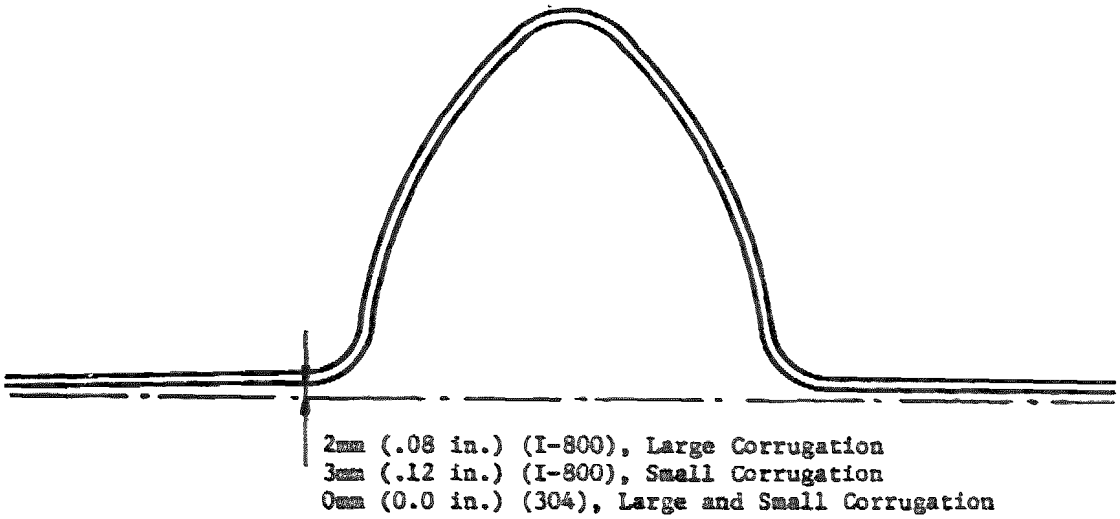

Fig. 3.1.1-2 Corrugation Profile Comparison

This degree of springback in the I-800 causes no problems in installation of the liner or performance of the tank, so no effort was made to eliminate it.

An analysis of the residual ferrite content was made on I800 samples in order to determine cold working effects. Residual ferrite content remained at a constant 0.05% for sheets before forming, after forming a knot, and in a knot after fatigue cycling had been performed.

Vickers hardness measurements were taken in the smaller radius I-800 liner knots and angle pieces to get an estimate of the cold work taking place. The values of these measurements and the % change due to cold working are given in Table 3.1.1-1. These values compare very favorably with estimated values for 304 stainless steel and are no cause for concern when compared to an acceptable value of 35%.

Table 3.1.1-1 Cold Working Estimate for I-800

		Hardness (Vickers)	Cold Reduction (Percent)
Knot	Min	176	6
	Max	236	17
Angle	Min	180	7
	Max	255	22

3.1.2 Liner Corrosion Testing

The corrosion question has already been pursued in other DOE-sponsored programs conducted by Martin Marietta and Sandia. Results of the ACR Phase II material compatibility tests provided a basis for selection of Incoloy 800 as the primary liner material candidate, since it underwent minimal corrosive degradation during long term high-temperature service up to 580°C (1075°F).

3.1.3 Liner Stress Testing

A buckling test of liner corrugations and knots was performed on 1.20 mm (0.047 in.) thick 304 stainless steel. Although this testing was not performed under this contract, the results are presented because it supports the selection of the liner design parameters. Strain gauges were placed on the top and side of the large corrugation as shown in Figure 3.1.3-1. The small corrugation had strain gauges placed on each side.

Figure 3.1.3-1 Strain Gauges Installed on Large Corrugation

The testing took place at room temperature with static pressure on the membrane being gradually increased to 1.96 MPa (280 psi). The panel began to collapse at the large corrugation at approximately 0.39 MPa (56 psi). The small corrugation maintained structural integrity up to 1.19 MPa (170 psi). A photograph of the buckled membrane is shown in Figure 3.1.3-2.

The thicker material used on this program will increase the buckling strength of the corrugations, but the loss of modules at elevated temperature will slightly reduce the bucking strength. A nominal design pressure of 0.3 MPa (43.5 psi) was selected, to provide a factor of safety. It should also be noted that the membrane will be backed up by the insulating firebricks and the corrugation ends will be constrained which will further enhance the membranes structural rigidity.

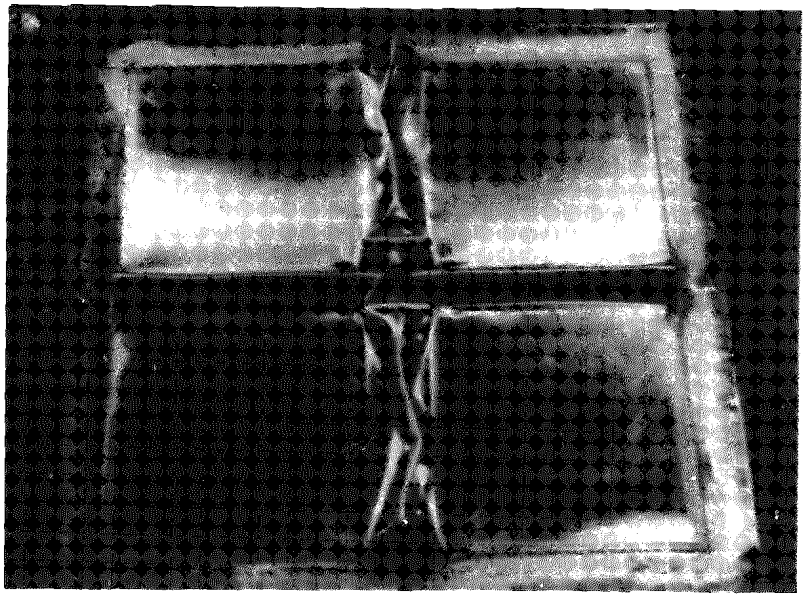

Figure 3.1.3-2 Buckled Membrane After 1.96 MPa (280 psi) Pressure

3.1.4 Liner Fatigue Testing

A number of fatigue tests were performed on liner elements. The liner is subjected to two types of fatigue loading in service; salt pressure loads due to filling and draining the tank each day and thermal expansion loads. The latter consists of small amplitude diurnal temperature variations, larger amplitude (but longer frequency) temperature variations due to variations in the weather (such as storms, clouds, etc), and finally complete tank cooldown to ambient temperature for inspection and maintenance. These variations are difficult to quantify in general since they will depend upon solar plant specifics and weather behavior. For the purposes of this study, we have adopted the following design environments:

Fluid pressure:	0-0.3 MPa (43.5 psi) once per day for 30 years
Liner thermal expansion	700-839K (800-1050°F) once per day for 30 years

The liner was tested in these fatigue environments in a series of tests of ever increasing realism. We began with a set of tests on the small elements described above. Six different kinds of tests were run:

1) Biaxial knot strain tests at room temperature.
2) Uniaxial angle piece strain tests at room temperature.
3) Knot pressure tests at room temperature.
4) Angle piece pressure tests at room temperature.
5) Biaxial knot strain tests at 566°C (1050°F).
6) Uniaxial angle piece strain tests at 566°C (1050°F).

3.1.4.1 Room Temperature Fatigue Strain Tests - Two knot samples formed from Incoloy 800 were fatigue tested under elongation. The knot material was 1.27 mm (0.050 in.) thick. Table 3.1.4.1 below shows the results of the testing and a comparison to data previously obtained by Technigaz on their 304L stainless steel LNG liners. Failure were defined as crack initiation. Crack propagation through the material often takes considerable more cycles.

Table 3.1.4-1 Knot Fatigue Test Results--Room Temperature

Material	Elongation				Number of Cycles To crack Initiation
	Small Corrugation		Large Corrugation		
	mm	in.	mm	in.	
I-800	0.86	0.034	0.86 ± 0.72	0.034 ± 0.028	91,200
	0.86 ± 0.54	0.034 ± 0.021	0.86	0.34	61,260
304L	0.86	0.034	0.86 ± 0.72	0.034 ± 0.028	77,740
	0.86 ± 0.54	0.034 ± 0.021	0.86	0.34	87,150

The fatigue life of the I-800 and 304L samples compare reasonably well and failure occurs well above the number of operating cycles anticipated.

3.1.4.2 High Temperature Fatigue Strain Tests - A fatigue strain testing machine was adapted to permit radiant heating by electrical heaters up to 566°C (1050°F). Three knot samples were tested at this temperature, under simultaneous compression along two axis, using different strain levels for each sample. The test procedure used was;

- o heat sample to 566°C (1050°F)
- o cycle under maintained temperature
- o Visual inspection at regular intervals until appearance of first crack

The results of the knot tests are shown in Table 3.1.4-2 and the location of the cracks are depicted in Figure 3.1.4-1.

Table 3.1.4-2 Knot Fatigue Strain Test Results - High Temperature

Corrugation	Elongation Min mm.(in.)	Elongation Max mm.(in.)	Amplitude Elongation mm. (in.)	Crack Location	Freq	Number of Cycles	Remarks
Large	0	1.94 (0.076)	1.94 (0.076)	I	6 Hz	91,000	Four Through Cracks
Small	0	1.37 (0.054)	1.37 (0.054)				One on the top of the knot
Large	0.54 (0.021)	1.94 (0.076)	1.4 (0.055)	II	5 Hz	101,000	No Through Crack
Small	0.38 (0.015)	1.37 (0.054)	0.99 (0.038)				One Crack
Large	0	2.5 (0.098)	2.5 (0.098)	IV	4 Hz	10,000	One Crack on the Top of the Knot
Small	0	1.76 (0.069)	1.76 (0.069)				

Similar testing as was performed on the knots was also performed on liner angle pieces using the same heating procedure, identical strain levels and the same number of elements. The tests were performed under compression along a single axis in the direction of the edge of the angle piece. The results of this test are given in Table 3.1.4-3 and the location of the cracks are illustrated in Figure 3.1.4-2.

Table 3.1.4-3 Angle Piece Fatigue Strain Test Results

Elongation Minimum mm.(in.)	Elongation Maximum mm.(in.)	Amplitude Elongation mm.(in.)	Crack Location	Freq	Number of Cycles	Remarks
0	1.37 (0.054)	1.37 (0.054)	I	10 Hz	189,000	Two Through Cracks
0.38 (0.015)	1.37 (0.054)	0.99 (0.039)		10 Hz	stop at 600,000	No Cracks
0	1.76 (0.069)	1.76 (0.069)	IV	10 Hz	87,000	Two Through Cracks

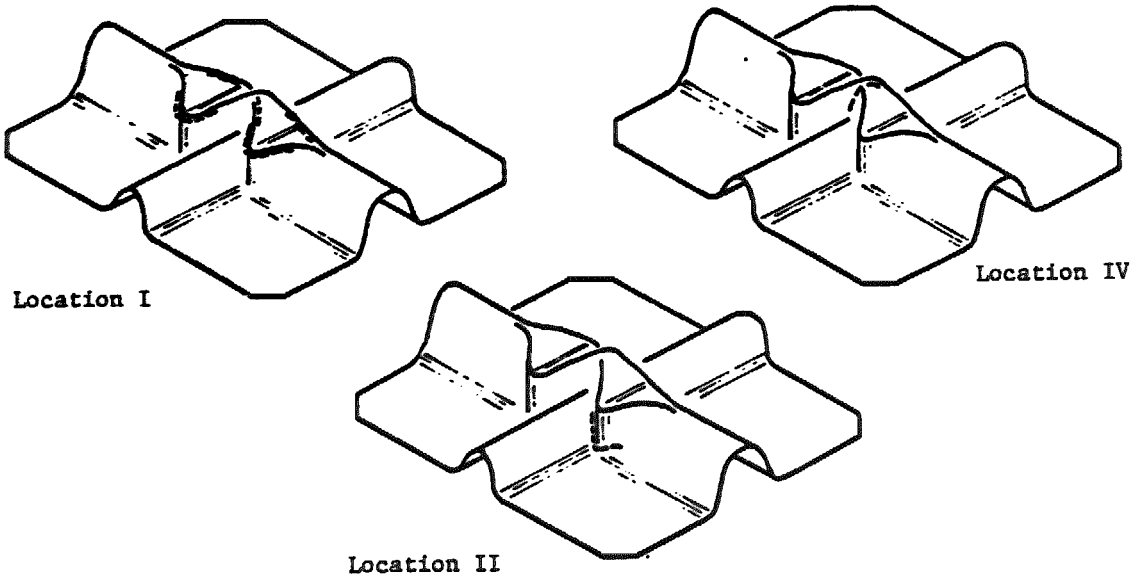

Figure 3.1.4-1 Knot Fatigue Failure Locations

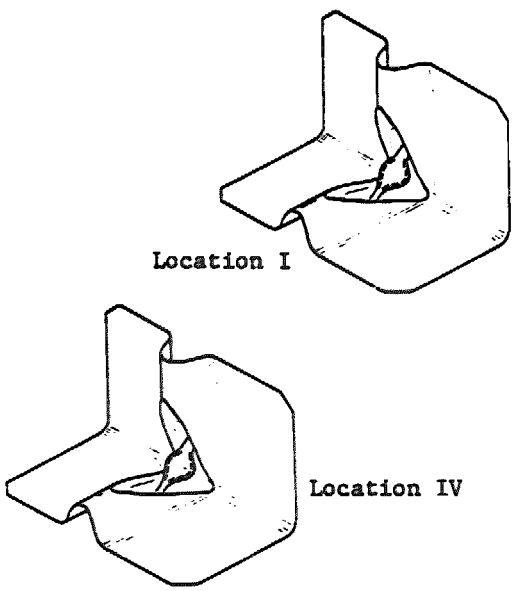

Figure 3.1.4-2
Angle Piece Fatigue Failure Locations

Fatigue testing performed at room temperature correlates very well with tests run at elevated temperatures. This indicates there is no appreciable effect of high-temperature on the fatigue behavior of the liner elements.

It is realized that the creep-fatigue failure of the liner elements were not tested. Due to the complexity of the shape an analytical evaluation can not be performed. The large margin in fatigue life above the required life gives confidence that a 30-year life of the liner is possible. An evaluation of the creep-fatigue life is addressed in Appendix I. The history of one high-temperature application of the liner showed no problem attributed to creep.

3.1.4.3 Room Temperature Pressure Tests of Liner Elements

The purpose of these tests was to evaluate the fatigue behavior of Incoloy 800 liner elements under cyclic pressure. The maximum pressure the elements would experience in regular service would be 0.224 MPa (32 psi) and the number of pressure cycles approximately 11,000. Under test the elements were subjected to cyclical pressure between 0 and 0.3 MPa (44 psi) at room temperature for a maximum of 150,000 cycles. To investigate the effect of installation inaccuracies a discontinuity of 2mm (0.8 in.) and 4mm (.16 in.) was purposely maintained in the back-up support for selected elements.

The tests were not performed at elevated temperatures because the liner and the attendant insulating brick structure would be tested in this manner in the 1 cubic meter test.

To run the test, two samples are installed at the same time in a testing chamber filled with water. The cyclic pressure is applied on the corrugated side by means of a water piston actuated by a hydraulic jack which is controlled by a servo loop.

The samples were installed and tightly welded (the welds were submitted to the ammonia test) on a support, and holes were drilled under each sample. A crack through is detected and cycling is stopped as soon as a water flow is detected.

After the completion of the tests, a dye check is carried out on all the samples to find eventual nonpenetrating cracks.

The results of the knot element pressure testing is shown in Table 3.1.4-4 and the crack locations in Figure 3.1.4-3. The same data for angle piece elements is given in Table 3.1.4-5 and Figure 3.1.4-4.

Table 3.1.4-4 Knot Pressure Test Results

Number of Samples	Pressure Level	Sample Installation	Number of Cycles	Remarks
2	0 - 0.3 MPa (0 - 44 psi)	applied directly on a flat support 	test stopped at 150 000 cycles	no leak no crack
1	0 - 0.3 MPa (0 - 44 psi)	installed with a 1 mm gap from the flat support 	test stopped at 150 000 cycles	no leak no crack
1	0 - 0.3 MPa (0 - 44 psi)	installed with a gap of 2mm from the flat support 	test stopped at 150 000 cycles	no leak no crack
1	0 - 0.3 MPa (0 - 44 psi)	installed with a gap of 2 mm from the flat support  The gap is maintained by a 2mm thick gauge installed under one of the four feet, during all the test	107 000 cycles	one leak one through crack
1	0 - 0.3 MPa (0 - 44 psi)	Installed with a gap of 4mm, maintained by a 4mm gauge put under one of the four feet, during all the test 	34 000 cycles	leak 6 cracks

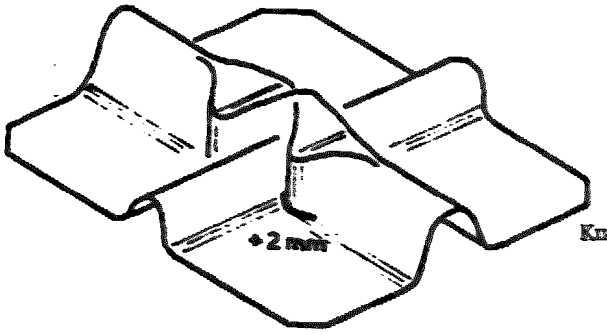

Knot with 2 mm Gage

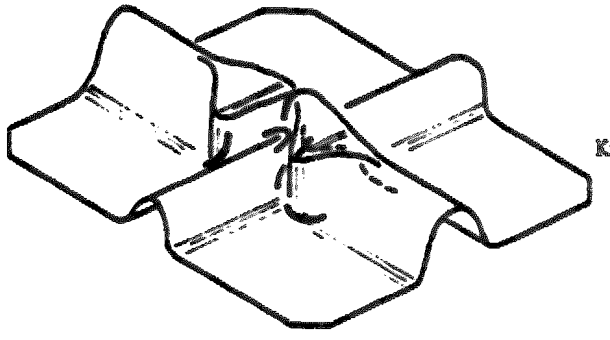

Knot with 4 mm Gage

Figure 3.1.4-3 Knot Pressure Test Failure Locations

Table 3.1.4-5 Angle Piece Pressure Test Results

Number of Samples	Pressure Level	Sample Installation	Number of Cycles	Remarks
2	0 - 0.3MPa (0 - 44 psi)	applied directly on the flat support 	test stopped at 150 000 cycles	no leak one non-penetrating leak
1	0 - 0.3MPa (0 - 44 psi)	installed with a 1mm gap from the flat support 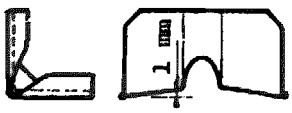	test stopped at 150 000 cycles	no leak no crack
1	0 - 0.3MPa (0 - 44 psi)	installed with a 2mm gap from the flat support 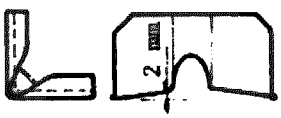	test stopped at 150 000 cycles	no leak one non-penetrating crack
2	0 - 0.3MPa (0 - 44 psi)	installed with gaps of 2mm and 4mm at the same time. Gap maintained during all the tests by means of gauges welded on the support 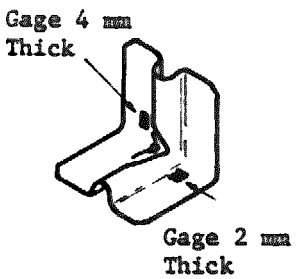	test stopped at 150 000 cycles	no leak one time crack beginning on one of the two samples

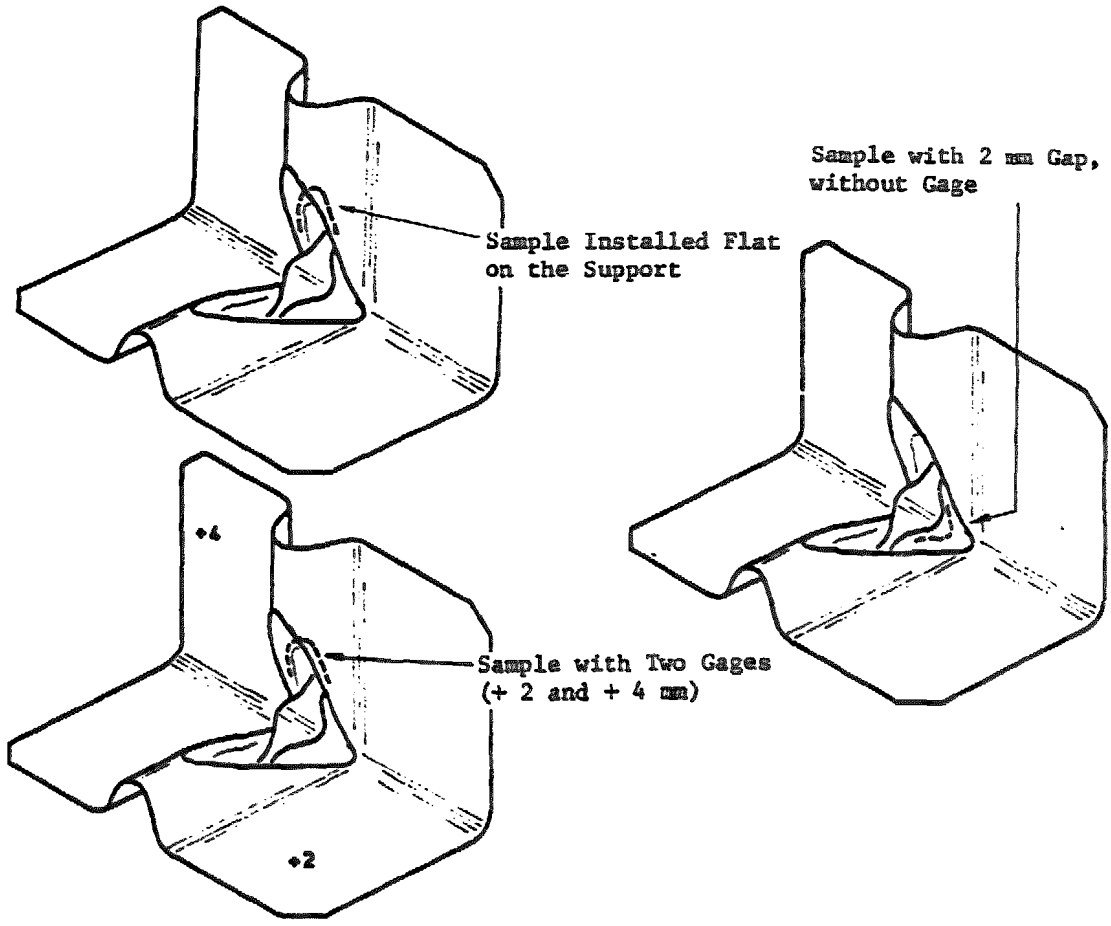

Figure 3.1.4-4 Angle Piece Pressure Test Failure Locations

The results of the strain tests on the knots are shown in Figure 3.1.4-5. It can be seen that the fatigue life of the knot is well above the required values. The elevated temperature strain tests gave essentially the same results. The pressure tests were all conducted at 0.3 MPa (43.5 psi) maximum load, and variations in manufacturing tolerances on the wall smoothness were simulated. It was found that there were no through cracks in any of the elements after 150,000 cycles of testing for reasonably smooth walls. An abrupt discontinuity of 2 and 4 mm under one of the feet of a knot reduced the fatigue life to 107,000 and 34,000 cycles respectively. The fatigue testing of liner elements has shown that the liner should withstand the design loads for a number of cycles that far exceeds the requirements for a hot tank at a solar plant.

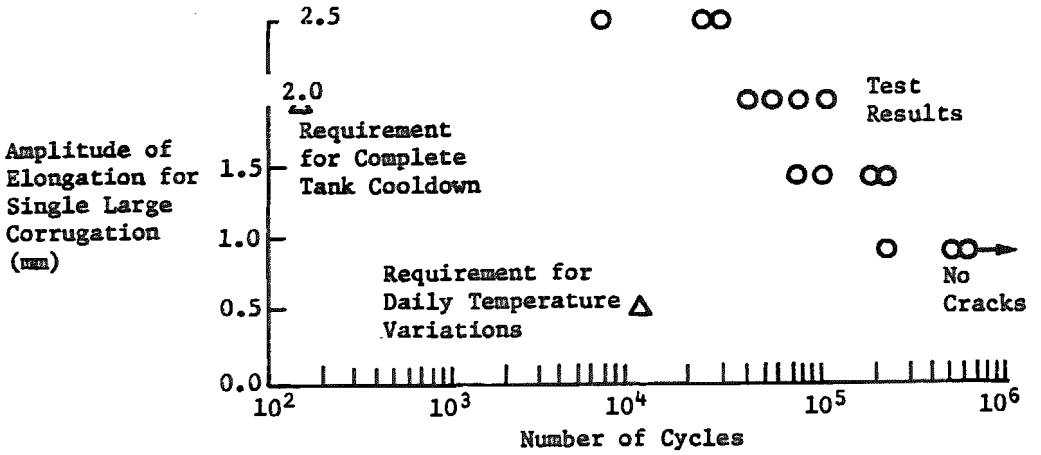

Figure 3.1.4-5 Knot Fatigue Test Results

3.1.5 Liner Welding Technique and Requirements

Another key element in the acceptability of Incoloy 800 as the molten salt storage tank liner is its weldability. Technigaz has 17 years experience welding 304 stainless steel liners for LNG applications. They were therefore selected to establish welding techniques and requirements for I-800. The resulting requirements are set forth in Technigaz report 11,258,20 CZ/CM, dated Feb. 12, 1981, titled Instructions For Welding of Membrane Tanks Made of Incoloy 800. The process set forth, requires use of the tungsten electrode inert gas process using direct current. The inert gas specified is 99.99% pure Argon containing less than 10 ppm water or oxygen. Gas flow rates, values for current and welding rates are specified for various types of welds.

Performance of the welding of the liner was entrusted only to qualified welders. These welders were checked periodically in accordance with procedures set forth in the above mentioned report. Each welder was required to have a welder registration book which the contractor regularly updated as to the types of weld for which qualification was granted.

Included in the report is a list of approved manual and automatic welding equipment, and approved electrode and filler material.

The effect of welding on the corrosion rates of Incoloy 800 was evaluated under the ARC Phase II contract. It was found that the welded area had a slight increase of corrosion rate as compared to an unwelded section. The tensile strength of welded specimens were almost identical to parent material after exposure to molten salt at 580°C (1075°F) throughout the test period of 10,000 hours. The welding of the liner is outside the high stress area of the knots. Thus the welding is not considered to have an effect on liner life.

3.1.6 Leak Detection of Molten Salts Through Internal Liner

An important issue in the integrity of the molten salt storage tank is elimination of salt leaks. Analysis and testing was performed to determine molten salt flow rates under pressure and at maximum operating temperature (566°C (1050°F)).

It is possible to determine the critical hole size (the smallest hole through which molten salts can pass) in the liner based on the capillarity theory. The formula used is:

$$D = \frac{4A \cos\Theta}{P}$$

where: D = diameter of the hole in meters
A = surface tension of the liquid Newton/Meter
Θ = Angle formed by the liquid and the solid surface
P = pressure in Pascals

For molten salts:

$A = 115 \times 10^{-3}$ N/m

$\cos\Theta = 1$

and $P_{max} = 3 \times 10^{5}$ Pascals (0.3 MPa)

therefore: $D_{critical} = 1.5 \times 10^{-6}$ m

This hole size is smaller than the minimum size of crack through the Incoloy 800 liner material, which means that cracks in the internal liner can be detected by leakage of the molten salts.

Tests were run to determine molten salt flow rate under variable pressure through holes of varying surface area when at the maximum service temperature of 566°C (1050°F). The testing apparatus is shown in Figure 3.1.6-1

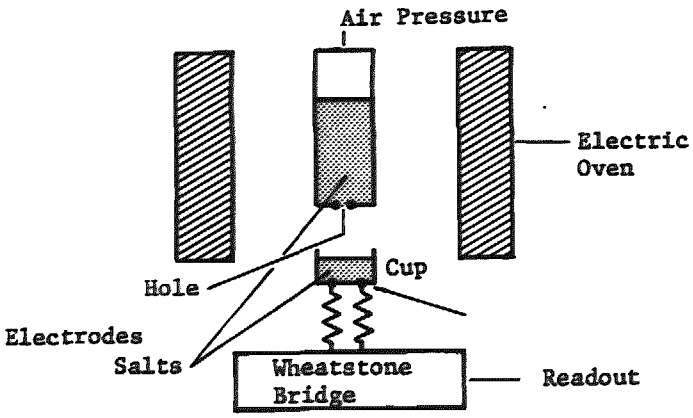

Figure 3.1.6-1
Molten Salt Leak Detection Apparatus

The molten salt passing through the hole in the liner material is collected in a small cup. The molten salt collected in the cup establishes an electric current between the two attached electrodes.

The results of the testing performed is shown in Figure 3.1.6-2. For the smallest hole tested, (surface area of 0.014 in.^{2} [1 x 10^{-5} m^2]) it has been verified that quick detection is easily accomplished using an ammonia gas procedure (described in more detail in Section 5.)

Several methods of detecting salt leakage through the liner into the brick are possible.

a) Temperature measurement on the tank shell will indicate a gradual increase as the brick thermal conductance is increase due to their being saturated with molten salt.

b) Infrared scanning of the tank sheathing will detect any sheathing temperature increase which results from an increase shell temperature.

c) Measurement of the electrical resistance of parallel wires can detect leaks. Molten salt is electrically conductive; thus insulated parallel wires (i.e. woven glass insulated thermocouple wire) will change from an open circuit to some measurable conductance when saturated with molten salt.

None of these methods give a quick localized detection of a leak. The electrical resistance change of wires can occur at any point along the wires. Testing this concept is necessary to determine its accuracy. Relying upon the temperature measurements of the shell or sheeting will detect a leak only when several square feet of brick have been saturated with molten salt. However this is adequate to detect leakage which could cause a rupture of the tank shell.

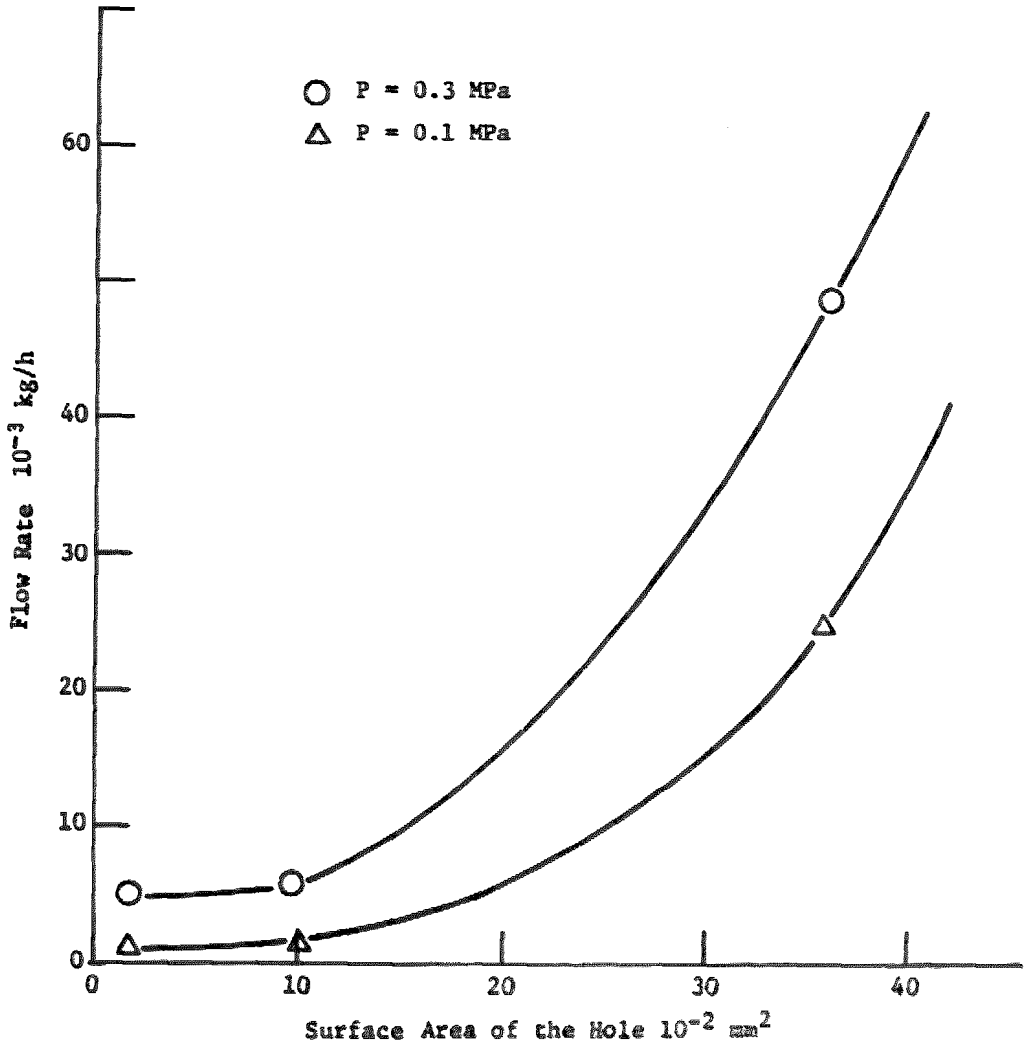

Figure 3.1.6-2 Flow Rate of Molten Salt Through a Hole

3.2 INTERNAL INSULATION

Extensive testing was performed on internal insulation material candidates. Seven different insulating firebrick materials underwent various phases of molten salt compatibility and compressive strength testing between June, 1980 and May, 1981. The three phases of testing included:

- Molten salt compatibility test with samples immersed in molten salt at 566°C (1050°F).

- Wet crush test with samples immersed in molten salt at 566°C (1050°F) and under a constant compressive load of 0.24 MPa (35 psi)

- Dry crush test with samples kept at a temperature of 566°C (1050°F) and under a constant compressive load of 1.05 MPa (150 psi).

The results of the molten salt compatibility testing phase is given in Table 3.2-1. Upon completion of this phase of testing Johns-Manville firebrick materials JM 25 and JM C22ZSL showed the least degradation in the molten salt environment.

Table 3.2-1 Molter Salt Compatibility Test Results

Material	First Indication of Degradation After Start of Test (Months)	Appearance	Total Test Period (Months)	Final Appearance
JM 20SL	3	Some Cracks, No Swelling	11	Same as Month 3
JM C22ZSL	-	-	7	No Apparent Change
JM 23SL	3	Some Cracks, Some Corners Gone	11	Same as month 3
JM 25	-	-	9	No Apparent Change
JM 28	3	Some Cracks, Some Corners Gone	11	Same as month 3
Krilite 26	3	Many Cracks, Swollen	11	More Cracks, Swollen Worse
Krilite 55	1	Swollen	9	Many Cracks, Very Swollen

The wet crush test was initiated two months after the start of the compatibility testing and was run concurrently. Weights were placed on each sample in the oven to provide a constant load of 0.24 MPa (35 psi) at 566°C (1050°F). The results of this test is given in Table 3.2-2. Inspection of the firebrick samples, upon completion of the test, indicated that JM 25 and JM C22ZSL best maintained their structural integrity.

Table 3.2-2 Wet Crush Test Results

Material	Test Period (months)	Observations
JM20SL	1/2	Corner fracture
JMC22ZSL	6	No obvious cracks
JM 23SL	1	Cracked, possible fracture
JM 25	2 1/4	No obvious cracks
JM 28	1 1/4	Few Slight cracks
Krilite 26	1	Cracked and swollen; fell apart
Krilite 55	1 1/4	Fractured into many pieces

Based on the results of the compatibility and wet crush testing, four leading material candidates were selected to undergo a high temperature, high load crush test in a dry environment. Samples of JM C22ZSL, JM 23SL, JM 25 and JM 28 were placed on each sample to provide a constant 1.05 MPa (150 psi) load. The JM 23SL sample crushed into powder within one to two minutes after start of the test. Three days later the JM 25 sample was found in the same condition. The other two samples remained in the oven under load for 6 1/2 months. Upon removal from the oven it was found that the JM 28 sample had fractured all the way through but had not crushed. The JM C22ZSL sample, however, showed no cracks or fractures, although it had experienced a small amount of permanent deformation. The result of this preliminary test phase clearly indicated that JM C22ZSL insulating firebrick was the best material. Consequently, this material was selected to undergo additional testing under the direction of Technigaz personnel.

3.2.1 Compressive Tests

Ambient tests were performed on a Houndsfield Laboratory machine and high-temperature tests on an Instron Machine with an oven adapted to it. A stress strain curve was recorded for each sample and compressive strength was determined from the first abrupt slope change in the curve (see Fig. 3.2.1-1). Samples were 40 mm (1.57 in.) cubes and three from each of 10 bricks were tested at ambient and at high-temperature to determine compressive strength along each axis. The detailed results of all firebrick tests are included in Appendix B. It has been concluded from these tests that compressive strength does not vary with axis direction and is also unaffected by increased temperature. The minimum compressive strength of any sample in the test was 1.6 MPa (232 psi) which is more than five times the strength required for this application.

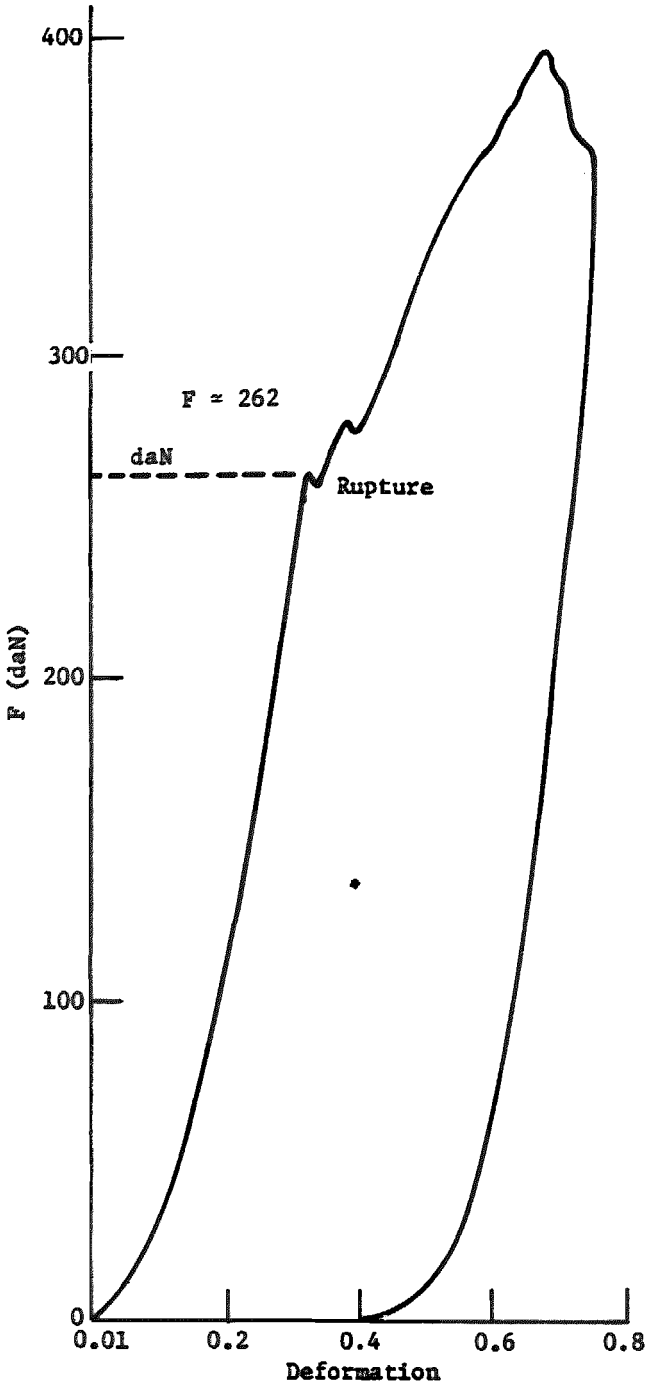

Figure 3.2.1-1 Compressive Stress Strain Curve For JM C22ZSL Brick

3.2.2 Compressive Strength Test Under Thermal Cycling

Samples of 40 mm (1.57 in.) cubes were cut from 6 bricks and tested for compressive strength under thermal cycling. A thermal cycle consisted of raising the temperature 250°C (482°F)/hour up to 566°C (1050°F), maintaining temperature there for two hours and then cooling back down to ambient temperature. The compressive strength of the specimens was then checked at ambient temperature after 3, 6, 9, and 12 cycles, in order to compare to the compressive strength of reference specimens. Load was always applied along the same axis for all specimens. Results of the testing showed no degradation of compressive strength due to thermal cycling. (See Appendix B for detailed data.)

3.2.3 Flexure Testing

Flexural testing on JM C22ZSL was performed on a Shenck Trebel machine (5% accuracy) which was adapted to permit high-temperature tests. Specimens were 225 mm (8.86 in.) long with 25 mm (1 in.) square cross sections. Each specimen was loaded as shown in Figure 3.2.3-1. Half of the specimens were tested at ambient temperature and the other half at 566°C (1050°F). Taking into account average values, the maximum bending strength of the material is 0.85 MPa (123 psi) at room temperature and 1.14 MPa (164 psi) at elevated temperature. Both are well above anticipated bending stress levels. (See Appendix B for detailed data.)

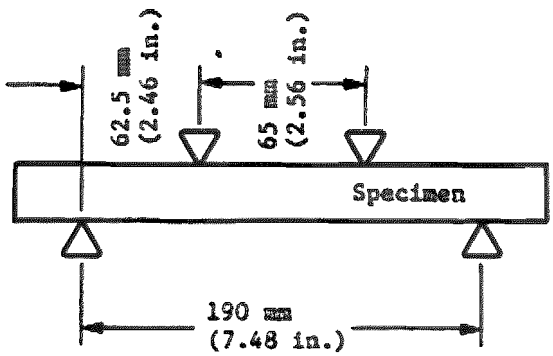

Figure 3.2.3-1 Specimen-Loading Arrangement

3.2.4 Fatigue Testing

Fatigue testing on the firebrick samples was performed at 566°C (1050°F). Tests of 50 mm (1.96 in.) cubic samples were performed on a Shenck Trebel machine adapted for high-temperature testing at a cyclic frequency of 3hz. During the test, deflection was continuously monitored and at regular intervals the stress/strain curve between 0 and

the selected maximum pressure was checked to verify that the specimen had not been damaged. Specimens were subjected to cyclical pressures of 0.3 MPa (43.5 psi) for 150,000 cycles with only 1 failure at 147,000 cycles.

The remaining samples were then tested at 0.45 MPa (65.3 psi) and reached over 400,000 cycles without rupture. The anticipated number of cycles expected in normal operation for 30-year service life is approximately 11,000, well below the tested values.

3.2.5 JM C22ZSL Testing Summary

- The average compression strength was 2.5MPa (363 psi) with a standard deviation of 0.7MPa (102 psi) at room temperature, and 2.4MPa (348 psi) and 0.4MPa (58 psi) at 566°C (1050°F) respectively.

- There was no significant effect of direction, temperature or thermal cycles on compressive strength.

- The brick was undamaged after 145,000 cycles of compressive fatigue testing at applied load levels of 0-0.3 MPa (43.5 psi) or 0-.45 MPa (65.3 psi) at 566°C (1050°F), and several samples survived over 500,000 cycles.

- Brick at 566°C (1050°F) withstood a constant load of 1.0 MPa (150 psi) for 6 months without breaking.

Samples of this brick were also immersed in molten salt at 566°C (1050°F) for 6 months without any catastrophic damage due to chemical attack. These results give confidence that this brick is more than adequate to withstand the loads imposed in this application.

The vendor does not determine the physical properties of his product for each batch. The vendor's published data are considered to be of average value. The variation of brick properties between batches is not known, because there is no batch control by the vendor. The C222SL brick has a large margin, so variation between batches would not cause a failure. It may be desirable to do some spot testing in commercial applications in the future.

4.0 One Cubic Meter Test

4.0 ONE CUBIC METER HOT TANK TEST

4.1 PURPOSE OF THE TEST

The purpose of the test was to evaluate the fatigue life of the insulated structure under cyclic pressure, in a hot 566°C (1050°F) molten salt pressurized environment. The test consists of 19,000 cycles from 0.0 to 0.3 MPa (43.5 psi).

The tested structure used liner material, insulating material and design identical to the TES, including a typical corner section. The pressure applied during the cyclic test corresponds to the TES commercial size hot tank service conditions for 30 years. The testing included the effects of fatigue and high temperature on the liner but did not simulate the effects of creep or creep-fatigue interactions. The test also demonstrated the interaction of the liner with the rest of the tank.

In addition to the cyclic test, the subassembly tests included the following:

- Evaluation of construction methods of the insulating structure: brick and liner (welding)
- Use of weld leak check technique with ammonia
- Use of proposed operational electrical leak check technique
- Demonstration of tank liner repair

4.2 TEST SYSTEM DESCRIPTION

4.2.1 Test Article Assembly

A cross section of the test tank is shown in Figure 4.2.1-1. The internal volume of the tank (location of Incoloy 800 liner) is $1 m^3$. The Incoloy 800 liner is the same design (i.e., thickness and corrugations) as the TES design. The internal insulation material (JM C22ZSL) and thickness [0.34 m (13.4 in.)] is also the same as in the TES. The stiffened carbon steel tank was designed to withstand 0.5 MPa (73 psi) at 288°C (550°F). The cover consists of a stiffened carbon steel structure with a 0.6 m (23.6 in.) diameter 316 stainless steel heater enclosure welded into the center. The heater enclosure is immersed in Partherm 430 salt. The 25 thermocouple locations are also shown in Figure 4.2.1-1.

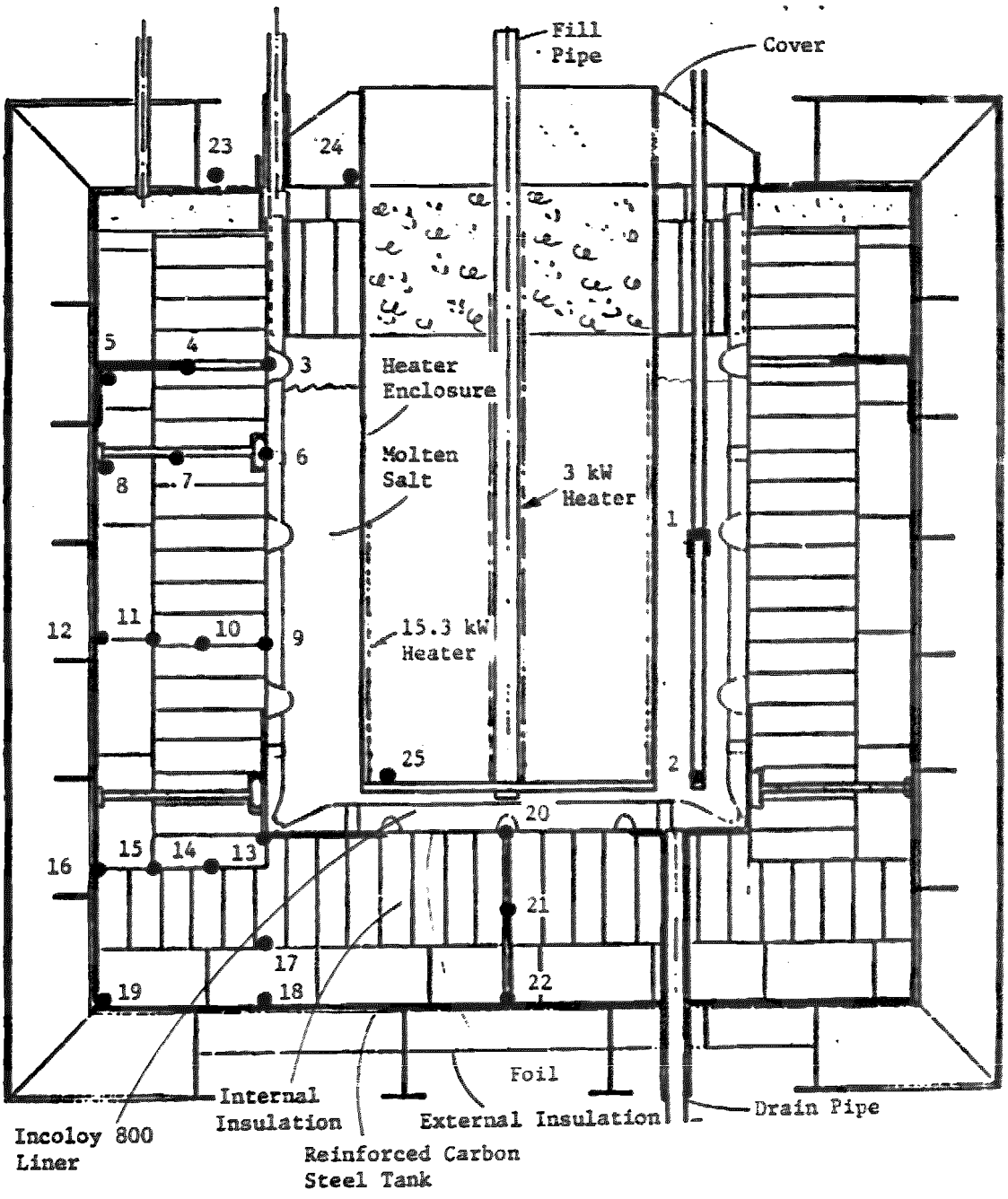

Figure 4.2.1-1 One Cubic Meter Test Tank and Thermocouple Locations

The salt heater and tank lid assembly is shown in Figure 4.2.1-2. The stiffened carbon steel tank without the external insulation is shown in Figure 4.2.1-3. The heater and tank lid assembly can be seen in the foreground.

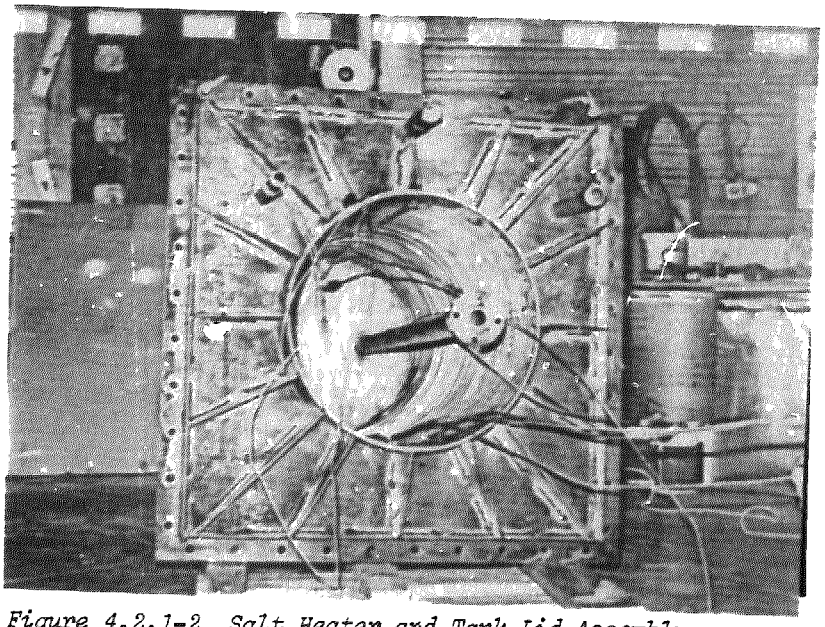

Figure 4.2.1-2 Salt Heater and Tank Lid Assembly

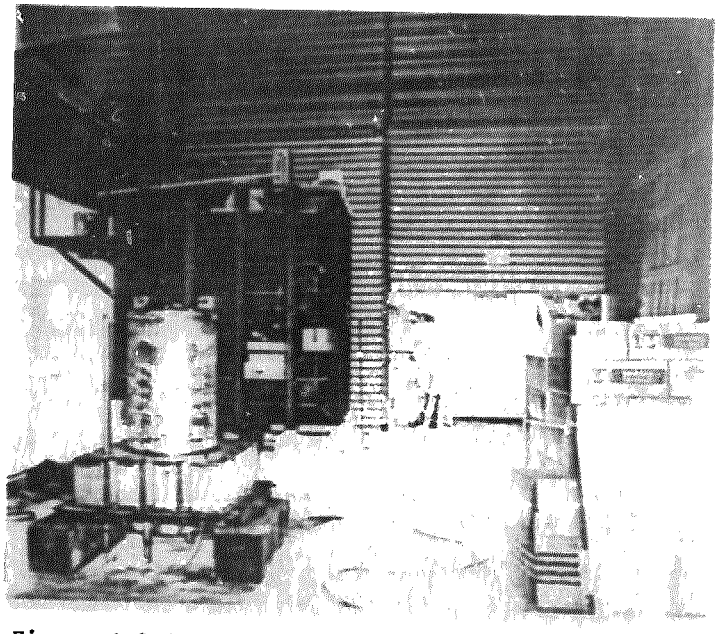

Figure 4.2.1-3 Carbon Steel Tank

The tank interior was prepared for installation of the insulating brick and thermal expansion liner. The internal tank details including the brick shelves and anchor nuts are shown in Figure 4.2.1-4. The brick insulation on the floor is shown in Figure 4.2.1-5.

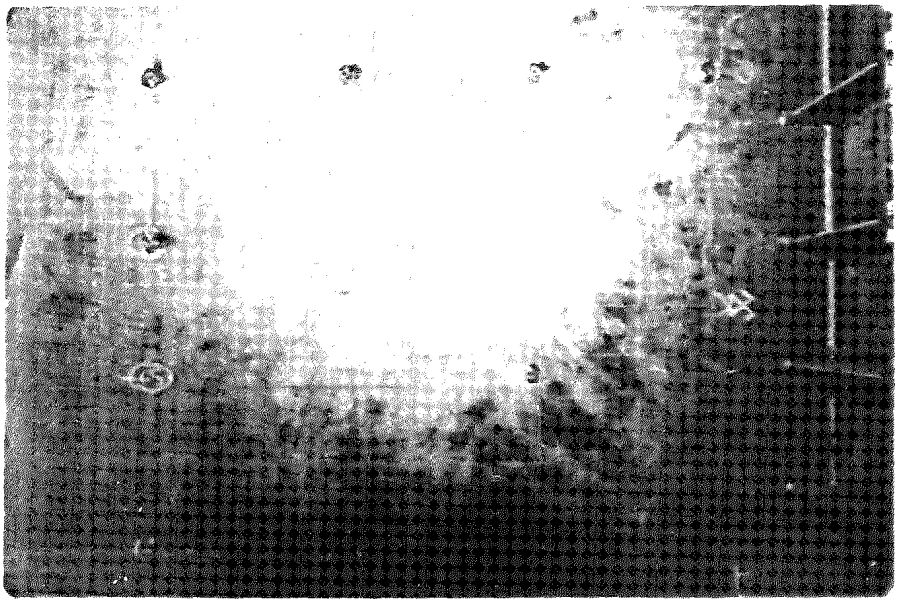

Figure 4.2.1-4 Internal Tank Details

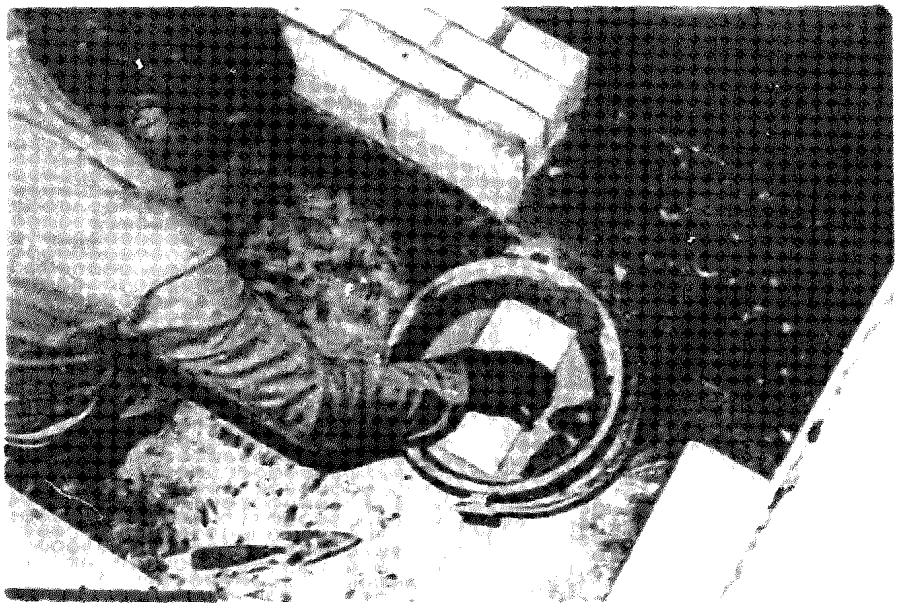

Figure 4.2.1-5 Brick Installation on Tank Floor

The entire interior surface of the carbon steel tank was lined with JM C22ZSL brick, using the shelves shown in Figure 4.2.1-4 to support the bricks. Care was exercised to locate the liner support anchor bolts in mortar joints. Two layers of brick were utilized in the assembly. The outer layer was installed vertically and an inner layer was placed horizontally. Figure 4.2.1-6 shows the assembly partially completed. Two anchor bolts can be seen at the top of the wall and the expansion joint in the middle of the wall.

Figure 4.2.1-6
Partially Completed Insulating Firebrick Installation

Heavy angle pieces were installed at all wall intersections for reinforcing to minimize cyclic angular deformation of the liner angle pieces. Figure 4.2.1-7 shows the tank interior after most of the heavy angle pieces have been installed. Each angle piece is held in place by an anchor bolt.

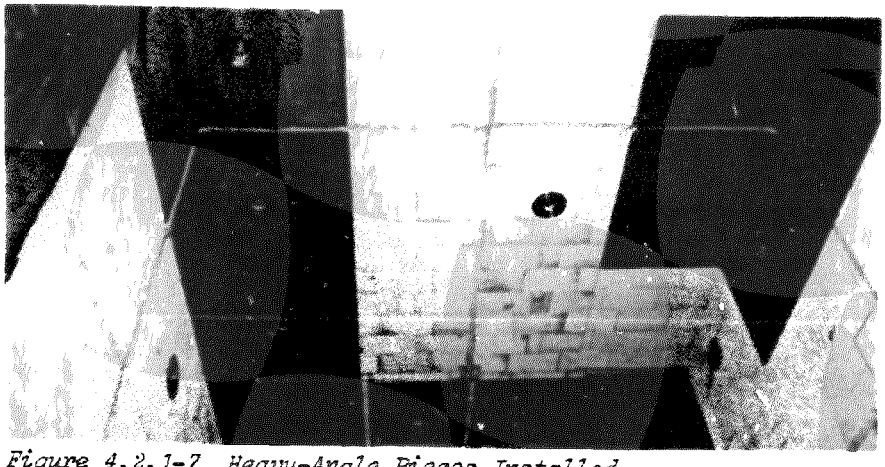

Figure 4.2.1-7 Heavy-Angle Pieces Installed

One concern of the proposed design was wear of the internal Incoloy 800 expansion liner due to abrasion by the firebrick during thermal expansion cycles. To eliminate this concern, the entire bricked surface was covered with a stainless steel foil as shown in Figure 4.2.1-8.

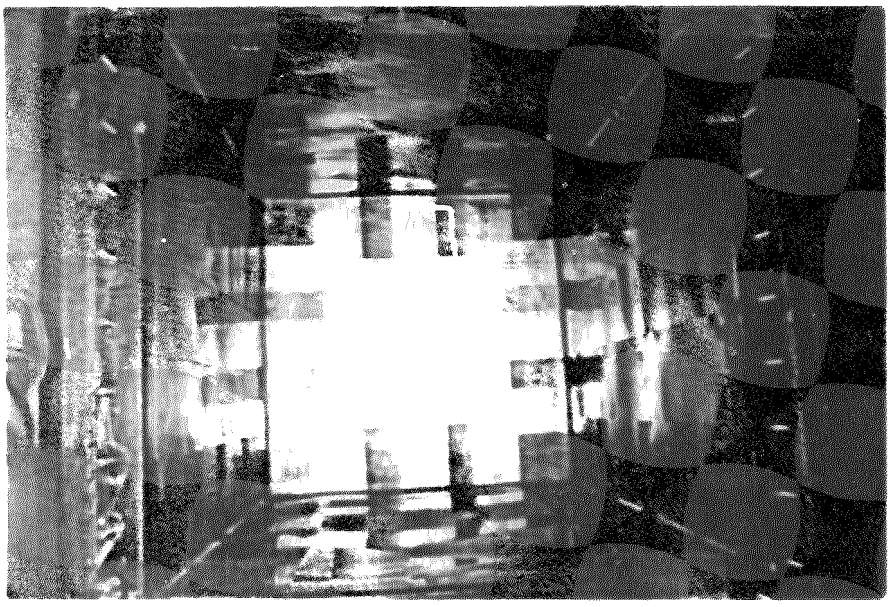

Figure 4.2.1-8 Completed Foil Installation

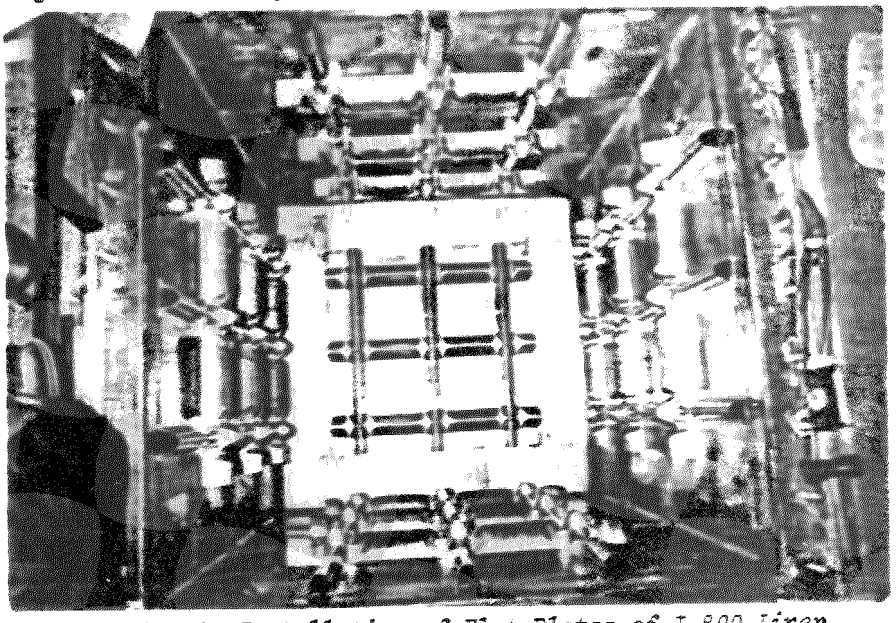

Figure 4.2.1-9 Installation of Flat Plates of I-800 Liner

Upon completion of the foil installation, large flat sheets of the Incoloy 800 liner were put in place as shown in Figure 4.2.1-9. The specially formed corrugations in these panels are designed to permit thermal expansion and contraction cycling with minimum stress concentration in the liner. An anchor point for the heavy angle pieces, the foil and the I-800 liner is shown in Figure 4.2.1-10.

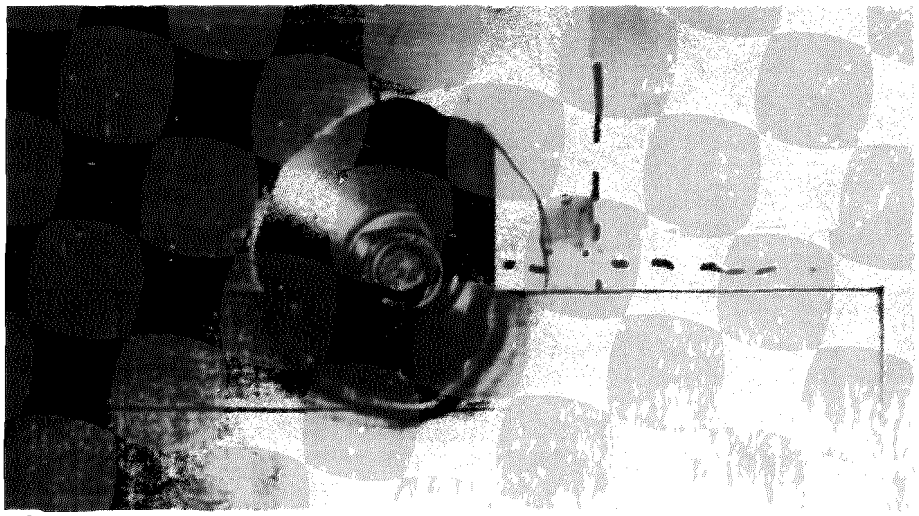

Figure 4.2.1-10 Anchor Point

Once the flat liner panels were in place, the corners of the tank were covered using corrugated angle pieces. All overlapping liner segments were welded in place to provide a totally leakproof liner assembly. Figure 4.2.1-11 shows the completed liner installation.

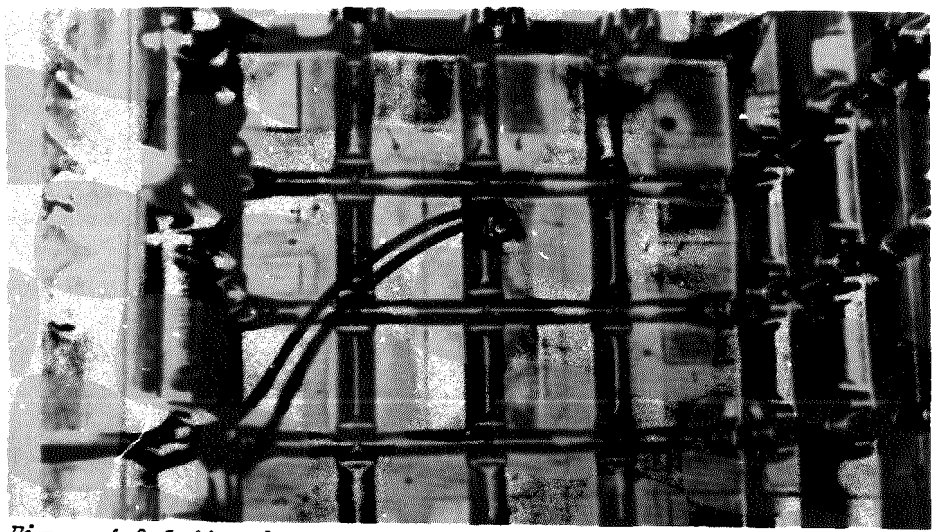

Figure 4.2.1-11 Liner Installation Completed

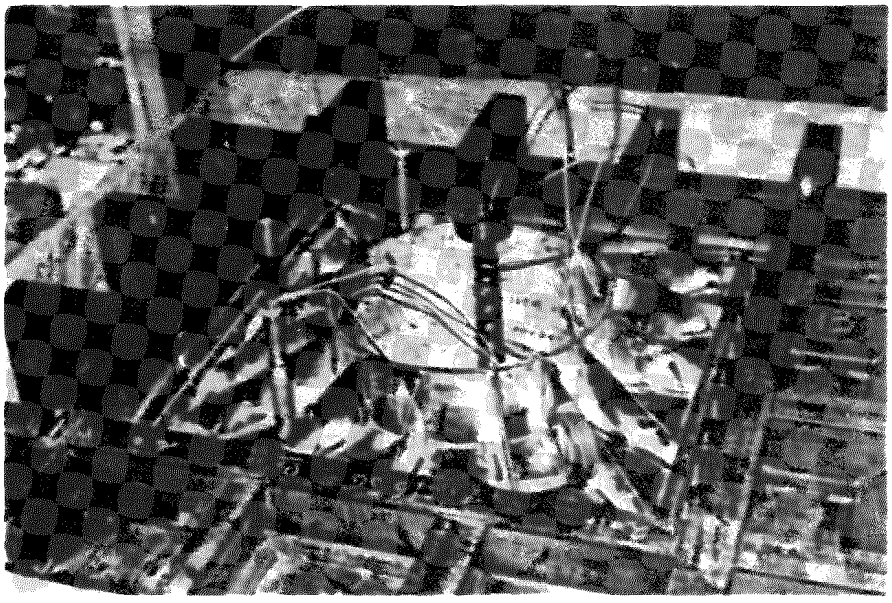

Figure 4.2.1-12 Tank Lid Installed

After installation and leak testing of the internal liner, the tank lid with integral salt heater was lowered into place and sealed to the tank. (See Fig. 4.2.1-12.) The entire tank was then encased in insulation bats. The fully assembled and insulated tank is shown in Figure 4.2.1-13 prior to testing. The insulating blocks upon which the tank was placed may also be seen. A catch tank was placed under the tank to hold the molten salt after draining.

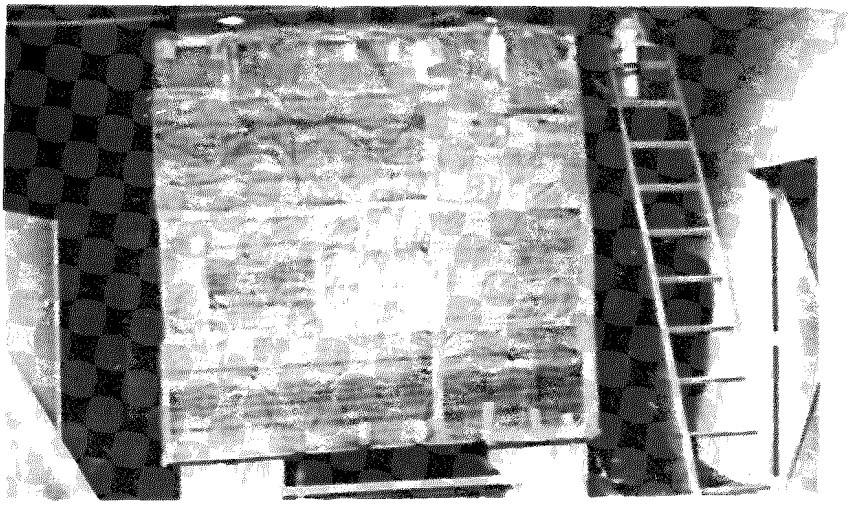

Figure 4.2.1-13 One Cubic Meter Tank Assembly

An important feature of a commercially used hot salt storage tank is its repairability. After completion of the testing, the tank was drained and a section of the I-800 liner was removed as shown in Figure 4.2.1-14. A portion of the foil between the liner and the insulating brick has also been removed. The tank was then repaired and checked for leaks, thereby demonstrating a successful liner repair technique. The repaired piece is shown in Figure 4.2.1-15.

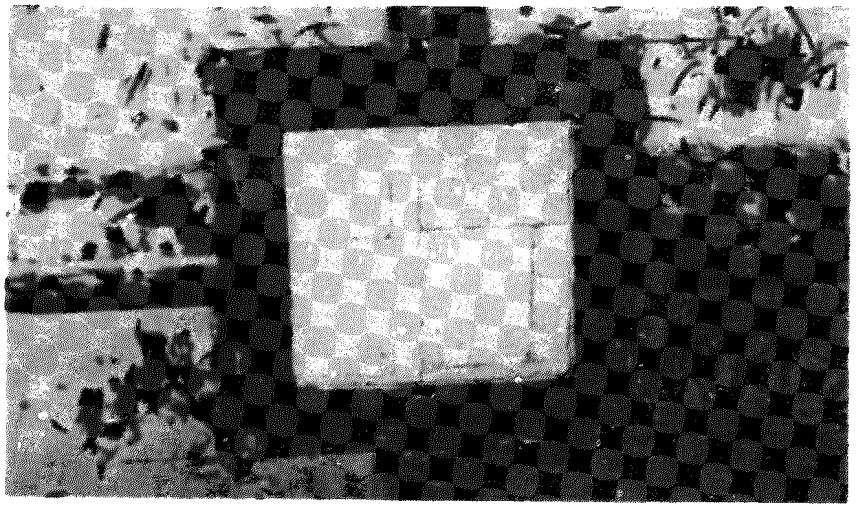

Figure 4.2.1-14 Liner and Foil Pieces Removed

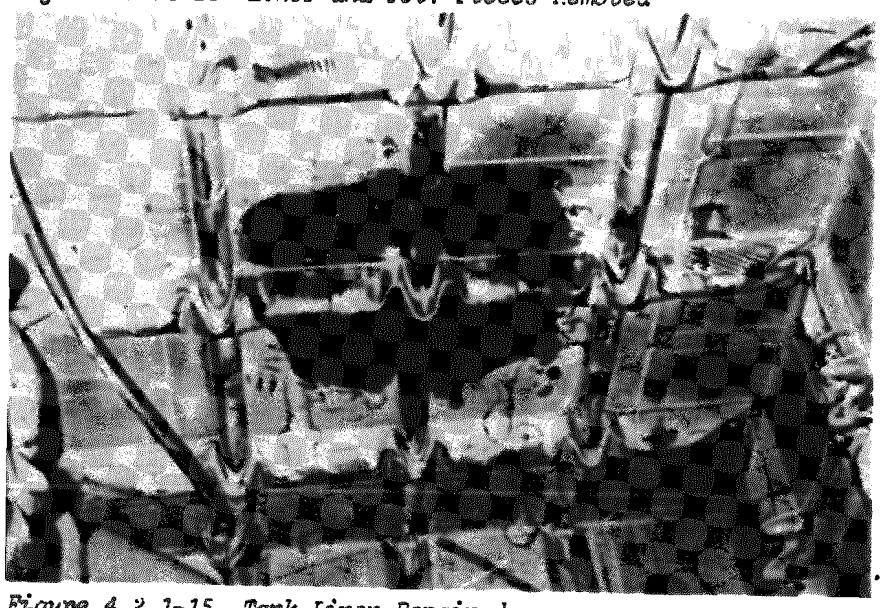

Figure 4.2.1-15 Tank Liner Repaired

4.2.2 Leak Detection System

The molten salt tank was fitted with an electrical leak detection system. Four leak detectors were installed under the liner in the locations shown in Figure 4.2.2-1. Each detector consisted of a small pan which would collect molten salt in the event of a leak. Two wires were routed to the pan where a circuit would be completed by the molten salt if it leaked into the pan. This bridge circuit was sized to account for salt's electrical resistance, which is dependent on temperature. This circuit was connected to an extensometry bridge, which was in turn connected to a recorder.

Before test, all of the liner welds were leak tested using an ammonia leak test method employed for many years for LNG tank applications. This test consisted of applying an ammonia sensitive paint to all the welds and applying a low pressure ammonia between the liner and the carbon steel tank. Leaks could be easily detected since the yellow paint turns blue in the area of a leak.

4.2.3 Tank Pressurization System

The tank pressure was cycled using the system shown schematically in Figure 4.2.3-1. Air is delivered by a compressor at 0.7 MPa (100 psi) and is dried to less than 10% relative humidity. The pressure controller opens the valve and allows the pressure in the tank to increase to 0.3 MPa (44 psi) at which point the tank is vented through the exhaust valve. The resulting pressure wave is shown in 4.2.3-2. The number of cycles and the amplitude of the cycles required were determined as shown in 4.2.3-3. This is in accordance with the ASME pressure vessel code (Appendix II, Article II, 1.000).

4.2.4 Salt Filling

Salt filling was done at a temperature of approximately 420°C (790°F) which was monitored by thermocouple 25. The salt supplied had not been kept dry and consequently solidified in the drums. It was necessary to reduce the salt to powder to fit through the filling tube.

The tank contained about 675 liters (23.8 ft^3) of salt. The maximum level was a few centimeters from the tank cover insulation to allow adequate pneumatic pressure cycling during the test. The space left above the liquid surface [assumed to be 10 liters (0.35ft^3)] must be small to allow a reasonable cycling frequency. It is worth noting that the cycling frequency was increased during the test from 860 cycles to 1200 cycles per hour. This was because the tank temperature rise caused salt expansion, thereby reducing the ullage air space.

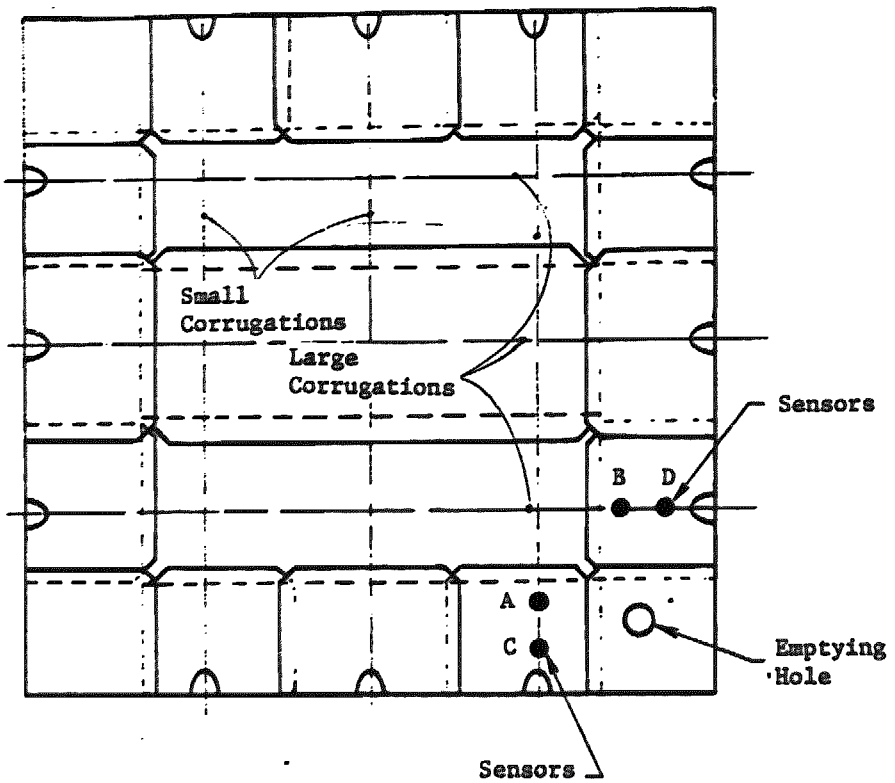

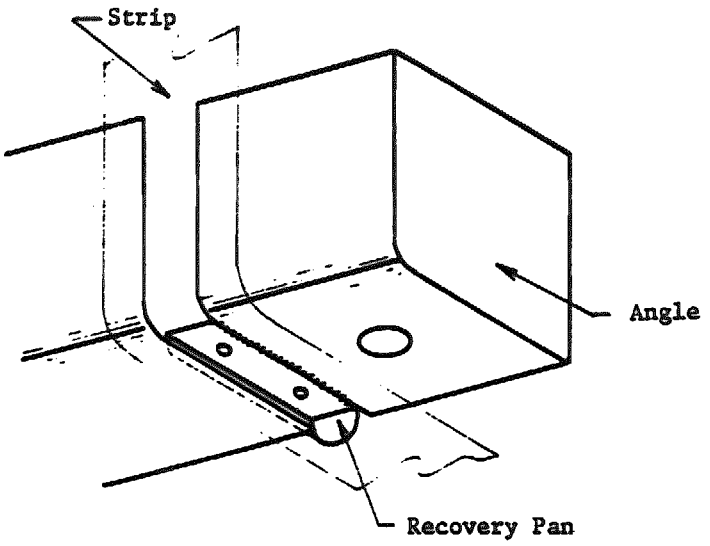

Figure 4.2.2-1 Molten Salt Leak Detection

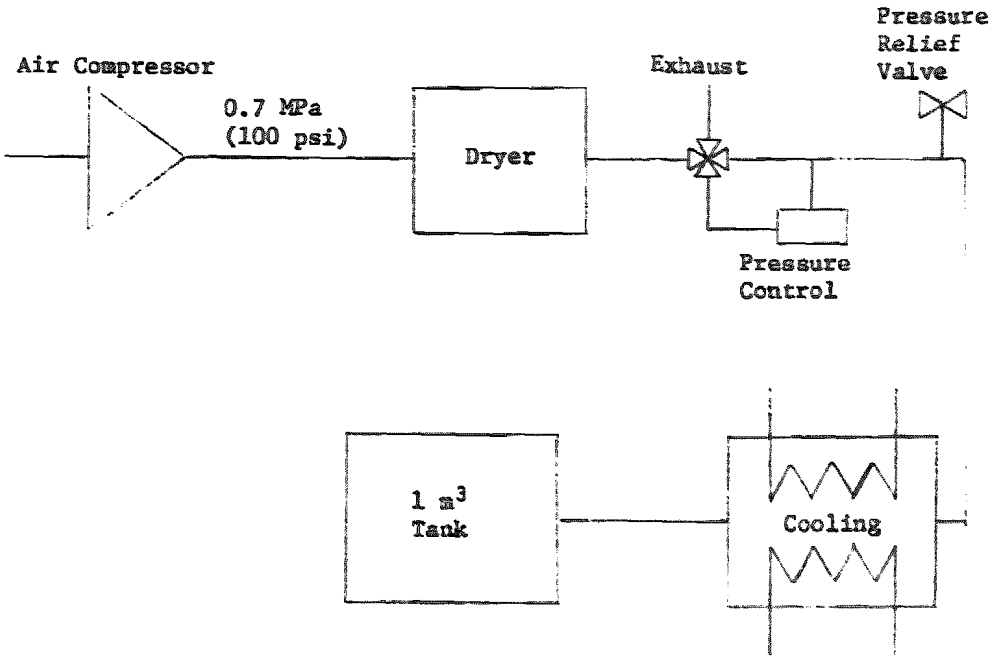

Figure 4.2.3-1 Pressure Cycling System

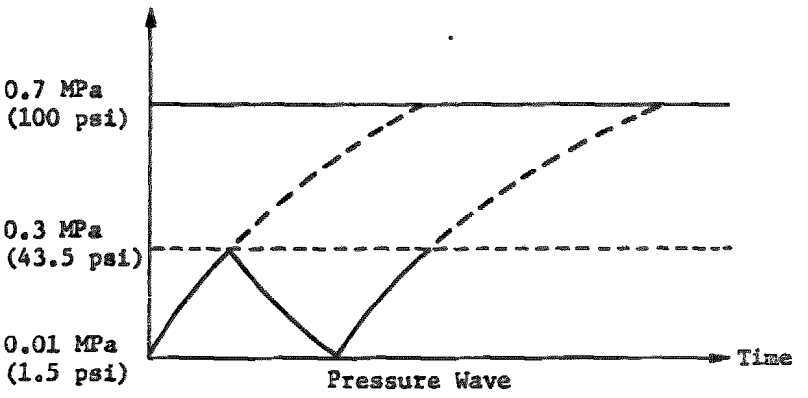

Figure 4.2.3-2 Tank Pressure Wave

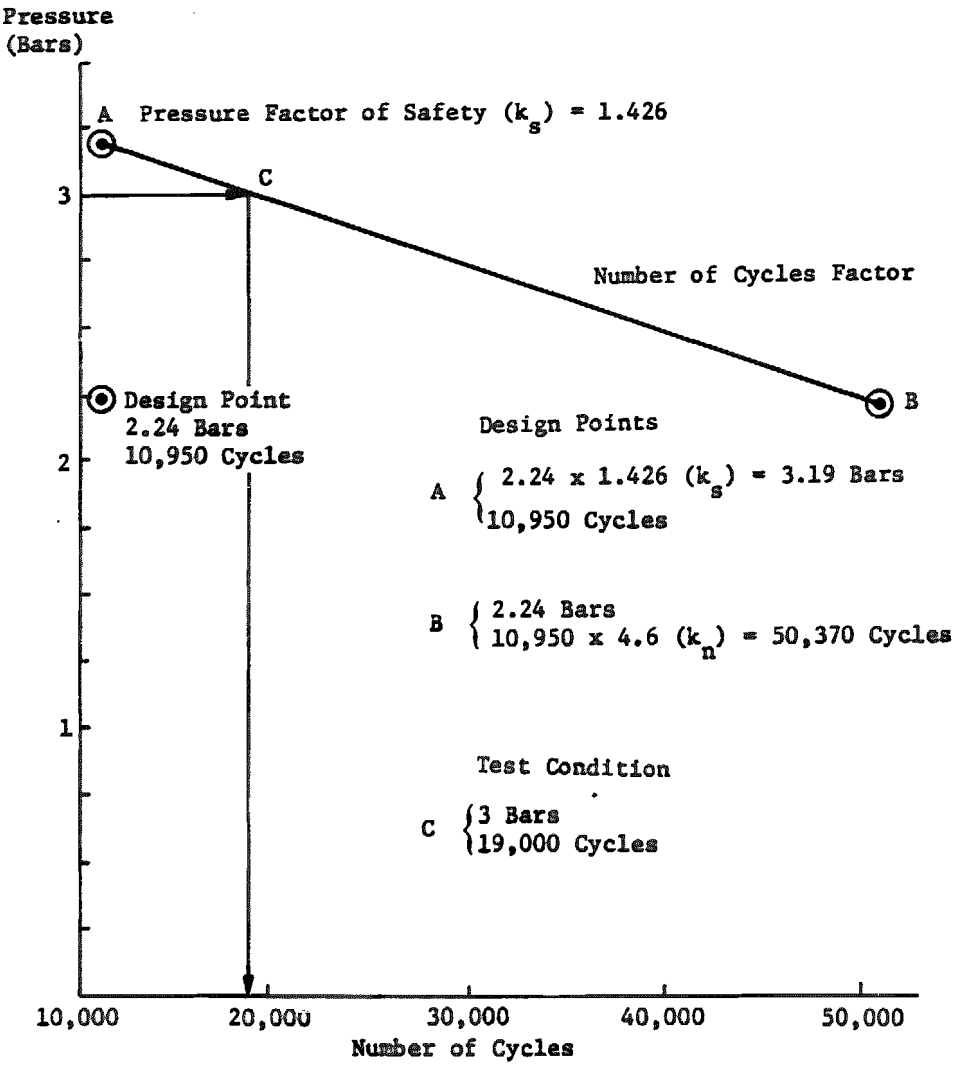

Figure 4.2.3-3 Pressure Test Parameters

4.3 TEST

Figure 4.3-1 shows the temperature versus time history of the molten salt after filling, as measured by thermocouple number 6 (see Fig. 4.2.1-1 for thermocouple locations). Table 4.3-1 gives all the temperature measurements throughout the cycling tests which began at 15:34 hours on July 23, 1981. Also, the number of cycles is shown in the right hand column. Thermocouples numbers 1 and 24 were not working. The salt temperature was uniform as seen by the thermocouples on the

liner (nos. 2, 3, 6 & 9). At the start of the test the salt temperature was low [540°C (1004°F], but was up to over 566°C (1050°F) by 0.0 on July 24, 1981 after 5780 cycles. The temperature readings of thermocouple no. 6 is plotted versus time (and number of cycles) in Figure 4.3-2. The steady-state temperatures are shown on Figure 4.3-3 (after 18,000 cycles at 11.0 hours on July 24, 1981). The salt temperature, as measured by liner thermocouples (nos. 2, 3, 6 & 9), was very uniform at approximately 567°C (1053°F). Note that thermocouple 13 (in the corner) is on the heavy angle (not the liner). Also, thermocouple 20 (bottom center) is on an anchor bolt under a liner corrugation. The temperature of the carbon steel tank varied between 86°C (187°F) and 212°C (414°F). The design temperature for the carbon steel tank was 288°C (550°F). The external insulation proved to be inadequate to maintain the desired tank temperature probably due to the extensive external support structure. The external support structure and insulation are unique to this test and are in no way typical of a commercial tank design. However, the lower carbon steel tank temperature results in a conservative test because there was a larger temperature difference between the tank and the liner than in the design model. This resulted in larger membrane stresses in the $1m^3$ test. As noted previously in paragraph 4.2.4 the pressure cycle frequency increased from 800 to 1200 cycles per hour during the test as a result of salt temperature rise (expansion) and an attendant reduc- tion in ullage air space. No leaks were detected during the test.

After the test was completed, the tank was emptied. The tank was then thoroughly cleaned to remove any salt remaining which might be blocking cracks. The ammonia leak test was then repeated and the results verified there were no cracks in the liner.

4.4 CONCLUSION

The one cubic meter subassembly, consisting of full scale materials simulating the actual commercial size of the salt storage tanks, was tested under conditions simulating a service life of 30 years, according to the ASME pressure vessel Code (Appendix II, Article II, 1.000). However, it must be understood that although the stress level, fatigue cycles, and temperatures were simulated, the effects of creep or creep-fatigue interaction were not simulated.

No evidence of deformation of the liner, damage to the insulation or the liner was found after the test.

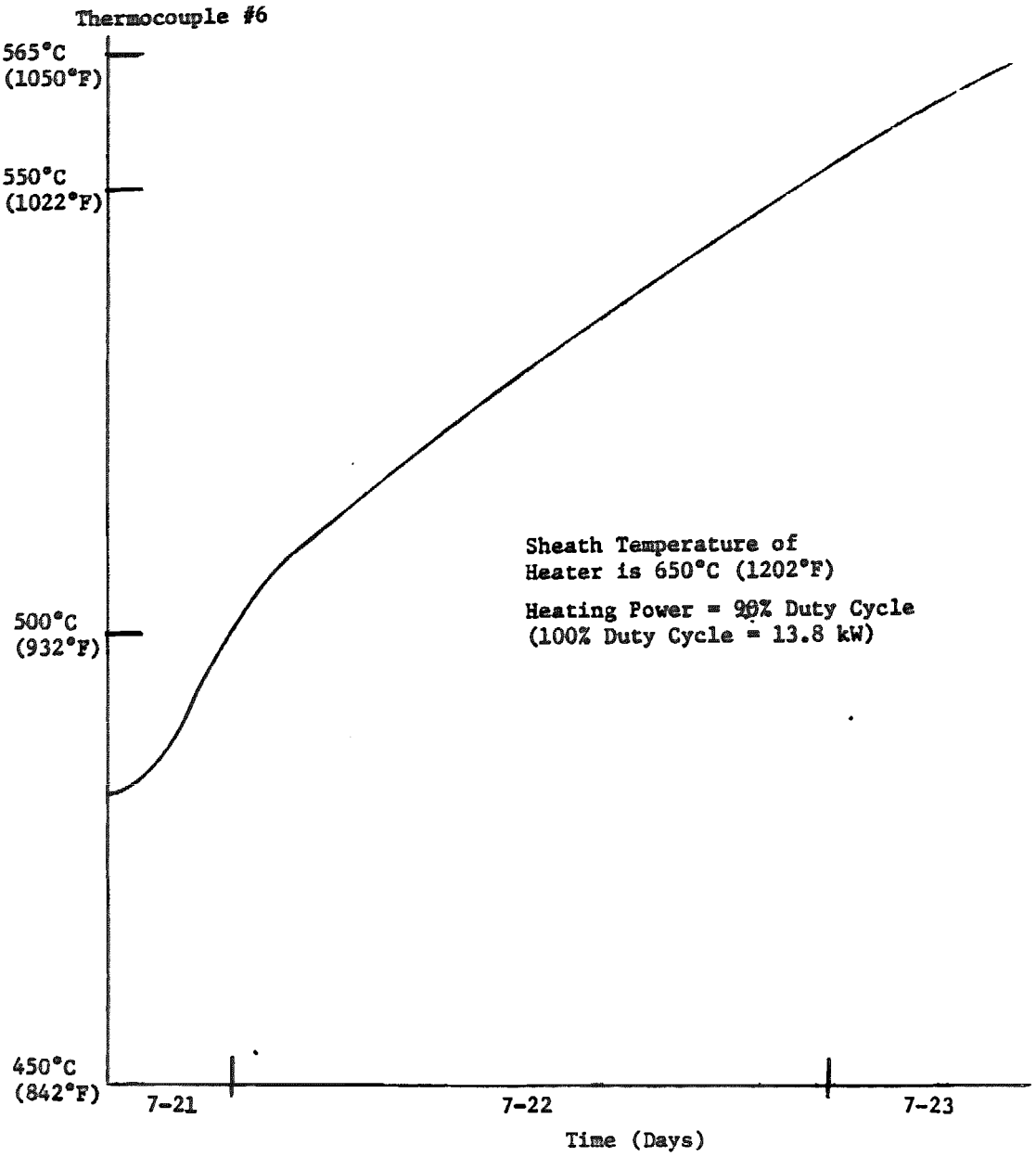

Figure 4.3-1 Tank Warmup When Filled With Salt

Table 4.3-I Thermocouple Temperatures, °C

	Begin Test							
Date	23/7							
No. Cycles	0				2285			
Time / Gage	15 h 34	19 h	19 h 30	20 h	20 h 30	21 h	21 h 30	22 h
1	Out of Service →							
2	536	538	544	543	545	547	549	554
3	540	544	545	547	549	550	552	553
4	290	289	288	288	287	287	287	287
5	197	197	196	196	196	196	197	198
6	545	546	548	549	551	553	554	556
7	347	347	346	346	346	345	345	345
8	133	133	132	132	131	134	137	139
9	543	545	546	548	550	552	553	555
10	450	450	450	451	451	452	453	454
11	300	299	299	298	297	297	296	296
12	140	139	138	138	138	138	137	137
13	495	497	499	500	502	504	506	507
14	213	213	213	213	213	213	213	213
15	126	126	126	127	127	127	128	128
16	100	100	100	100	99	99	99	99
17	139	139	139	139	139	139	139	139
18	96	96	96	95	95	95	95	95
19	89	89	89	89	88	88	88	87
20	513	514	517	519	521	523	524	526
21	320	320	319	319	319	319	319	319
22	101	101	101	101	101	101	101	101
23	292	300	322	329	339	356	367	380
24	Out of Service →							
25	574	576	578	580	582	583	585	587

Table 4.3-1 Thermocouple Temperatures, °C (cont)

Date	23/7			24/7				
No. Cycles	5780							
Time / Gage	22 h 30	23 h	23 h 30	0 h	0 h 30	1 h	1 h 30	2 h
1	Out of Service →							
2	553	554	556	558	560	562	561	561
3	555	557	559	560	562	564	560	562
4	287	287	288	289	290	291	292	293
5	199	200	202	203	204	205	206	207
6	558	560	562	564	566	568	564	565
7	345	345	345	346	346	346	347	347
8	141	142	144	145	145	146	147	147
9	557	559	560	562	564	566	564	564
10	455	456	457	459	461	462	464	465
11	296	296	296	297	297	298	299	300
12	137	138	138	139	139	139	140	140
13	509	512	512	514	516	518	519	519
14	214	214	214	214	215	215	215	216
15	128	128	128	128	128	129	129	129
16	99	99	99	99	99	99	99	99
17	139	139	139	139	140	140	140	140
18	94	94	94	94	95	95	95	95
19	87	87	87	87	87	87	87	87
20	528	529	531	533	535	537	537	537
21	319	320	320	320	320	321	321	321
22	100	100	101	101	101	101	101	101
23	387	392	395	403	403	405	398	389
24	Out of Service →							
25	589	591	592	593	596	598	594	596

Table 4.3-1 Thermocouple Temperatures, °C (cont)

Date	24/7							
No. Cycles	10180							
Time / Gage	2 h 30	3 h	3 h 30	4 h	4 h 30	5 h	5 h 30	6 h
1	Out of Service →							
2	563	563	563	564	566	567	568	567
3	563	563	563	563	564	565	565	563
4	293	294	295	296	296	297	297	298
5	208	208	208	209	209	209	210	210
6	568	566	566	568	569	570	570	567
7	348	348	349	349	350	351	351	352
8	147	148	148	148	148	148	148	149
9	567	565	565	567	568	569	569	567
10	466	467	467	468	468	469	469	470
11	300	301	302	302	302	303	303	303
12	140	140	141	141	141	141	141	141
13	520	521	521	522	523	525	526	526
14	216	216	217	217	218	218	219	219
15	129	130	130	130	131	131	131	131
16	99	99	100	100	99	99	99	99
17	141	141	141	141	142	142	142	143
18	95	95	95	95	95	95	94	94
19	87	87	87	87	87	87	87	87
20	538	538	539	540	541	542	543	543
21	322	322	323	323	324	324	325	325
22	101	101	101	101	101	101	101	101
23	392	392	393	394	403	404	403	398
24	Out of Service →							
25	599	595	589	596	598	596	594	580

Table 4.3-1 Thermocouple Temperatures, °C (cont)

Date	24/7							
No. Cycles								
Time / Gage	6 h 30	7 h	7 h 30	8 h	8 h 30	9 h	9 h 30	10 h
1	Out of Service →							
2	566	568	568	567	568	570	570	568
3	565	565	565	565	566	567	566	566
4	298	299	299	300	300	300	301	301
5	210	211	211	211	211	211	212	212
6	569	570	570	569	570	571	570	569
7	352	252	353	353	354	354	354	355
8	149	149	149	149	149	149	149	149
9	567	569	569	568	569	571	570	568
10	470	470	471	471	471	472	473	473
11	303	304	304	304	305	305	305	306
12	141	141	141	141	141	141	141	142
13	526	526	527	527	528	529	529	529
14	219	220	220	221	221	222	222	222
15	132	132	132	132	133	133	133	133
16	99	99	99	99	99	99	99	99
17	143	143	144	144	144	145	145	145
18	94	94	94	94	94	94	94	94
19	86	86	86	86	86	86	86	86
20	543	544	545	545	545	546	547	546
21	326	326	327	327	328	328	329	329
22	101	101	101	101	101	101	101	101
23	395	398						
24	Out of Service →							
25	600	597	595	596	600	601	590	591

Table 4.3-1 Thermocouple Temperatures, °C (concl)

Date	24/7		End Test	Extreme Temperatures During Test	
No. Cycles			19,000		
Time / Gage	10 h 30	11 h	11 h 30	Min	Max
1	Out of Service →				
2	567	567	567	538	570
3	565	566	566	540	567
4	302	302	302	287	302
5	212	212	212	196	212
6	568	567	569	545	571
7	355	355	356	345	356
8	149	149	150	131	150
9	567	568	568	543	571
10	473	473	473	450	473
11	306	306	307	296	307
12	142	142	142	137	142
13	529	528	528	495	529
14	223	223	223	213	223
15	134	134	134	126	134
16	99	99	100	99	100
17	146	146	146	139	146
18	94	94	94	94	96
19	86	86	87	86	87
20	546	545	545	513	547
21	330	330	330	319	330
22	101	101	101	100	101
23	392	390	390	292	406
24	Out of Service →				
25	592	594	593	574	601

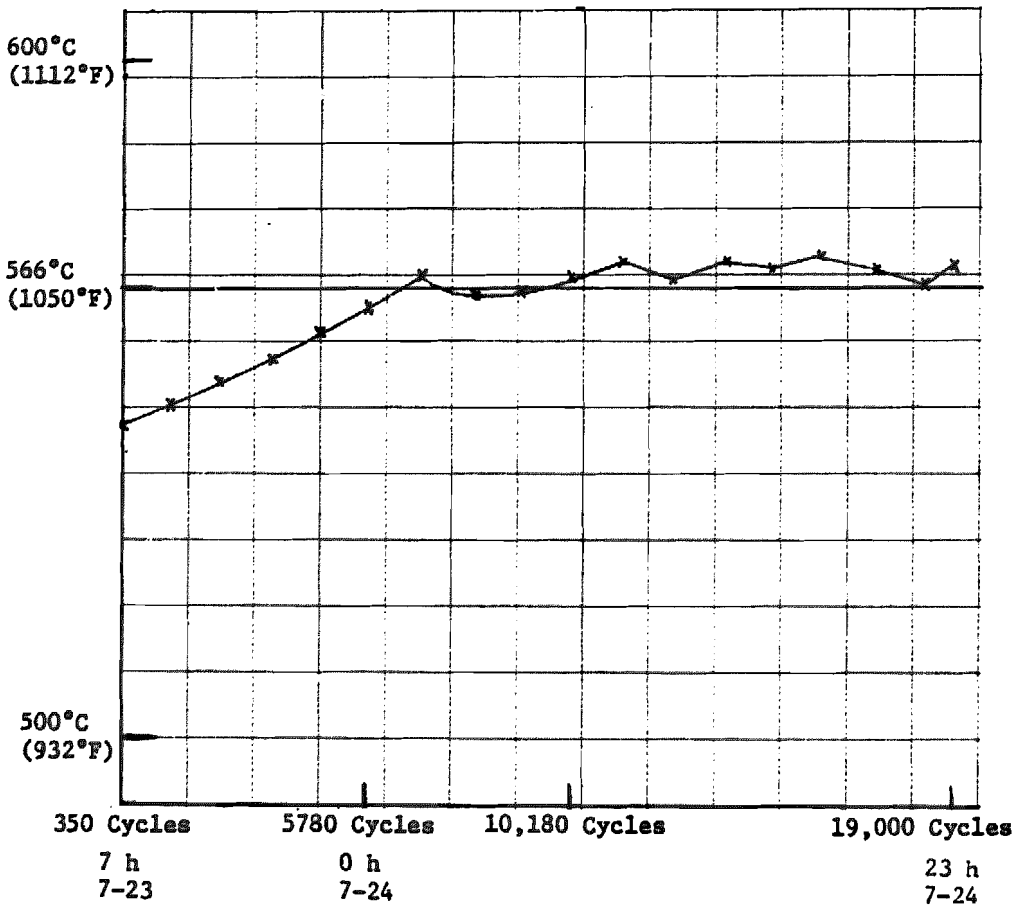

Figure 4.3-2 Temperature of Number Six Thermocouple during Pressure Test

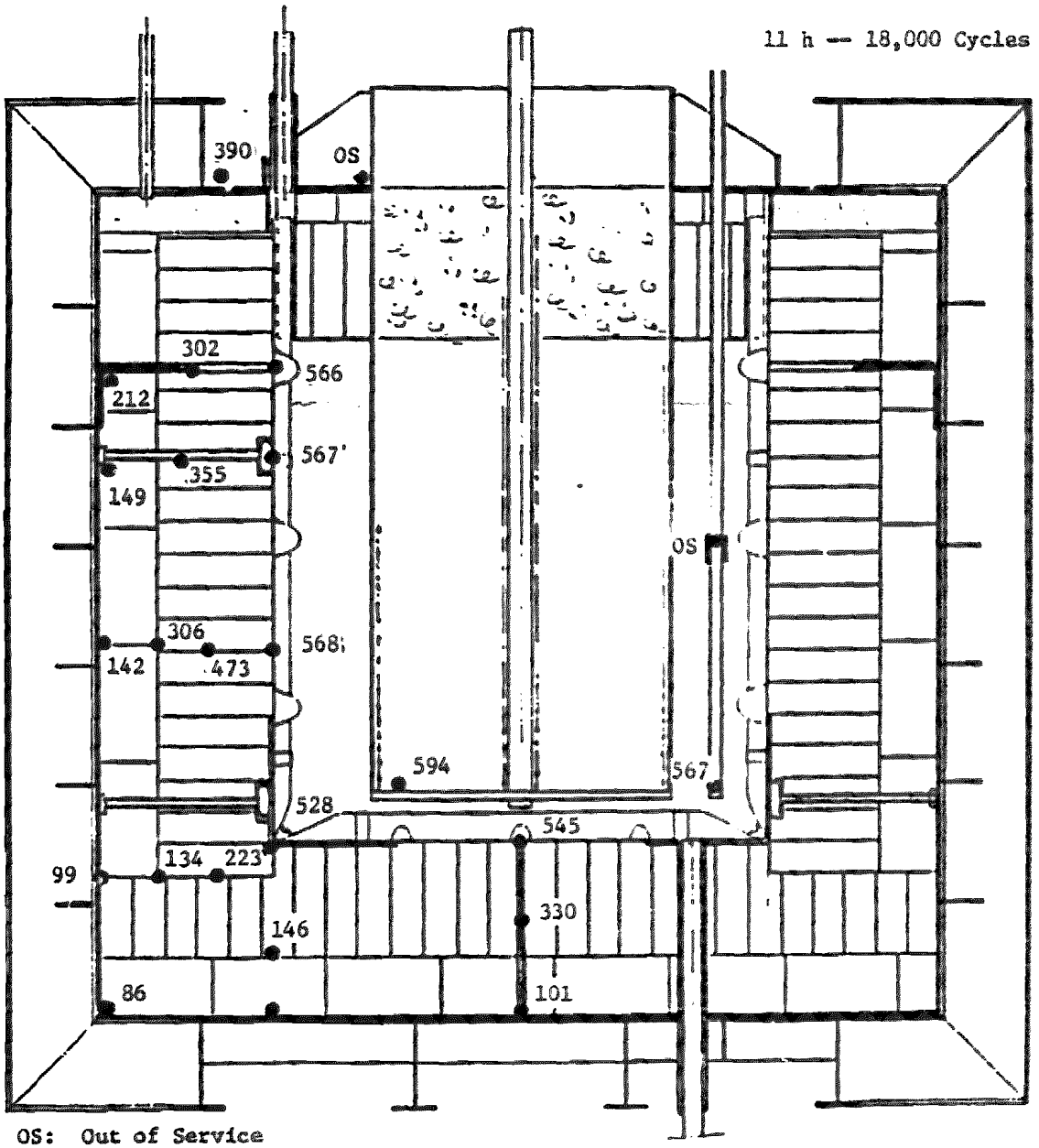

Figure 4.3-3 Steady-State Temperature (^{o}C) during Pressure Test

5.0 SRE Design

5.0 SUBSYSTEM RESEARCH EXPERIMENT (SRE)

The objective of the SRE was to design, construct and test a subscale prototype molten salt thermal energy storage system (TES) employing the dual-tank (i.e., hot and cold tank) approach. The purpose of this subsystem research experiment was to resolve all design, fabrication, operational and performance uncertainties associated with the full-scale TES system. To achieve these objectives, the SRE storage tanks were designed and constructed using the same techniques that would be used for a full-scale TES system, e.g., full-size liner panels with welds and attachments to the rest of the tank, full-size insulation thicknesses, water-cooled concrete foundations, etc. Only the overall tank size was scaled down to stay within the budgetary constraints of the SRE. The solar heating of the salt in a commercial plant was simulated by using a fossil-fired heater, and the cooling of the salt associated with generating steam for the commercial plant was simulated by an air cooler. The SRE was tested in all operational modes employed by a full-size plant. The net result was that the SRE simulated all aspects of the design, construction and operation of a TES for a full-scale plant, only on a smaller scale.

To summarize, the SRE design consisted of (1) one internally and externally insulated hot tank, 7.2 m (23.6 ft) high and 3.7 m (12.3 ft) in shell diameter, with a Technigaz Incoloy 800 liner and a carbon steel shell, (2) one externally insulated cold tank, 3.7 m (12 ft) high and 3.7 m (12.3 ft) in shell diameter, with a carbon steel shell, (3) operating temperatures of 566°C (1050°F) in the hot tank and 288°C (550°F) in the cold tank, (4) thermal storage capacity of 6.9 MWht (2.35×10^7 Btu), (5) each surrounded by a safety dike, (6) one fossil-fired heater with a 3 MW (10.4×10^6 Btu/h) salt heating capacity, (7) one air cooler of 5 MW (17×10^6 Btu/h) salt cooling capacity, (8) one hot sump with a 5.7 kW (7.5 HP) cantilever pump, (9) one cold sump with a 45.6 kW (60 HP) cantilever pump, (10) a total of 79,400 kg (174,700 lb) of 60% sodium nitrate/40% potassium nitrate molten salt, (11) all necessary piping and valves, all of which have electrical trace heating, (12) a semiautomatic control system, and (13) temperature, pressure and fill level instrumentation at key points throughout the system.

The cooler, cold pump and sump, and the cold salt valves were taken from the ACR Phase II program. This considerably reduced the cost for this program as well as maximizing component reliability. The SRE was designed to easily accommodate future improvements in the basic setup. This includes the possible future addition of a molten salt-to-water/steam generator (heat exchanger) in the loop. This heat exchanger would simply replace (or augment) the air cooler in the present SRE design. It could also include a potential hookup with the Martin Marietta salt receiver SRE.

Briefly, the SRE test plan consisted of (1) cold startup including mixing of salts, salt meltdown, and salt loading, (2) tank heat loss tests, both steady-state, cyclic charge/discharge and transient cool-down, (3) normal diurnal startup and shutdown tests, (4) emergency shutdown test, (5) maintenance exercises, and (6) cyclic charge and discharge at anywhere between maximum rate and 10% of maximum rate.

This task involved three main elements--design, fabrication, and test. In the text that follows, there is first described the rationale used to scope the size of the SRE (Subsection 5.1). Next is described the preliminary design of the SRE and its components (Subsection 5.2). This is followed by a discussion of the SRE fabrication and installation in Section 6.0 and finally the SRE testing and analysis (Section 7.0).

5.1 SIZING AND DESIGN RATIONALE

In view of the basic objective of the SRE, the specific objectives of this task were to (1) demonstrate design and fabrication techniques for a dual-tank commercial-size TES by designing and constructing a subscale SRE employing full-scale designs and fabrication techniques at each step (full-scale liner panels and insulation thicknesses, liner attachments, water-cooled concrete foundations, welds, etc), (2) demonstrate actual TES hot and cold tank operations and procedures by testing the SRE in all modes expected in a commercial operation (startup, shutdown, diurnal cyclic charge/discharge over a range of flow rates, storage, emergency shutdown, maintenance), (3) measure tank heat losses under actual operational conditions to verify thermal modeling and confirm TES system performance predictions, (4) provide an experimental means of identifying and resolving any uncertainties in the commercial TES system, (5) provide a firmer basis for refining cost estimates for commercial-sized tanks, and (6) provide a test bed for potential future long-term materials, procedures and solar system testing.

To meet these objectives the SRE was sized using the following rationale. First, it was deemed vital to the success of this program to use exactly the same salt, tank materials, insulation thicknesses, and operating temperatures in the SRE as in the TES to (1) have the same heat loss rate (per unit surface area) for each element of the tank (side, top, bottom) to minimize the uncertainty in area scaling up to TES size, (2) have the same operating temperatures in each material so there is no uncertainty in material strength and compatibility with molten salt, (3) have the same thermal gradients so the relative thermal expansions of one member to another are the same, even if the absolute values cannot be matched in a subscale experiment [particularly important for the hot tank at the liner-insulation-shell interfaces in both the vertical and radial directions, and for both tanks at (and near) the tank shell-foundation interfaces], and (4) have the same salt at the same operating temperatures to reduce any uncertainties in material compatibilities of pumps, valves, pipes, controls and salt handling and conditioning equipment, leaving only component sizing as a tasks for specific TES designs.

Second, to meet the schedule constraints of this program and to make the program as economical as possible, while still achieving technical success, there was a reduction of the tank height, tank diameter, salt flow rates and total number of charge/discharge cycles for the SRE relative to the TES. The primary effect of this reduction in scale was that, relative to the TES, the SRE obviously has much smaller thermal storage capacity, charge/discharge rates and heat losses. Since all the materials, thicknesses and operating temperatures are the same, the

SRE heat capacity, heat charge/discharge rate and heat loss rate are easily and reliably scaled up to the TES with virtually no uncertainty since these parameters are known to be directly proportional to the mass of working salt in the tank, the mass flow rate during charge/discharge and the total tank surface area (after simple adjustment for proportions of total area in top, side and bottom).

In addition to the basic differences between the SRE and TES noted, (which are easily scalable), there are some other (and more subtle) consequences of the scaled down size. First, since the salt height at full charge was lower in the SRE, so was the maximum salt pressure and hence loads on the liner and walls. Since the liner panels were sized for the TES height and pressure, stresses in the SRE liner were lower. Second, since the SRE test time was considerably shorter than the 30-year service life of the TES tank (3 months vs 30 years), the total number of SRE cycles for fatigue effects was considerably smaller. However, this issue was resolved by fatigue-testing a 1 m^3 hot tank subassembly. The 1 m^3 test program produced liner/tank exposure to pressure and number of cycle environments in excess of what the TES will experience.

Because of the smaller dimensions, the convection heat transfer coefficients between the salt and the wall and between the external sheathing and the ambient air was somewhat different in the SRE than in the TES. This is because the Grashof number (for natural convection) and the external Reynolds number (for wind) was smaller. These differences will have only a small effect on the SRE heat transfer rate per unit area, however, because most of the thermal resistance is in the insulation and these resistances will be identical. In any event, these differences will be accounted for in the thermal modeling and data evaluation. Because the hoop stress in the carbon steel shell walls is directly proportional to the product of salt pressure and tank diameter, these stresses are lower in the SRE than in the TES. Although the absolute value of the thermal expansion growth is lower in the SRE, the thermal strains and stresses are comparable. Last, the concrete foundation loads and stresses in the SRE are lower because of the reduced height which cannot be compensated for. Water cooling to keep the concrete near ambient temperature was used.

There is a practical lower limit in the scaling of the SRE. In particular, the overall tank dimensions could not be reduced so the use of full-scale fabrication techniques was precluded or unreasonably low pressures were produced. Thus the lower limits on SRE size were set by the requirements to provide (1) a full-scale liner panel (i.e., widths and heights) for the hot tank sides, bottom and top [a sidewall panel is approximately 1 x 3 m (3 x 9 ft)], (2) sufficient inside diameter and height for the hot tank so the liner panels can be installed and welded by personnel inside the SRE tank, as would be done for the TES, (3) sufficient height of both hot and cold tank to get reasonable pressure loads on the sides and bottom, and (4) sufficient height on the hot tank to get reasonable vertical thermal expansion growth of the liner to properly simulate the interaction of the liner and its attachments with the insulation and shell.

Based on these considerations, the hot tank was sized at 7.2 m (23.6 ft) high and 3.7 m (12.3 ft) in diameter (outside shell dimensions). This height allowed the use of full-scale liner panels while also providing reasonable thermal expansion growth of the walls in the vertical direction and reasonable pressure loads at the bottom of the tank. The minimum practical diameter to permit installation of liner panels was 3 m (10 ft). The tank shell diameter resulted from this minimum diameter and the brick thickness. The small diameter also increased the linear velocity of the liquid salt-ullage gas interface, which better simulates the TES.

Similarly, the 3.7 m (12.3 ft) height and 3.7 m (12.3 ft) outer shell diameter for the cold tank was used. These dimensions were selected so the cold tank shell design would be the same as for the hot tank, thus providing a cost savings. Another important feature of both SRE tanks was that each used a manhole for ingress/egress, and a water-cooled insulating concrete foundation, as in the TES.

As previously mentioned, the SRE tanks used full-scale TES materials and thicknesses; only the height and diameter were smaller. In the case of the liner for the hot tank, full-scale liner panels were used. Only the number of panels in the tank was smaller (their curvature, of course, was different). The SRE used the liner thickness, corrugation geometry and knot shapes selected for the TES. The liner and internal insulation were installed and welded in the SRE tank in identical manner to a full-scale TES.

Once the basic SRE tank sizes were selected, it was necessary to select the flow rates and heater and cooler capacities. Because the SRE thermal storage capacities are much smaller than the TES values, the SRE thermal charge and discharge rates were also much smaller. As previously noted, this was not considered a problem since these thermal rates will scale up directly with the flow rate because of the identical working fluid and operating temperatures used in our system. Thus the capacity of a practical and economic salt heater became the driving function for the flow rate selection. Based on a survey of vendors, a 3 MW (10.2×10^6 Btu/h) fossil-fired heater was selected. This heater is a large salt heater having a design that has been produced and that is reasonably economical in both capital and operating costs. Since the purpose of the heater was to simulate the solar receiver, there was no attempt to go into a development program for fossil-fired salt heaters in this thermal energy storage system program. The extra risk and cost would have added little in value to the program. At a salt temperature rise of 278°C (500°F), this heater can heat a maximum salt flow rate of 25,335 kg/h (55,738 lb/h). This flow rate was sufficient to completely charge the hot tank in 2.3 hours.

The fan-type air cooler used in the salt receiver SRE program was also selected to cool the salt in the thermal storage SRE. This resulted in considerable savings for this program. The maximum cooler capacity is 5 MWt.

The cold pump, sump tank and cold salt valves were taken directly from the ACR Phase II program. This not only reduced the cost of the program, but also maximized reliability since these components had already been extensively operated.

The pipes and controls that make up the rest of the SRE system were sized to be compatible with the maximum salt flow rates, tank capacities and charge/discharge times. The SRE charge (or discharge) rate could be reduced to as little as 10% of its maximum value. The system was then designed to easily accommodate such future improvements as the addition of a salt/water-steam heat exchanger in place of the cooler and to connect with the salt solar receiver SRE.

It should be reemphasized that the rationale used in the size selection process was keyed to resolving all the TES uncertainties noted at the beginning of this section, while keeping SRE costs to a minimum.

A summary-type comparison of the SRE and TES characteristics is given in Table 5.1-1. The Table shows that while the various SRE capacities were considerably smaller than the TES, key parameters such as type of salt, operating temperatures and materials and thicknesses were identical so the SRE performance data can be easily and reliably scaled up to the TES size.

5.2 DESIGN DESCRIPTION

A functional schematic of the SRE is shown in Figure 5.2-1. The basic system consists of the two storage tanks, one heater, one cooler, two sumps and two pumps. During the charging process, salt was drained from the cold tank at 288°C (550°F) and was gravity fed into the cold salt sump. The cold salt pump then pumped the fluid through the fossil-fired heater where the salt was heated to 566°C (1050°F) prior to entering the hot tank. During the discharge process, hot salt drained from the hot tank and flowed into the hot sump by gravity. The hot salt pump then pumped the fluid through the air cooler where the salt was cooled to 288°C (550°F) and returned to the cold tank. During the cold startup process, the salt was mixed and melted at the SRE site. The vendor used his own equipment (including a fossil-fired heater) and loaded molten salt at about 288°C (550°F) directly into the cold tank outlet line.

Special precautions were taken in the SRE design to prevent salt freeze-up problems. All pipes and valves were electrically trace-heated in the same manner as used in the ACR Phase II program. Both sumps and tanks had electrically controlled heaters to maintain proper operating temperatures. The two sumps and the cold tank used heaters outside the steel shells, while the internally insulted hot tank used an immersion heater, fed in through the top of the tank with the heating elements located near the floor. In addition, there were electrical heaters in the cooler to prevent freezing during startup and no-flow conditions. These heaters, as well as the trace heaters, were also used to bring the temperature of the components up before cold startup. The tank heaters can also be used to thaw residual salt if required.

Table 5.1-1 Comparison of TES and SRE Characteristics

Parameters	TES	SRE
System Characteristics		
Storage Fluid	60% $NaNO_3$/40% KNO_3 Molten Salt	Same as TES
Tankage Configuration	Dual Tanks	Same as TES
Operating Temperatures	566°C (1050°F) Hot Tank, 288°C (550°F) Cold Tank	Same as TES
Thermal Storage Capacity	1200 MWht	6.9 MWht
Working Salt Storage Capacity	10.2×10^6 kg (22.4×10^6 lb)	5.9×10^4 kg (1.3×10^5 lb)
Maximum Charge Rate	480 MWt (1.9 h)	3 MWt (2.3 h)
Minimum Charge Rate	48 MWt (25 h)	0.1 MWt (7 h)
Maximum Discharge Rate	300 MWt (4 h)	5 MWt (1.4 h)
Minimum Discharge Rate	30 MWt (40h)	0.1 MWt
Hot Tank Characteristics		
Shape	Cylindrical	Same as TES
Height (Shell)	15.8 m (51 ft, 10 in.)	7.2 m (23.6 ft)
Diameter (Shell)	25.2 m (82 ft, 7 in.)	3.7 m (12.3 ft)
Insulation Concept	Internal Plus External	Same as TES
Materials & Thicknesses	See Section 2	Same as TES*,†
Maximum Heat-Loss Rate	0.27 MWt	0.0275 MWt
Maximum Salt-Cooling Rate	4.8 K/24 h (8.6°F/24 h)	27 k/24 h (48°F/24 h)
Cold Tank Characteristics		
Shape	Cylindrical	Same as TES
Height (Shell)	12.2 m (40 ft)	3.7 m (12.3 ft)
Diameter (Shell)	25.2 m (82 ft, 7 in.)	3.7 m (12.3 ft)
Insulation Concept	External Only	Same as TES
Materials & Thicknesses	See Section 2	Same as TES†
Maximum Heat-Loss Rate	0.08 MWt	0.009 MWt
Maximum Salt-Cooling Rate	1.3 °C/24 h (2.4°F/24 h)	8.5°C/24 h (15°F/24 h)

*Except internal insulation in SRE hot tank is thermal equivalent of TES brick.

†Except SRE steel-shell thicknesses are less (sized for SRE loads at the TES design stress level).

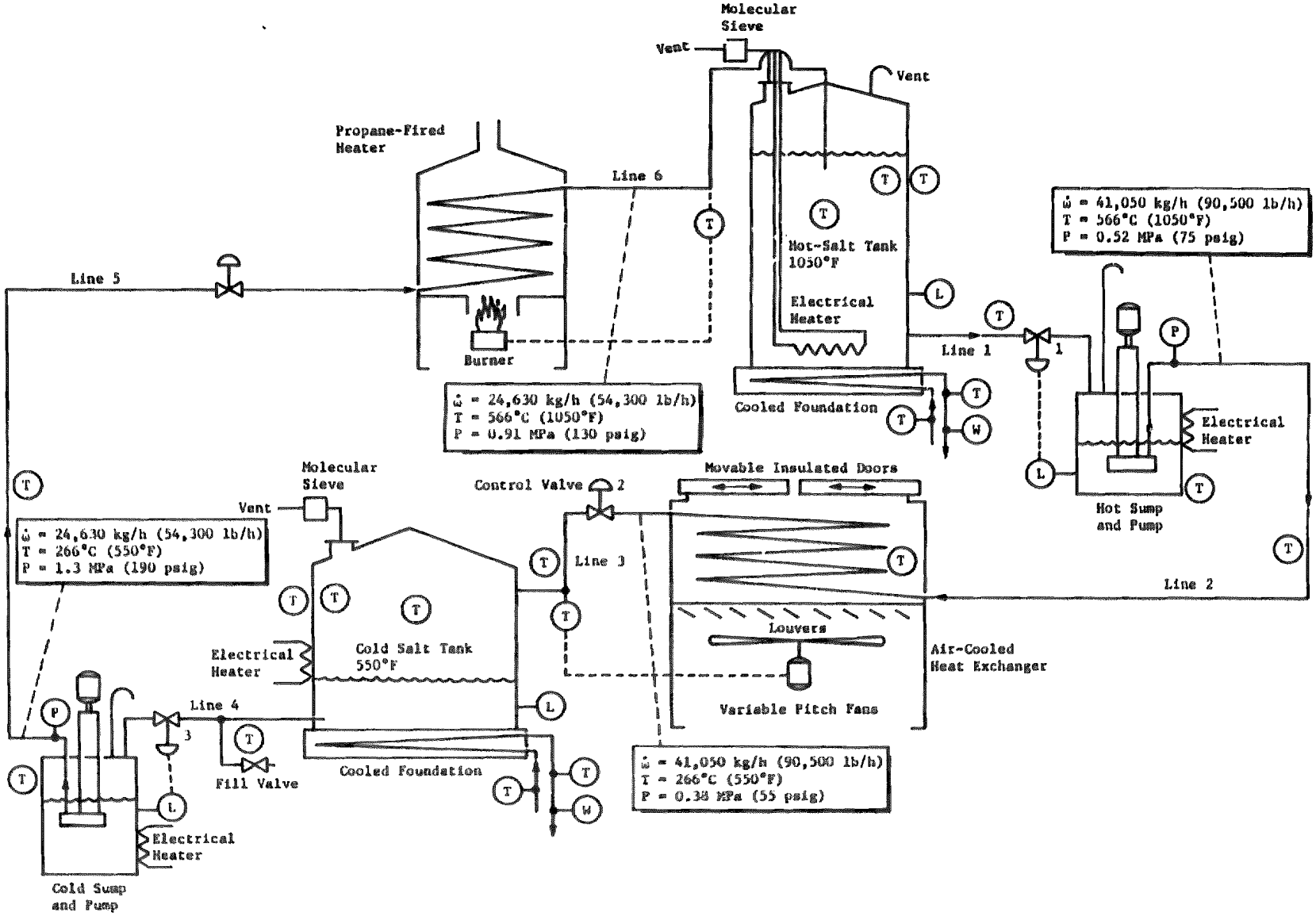

Figure 5.3-1 SHE Flow Schematic

Ullage gas was vented to the atmosphere in each tank and sump.

The control system was semiautomatic. All controls were mounted at a single console. The operator initiated the particular operational mode being tested by turning on the appropriate pumps and valves. Once the charge (or discharge) process had been initiated, the system operated automatically until the operator terminated it. There were automatic overrides to kill the heater or the cooler in the event no-flow conditions occurred.

Comparison of the SRE functional schematic (Fig. 5.2-1) with the TES schematic (Fig. 2.0-1) shows that the two are very nearly identical within the boundaries of the thermal energy storage subsystem part of the plant. Outside these boundaries, the TES solar receiver was simulated in the SRE by a fossil-fired heater, the TES salt-steam generator was simulated by the SRE cooler, and the TES main circulating pump was simulated by the SRE cold sump and cantilever pump. Within the thermal energy storage subsystem boundaries there was a one-to-one match of the major components, except there was no salt reprocessor in the SRE. Since the SRE contains smaller amounts of salt, has a shorter operating time than the TES and since the TES reprocessing requirements were not clear at this time, in the interests of economy, a salt processor unit in the SRE was not included.

Another slight difference was that the SRE used a temporary one-time-only vendor's service to melt and load the salt, whereas the TES plan is to have permanent equipment installed at the site to perform this function. Nevertheless, the SRE loading techniques are essentially identical in principle to the TES. Finally, one other difference was that the TES has three bypass lines to provide flexibility in system operation. The SRE simulates these options by varying the cooler heat transfer rates to produce either hotter or colder than nominal salt temperatures into the cold tank, and by varying the heater rate to produce colder than nominal salt temperatures into the hot tank. Thus the SRE simulated all major functional components and all operational modes of the TES.

5.2.1 Hot Salt Storage Tank

The hot salt storage tank was the principal element of the SRE system and the only one that required any development. Because the development work required for the stainless steel liner in this tank has been described in detail in Section 3.0 it will not be repeated. The rationale used to arrive at the specific size for the SRE has been described in Subsection 5.1 of this section. Figure 5.2.1-1 shows the elements of our hot tank design for the SRE. The overall exterior dimensions were 7.2 m (23.6 ft) in height and 3.7 m (12.3 ft) in diameter. The salt operating temperature was 566°F (1050°F).

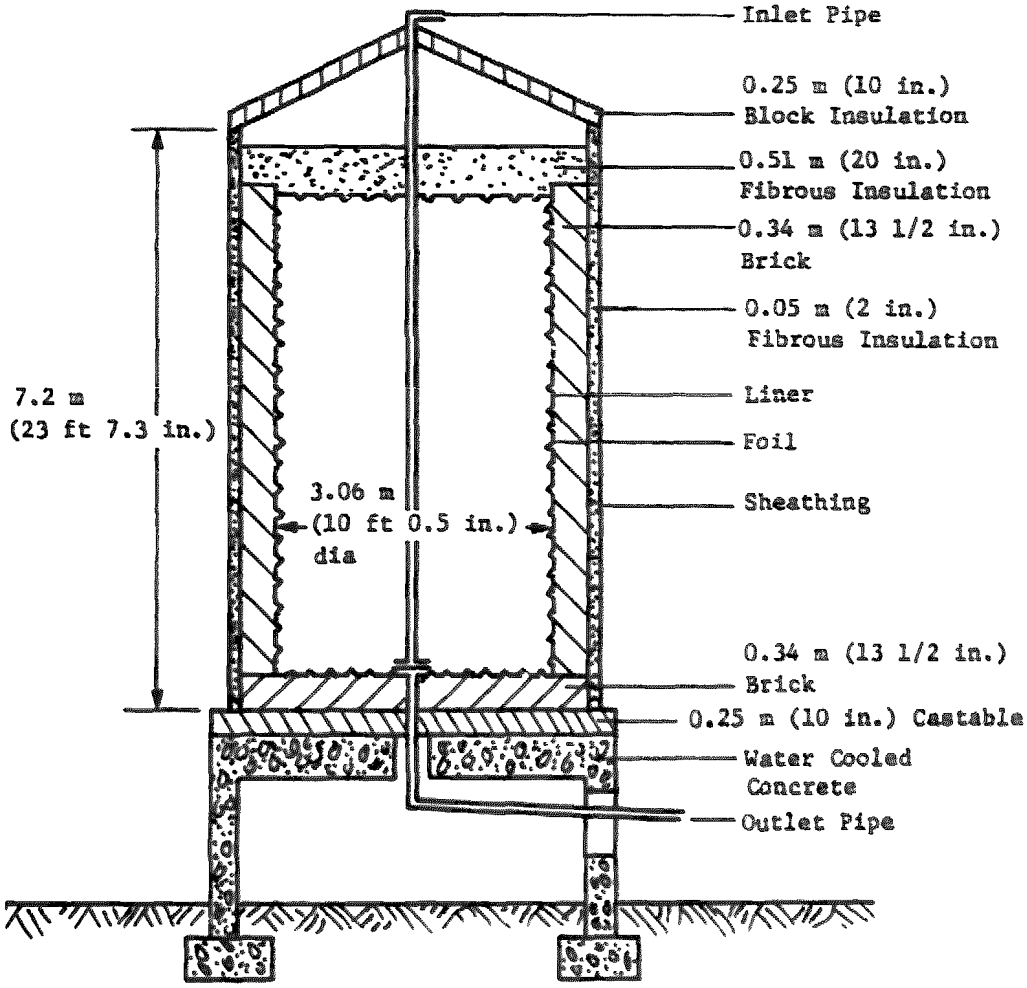

Figure 5.2.1-1 SRE Hot Tank

The important design features of the SRE hot tank are summarized in Table 5.2.1-1.

The maximum salt height in the tank was 5.0 m (16.5 ft) and 0.3 m (1.0 ft) for ullage gas. The minimum salt height in the tank was 0.4 m (1.3 ft), which allowed sufficient salt to cover the immersion heater. This amount of salt maintained the tank walls, top and bottom at (or very near) their operating temperatures.

The shell of the hot tank was made of carbon steel (e.g., SA516 grade 70). The thickness was sized to keep the hoop stress in the shell walls at the same safe working level as in the TES and in conformance with all applicable codes.

As a result, the normal shell temperature (i.e., with dry brick) will be only 163°C (325°F).

The above approach was compared to the approach of maintaining the shell temperature at 288°C (550°F). When the design temperature of the shell was 288°C (550°F) a less expensive tank system was achieved due to the effect on the insulation. This allowed a 56°C (100°F) temperature margin below the material coded values at which the strength of the material will decrease. If the liner were to leak the shell temperature could exceed the 343°C (650°F) temperature limit. However, any leakage would be slow and would allow time to remove external insulation from the tank to limit the shell temperature. This approach was used in the insulation design.

An important feature of our SRE design was that, since the same salt and salt temperature and the same materials and thicknesses were used, the SRE liner, insulation and shell temperatures would be close to the TES values. This minimized the need for temperature-scaling SRE results up to the TES size.

The key to the success of this internally insulated hot tank design approach is the liner. The liner must be extremely leak resistant and corrosion resistant to protect the refractory brick from the hot salt. The liner must also be flexible enough to withstand considerable thermal expansion during tank startup, and numerous pressure loading cycles (up to 50,000 in 30 years) during cyclic charge/discharge. These desirable characteristics are available in the Technigaz liner. Note that the liner is not a primary load-carrying structure; rather, it transmits the salt pressure loads through the internal insulation into the steel shell.

The salt outlet piping included a drain with an anti-vortex baffle to preclude sucking air into the lines during discharge (i.e. avoid the "bathtub vortex effect"). The hot tank also used a water-cooled insulated concrete foundation capable of withstanding soil loadings up to 239 kPa (5000 lb/ft^2). This approach kept the soil at essentially ambient temperature and avoided hot soil problems (heated water vapor, strength, etc). Our earlier studies indicate that hot foundations are not state of the art, and that a convection cooling approach on the bottom was inadequate.

5.2.2 Cold Salt Storage Tank

The SRE cold tank is shown in Figure 5.2.2-1. This design was a straightforward carbon steel (e.g., SA516 grade 70) shell with external insulation. The SRE materials and thicknesses are the same as for the TES cold tank, except that the shell thickness is reduced to produce the same hoop stress as in the TES. This design also used a drain manifold and a water-cooled insulating concrete foundation. Both the hot and cold SRE tanks have manholes and ullage gas vents to the atmosphere.

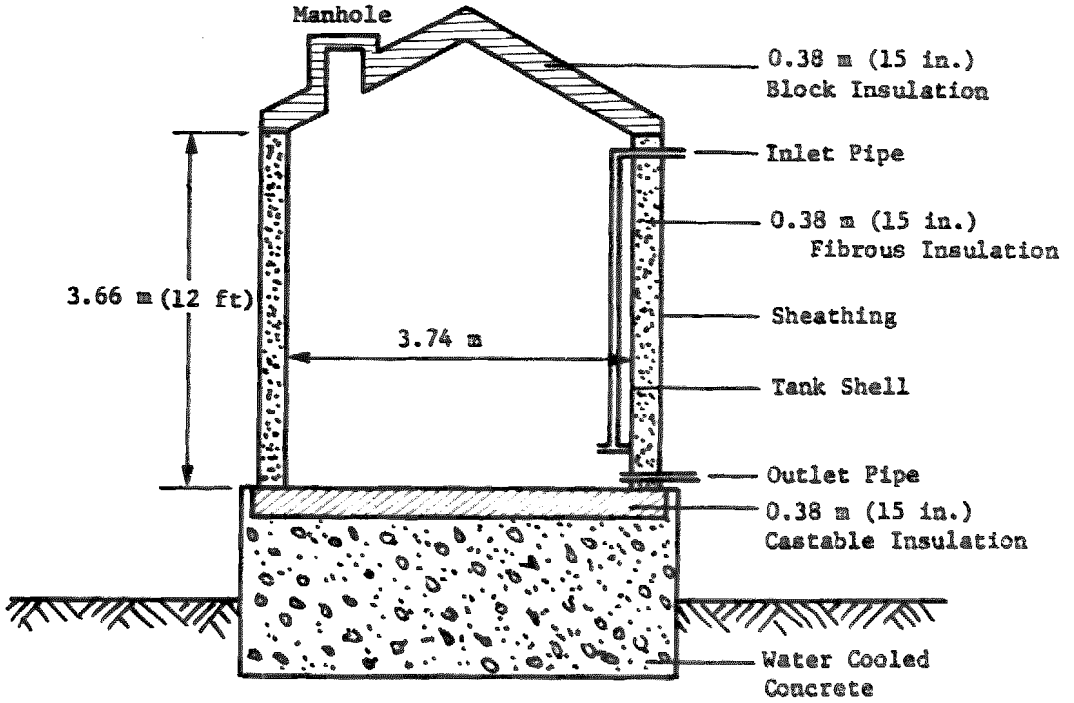

Figure 5.2.2-1 SRE Cold Tank

5.2.3 Ancillary Equipment

The fossil-fired heater was a standard design with a 3 MW (10.2×10^6 Btu/h) salt heating capacity. The salt inlet temperature was 268°C (550°F) and the outlet temperature was controlled to 566°C (1050°F) by throttling the heater fuel flow. The maximum flow rate was 0.20 m^3/min. (53 gal/min); the minimum flow rate could be a factor of 20 less. The heater was 7.3 m (24 ft) high, 2.7 m (9.0 ft) in diameter, and weighs 15,870 kg (35,000 lb) dry. The heating coils were 80 mm (2.12 in.) tubes made of 316 stainless steel.

The fan-driven air cooler was the one used in ACR Phase II, and was a custom design by the Happy Division of Therma Technology, Inc. The cooler was about 7.3 m (24 ft) long, 4.0 m (13 ft) high and 2.4 m (8 ft) wide. The cooler used two large fans to blow air over the tubes containing salt. It had a 5 MW (17×10^6 Btu/h) nominal salt cooling capacity. The salt outlet temperature was automatically controlled by varying the pitch on the fan blades.

The hot salt pump was installed on the hot sump. The pump was a standard Lawrence Pump and Engine Company model of the cantilever design. It had a head rise of 21 m (68 ft) at a 0.40 m^3/min (106 gpm) flow rate. It used a 5.7 kW (7.5 HP) electric motor. The lower bearing was water-cooled. The impeller and housing were made of 316 stainless steel. The hot sump was 1.2 m (4.0 ft) in diameter with a height of 1.2 m (4.0 ft) and was made of 316 stainless steel.

The cold pump was located on the cold sump, and came from the ACR Phase II program. The cold pump was similar to the hot pump except it has a carbon steel impeller and housing and has a maximum head rise of 62.5 m (205 ft). The obvious advantage of using cantilever pumps was that they avoid seal and bearing problems with molten salt. The cold sump was 1.5 m (5 ft) in diameter and 1.5 m (5 ft) in height.

Bellows-sealed valves were used for the SRE. This avoided the problem of salt creeping up the stem and freezing. The valves had dome motors (i.e., pneumatically driven) with limit switches. The valves also had mechanical override handles. For hot salt valves, 316 stainless body material was used and for cold salt, carbon steel body material.

Several kinds of piping were used. All hot salt lines were made of 316 stainless steel, while all cold salt lines were made of carbon steel.

5.2.4 Controls and Instrumentation

The monitoring and control of the SRE was accomplished from the control console. This includes the following:

1) Stop/start of motors
2) Start heater pilot light sequence
3) Heater stop
4) Cooler fan pitch
5) Cooler Louver position
6) Open/close cooler insulated door
7) Control valves No. 1 through No. 4
8) Salt level in sumps and tanks
9) Temperature of hardware

Interlocks were used to provide control and prevent hardware damage. Alarms were used to warn of conditions which were out of design limits. Automatic control of valves No. 1 and No. 3 was used to maintain specified heights of salt in the sumps. Automatic control of the outlet temperature was accomplished by the variable pitched fans. Manual override of all automatic controls was possible. The heater provided automatic control of the outlet temperature by adjusting the burner fuel flow.

All lines and components were provided with thermocouple instrumentation. The temperature of the piping could be heated to a temperature above the salt freezing point prior to salt introduction. The poor thermal conduction of the tubing required a thermocouple about every four feet. Sufficient instrumented points were provided to characterize the heat loss and the salt temperature gradients .

5.2.4.1 Controls

a) Hot Sump Level Control - The level sensor indicated the sump salt height from 0.15 m (6 in.) to 1.22 m (4 ft). The level sensor was used to provide automatic control of valve #1 (hot sump inlet valve) so that the sump was maintained at 0.58 m (23 in.) $\pm$ 0.10 m ($\pm$ 4 in.). Valve 2 has a head pressure variation in the hot tank

which varied from 84.3 KPa (12.24 psi) to 6.8 KPa (1.00 psi). Flow through the valve varied from 11.43 kg/s (90,500 lb/h) to 1.14 kg/s (9,050 lb/h). An audible alarm sounded when the salt exceeded 1.12 m (3 ft-8 in.). Manual or automatic control of the valve was available. Sump level valve position, and open/close lights were indicated on the control console.

b) Cold Sump Level Control - The level sensor indicated the sump salt height from 0.15 m (6 in.) to 1.78 m (5 ft - 10 in.). The level sensor was used to provide automatic control of valve #3 (cold sump inlet valve) so that the sump level was maintained at 0.38 m (15 in.) $\pm$ 0.08 (3 in.). The head pressure in the cold tank varied from 61.9 kPa (8.99 psi) to 7.63 kPa (1.11 psi). Flow through the valve varied from 6.86 kg/s (54,300 lb/h) to 0.69 kg/s (5430 lb/h). An audible alarm sounded when the salt level exceeded 1.5 m (4 ft - 11 in.). Manual/automatic control of the valve was provided. Valve position and sump level was indicated at the console.

c) Control Valve for the Hot Pump - Valve #2 controlled the flow from the hot pump through the cooler to the cold tank. This flow was set manually with no automatic feedback. A valve position indicator was necessary so that the flow could be set to previously determined values. Open and closed indicator lights were used.

d) Control Valve for the Cold Pump - Valve #4 controlled the flow rate from the cold pump through the heater to the hot tank. This flow was set manually and no automatic feedback was necessary. A valve position indicator was used to set the flow rate. Open and closed indicator lights were used.

e) Fossil Fired Heater Control - The heater was supplied with its own control panel which included burner safety features and start sequence. Several functional items were available at the console, a start button to start the pilot light sequence, a pilot light indicator light. The salt outlet temperature was controlled by the controller (Bartlow 76) which was set in the console. Initial preheat of the heater was accomplished by setting the controller at 700°F. The controller monitored flue gas exit temperature. A stop button was available at the console to turn off the burner. A main burner switch in the control console was required to lockout the main burner until flow was established through the heater.

f) Air cooler - The controls for the air cooler were GFE. A manual/automatic control was provided for the variable pitched fans to control the salt outlet temperature. It had single or double fan pitch control. Both fans could be stopped and started from the console. The louver pitch was manually controlled. Insulated movable covers on the air cooler were pneumatically operated with switches from the console. Indicator lights for open and closed positions were provided.

g) Foundation Coolant Flow - The valves for controlling the coolant flow through the tank foundation were manual valves. Coolant flow through the foundations was parallel flow with a valve at each foundation. Each flow was measured locally.

h) Electrical Trace Heaters - The controls for the majority of the trace heaters were off/on switches. The heater power is designed to obtain the correct temperature without cycling. The heater switches on the console operate relays in the "J" box.

j) Fill Valve - The fill valve, to initially fill salt into the system, was a manual valve only.

k) Control Equipment - An existing piece of equipment was used for electrical control switching. This large electrical box has the 480/277 supply with a 300 amp breaker. There is a 110 V transformer inside the "J" box. There are 27 relays which switch on electrical trace heaters via a 24 volt signal from the console. The relays to pull in the 110 V circuits to start the pump and fan motors are also located in "J" box.

5.2.4.2 Instrumentation

a) Thermocouples - Chromel alumel thermocouples were used. Components had thermocouples as identified under each component. The thermocouples on the lines were placed approximately every four feet and attached by spot welding to the exterior of the tube. The wires were bundled together.

The temperature rakes inside both tanks were tubes containing thermocouples which were sealed from the salt. One tube was placed 0.08 m (5 in.) from the tank wall and a second tube was place in the center of the tank.

b) Instrumentation Readout - The instrumentation readings which were displayed on the console are listed in Table 5.2.4-1. All the other thermocouple data was displayed and printed by GFE equipment. The experimental data was printed on computer paper at the interval specified by the test operator.

5.3 DESIGN ANALYSIS

Proper sizing of the critical components of the SRE required a significant amount of analysis. Heat loss analysis was performed on the hot tank, cold tank, transfer lines and pumps. In addition stress analyses were performed on all major components (i.e., hot tanks, cold tank, tank foundations, sumps, support structure, etc.) A line pressure loss analysis was also completed.

5.3.1 Hot Tank Thermal Analysis

The internally insulated hot tank has a layer of low density fire brick on the walls and floor, with fibrous insulation on top. This internal insulation is protected from the molten salt by a thin corrugated metal liner. The internal insulation reduced the shell temperature to near 288°F (550°F) so that a carbon steel shell could be used. Exterior insulation is used on the shell to maintain its temperature at 288°C (550°F). A fibrous insulation is used on the side and a block insulation is used on the top.

Table 5.2.4-1 Measurements Displayed on Console

1. Air Cooler
   - A. Pitch Control
   - B. Louver
   - C. Open/Close Ins. Door - Switch
   - D. Door - Open/Close Lights
   - E. Outlet Temperature
   - F. Overtemperature alarm
   - G. Undertemperature alarm

2. Heater
   - A. Start/Stop Switch
   - B. Temperature Controller (Supplied) Bartlow Series 76
     Stack Temperature (on Controller)
   - C. Overtemperature Kill-Controller Stack Temperature (on Controller)
   - D. Burner Override - Switch
   - E. Outlet temperature
   - F. Indicator Lights 0 Timer, Pilot, Burner
   - G. Overtemperature Alarm

3. Hot Tank
   - A. Temperature
   - B. Level Gauge

4. Cold Tank
   - A. Temperature
   - B. Level Gauge

5. Hot Sump & Valve
   - A. Level - (Control of Sump Inlet Valve)
   - B. Valve Control (with Manual Override)
   - C. Valve Stem Position (0-10 V, Bailey)
   - D. Overheight Alarm
   - E. Open/Close Lights on Valve Travel

6. Cold Sump & Valve
   - A. Level - (Control of Sump Inlet Valve)
   - B. Value Control (with Manual Override)
   - C. Value Stem Position
   - D. Overheight Alarm
   - E. Open/Close Lights

7. Cooler Flow Valve
   - A. Manual Valve Control
   - B. Open/Close Lights

8. Heater Flow Valve
   - A. Manual Valve Control
   - B. Open/Close Lights

9. Pneumatic Indicator
   - A. Loss of pressure

Herein is presented the predicted thermal performance of the tanks. The analytical data are based upon a small computer program called STS (Solar Thermal Storage). The code is written as a design tool and is intended to produce accurate predictions inexpensively. The output from the code is a time history of the salt and tank temperatures. A running total of heat loss and charge rates are kept. From these numbers the thermal performance of the system can be determined. In Section 7.4 analytical results of the STS are compared with the experimental data from the thermal storage Subsystem Research Experiment (SRE) conducted at the Sandia National Labs in Albuquerque, New Mexico. The data from both the hot and cold tank are presented, as well as analytical results for a commercial size system.

5.3.1.1 Analytical Model - The analytical model (STS) was developed in order to support the thermal design of the salt storage tanks. This model was formulated to provide a balance between accuracy, flexibility, and computer costs.

An overall energy balance performed on a tank yields the following equation;

$$\dot{m}_c h_c - \dot{m}_d h_d - Q = \frac{d(mu)_s}{d\tau} + \frac{d(mu)_t}{d\tau} \qquad (1)$$

a mass balance results in;

$$\frac{d m_s}{d\tau} = \dot{m}_c - \dot{m}_d \qquad (2)$$

and, obviously;

$$\frac{d(m)_t}{d\tau} = 0 \qquad (3)$$

where:

h = enthalpy
m = mass
Q = heat loss from tank (positive number)
τ = time
u = internal energy
c = salt charging
d = salt discharging
s = salt in the tank
t = tank structure and insulation

Differentiating the right hand side of equation (1) and combining the result with equations (2) and (3) yields:

$$\dot{m}_c h_c - \dot{m}_d h_d - Q = u_s(\dot{m}_c - \dot{m}_d) + \dot{m}_s \frac{du_s}{d\tau} + m_t \frac{du_t}{d\tau} \qquad (4)$$

Applying the following assumptions:

1) The salt within the tank is at a uniform temperature at any given time.

2) The specific heat of the salt is a constant.

The heat transferred from the salt to the roof and walls above the salt level is determined using both radiation and free convection. The view factor of the roof is based on that between two parallel disks. The view factor from the salt to the wall is one minus the viewfactor from the salt to the roof. The free convection coefficients are based upon data for enclosed air spaces. As in the other sections the heat is conducted from the interior surfaces through the insulation. The effect of the attic space (small region between the internal insulation and shell) has been neglected. Forced convection from the wall is assumed to be that of a cylinder in cross flow, and the roof is treated as a plane in parallel flow. An average windspeed is used in the calculations of these parameters.

An overall heat transfer coefficient is calculated for the tank from the four individual coefficients. An area-weighted average system is used and is based upon the liner areas. The average ground or foundation temperature, the average windspeed and the ambient air temperature are supplied by the user.

The analytical technique described in this section was used to size the insulation for the system and to estimate the thermal performance of the salt storage tanks for several situations. The most common scenarios include the "normal day" where the system is charged and discharged for 8 hours, the "poor day" with 6 hours of charging and discharging, the "good day" with 14 hours of operation, and the solar outage where the system is charged to a certain level and held there for several weeks.

5.3.1.2 Analytical Model Results - From the various charge/discharge scenarios of the storage system the insulation thicknesses were selected as shown in Table 5.3.1-1. Other parameters of the TES sized system were discussed in Section 2.1. The STS model was used to predict heat loss and temperature profiles of the SRE tank. A charge/discharge scenario for the system is shown in Figure 5.3.1-1 where the charge and discharge rates are 3 MW. Simultaneous transfer occurs for 2 1/2 hours. The temperature profiles for the hot and cold tank are shown in Figure 5.3.1-2 and Figure 5.3.1-3. In this scenario the salt was stored in the cold tank for overnight conditions. The sensitivity of various environmental conditions were also evaluated. This was used to verify that the hot tank shell temperature would not exceed the design temperature of 288°C (550°F). Table 5.3.1-2 shows the effect of the environment on the hot tank. Very little effect is observed due to cold or hot days. The power loss was also used to size the electrical trace heaters for both tanks.

Table 5.3.1-1 SRE Insulation Materials and Thicknesses

Tank	Component	Material	Design Thickness	
			m	in.
Hot	Internal Insulation			
	Top	Holmes Flexwhite 1260 Fibrous Batt	0.508	20.0
	Side	JM C22ZSL Brick	0.343	13.5
	Bottom	JM C22ZSL Brick	0.343	13.5
	External Insulation			
	Top	Holmes 1212 Blok Board	0.254	10.0
	Side	Flexwhite 1260 Fibrous Batt	0.051	2.0
	Bottom	JM 2100 Insulating Castable	0.254	10.0
Cold	External Insulation			
	Top	Holmes 1212 Blok Board	0.381	15.0
	Side	Flexwhite 1260 Fibrous Batt	0.381	15.0
	Bottom	JM 2100 Insulating Castable	0.381	15.0

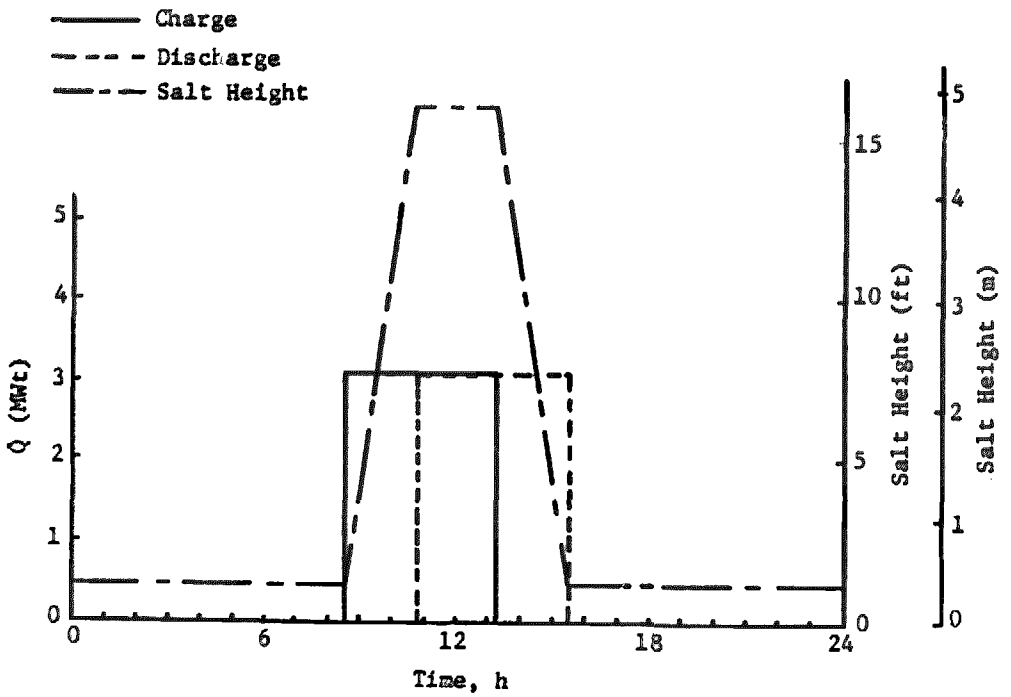

Figure 5.3.1-1 Charge/Discharge Scenario for SRE Hot Tank

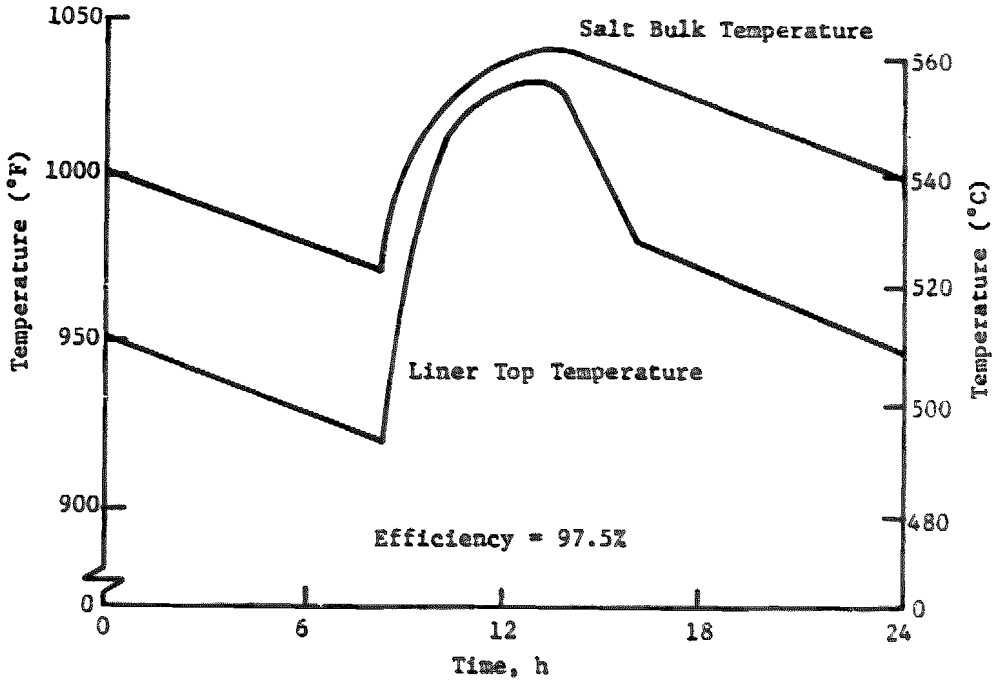

Figure 5.3.1-2 SRE Hot Tank Temperature Prediction

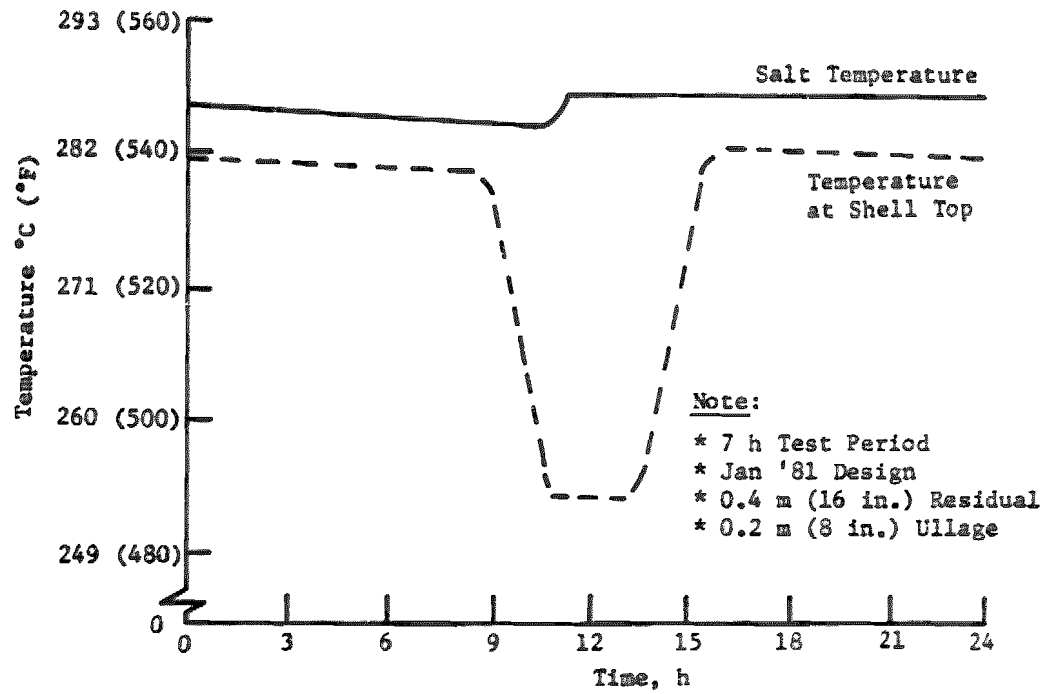

Figure 5.3.1-3 SRE Cold Tank Temperature Prediction

Table 5.3.1-2 SRE Hot Tank Thermal Predictions

Parameter	Hot Day[a] °C (°F)	Nominal Day[a] °C (°F)	Cold Day[a] °C (°F)
Salt Bulk Temperature[b,c]	559 (1038)	558 (1037)	558 (1037)
Top Shell Temperature[b,c]	269 (516)	283 (461)	231 (448)
Side Shell Temperature[b,c]	272 (522)	257 (495)	251 (484)
Bottom Shell Temperature[b,c]	265 (509)	242 (467)	231 (448)
Heat Loss Rate[b,c]	20.6 kWt	21.5 kWt	21.9 kWt

Note:

a)

Type of Day	Ambient Air Temp °C (°F)	Wind mps (mph)	Solar Flux W/m^2 (Btu/h-ft^2)
Hot	36 (96)	0 (0)	16.3 (310)
Nominal	4 (40)	2.2 (5)	0 (0)
Cold	-10 (14)	6.7 (15)	0 (0)

b) Maximum Value of Average Temperature during a Daily Charging and Discharging Scenario

c) Predictions Include Effects of Metal Shelves (Inside and Out), Anchor Pieces, Nonflat Roof, Corners, and Tank Heat Capacity--They Do Not Include Transient Diffusion or 2-D Conduction Effects

From the analysis it was determined that exterior sheathing should have a low solar absorption surface. Temperature variation through out the hot tank shell can exist due to solar heating. This increases the stress within the shell. The tank sheathing was specified to have a solar absorption of less than 0.30 and an infrared emittance greater than 0.83. Although the cold tank did not require this same coating on the sheathing it was used for commonality.

The results of the preliminary hot tank thermal analysis predicted an overall heat loss 15.18 kW, based on idealistic conditions. The effect of the following parameters were added to the program by increasing the thermal conductivity of the associated insulation:

- Brick shelves
- Insulation support rings
- Heater, piping and instrumentation penetrations
- Liner anchor ties
- Attic area

With these changes the predicted heat loss was 18.07 kW. By degrading the block and fibrous insulation by 74 and 33 percent respectively, the heat loss became 18.33 kW. Degrading the insulation values allowed for installation gaps and other effects at the joints. These values are compared to actual measured heat loss of the SRE in Section 7.0.

A commercial size system has been designed. The system is sized to have a thermal capacity of 1200 MWht. It is capable of operating a 100 MWe plant for four hours. The general specifications of the system are presented in Table 5.3.1-3. The STS code predicted heat loss rate for a normal Barstow, CA day would be 1.5 MWt. This results in a salt temperature drop of 1°C (2°F) per day for a full hot tank. The calculated thermal efficiency of this system is 98%, based on equation (8).

Table 5.3.1-3 Commercial Storage System Specifications

Storage Media	Molten Salt (60% $NaNO_3$, 40% KNO_3 by wt.)
Tank Configuration	Dual Tanks (Hot and Cold)
Storage Capacity	1200 MWht
Hours of Storage	4 hours (120 MWe plant)
Hot Salt Tank	
Insulation Type	Internal
Liner Diameter	24.5 m (80.33 ft)
Maximum Salt Height	13.2 m (40.33 ft)
Nominal Salt Temperature	566°C (1050°F)
Cold Salt Tank	
Insulation Type	External
Shell Diameter	25.2 m (82.5 ft)
Maximum Salt Height	11.3 m (37.25 ft)
Nominal Salt Temperature	288°C (550°F)
Maximum Charge Rate	480 MWt
Maximum Discharge Rate	300 MWt

$$\text{Efficiency} = \frac{\text{Energy Discharged}}{\text{Energy Charged}} \qquad (8)$$

The high system efficiency indicates that this design is an excellent way of storing high temperature thermal energy.

The STS code effectively predicts the performance of the storage system. The comparison with the experimental results indicate that the program can be used with a high degree of confidence.

Preliminary experimental results indicate that internally insulated tanks are practical for this type of energy storage system. Also the overall energy storage concept presented here has been shown to be appropriate for solar thermal central receiver systems and, indeed, this technology is ready for commercialization.

5.3.1.3 Hot Tank Foundation Thermal Analysis

Thermal analysis on the hot tank foundation was performed using a standard heat transfer method. The representative area selected is shown in Figure 5.3.1-4. It contains a 0.3 m (1 ft) length of cooling pipe with its associated concrete, castable insulation, and tank floor. The cooling pipe was 25.4 mm (10 in.) standard steel pipe installed on 0.3 m (12 in.) centers. The pipe was located in the foundation to provide a minimum of 38 mm (1.5 in.) of concrete cover. The recommended thickness of the external castable insulation was 0.25 m (10 in.).

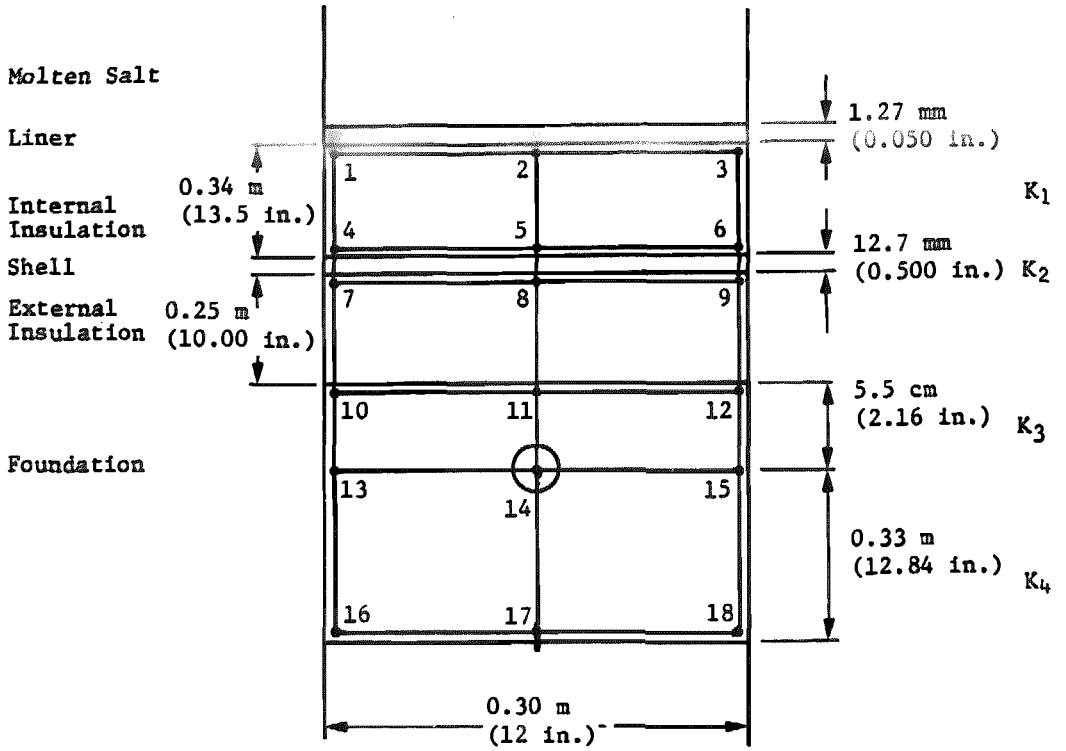

Figure 5.3.1-4 Representative Hot Tank Foundation Area

The thermal conductivity of the materials is given in Table 5.3.1-4. The molten salt temperature is 566°C (1050°F) and the ambient temperature was taken as 36°C (96°F) maximum. Based on the coolant heat rejection system the cold water inlet temperature assumed was 49°C (121°F). A maximum temperature rise of 5.6°C (10°F) was used. It was also assumed that the foundation temperature was maintained at 49°C (120°F) at the air or earth interface.

Table 5.3.1-4 Material Thermal Conductivities

Material	K (W/m-c°)	K (Btu/h-ft-F°)
Internal Insulation	0.265	0.153
External Insulation	0.242	0.140
Steel Shell	43.3	25
Concrete Foundation	1.21	0.70

The analytical results are given in Table 5.3.1-5 for the maximum hot day condition. The desired temperature of 288°C (550°F) at the tank shell was achieved within 2°C (3.6°F).

Table 5.3.1-5 Hot Tank Foundation Node Temperatures

	TEMPERATURE			TEMPERATURE	
Node	°C	°F	Node	°C	°F
T_1 =	566	1050	T_{10} =	68	154.3
T_2 =	566	1050	T_{12} =	63	145.7
T_3 =	566	1050	T_{13} =	68	154.3
T_4 =	289.6	553.2	T_{14} =	60	139.2
T_5 =	289.5	553.1	T_{15} =	52	126
T_6 =	289.6	553.2	T_{16} =	60	139.2
T_7 =	289.5	553.1	T_{17} =	49	120
T_8 =	289.4	553.0	T_{18} =	49	120
T_9 =	289.5	553.1	T_{19} =	49	120

The amount of coolant flow required to maintain these node temperatures was calculated as 7.0 liters/min. (1.85 gpm) based on a coolant Cp of 0.871 calories/gram-°C (0.871 Btu/lb-°F).

5.3.1.4 Hot Tank External Shell Stress Analysis - An analysis of the steel shell of the hot tank was performed using a finite element computer program. The program is titled SAP IV and was developed by the Earthquake Engineering Research Center at the University of California in Berkeley. Load cases for hydrostatic pressure, temperature gradient, seismic loading, and wind and snow were used.

Because of the size of the tank and the ratio of thickness to radius, 4 node, flat, shell elements were used. Due to the size of the PRIME 250 mini-computer two models were used. The first model, shown in Figure 5.3.1-5 includes the top inlet pipe but not the upper support ring, and was used to evaluate top cover stresses. The second model, shown in Figure 5.3.1-6 has the upper support ring but not the inlet pipe and was used to study the effects of the ring and of the thermal gradients near the ring.

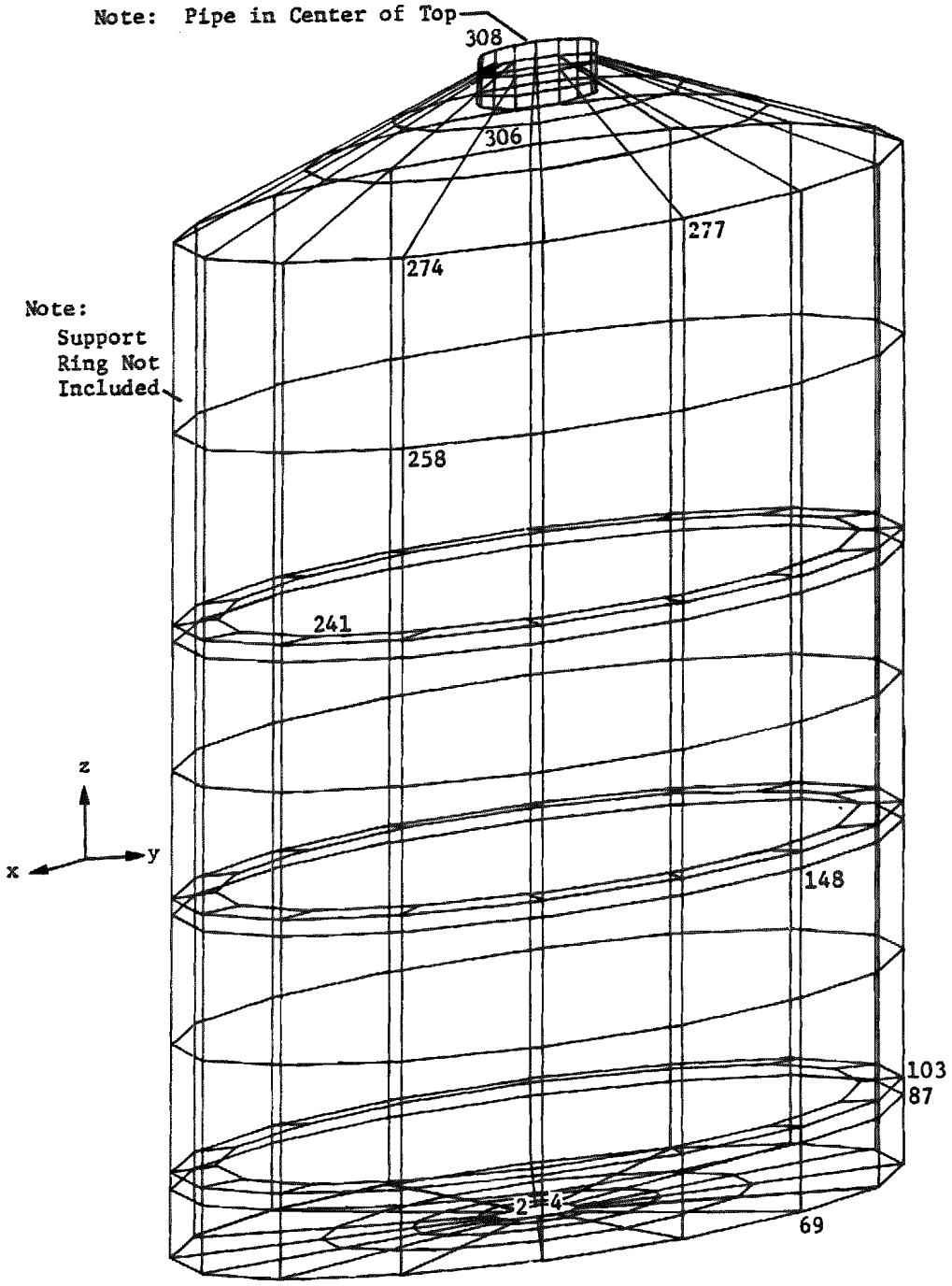

Figure 5.3.1-5 Hot Tank Model with Center Pipe

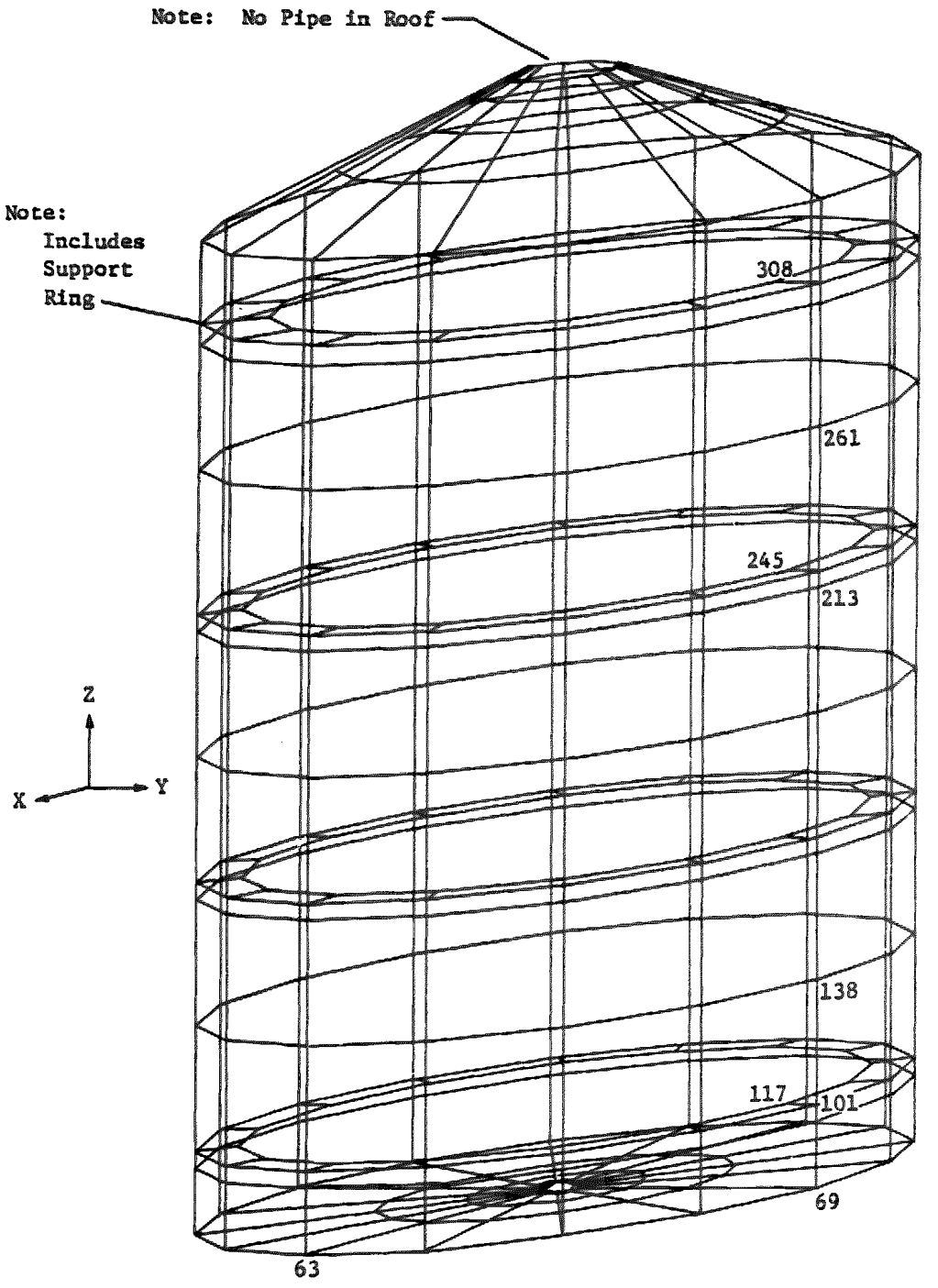

Figure 5.3.1-6 Hot Tank Model Without Center Pipe

Necessary input data for each element includes pressure normal to the surface, and the temperature at the center which was considered to be the mean temperature.

The modeling assumptions include; (1) fixing the inner and outer row of bottom node points in the Z direction as shown in Figure 5.3.1-7, (2) fixing of four center bottom nodes, as shown in Figure 5.3.1-8 to prevent rotation due to nonaxis-symmetrical seismic and wind loading, and to allow thermal expansion, 3) the ground exactly reacting any load against it, hence no pressure need be applied to the bottom elements and 4) fixing of all bottom nodes against rotation about the Z axis, due to type of elements used. Some loading assumptions are shown in Figures 5.3.1-9 and 5.3.1-10 and include hydrostatic pressure and seismic effect where seismic effect is obtained by multiplying the hydrostatic pressure by a seismic coefficient.

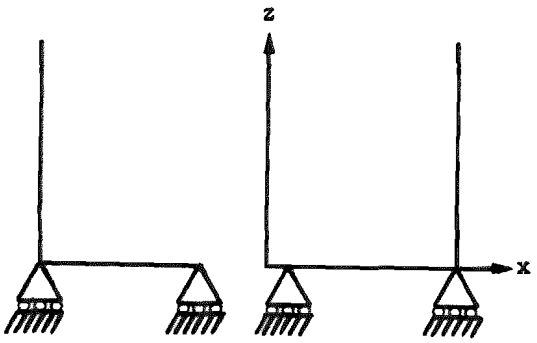

Figure 5.3.1-7 Vertical Fixity at Base

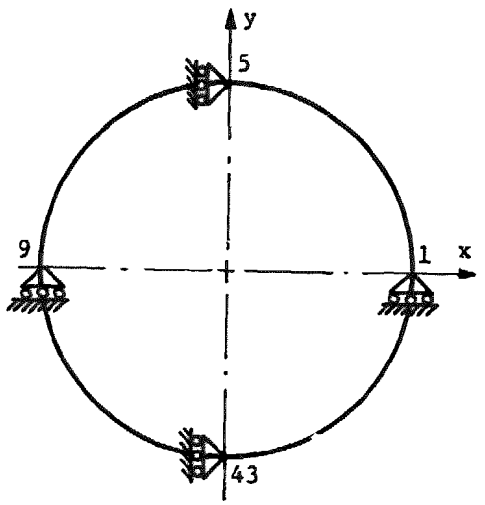

Figure 5.3.1-8
Rotational Fixity at Base

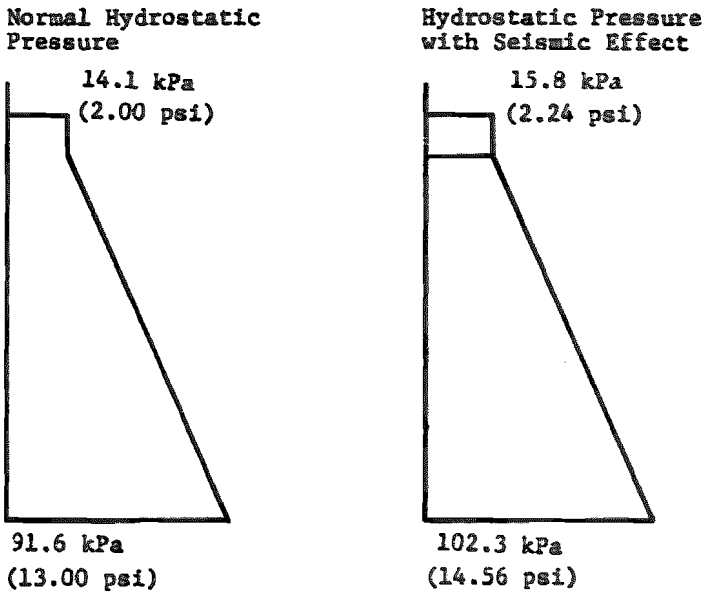

Figure 5.3.1-9 Hydrostatic Pressure Distribution

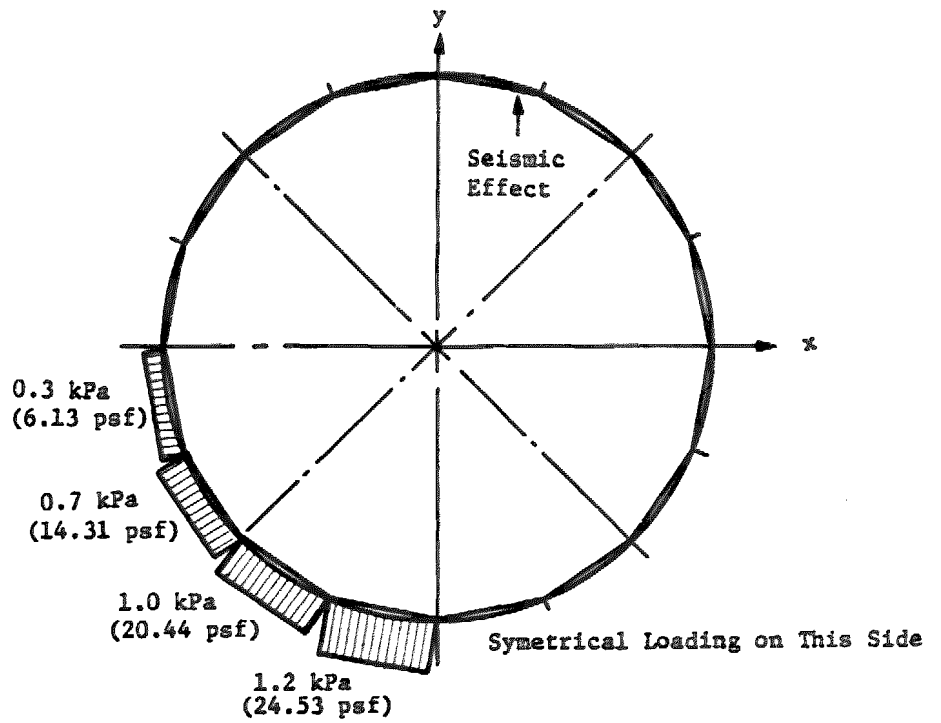

Figure 5.3.1-10 Environmental Loading of Steel Shell

The cover loads include pressure weight of suspended liner and insulation which is distributed to nodes approximating anchor points, and weight of bricks which is applied as a pressure at the corners. Thermal loading on the first model, with the inlet pipe and without the upper support ring, considered only the temperature gradient due to the corners. Thermal loading for the second model with the upper support ring and without the inlet pipe, consisted of both the thermal gradient due to the corners and at the level of the upper support ring.

The output from the SAP IV program consisted of node rotation and displacement for each axis, membrane stresses T_x, T_y, and T_{xy} for each element, and moment per unit length for each element. The principal stresses can then be derived from equations 1 and 2.

$$\sigma_1 = \frac{\sigma_x + \sigma_y}{2} + \sqrt{\left(\frac{\sigma_x - \sigma_y}{2}\right)^2 + T_{xy}^2} \qquad (1)$$

$$\sigma_2 = \frac{\sigma_x + \sigma_y}{2} - \sqrt{\left(\frac{\sigma_x - \sigma_y}{2}\right)^2 + T_{xy}^2} \qquad (2)$$

Examination of the first model output showed, as expected, that the pressure and weight loads give low stresses. The stresses resulting from thermal effects were somewhat higher. In the shell a maximum stress of 30 MPa (4270 psi) occurs on the bottom and on the lower part of the side, and for the support rings the maximum stress was 86.1 MPa (12,240 psi). Also, all of the side wall deflections are close to 6.5 mm (0.26 in.).

The second model (refer to Fig. 5.3.1-4) showed a maximum shell stress of 53.5 MPa (7600 psi) just below the upper support ring. The ring stresses and wall deflections were similar to those in the first model. The vertical displacement of nodes around the top of the wall is approximately 23.85 mm (0.938 in.).

Additional evaluation was done for the case of thermal gradients between the side and cover and between the side and bottom. These calculations showed that these thermal gradients must be kept less than or equal to 80°C (144°F). The maximum stress was then 95 MPa (13,500 psi).

The allowable stress in steel was 122 MPa (17,350 psi) which shows that the tank design is satisfactory.

5.3.1.5 Hot Tank Foundation Stress Analysis - Maximum soil bearing pressures were calculated by Stearns-Roger for the hot salt storage tank foundation. The maximum calculated bearing pressure was 0.127 MPa (2,590 psf) resulting from a combination of seismic and weight loads. This may be compared to an allowable of 0.13 MPa (2,660 psf).

The foundation was designed to an outside diameter of 4.4 m (14.5 ft). The foundation design is depicted in Figure 5.3.1.11. All concrete elements of the foundation were reinforced with steel rod varying in size from 12.7 mm (0.5 in.) to 19.0 mm (0.75 in.). Access to the air space within the ring wall was provided by two 0.91 m (3 ft) square opening, which were surrounded by additional reinforcing rod to provide the necessary strength.

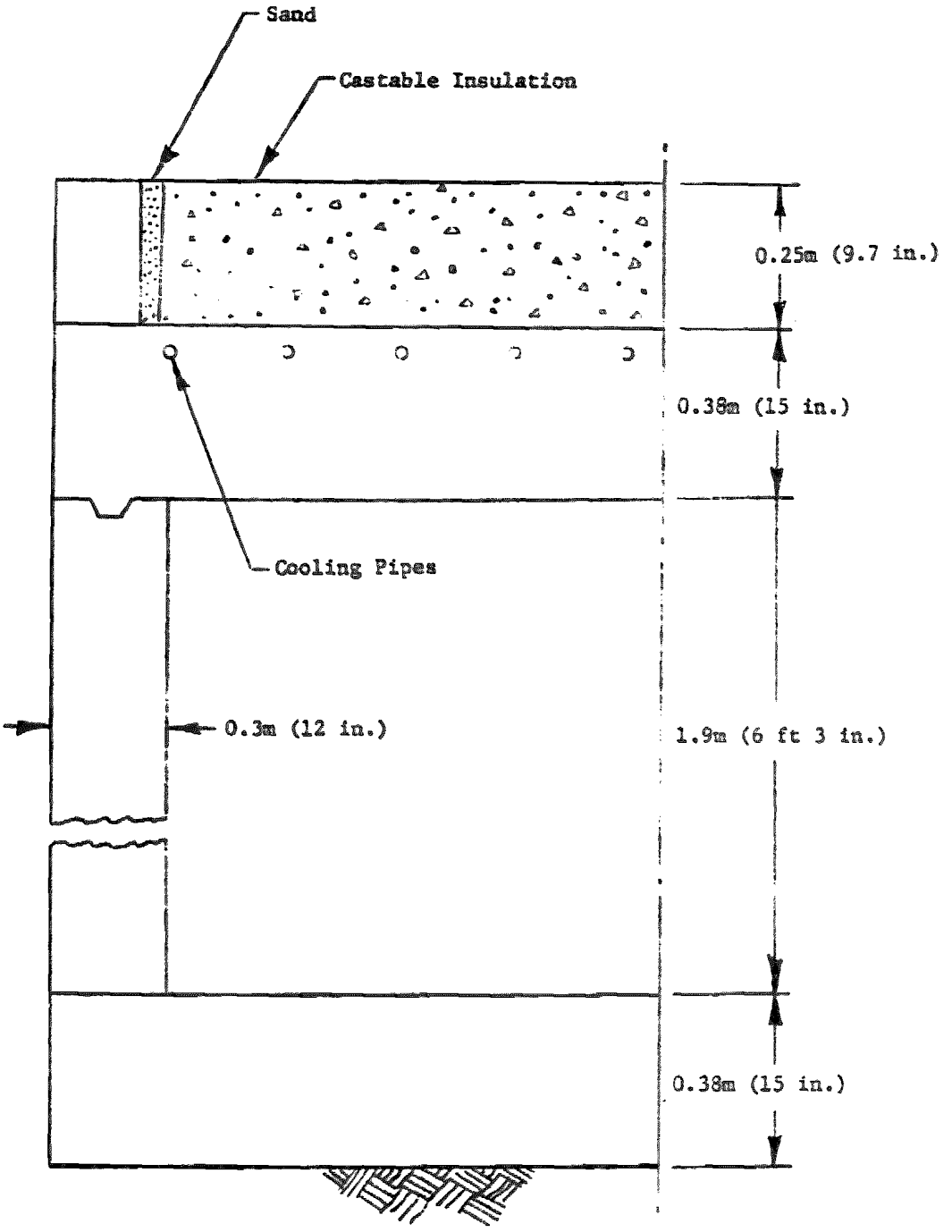

Figure 5.3.1-11 Hot Tank Foundation Configuration

5.3.2 Cold Tank Analysis

5.3.2.1 Cold Tank Thermal Analysis - For cold salt storage, the temperature of the molten salt [288°C (550°F)] was low enough to use carbon steel for the shell. While there was some decrease in strength allowable at this temperature, carbon steel still provides an adequate factor of safety for operational load conditions. This factor eliminated the requirement for an internal liner and permitted use of low cost fibrous external insulation to minimize tank heat loss. (Refer to Fig. 5.3.1-3).

The cold tank thermal analysis was performed using the same analytical model used for the hot tank (see paragraph 5.3.1.1).

The results of the cold tank thermal analysis indicate that for a salt height of 0.2 m (0.6 ft) the heat loss should be 4.94 kW. This prediction is compared with SRE experimental heat loss in Section 7.0.

5.3.2.2 Cold Tank Foundation Thermal Analysis - The thermal analysis for the cold tank foundation was a simplified version of the hot tank analysis, in that there is no internal liner and consequently fewer node points. The representative section of the foundation is shown in Figure 5.3.2-1. It contained a 0.3 m (1 ft) length of cooling pipe, foundation concrete, castable insulation and the tank floor. The cooling pipe was 25.4 mm (1.0 in.) standard steel pipe installed on 0.30 m (12 in.) centers. A minimum of 3.8 cm (1.5 in.) of concrete cover was provided over the cooling pipes. The recommended thickness of the castable insulation was 0.37 m (15 in.).

The molten salt temperature was 288°C (550°F) and the ambient temperature was taken at 36°C (96°F) maximum. It was assumed that the cooling water entered at 49°C (121°F) and that the outlet temperature increased 5.6°C (10°F). It was also assumed that the foundation was maintained at 38°C (100°F) at the air or earth interface.

The analytical method used was a two dimensional conduction heat transfer model using linear equations to describe the heat flow, as used for the hot tank foundation analysis (Section 5.3.1.2). Nodes 1, 2, and 3 were at 288°C (550°F) and nodes 10, 11, and 12 were held at 38°C (100°F). (See Fig. 5.3.2-1 for node locations.)

The results of this analysis is shown in Table 5.3.2-1.

Table 5.3.2-1 Cold Tank Foundation Node Temperatures

Node	TEMPERATURE °C	TEMPERATURE °F	Node	TEMPERATURE °C	TEMPERATURE °F
T_1 =	288	550	T_7 =	55.4	131.8
T_2 =	288	550	T_8 =	52.2	126
T_3 =	288	550	T_9 =	55.4	131.8
T_4 =	61.4	142.5	T_{10} =	37.8	100
T_5 =	59.4	138.9	T_{11} =	37.8	100
T_6 =	61.4	142.5	T_{12} =	37.8	100

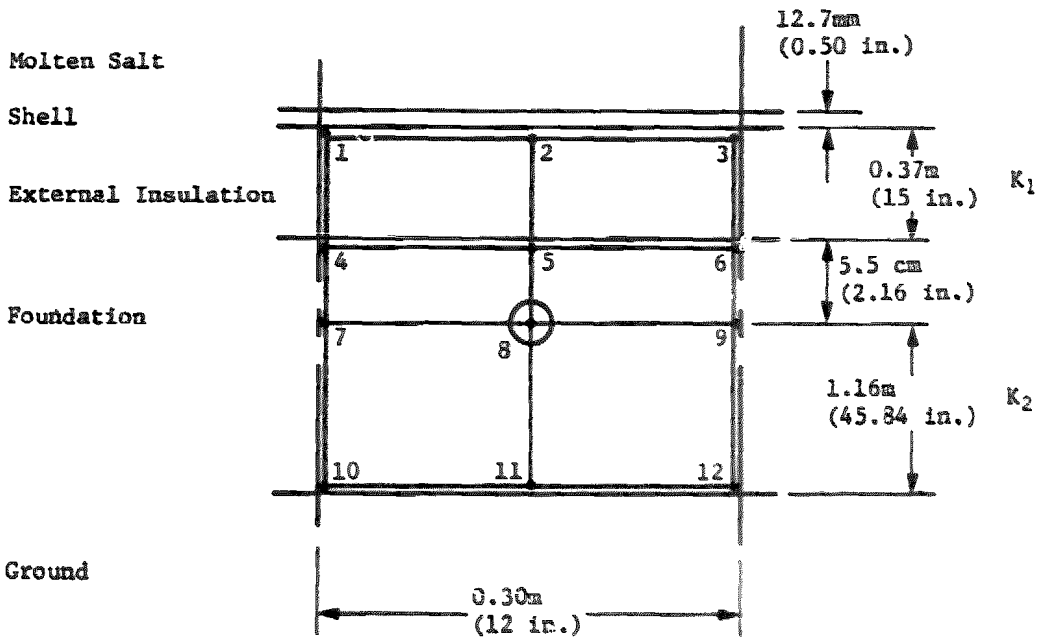

Figure 5.3.2-1 Representative Cold-Tank Foundation Area

The amount of coolant flow required to maintain these node temperatures, based on a coolant Cp of 0.087 calories/grams-°C (Btu/lb-°F) at 52°C (126°F) and a foundation diameter of 3.75 m (12.29 ft), was calculated as 4.7 l/min (1.25 gpm).

5.3.2.3 Cold Tank Shell Stress Analysis - Analysis of the cold tank steel shell indicated a maximum compressive stress level of 1.5 MPa (212 psi). The allowable compressive stress level for A516 grade 70 carbon steel is 3.15 MPa (4,500 psi), which provided a large factor of safety. Analysis also indicated that for the maximum seismic or wind loading, the resulting overturning moment was small enough that anchor straps to the foundation would not be required.

5.3.2.4 Cold Tank Foundation Stress Analysis - The cold tank foundation stress analysis was performed by Stearns-Roger to check the maximum bearing pressures. Under normal operating conditions the predicted bearing pressure was 0.08 MPa (1,740 psf) and under seismic conditions a value of 0.11 MPa (2,330 psf) was predicted. This may be compared to an allowable value of 0.13 MPa (2,660 psf). The foundation was reinforced with number 6 reinforcing rods [19 mm (0.75 in.) diameter] on 0.3 m (12 in.) centers.

5.3.3 Hot Sump Analysis

5.3.3.1 Hot Sump Thermal Analysis - The analysis assumed an outside ambient temperature of 37.8°C (100°F) and an internal temperature of

566°C (1050°F). Thermal conductivity of the fibrous insulation was 0.07 W/m-°C 0.045 (Btu/ft-h-°F). This insulation was placed on the top and sides of the sump.

Heat loss was calculated at 0.40 kW (1370 Btu/h) for the top of the tank, 1.61 kW (5,450 Btu/h) for the side and 0.40 kW (1,360 Btu/h) for the bottom. The total sump heat loss predicted was 2.41 kW (8,180 Btu/h). The heat loss through the pump was 550 watts. To replace the 2.96 kW loss, 3.9 kW electrical heaters were used.

5.3.3.2 Hot Sump Stress Analysis - The hot sump stress analysis was performed using a NASTRAN static analysis. The loading conditions are shown in Figure 5.3.3-1. This loading has the pump weight and the pressure which would occur if the full pressure head of the hot tank were applied to the sump. The tank material thicknesses were sized to provide a factor of safety of 2.0 over the allowable coded values of 304 stainless steel at 566°C (1050°F). The wall thickness was .32 cm (.125 inch); the top plate was 1.3 cm (.5 inch), and the bottom was a 0.64 cm (.25 inch) plate with stiffeners.

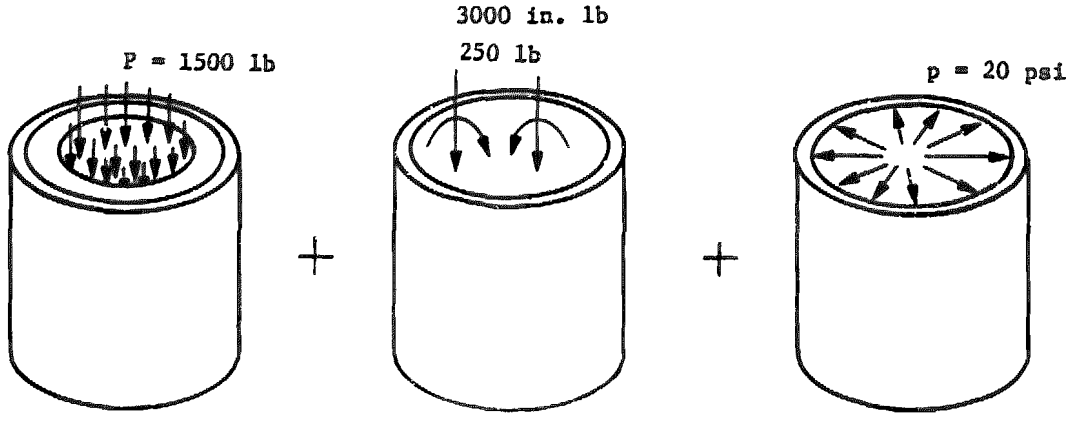

Figure 5.3.3-1 Hot Sump Loading Conditions

5.3.4 Cold Sump Analysis

5.3.4.1 Cold Sump Thermal Analysis - Re-evaluation of the cold sump thermal analysis was not performed for this test. Previous operations indicated adequate temperature margin. The tank had more trace heaters than necessary to maintain design temperatures.

5.3.4.2 Cold Sump Stress Analysis - The cold sump stress analysis was performed using a NASTRAN static analysis. The loading conditions are shown in Figure 5.3.4-1. This pressure loading accounted for a possible failure mode which would allow the full height of the cold tank to be applied to the cold sump. The maximum stresses in the sump occurred on the bottom plate; 171 MPa (24,316) in tension and 169 MPa (23,991 psi) in compression. At 316°C (600°F the value of the compressive yield allowable is 172 MPa (24,570 psi) and the tensile yield

allowable is 176 MPa (25,200 psi). This provided a margin of safety of 2.5% for worst case sump loading. The small margin was considered adequate since it would result in a failure mode which would have a limited time duration.

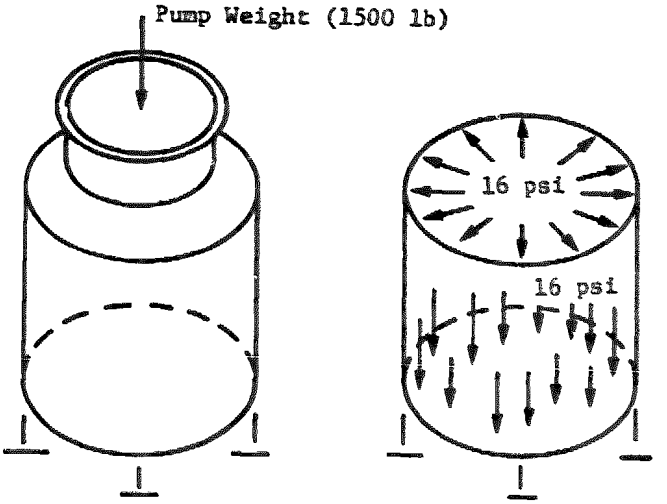

Figure 5.3.4-1 Cold Sump Loading Conditions

5.3.5 Salt Transfer Line Analysis

5.3.5.1 Salt Transfer Line Thermal Analysis - The insulation of the lines was not sized for optimum cost or for minimum heat loss. The insulation thickness was selected to maintain the external insulation below 50°C (140°F) when the line was at its maximum temperature. The lines were insulated with a calcium silicate, except at the elbows which had fibrous insulation. The heat loss to be replaced by the trace heaters was calculated with the lines at 332°C (630°F) [except for line #1 which was 566°C (1050°F)] and at 43°C (110°F) ambient temperature. It was necessary that line #1 be maintained at 566°C (1050°F) to prevent cold salt from causing thermal shock of the hot pump. The line insulation and heat losses are in Table 5.3.5-1.

Table 5.3.5-1 Heat Loss Salt Transfer Lines

Pipe No.	Pipe Size mm (in.)	Pipe Insulation mm (in.)	Heat Loss W/0.3m (W/ft)
1	50.8 (2)	63.5 (2.5)	35.9
2	50.8 (2)	114.3 (4.5)	27.4
3	101.6 (4)	127.0 (5)	36.6
4	76.2 (3)	114.3 (4.5)	33.5
5	76.2 (3)	76.2 (3)	41.2
6	76.2 (3)	76.2 (3)	41.2

There was no thermostatic control on the line heaters. The correct balance between the heaters and heat loss was used to maintain the temperature.

5.3.5.2 Salt Transfer Line Stress Analysis - Stress analysis of all salt transfer lines was performed by Stearns-Roger. Analysis included weight, pressure and thermal expansion loads. The results of the hot line (number one) between the hot tanks and the hot sump, is used as an example of the tasks completed. The line routing diagram is shown in Figure 5.3.5-1. The large number of bends in the line were inserted to allow the line to act as a spring, thereby reducing the magnitude of the thermal expansion stress loads which would be experienced in straight line segments. Pipe hangars were designed to permit unrestrained thermal expansion. The temperature of the molten salt was assumed to be 566°C (1050°F) and the pressure of the fluid in the line was taken 0.14 MPa as (20 psig) maximum. The pipe was a schedule 10, 316 stainless steel. The thickness of the calcium silicate insulation was 12.7 mm (5 in.). Deflection at line end points were used in conjunction with the above data and loads were determined using a computerized analysis. The number and location of expansion loops and pipe hangars were varied until the desired stress levels were achieved. The maximum stress level, based on these loads, was 190 MPa (27,187 psi) compared to an allowable of 256 MPa (36,625 psi). The equipment connection forces and moments are given in Table 5.3.5-2.

5.3.6 Pressure Loss Analysis

To determine valve and sump requirements it was necessary to determine the pressure loss in each of the salt transfer lines. Most of the valves and the cold sump were taken from ACR Phase II program so the SRE line designs were made compatible. Limiting the vertical drop of the tank outlet lines increased their diameters. The pipe sizing was an iterative process with the line stress analysis. As a line became larger in diameter, thus stiffer, it was necessary to add expansion loops which increased the line lengths. Sizing of the lines had to be compatible with the valve flow resistances. The pressure loss of the lines, as determined by a Stearns-Roger computer program, is listed in Table 5.3.6-1.

5.3.7 Miscellaneous

The analyses described above cover only the major components of the SRE. Analysis of numerous other components (i.e., pump and sump building foundation, ladder tower, pipe supports) was also performed. A complete list of analytical tasks performed is contained in Appendix C.

Table 5.3.5- Line No. One Connection Forces and Moments

Equipment Connections	Forces							
	x		y		z		Resultant	
	kg	lb	kg	lb	kg	lb	kg	lb
Hot Tank Outlet								
Thermal	64	141	44	96	3	6	78	171
Weight	-8	-17	-100	-220	5	11	100	221
Resultant	56	124	-56	-124	8	17	80	176
Hot Sump Inlet								
Thermal	-86	-190	-39	-87	75	166	121	267
Weight	0	0	-20	-44	0	0	20	44
Resultant	-86	-190	59	131	75	166	129	284

Equipment Connections	Moments							
	x		y		z		Resultant	
	kg-m	ft-lb	kg-m	ft-lb	kg-m	ft-lb	kg-m	ft-lb
Hot Tank Outlet								
Thermal	1.8	13	3.7	27	24.3	176	24.7	179
Weight	-2.4	-17	1.4	10	-2.9	-21	4.0	29
Resultant	-0.6	-4	5.1	37	21.4	155	22.0	159
Hot Sump Inlet								
Thermal	-29.3	-212	147	1066	-0.6	-4	150	1087
Weight	0	0	-0.6	-4	2.6	19	2.8	20
Resultant	-29.3	-212	147	1062	2.1	15	150	1083

Table 5.3.6-1 Pressure Losses in Salt Transfer Lines

Line No.	Pressure Loss	
	MPa x 10^{-3}	psi
1	18.8	2.69
2	15.8	2.26
3	3.5	0.50
4	5.8	0.83
5	10.1	1.44
6	4.7	0.67

6.0 SRE Fabrication

6.0 SRE FABRICATION

Most of the fabrication of the SRE was performed onsite at the CRTF except for the hot tank liner elements and tank subassemblies which were fabricated by Glitch Field Service, Inc. in Dallas, TX. The hot sump and the control console were built by Martin Marietta Denver Aerospace. All of the site preparation, foundations, piping and buildings were done by Stearns-Roger. All of the thermal insulation of the tanks and piping was done by American Enterprises, Inc. at Albuquerque, NM under subcontract to Martin Marietta Aerospace. Most of the electrical work including the installation of all the cable trays and conduit was performed by Sunrise Electric Co. under subcontract to Martin Marietta Aerospace. Martin Marietta Aerospace and Sandia supported all of the subcontractors and installed all of the instrumentation, controls, pneumatics, cooling water systems and performed the checks required. The fabrication started in June 1981 and was completed in January 1982.

6.1 SITE PREPARATION

Figure 6.1-1 shows the SRE site layout, which was located south and west of the CRTF tower. This location will provide easy hookup to a molten salt receiver prototype in the future. A view of the site in a preliminary construction stage is shown in Figure 6.1-2. This view is from the CRTF tower. The cylindrical structure seen at the far left of the picture is the hot tank foundation. The molten salt drain hole may be seen in the center of the foundation. To the lower right of the hot tank foundation is the cold tank foundation location. Framing for the concrete, reinforcing rod and foundation coolant tubes are being put in place. Directly above the cold tank foundation is the sump building which houses both the hot and cold sumps. To the left of the sump building is the pad which will support the propane heater. The control building for the SRE is located to the right of the sump building. At this stage only the floor slab has been poured.

Below the control building is a small pad where the electrical transformers will be located. The space between the transformer pad and the cold tank foundation is allocated for the air cooled heat exchanger. Preparation of this site included removal of two heliostat foundations and removal of the blacktop in the area. Figure 6.1-3 shows a side view of the SRE during this same stage of initial construction.

Once the hot and cold tank foundations had been poured and had adequately cured, the castable insulation was poured in place. This operation is taking place in Figure 6.1-4 and Figure 6.1-5 shows a side view of the foundation after completing this step. The air cooled heat exchanger may be seen in the background. This item had been previously used in two earlier power system programs, thereby reducing the overall cost of the SRE. Figure 6.1-6 is a view from the CRTF tower. At this stage the castable insulation task had been completed and some back filling of dirt had been done. In the upper right hand corner is the air cooled heat exchanger, which was being stored at this location prior to placement in the SRE.

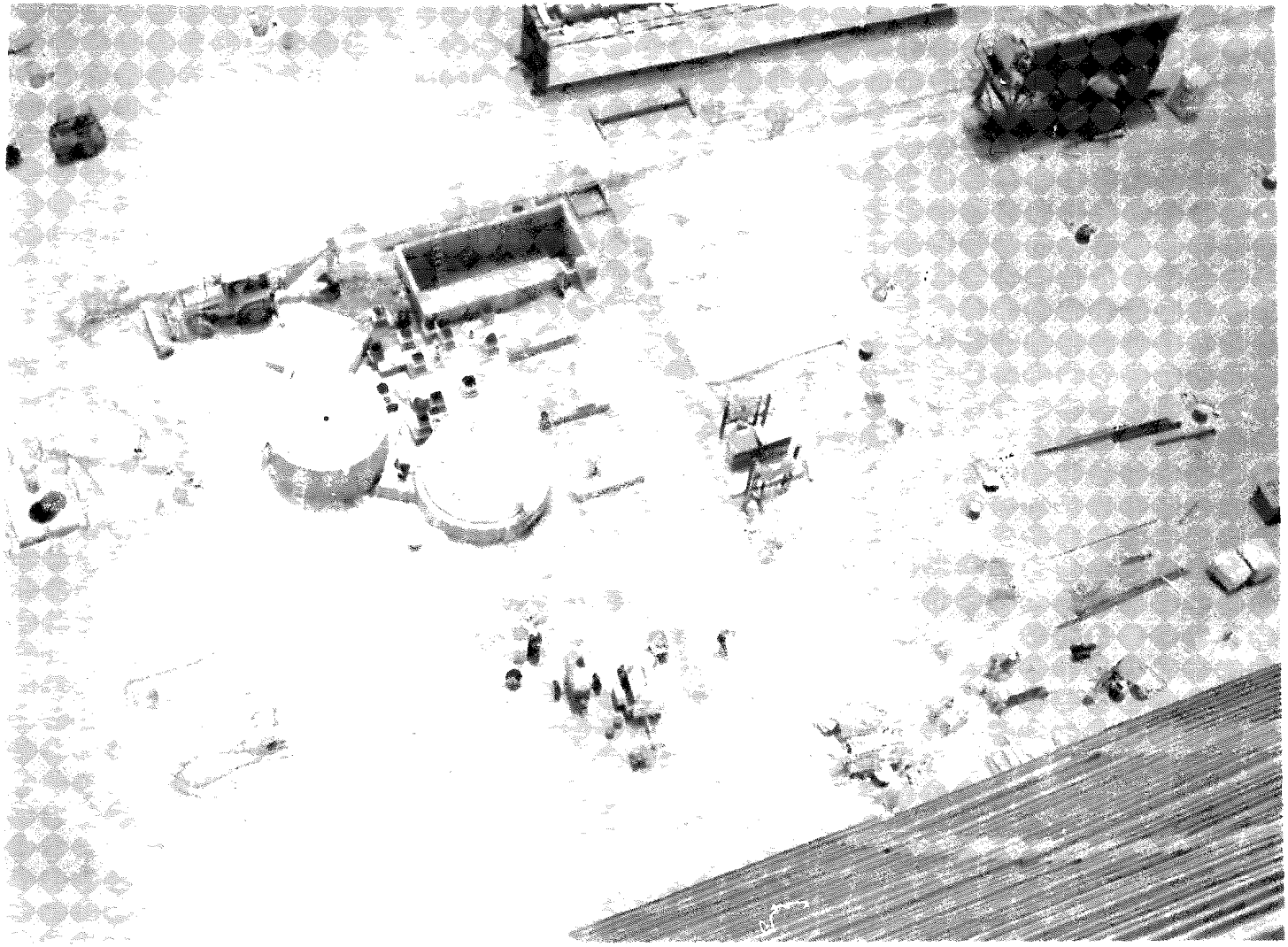

Figure 6.1-1 SRE Site Layout

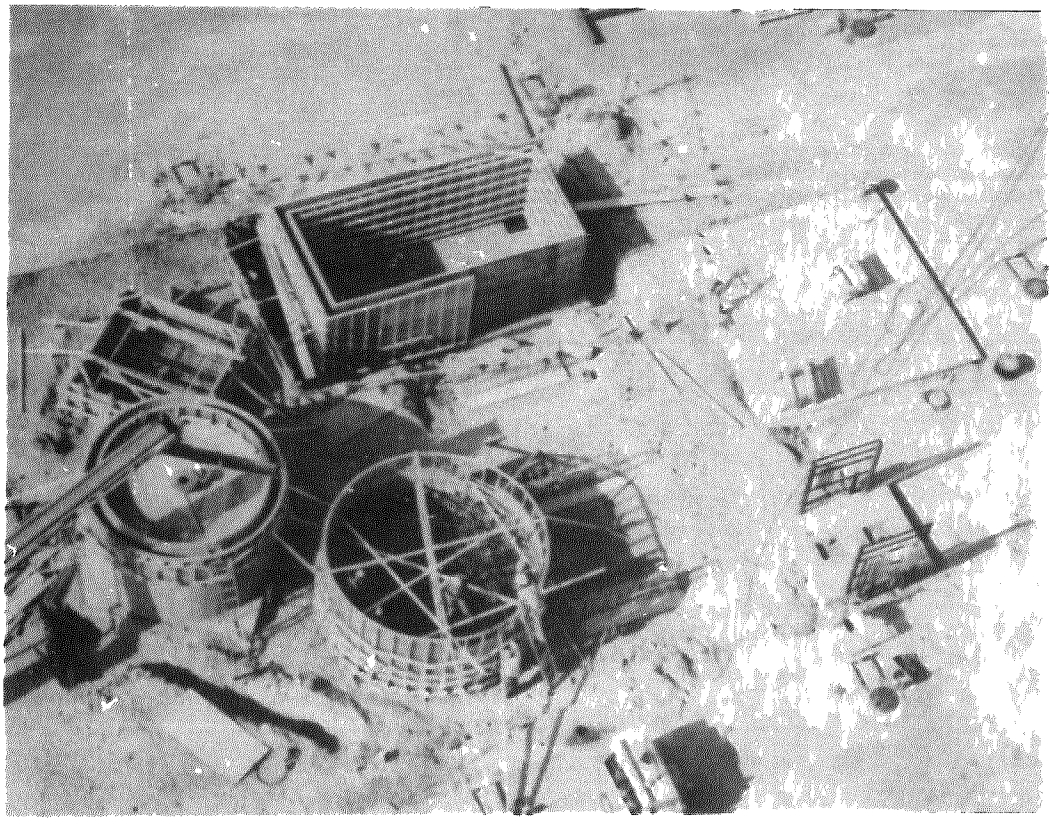

Figure 6.1-2 Early Site Construction Stage

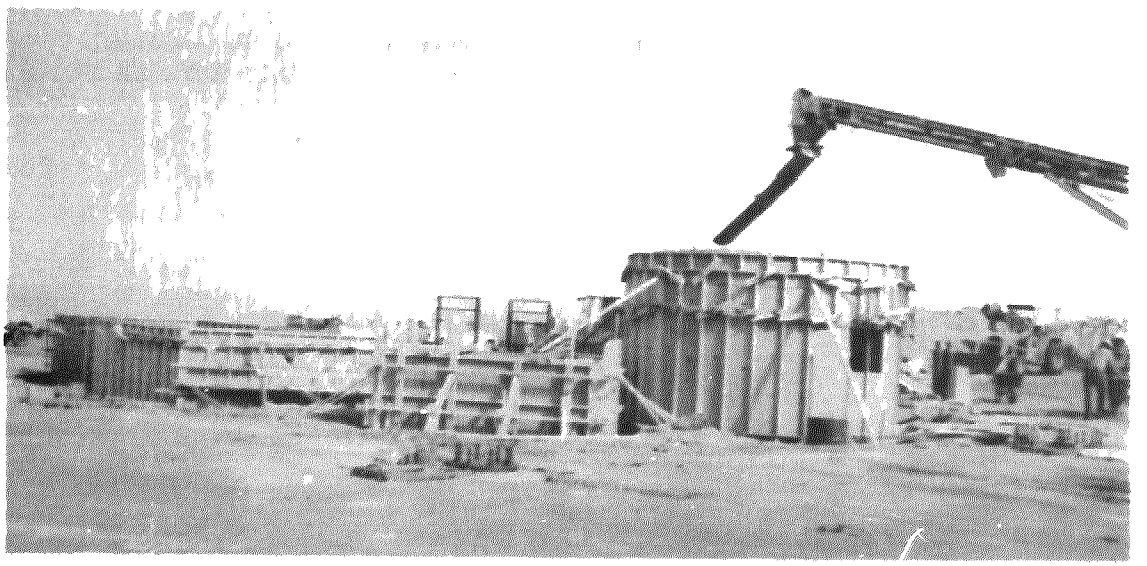

Figure 6.1-3 Side View of SRE Site During Initial Construction

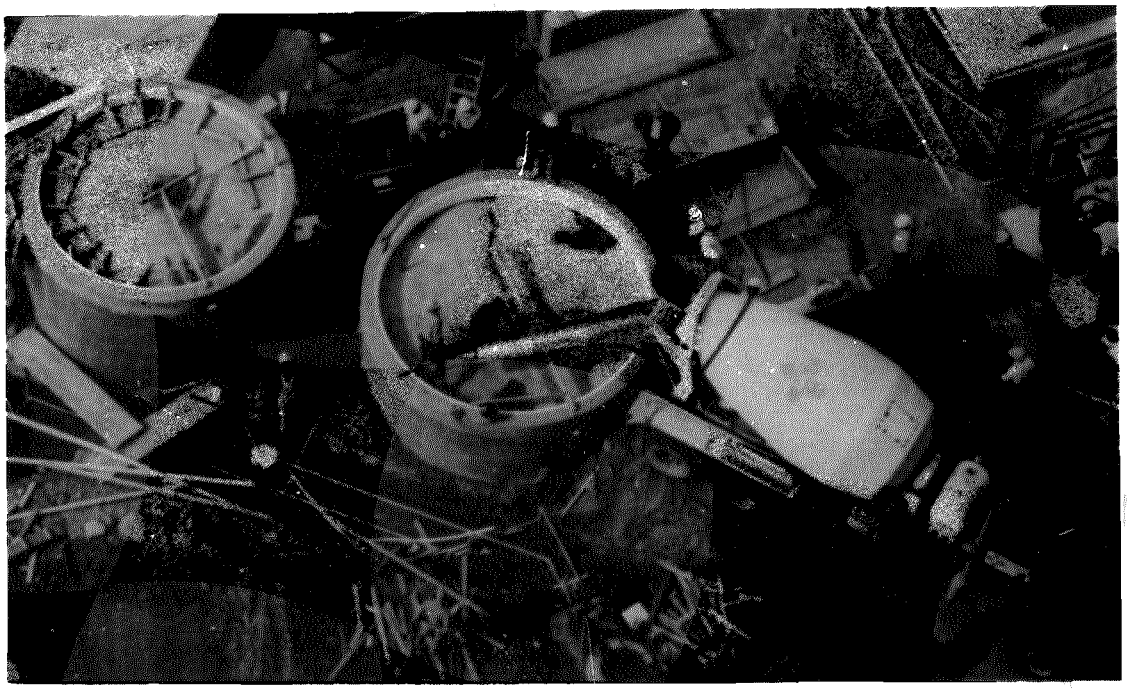

Figure 6.1-4 Pouring Castable Insulation

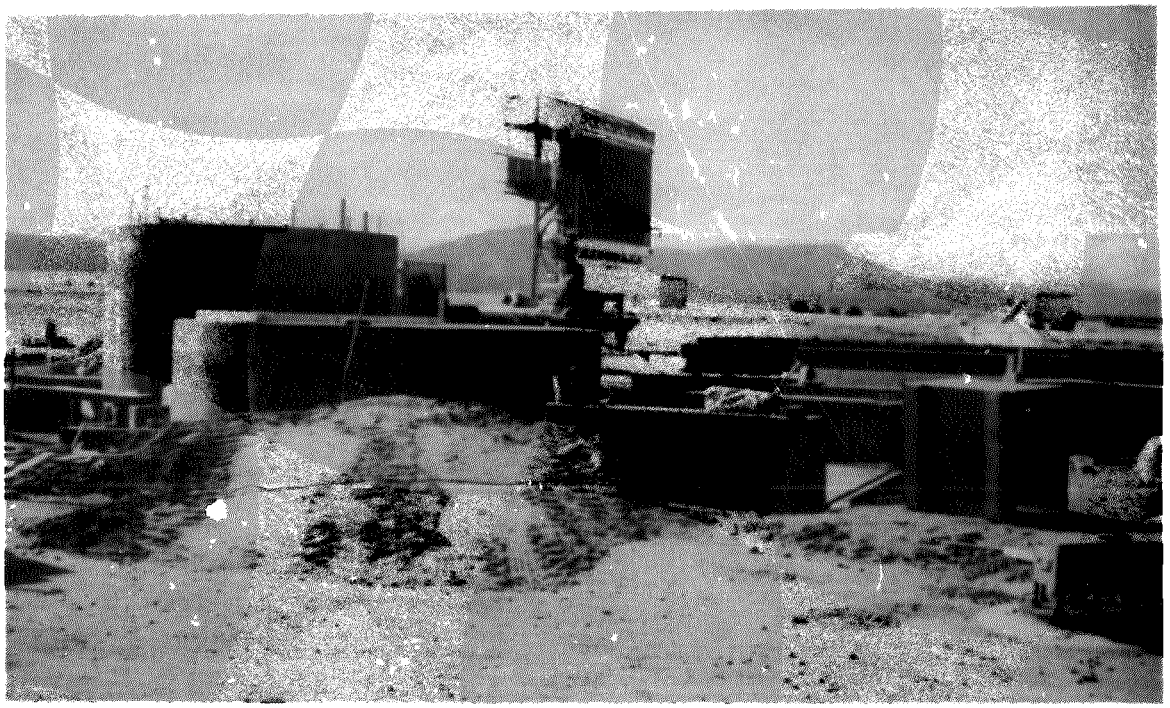

Figure 6.1-5 Side View of Completed Foundations

Figure 6.1-6 Castable Insulation Installed

In Figure 6.1-7 the air cooled heat exchanger has been placed in its permanent position. The walls of the control building have been erected and the 6 mm (1/4 in.) thick carbon steel plates, for the bottom of the hot and cold tanks, have been set into place. A tank shell half-ring can be seen being readied for lifting into place in the bottom of the figure. All back fill and formation of the hot salt overflow retaining dike has been completed at this stage. Figure 6.1-8 shows a side view of a tank shell half ring being readied for placement.

The shells of the hot and cold storage tanks have nearly been completed in Figure 6.1-9. The roof of the SRE control building has been completed. The cold sump and pump, which had also been used in Phase II of the ACR power system program, have been installed in the middle of the sump building. The sump of the hot pump has also been fabricated. The pump has been installed on the hot sump in Figure 6.1-10. At this point in time, some of the piping has also been installed.

Figure 6.1-11 shows the initial stages of the propane heater installation. The crane in the background is preparing to lift the base of the heater into place and the cabin of the heater is lying on its side to the left of the site. Installation of the cold tank roof has been completed. The insulation support ring gives it a hat-like appearance.

Installation of the propane heater has been completed in Figure 6.1-12. Several pallets of insulating firebrick can be seen in the foreground and some bricks have been placed at the top of the hot storage tank in preparation for installation of the internal insulation.

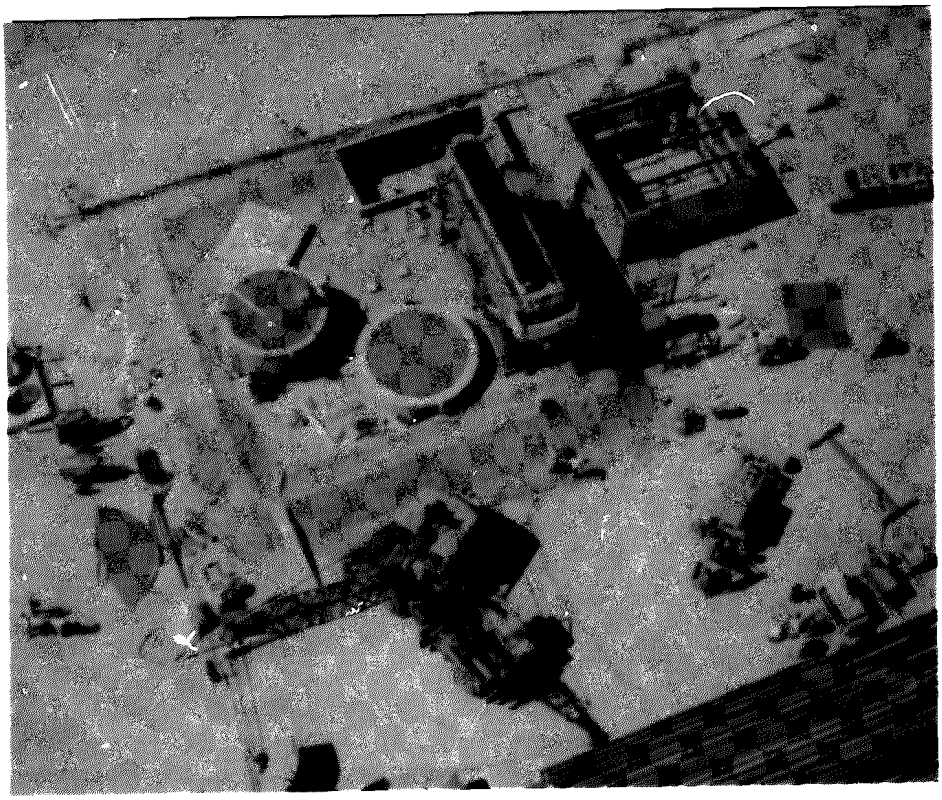

Figure 6.1-7 Cooler and Tank Bottoms Installed

An overall view of the SRE is shown in Figure 6.1-13. The propane tank can be seen in the upper right hand corner. The three small propane evaporators are located in the center of the picture on the other side of the chain link fence. Figure 6.1-14 shows a side view of the site. All major components of the SRE have been installed. The only tasks left to be completed are piping and electrical interconnects and insulating of the storage tanks.

6.2 HOT STORAGE TANK

Figure 6.2-1 shows nuts for the anchor bolts welded to the inside of the tank. The anchor bolts extend through the insulating firebrick to support the tank liner. The scaffolding used while laying the firebrick can be seen in Figure 6.2-2. Some bricking of the bottom of the tank has been completed. The steel rings on the inside of the tank lend stiffness to the tank as well as supporting the weight of the firebrick.

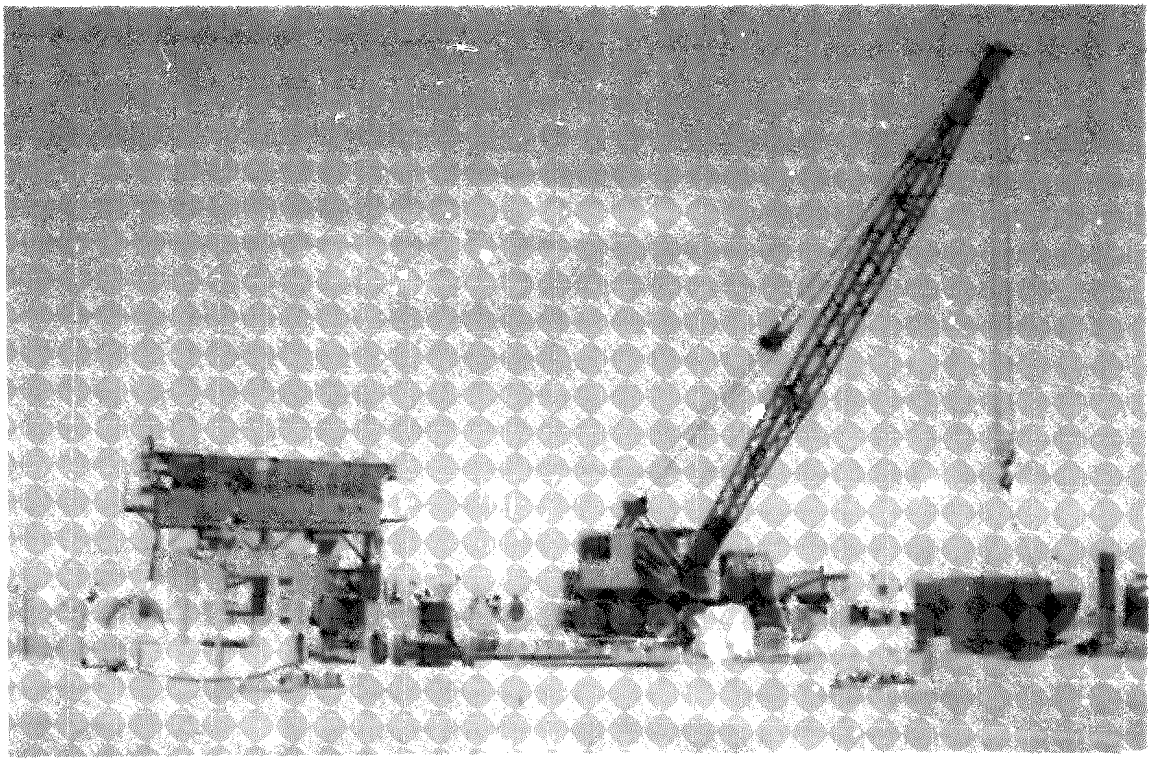

Figure 6.1-8 Lifting a Tank Segment

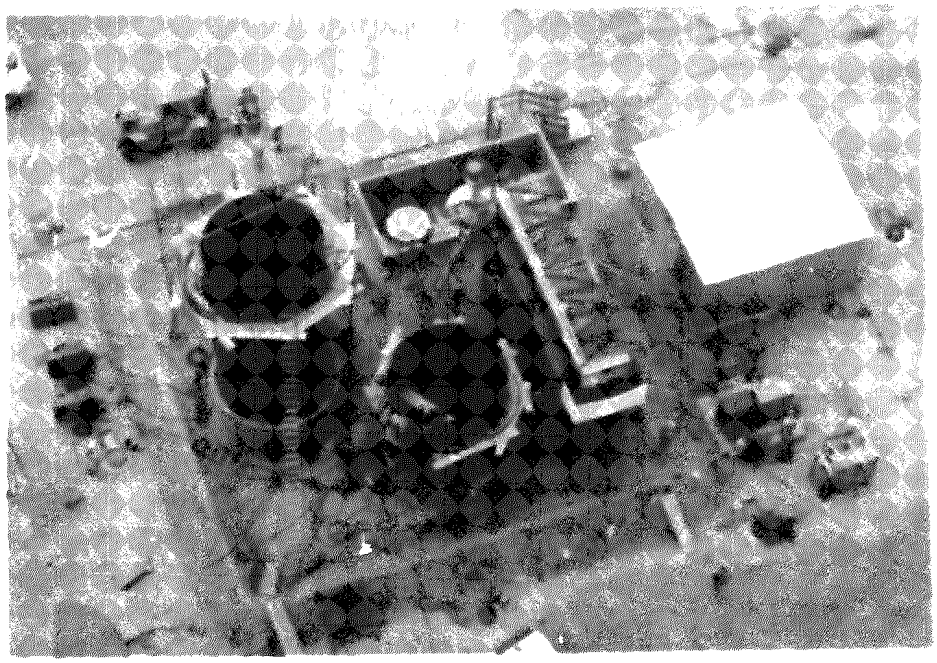

Figure 6.1-9 Tank Shell Assembly

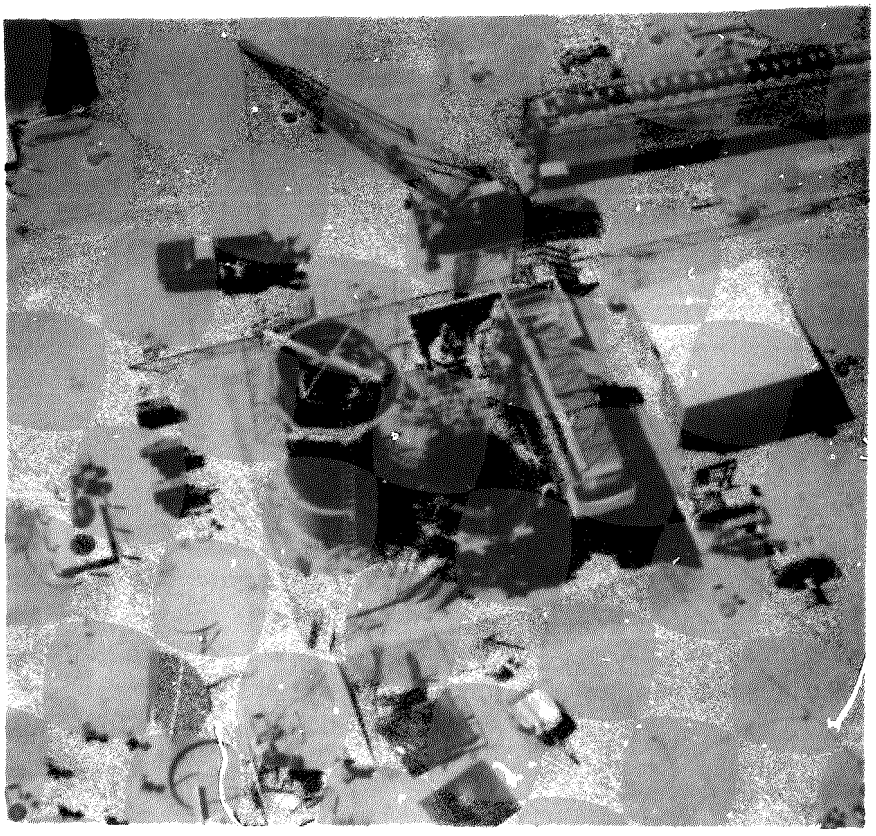

Figure 6.1-10 Interim Assembly Stage

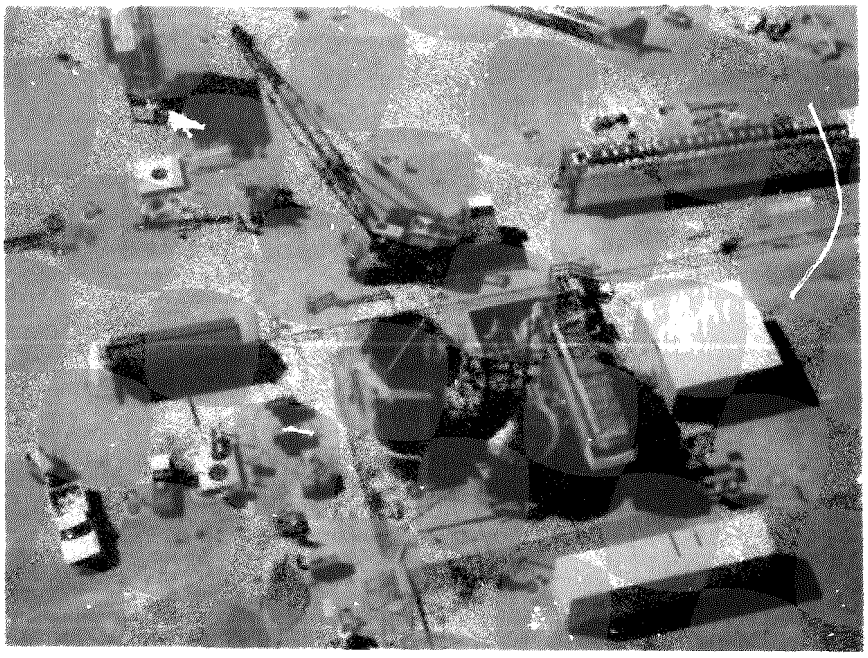

Figure 6.1-11 Propane Heater Installation

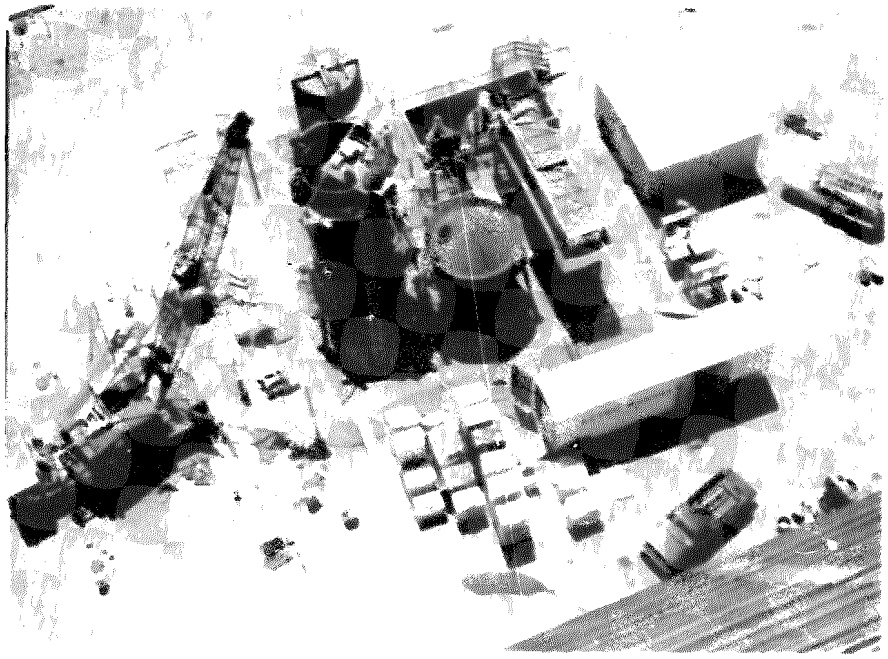

Figure 6.1-12 Bricking

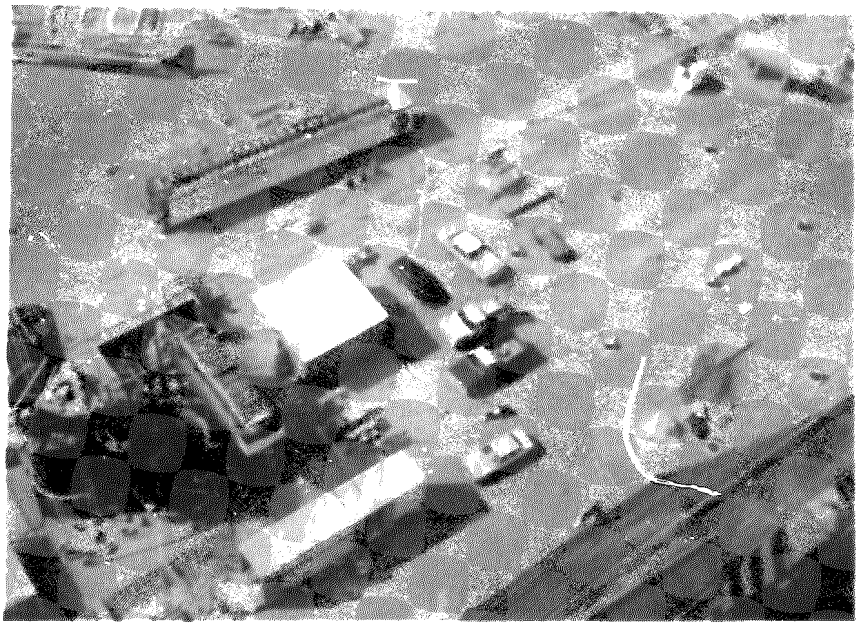

Figure 6.1-13 Overall View - Interim Construction Stage

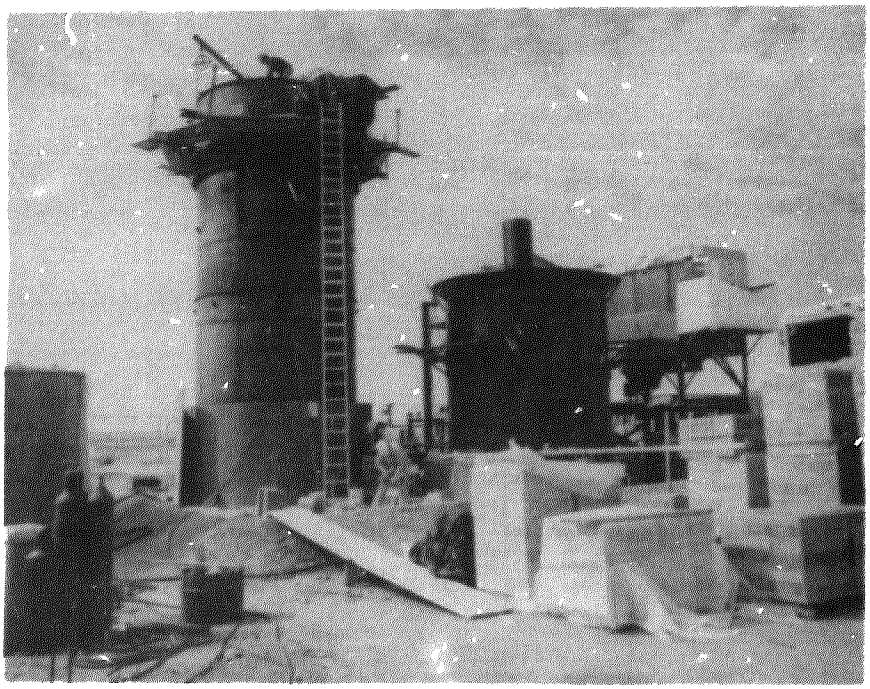

Figure 6.1-14 Side View During Bricking

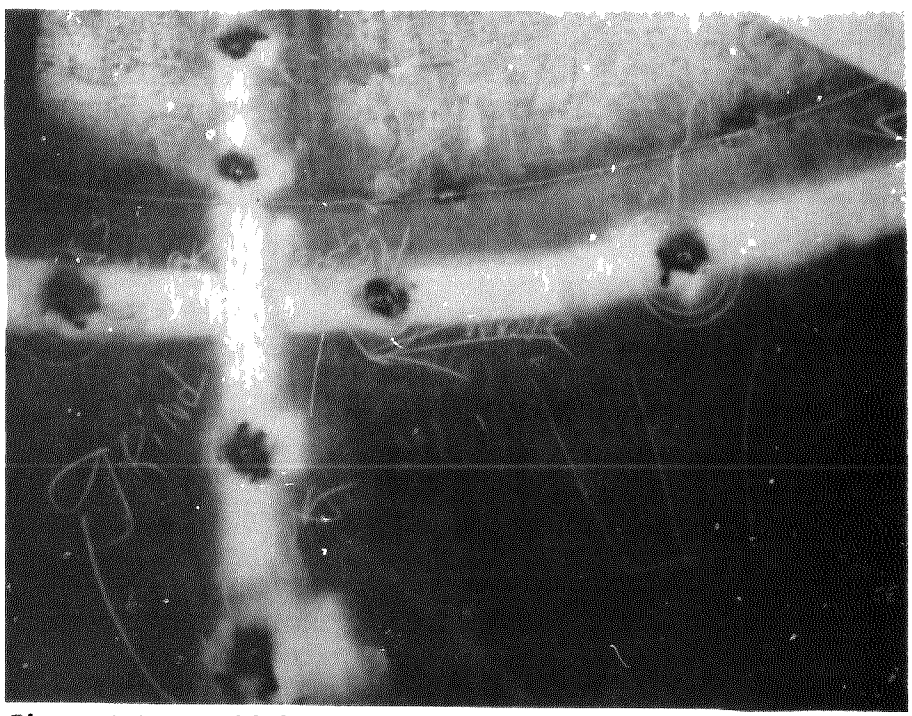

Figure 6.2-1 Welded Nuts For Anchor Bolts

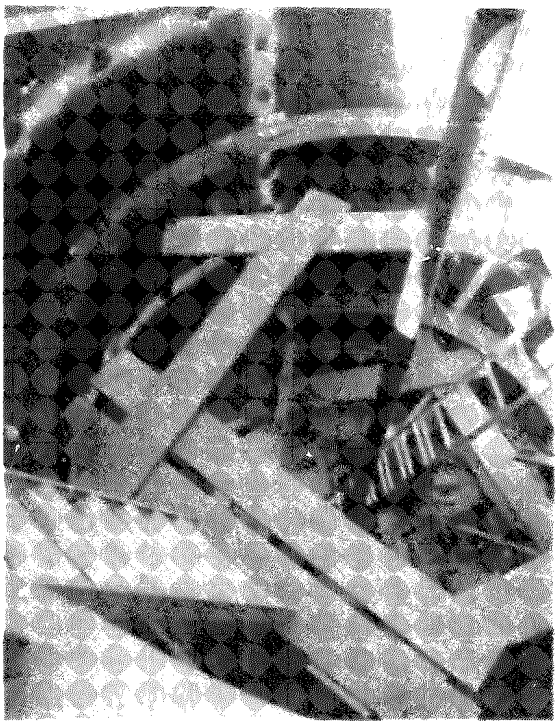

Figure 6.2-2 Hot Tank Interior

The top layer of the floor bricks is seen in Figure 6.2-3 and installation of the first course of tank side insulation has been started. The lowest support ring and several anchor bolts are also visible. The inner course of internal insulation is seen in Figure 6.2-4. The inner course is laid vertically and the inner course is laid horizontally. This provides a total insulation thickness of 0.34 m (13 1/2 in.). The mortar used to set the bricks is seen in the box in the foreground. The mortar is a slurry, so the bricks are dipped and pressed together, resulting in a very thin bond line. Anchor bolts were located at brick mortar joints as can be seen in Figure 6.2-5. In Figure 6.2-6 insulation is higher up the side of the tank and both the inner and outer courses can be seen.

To eliminate the high stress loads in the liner corner pieces at the intersection of the tank wall and floor, heavy back-up corner pieces (as shown in Fig. 6.2-7) are installed. These pieces are fabricated from 6 mm (0.25 in.) thick material and are attached to the anchor bolts. A foil liner can be seen above the corner pieces. The foil is 0.25 mm (0.010 in.) thick 304 stainless steel material and its function is to eliminate any abrasion, that could have resulted between the thermal expansion liner and the insulating firebrick, during thermal cycling. The foil is also attached to the anchor bolts.

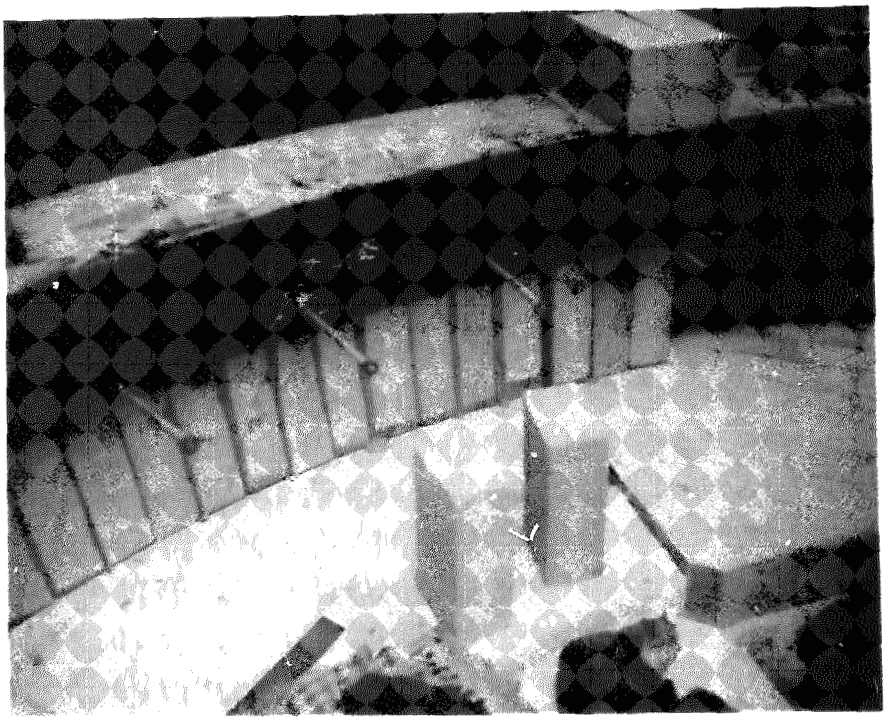

Figure 6.2-3 Insulating Firebricks at Tank Bottom

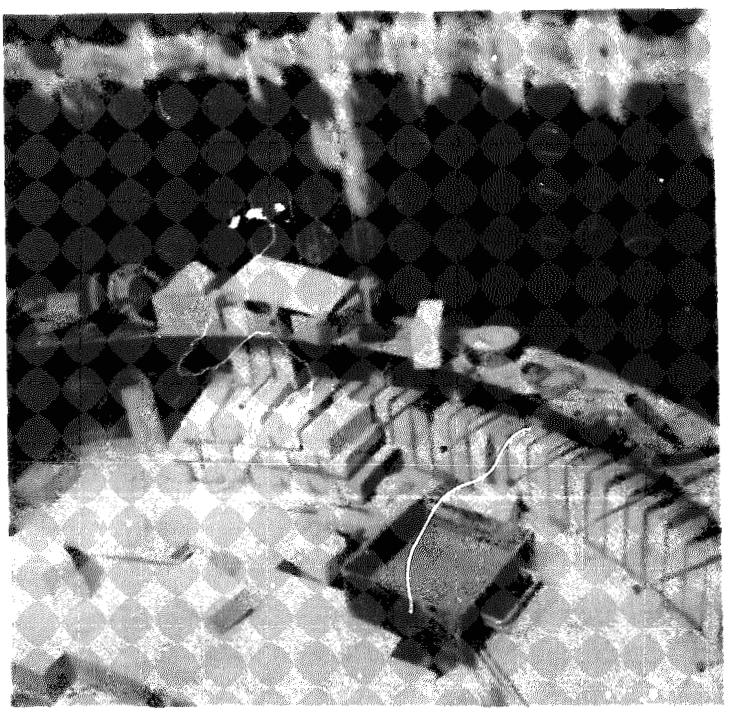

Figure 6.2-4 Internal Insulation - Side and Bottom

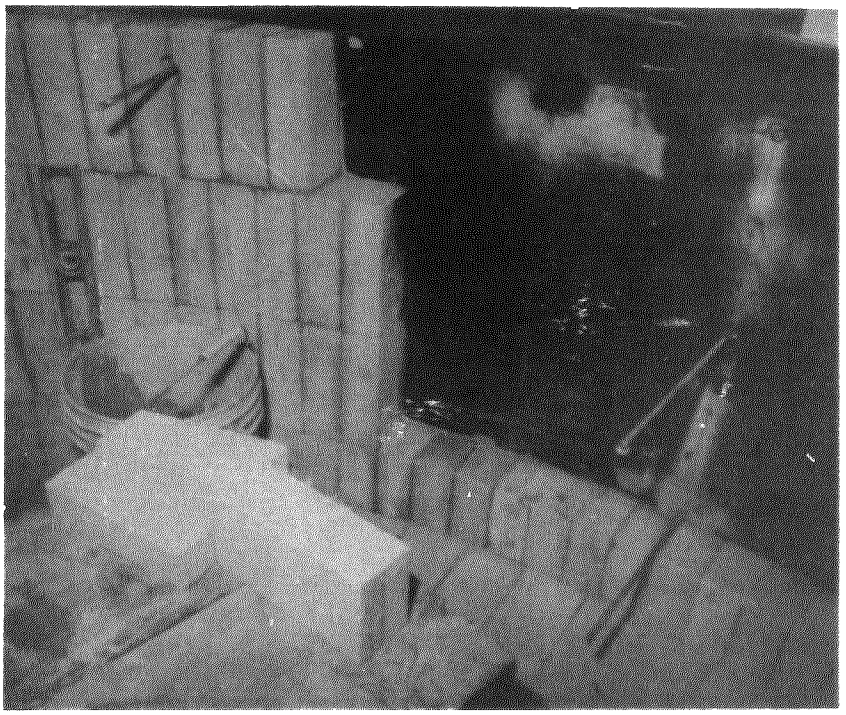

Figure 6.2-5 Inner & Outer Courses - Internal Insulation

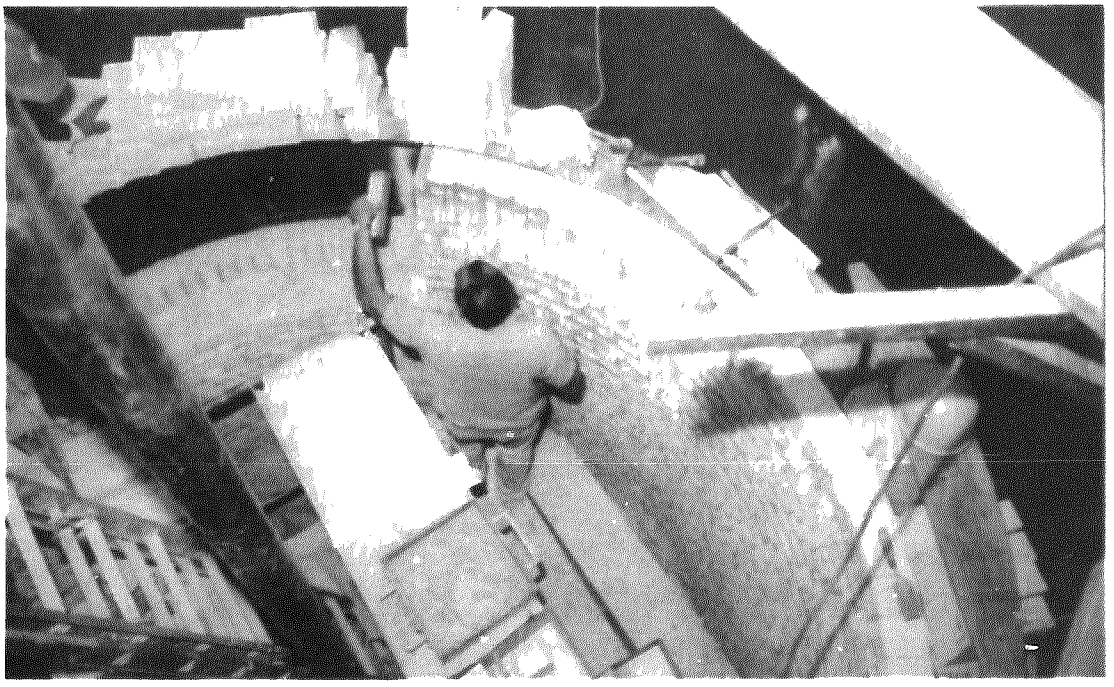

Figure 6.2-6 Internal Insulation Progress

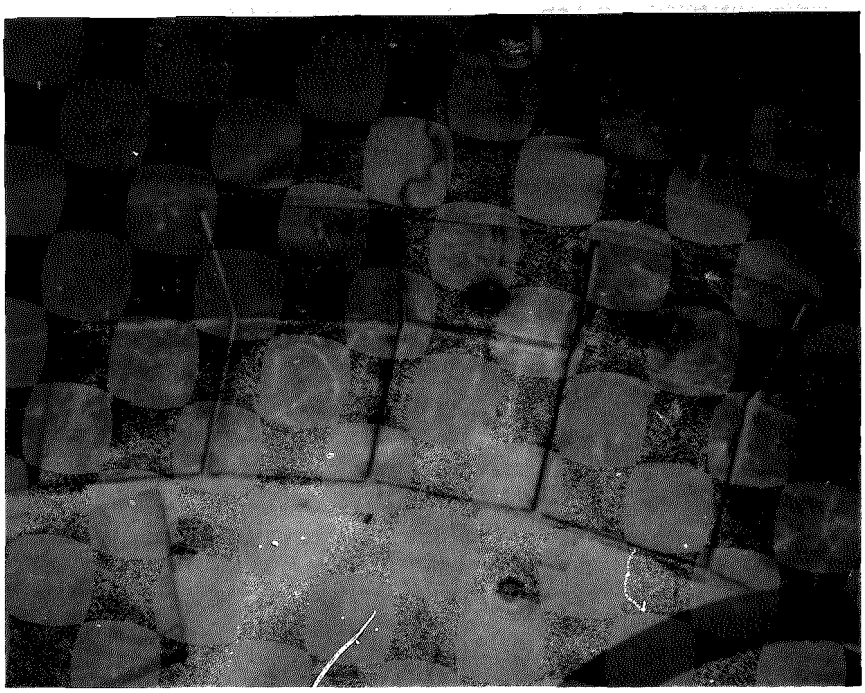

Figure 6.2-7 Corner Pieces and Foil

Figure 6.2-8 shows the attachment of the Incoloy 800 corrugated liner to the anchor bolt. The foil liner can be seen below it. The corrugated liner installation was started at the top of the tank and extends to the bottom, where it was overlapped by specially formed angle pieces. Installation of the lowest segment of corrugated liner and it's proximity to the heavy corner pieces can be seen in Figure 6.2-9.

The support jacks one of which is seen on the right side of Figure 6.2-10 serve dual functions. They supported the corrugated liner panel as it was being welded in place and also served to support scaffolding during tank assembly. Some of the instrumentation wiring to the thermocouples can be seen above the liner. Figure 6.2-11 illustrates the overlapping welding technique used on the liner panels at the top of the tank.

The outlet plate for the hot tank is shown in Figure 6.2-12. This plate was fabricated from Incoloy 800, since it would also be exposed to the corrosive action of the molten salts. The bottom corrugated liner panels were welded to this plate near the anchor bolt locations. A temporary cover has been placed over the drain hole located in the plate.

The hot tank salt heater is shown in Figure 6.2-13, prior to being installed in the tank. The propane tank is in the background.

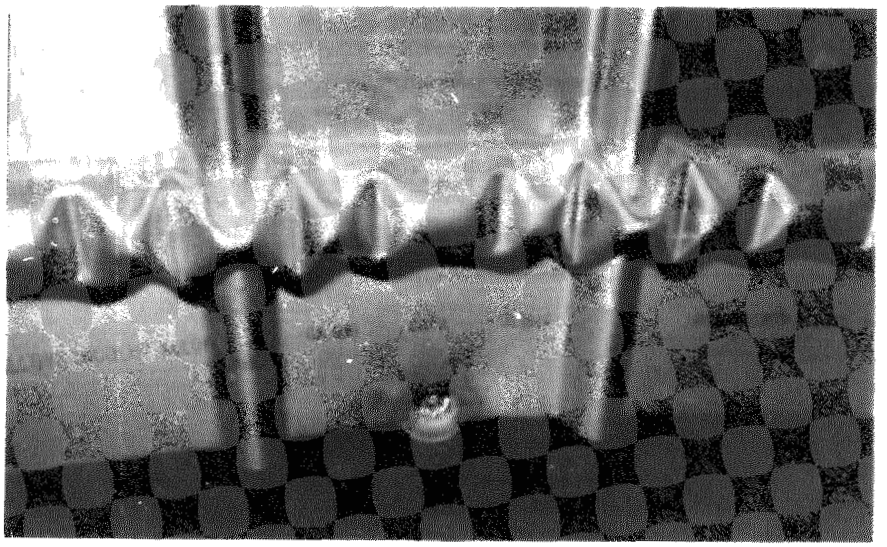

Figure 6.2-8 Liner Panel Attachment

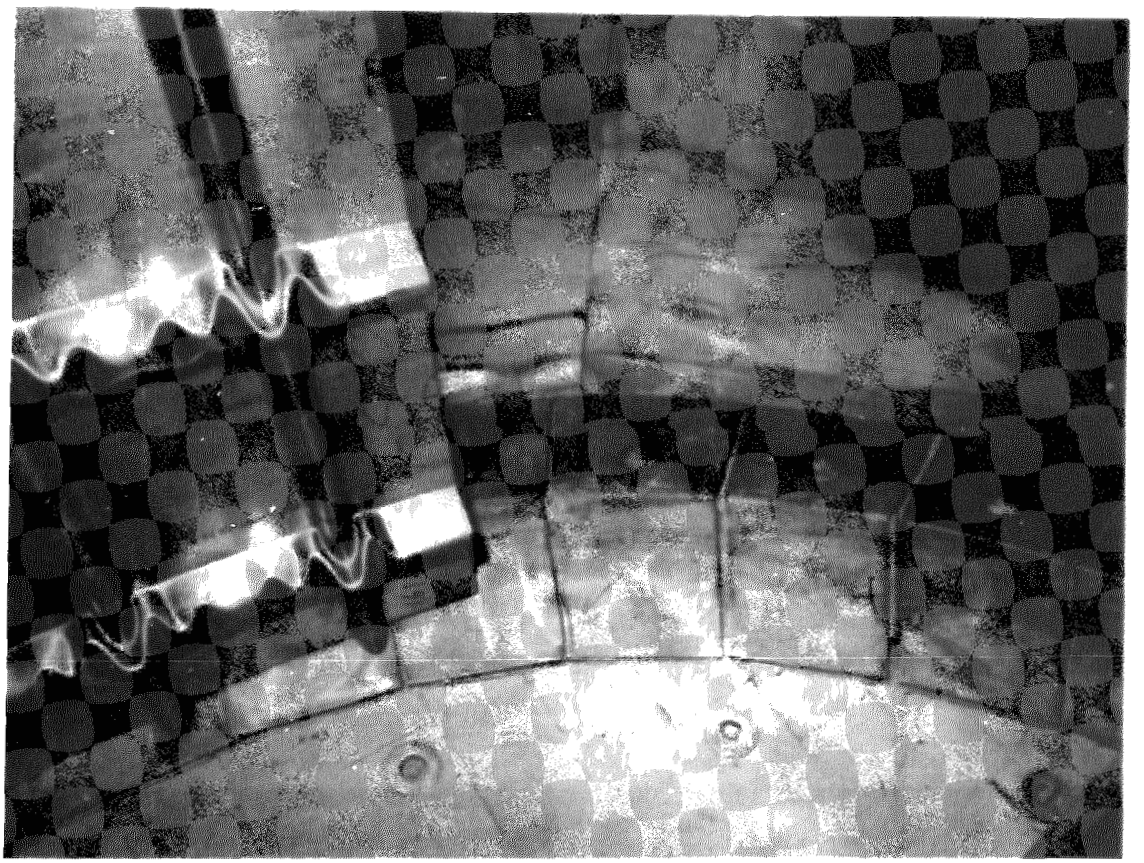

Figure 6.2-9 Liner Near Tank Bottom

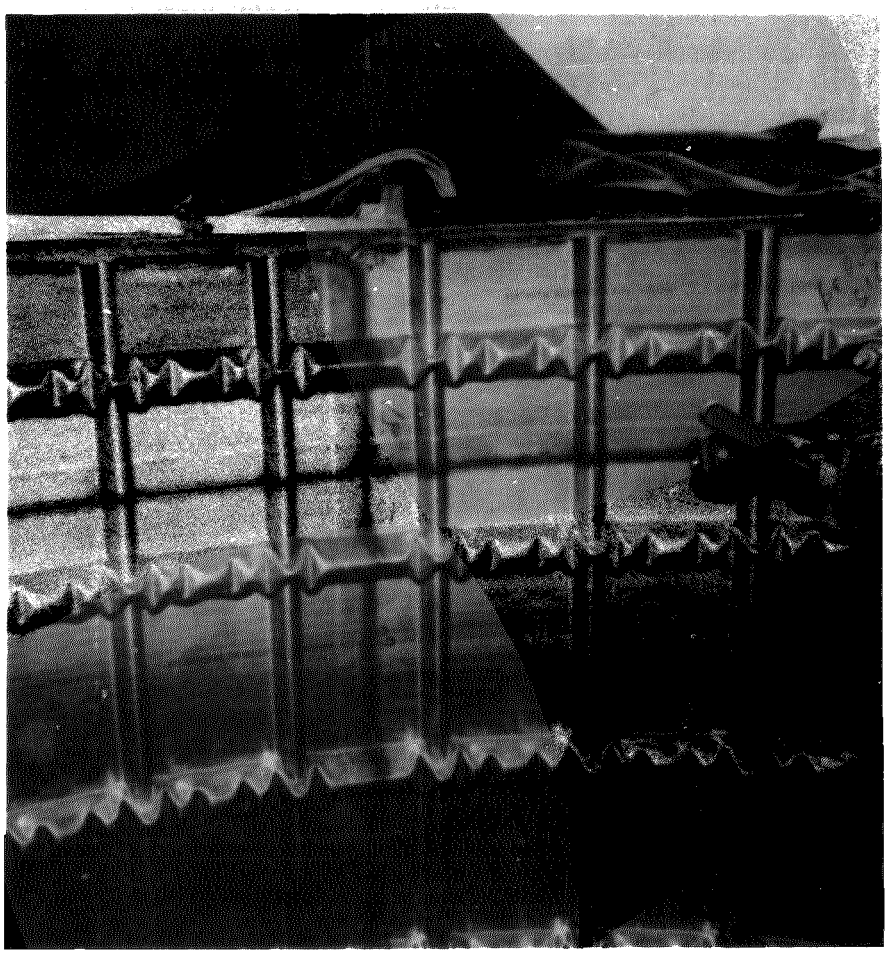

Figure 6.2-10 Upper Liner Panel and Instrumentation Wiring

Figure 6.2-14 is picture of the attic area of the hot tank. The vertical rods are supports for the suspended deck. An ammonia inlet tap, for the liner leak test, is on the ledge at the left hand side of the figure. Some of the thermocouple wiring can also be seen in this same area.

The accordion pieces which connect the corrugated liner with the suspended deck is shown in Figure 6.2-15. The end of each corrugation in the accordion pieces is welded shut and leak checked. The finished tank liner with the salt heater installed is shown in Figure 6.2-16.

6.3 COLD STORAGE TANK

Once the cold tank shell structure had been completed (refer to Fig. 6.1-14), fabrication of the interior of the tank was initiated. This was a rather straightforward and uncomplicated task, since all insulation was external and the carbon steel alloy selected for the shell could easily withstand the 288°C (550°F) salt temperature. Figure 6.3-1 shown the equipment installed in the bottom of the cold tank.

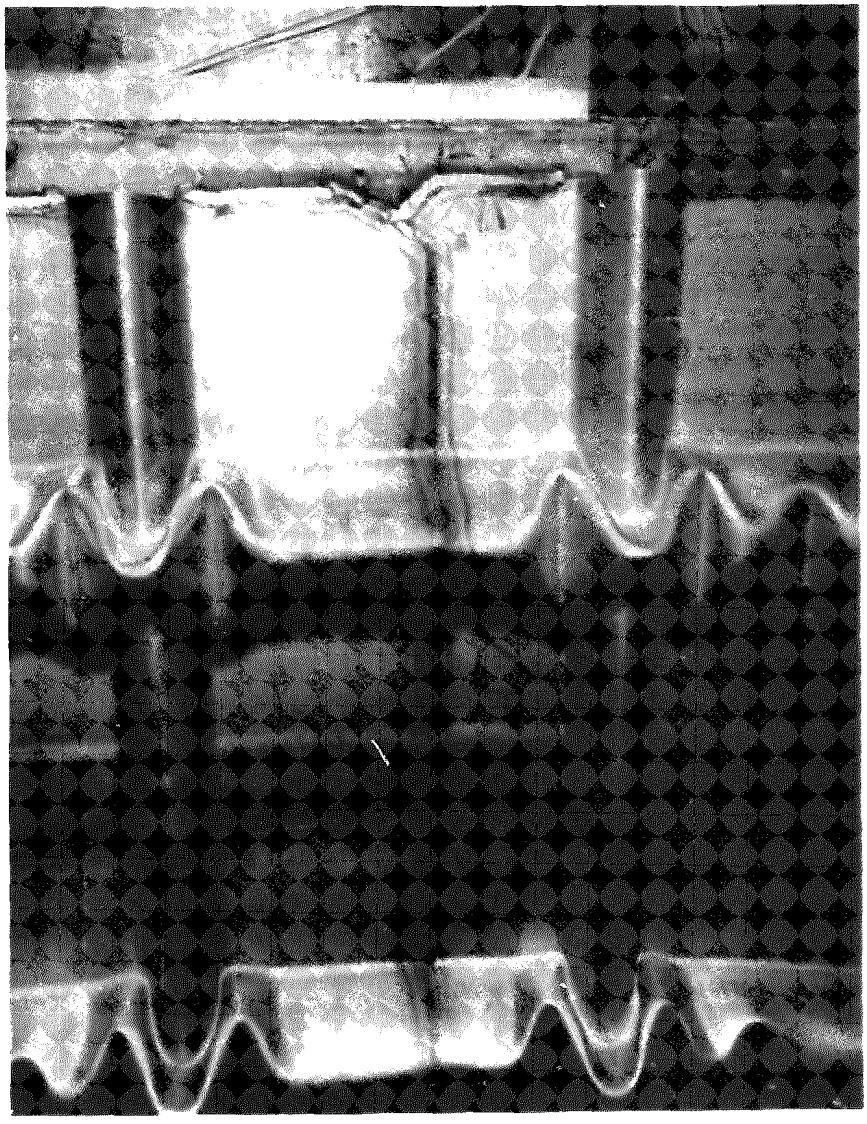

Figure 6.2-11 Overlapping Liner Welds

The tubes located in the center of the tank and in the upper left hand corner are temperature rakes. The tube in the lower left hand corner is a bubbling tube, used to provide a reliable yet inexpensive method of determining the height of the molten salt in the tank. In the upper left hand corner of the photograph, the tee shaped inlet pipe can be seen. Immediately below the inlet pipe is the outlet hole and a baffle above it to prevent vortex shedding during draining of the molten salt from the tank.

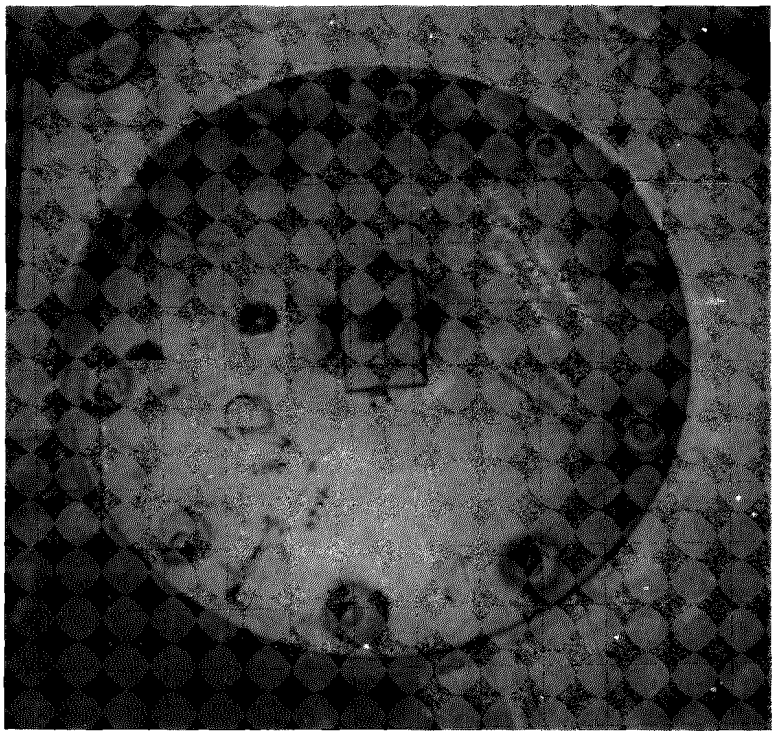

Figure 6.2-12 Hot Tank Outlet Plate

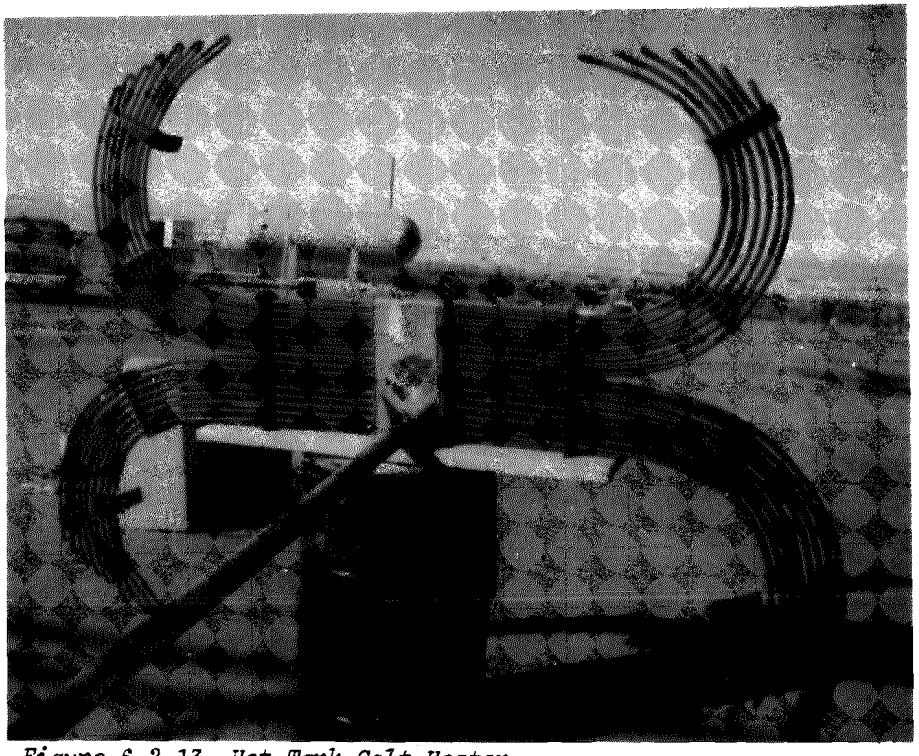

Figure 6.2-13 Hot Tank Salt Heater

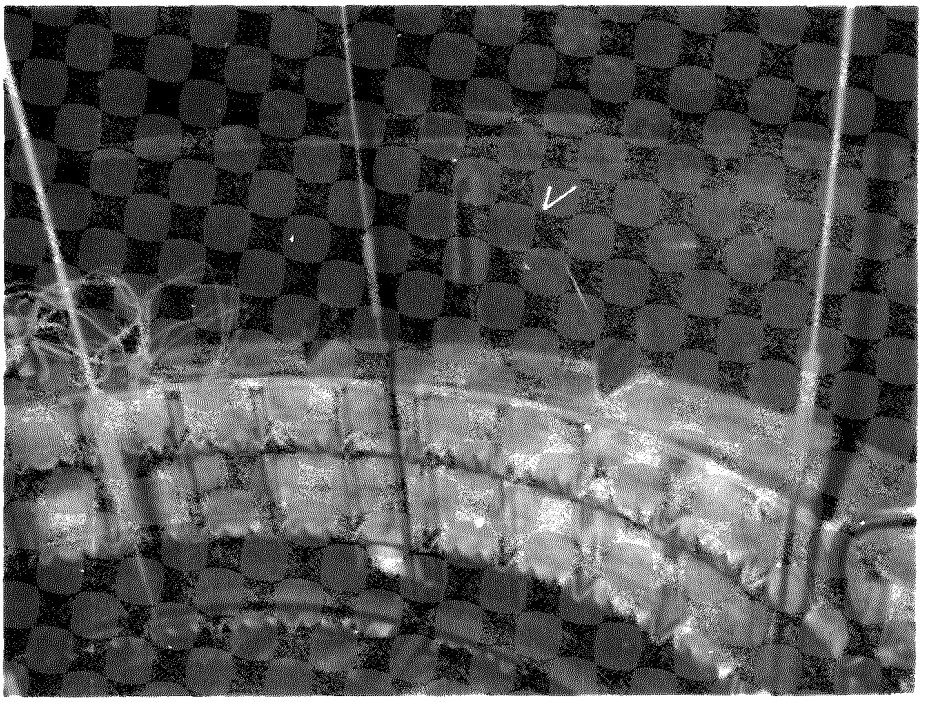

Figure 6.2-14 Hot Tank Attic Area

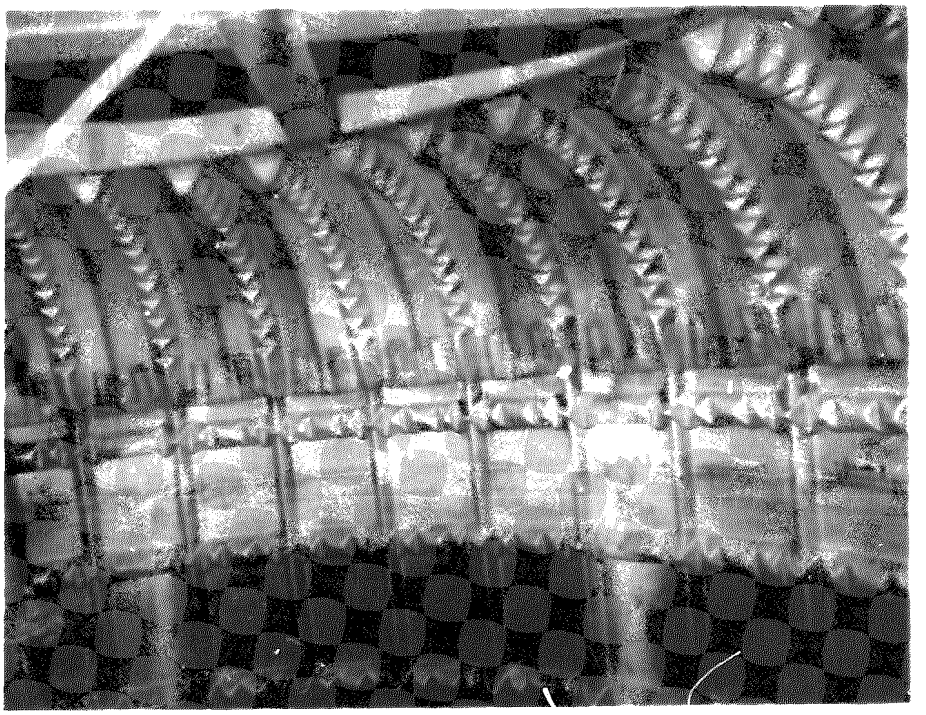

Figure 6.2-15 Accordion Pieces

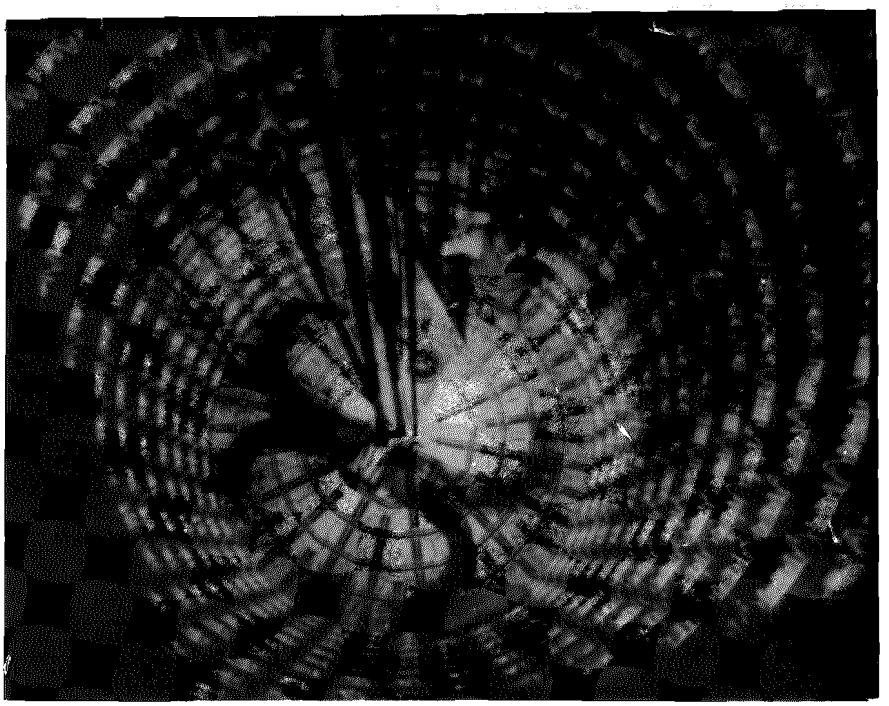

Figure 6.2-16 Completed Liner Installation

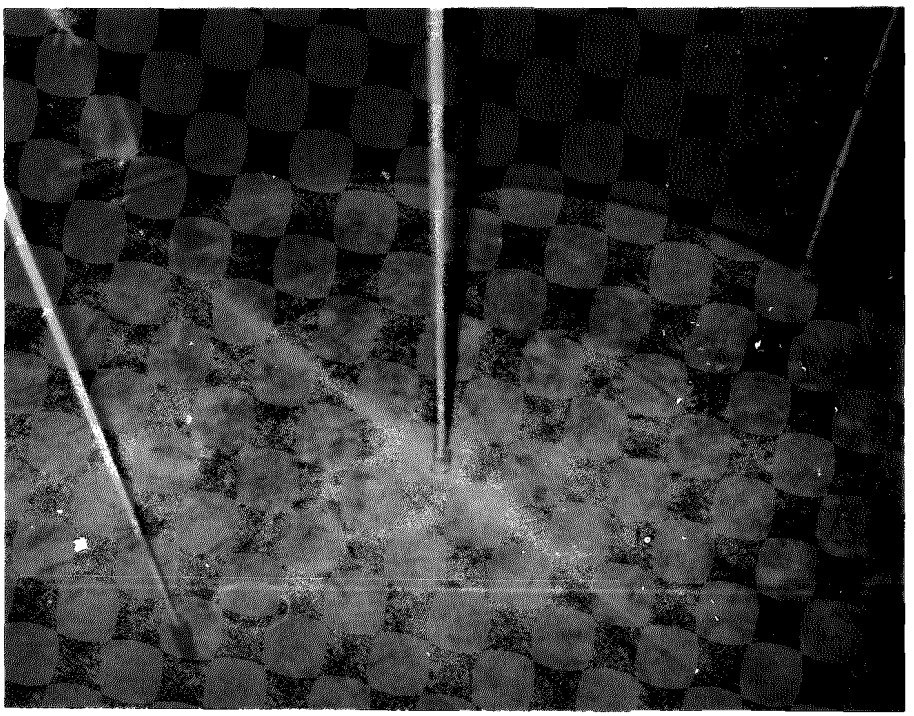

Figure 6.3-1 Bottom of Cold Tank Interior

The top of the inside of the cold storage tank is shown in Figure 6.3-2. The ladder can be seen exiting the manhole. The manhole provides access to the tank for final fabrication stages and to provide access to internal equipment during the experiment, should it be required. The tube located left of center in the figure is one of the temperature rakes and the tube located near center is the bubbling tube. A vent for the tank is located near the temperature rake tube close to a weld seam.

Figure 6.3-3 shows the wiring and foil insulation provided for 10 external trace heaters used on the cold storage tank. The sleeves placed around a section of the trace heaters prevented overheating where they penetrated the exterior insulation.

6.4 PUMP/SUMP ASSEMBLIES

The inside of the sump building is shown in Figure 6.4-1. The cold sump and pump, which was supplied from the ACR Phase II program, is shown installed in the foreground. The previously insulated sump is a tank 1.5 m (4.9 ft) diameter. The pump is mounted on top of the sump and the electric drive motor is mounted on top of the pump.

Figure 6.3-2 Top of Cold Tank Interior

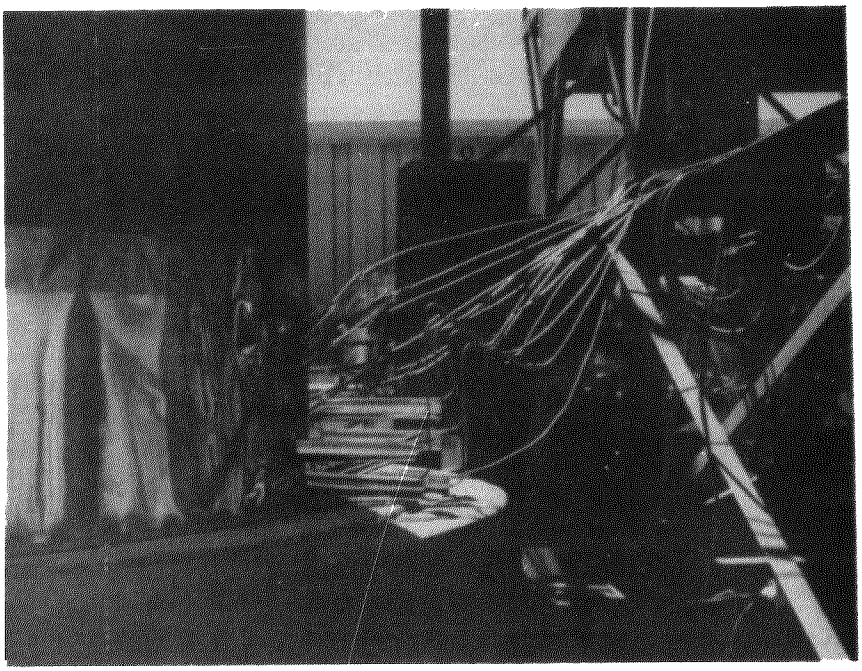

Figure 6.3-3 Cold Tank Trace Heaters

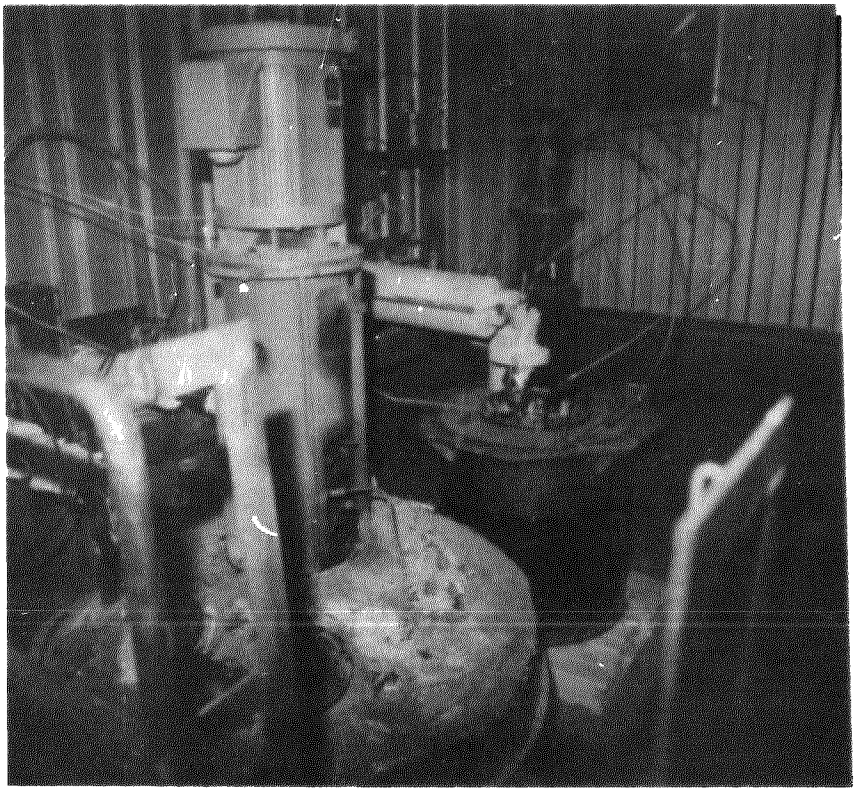

Figure 6.4-1 Pump/Sump Installation

The hot sump can be seen in the background. At this stage it has not been insulated. The hot pump and drive motor have been set in place. The lines in the figure are trace heater lines which have been brought into the sump building but have not been terminated. A thermostatically controlled fan used to keep the sump building cool can be seen in the upper right hand corner.

The finished installation of the sumps and pumps is shown in Figure 6.4-2. Electrical hookup of the pump motors has been completed. Note the rigid and flexible conduit coming from the ceiling. The valves and piping at the base of the cold pump provide an air supply to the pumps air cooled bearing. Piping to the hot pumps water cooled bearing has also been completed. The hot sump and molten salt transfer lines have all been insulated.

Figure 6.4-2 Sump Building Interior - Completed

6.5 PIPING

The piping leading into the sump building is shown in Figure 6.5-1. The line in the lower foreground is leading from the hot storage tank to the hot sump/pump. At this stage insulation has not been installed around the pipe. The method of supporting the salt transfer pipes may be seen in this figure. The line in the left hand center of the figure is leading from the cold sump/pump to the propane heater. Trace heaters have been installed on this line and covered with foil.

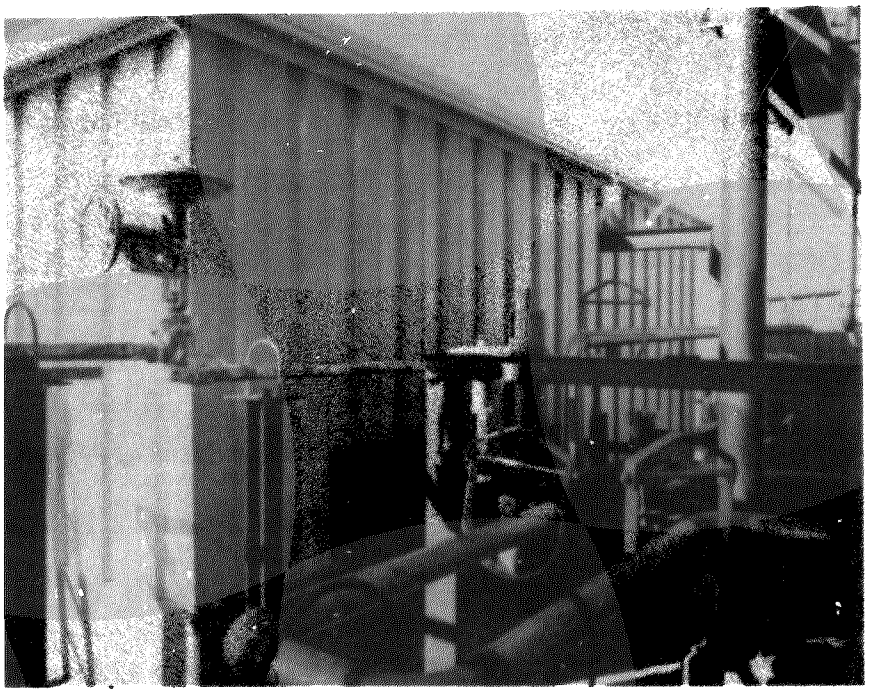

Figure 6.5-1 Salt Transfer Lines Leading to Sump Building

Figure 6.5-2 shows trace heaters and thermocouple wiring installed. The small wire parallel to the pipe is thermocouple which has been welded in place. The two larger diameter wires are the trace heaters, used to maintain adequate line temperature such that salt does not freeze in the line. Insulation has been placed over the line, thermocouples and trace heaters in Figure 6.5-3. Metal foil can be seen at the bend in the line and the thick external batts have been installed on the straight sections. The metal foil is used to thermally protect the trace heaters. Aluminum sheathing is placed over the thick insulation straight sections of the pipe leading from the hot tank to the hot sump/pump. Figure 6.5-4 is a view looking down on this line which shows installation of the pipe insulation nearly completed. Foil wrap of the other salt transfer lines has been finished.

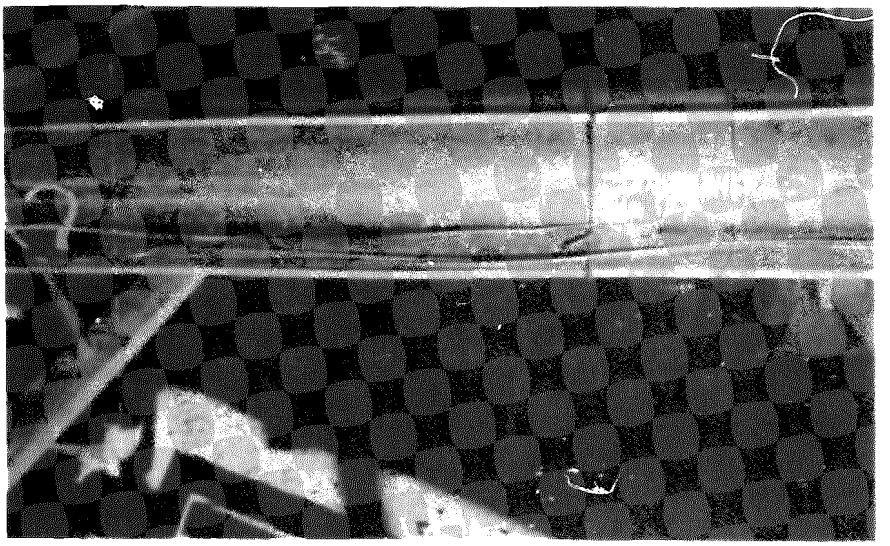

Figure 6.3-2 Salt Transfer Line Prior to Insulation Wrap

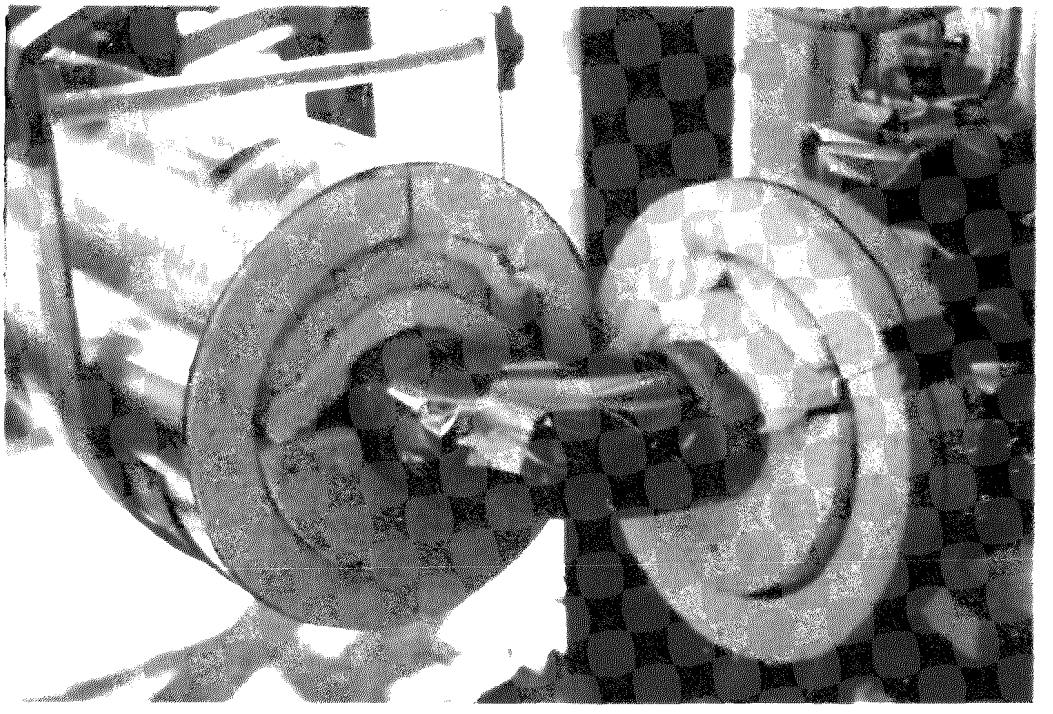

Figure 6.3-3 Pipe Insulation at Bend

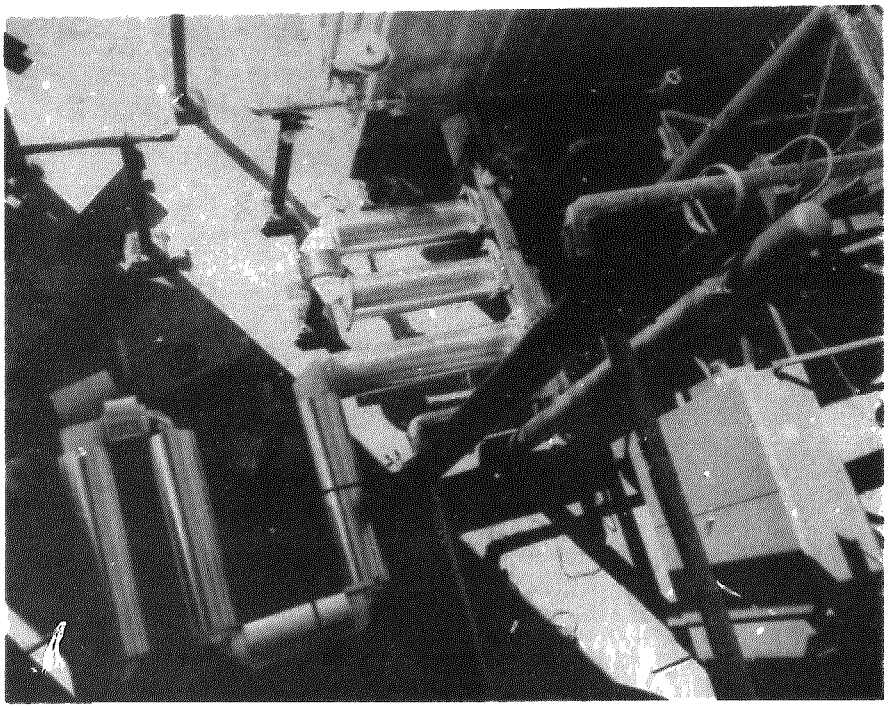

Figure 6.5-4 Insulated Salt Transfer Lines

6.6 PROPANE EVAPORATOR

Three propane evaporators are hooked in series to vaporize liquid propane for use in the burner section of the propane heater. The three units are shown in Figure 6.6-1 with the SRE in the background.

6.7 ELECTRICAL

The electrical distribution junction box used for the SRE is shown in Figure 6.7-1. This unit was also used in the ACR power system phase II program.

6.8 INSTRUMENTATION/CONTROL

The SRE control room housed all the experiment control devices and all the instrumentation readouts. Figure 6.8-1 shows the system control panel on the left. This panel controlled the propane heater, the air cooled heat exchanger, the sump pumps, all the valves and provided readout of the hot and cold tank levels as well as various component temperatures. The smaller panel or the right provided control of the trace heaters. Figure 6.8-2 shows the SRE data recording system which provided capability to record all instrumentation readout on tape or paper printout. Only the paper printout capability was used.

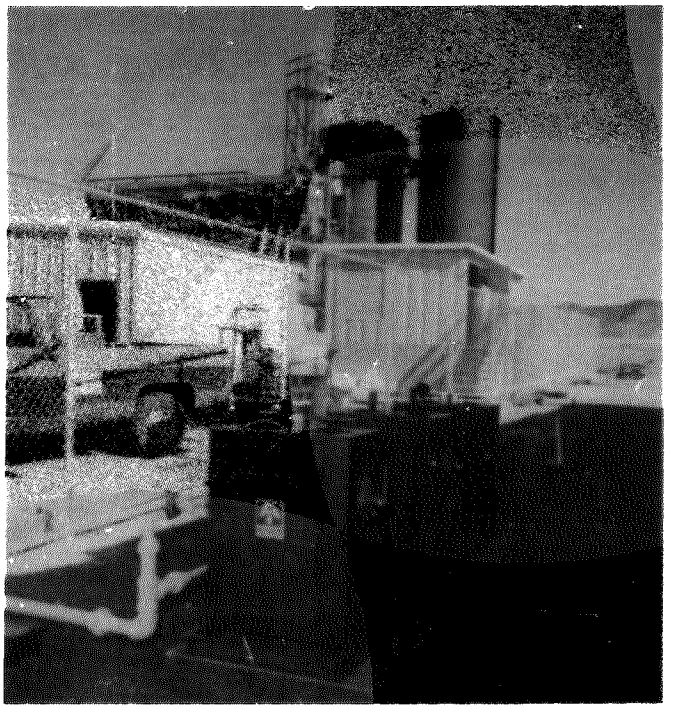

Figure 6.6-1 Propane Evaporators

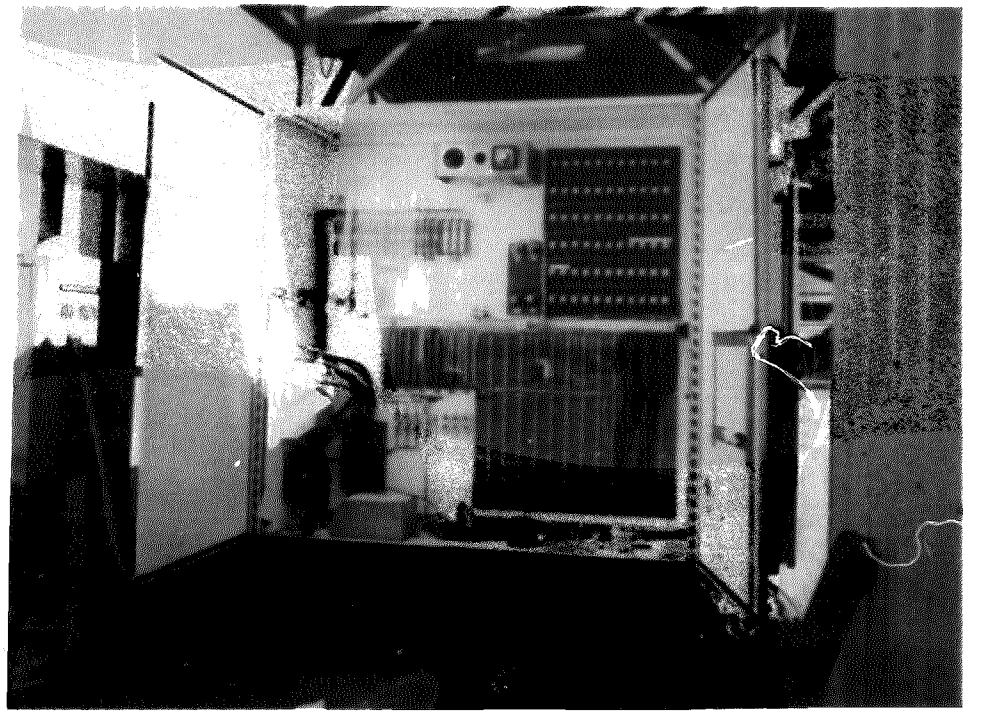

Figure 6.7-1 SRE Electrical Distribution Box

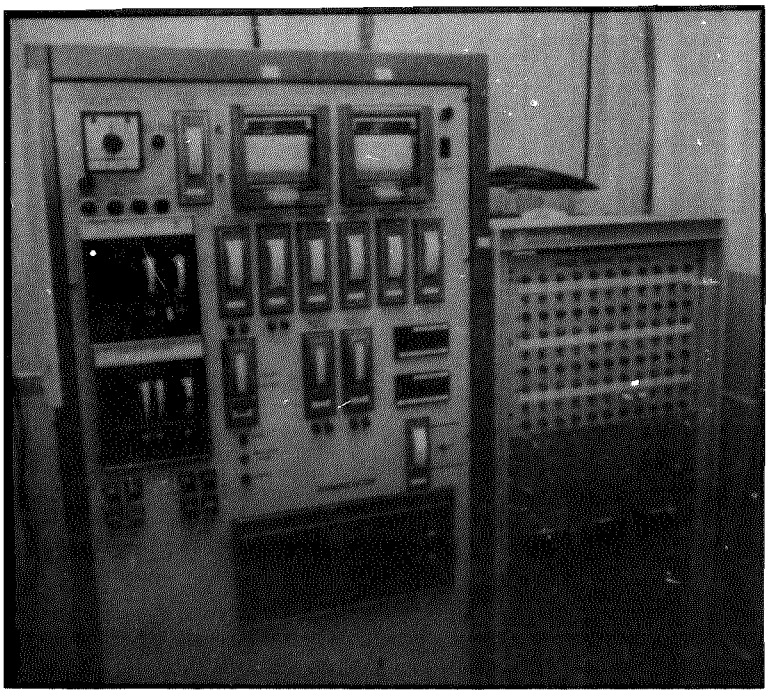

Figure 6.8-1 System and Trace Heater Control Panels

Figure 6.8-2 SRE Data Recording System

6.9 SRE COMPLETED

The completed SRE installation is shown in Figures 6.9-1, 6.9-2 and 6.9-3. Figure 6.9-1 is a side view looking from the north east. From right to left is the insulated hot tanks, the propane heater and the sump building. All lines and line support hangars are in place. The coolant inlet line to the water cooled foundation is located at the base of the hot salt storage tank. A view from the northwest is shown in Figure 6.9-2. To the right is the control building. In the center foreground is the air cooled heat exchanger. To the left in back of the cooler is the cold tank. The hot tank (with its ladder platform) and the propane heater are directly behind the cooler. Figure 6.9-3 is a view from the CRTF tower of the entire SRE system. SRE fabrication was started in June of 1981 and was completed by January of 1982. A more detailed schedule of the construction effort is listed in Table 6.9-1. Fabrication proceeded with no major problems, demonstrating that the proposed thermal storage tank construction techniques are feasible for commercial application.

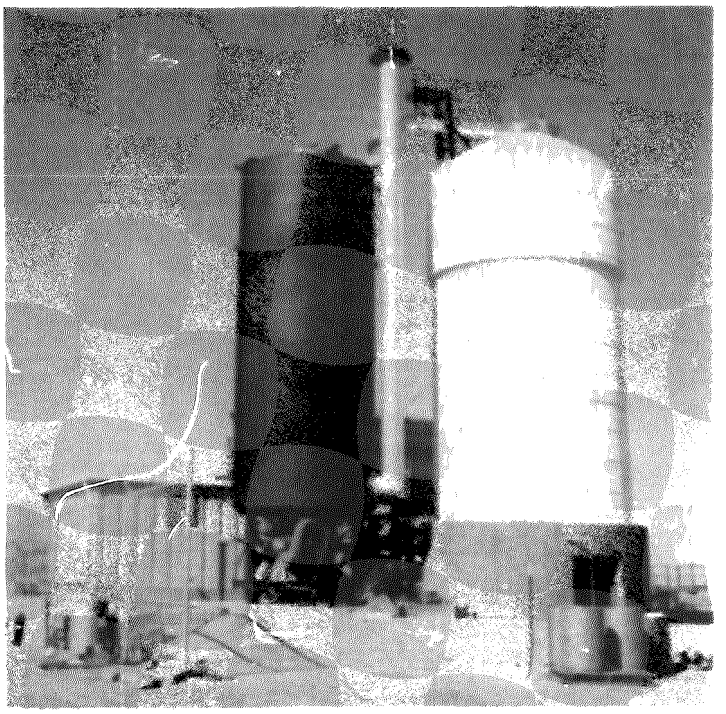

Figure 6.9-1 SRE View from Northwest

Figure 6.9-2 SRE View from Southeast

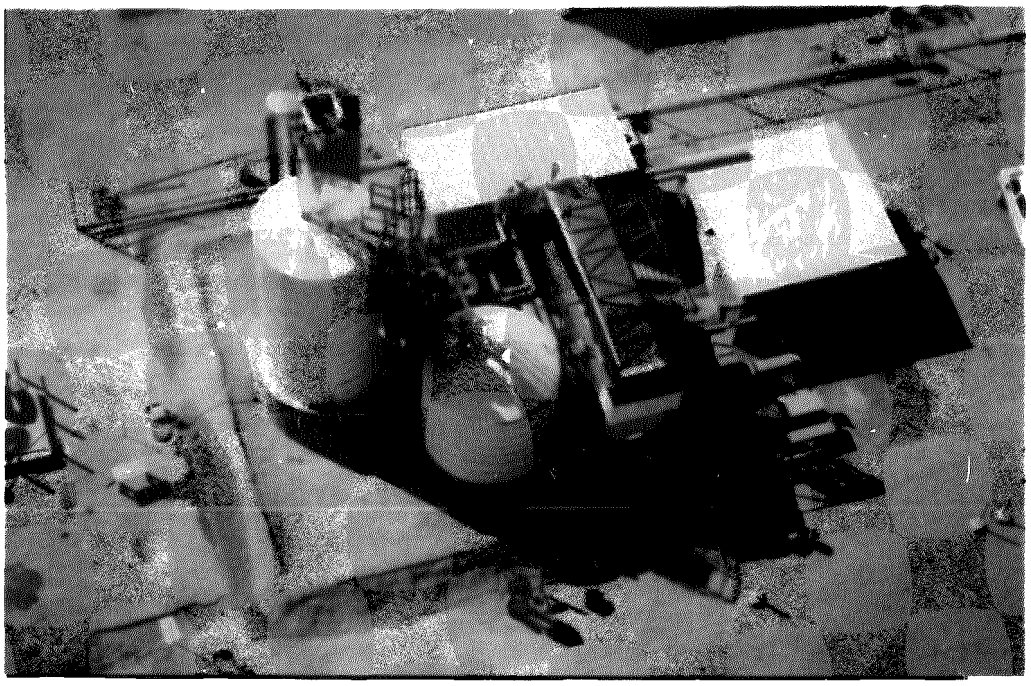

Figure 6.9-3 SRE View (Looking Down)

Table 6.9-1 SRE Build Schedule

May -	Two heliostat foundations were removed and buried electrical conduit was installed. Construction personnel were on site at the end of the month.
June -	Earth work and concrete foundations were completed.
July -	Both the sumps and the air cooler were set. Pipe foundation was started. Shell fabrication of both tanks was initiated. The control building was erected.
August -	The propane heater was erected. All the piping was completed except for the lines to the hot tank. The hot tank shell fabrication was completed except for the roof. Anchor nuts were welded to the hot tank shell. Bricking of the hot tank internal insulation was initiated.
September -	Bricking of the hot tank was completed. Welders for the liner fabrication were qualified. The anchors and the stainless steel foil between the bricks and the liner were installed. Hot tank lines were installed. Installation of the thermocouples and trace heaters for the lines was started. The control console was installed in the control building. Erection of the sump building was initiated.
October -	The internal liner for the hot tank was completed. The thermocouples and trace heaters on all the line except the hot tank inlet were completed. Thermocouples were installed on the cold tank. Insulation of salt transfer lines and the cold tank was started. Completion of the sump building was accomplished. Electrical wiring and instrumentation was begun.
November -	The floor liner, shell roof, suspended deck and accordion pieces were installed in the hot tank. The cold tank was completed including a leak check.
December -	The ammonia leak test of the hot tank liner was performed. Instrumentation of the hot tank was initiated. The cable trays and conduits for both the electrical and instrumentation wires were finished. The total pneumatic system was plumbed. The coolant system for the foundation was installed. The electrical system was checked out.
January -	The hot tank was completed. All remaining thermocouples were installed and the data system checked out.

6.10 QUALITY CONTROL

6.10.1 Salt Transfer Lines

The line welds were checked with die penetrant as they were completed. The stainless steel lines which were constructed of 10 schedule pipe were Tungsten Inert Gas (TIG) welded (both the root and finish weld). The mild steel lines were constructed of 40 schedule pipe. The root pass was TIG welded and the finish weld was done using a standard type electrical arc process. After line assembly the section of lines between the hot pump outlet and the valve upstream of the cold tank inlet was pressure checked to 0.78 MPa (113 psig). This included the lines to and from the air cooler. The line between the cold pump outlet and the control valve into the heater was hydro tested to 1.92 MPa (278 psig). No line leakage was found.

6.10.2 Propane Heater

The total length of coil in the heater was 500 m (1640 ft). The coil was air pressurized to 103 kPa (15 psig) and all welds were bubbled checked. The coil was also hydro tested to 1.38 MPa (200 psig).

6.10.3 Tank Shells

Visual inspection of the tank shell welds was performed. Radiographic inspection was also done on welds between plates where "tee" intersection were made. Only a few sections were welded due to visual inspection and no faulty welds were found by radiographic inspection.

6.10.4 Liner

The corrugated liner in the hot tank was checked by visual, dye penetrant and ammonia leak inspections. The first inspection performed was buffing the welds with a powered stainless steel wire wheel followed by visual inspection. The three areas of the liner where dye penetrant was used for the leak check were on the wall behind the accordion pieces, the accordion pieces and the suspended deck. Leakage of the liner behind the accordion pieces would not cause a problem with the molten salt since they would not be in contact. This dye penetrant test was performed to eliminate any possibility of a large ammonia leak. The accordion pieces and the suspended deck were not subjected to the ammonia test.

The ammonia test was performed by evacuating most of the air between the liner and the shell and then backfilling this volume with ammonia. The welds had all been previously coated with an ammonia sensitive paint. Leakage of the ammonia would cause the paint color to change locally from yellowish orange to blue. If leakage was detected the area was cleaned and rewelded and another cycle of the ammonia test was performed. The volume behind the liner was pumped down by-21 kPa (-3.0 psig) before and after each leak check. An initial evacuation was used to reduce the moisture which could absorb ammonia. After each test the volume was pumped down and backfilled with nitrogen to reduce the ammonia concentration thereby reducing corrosion potential during the

rewelding. The following number of leaks were found during the leak testing of the liner.

Cycle	No. of Leaks
1	70
2	33
3	30
4	1

6.10.5 Tank Insulation

Careful checks were made of the tank shell after fabrication. The installation of the bricks was monitored to guarantee their surface smoothness to the liner and the position of the anchors. Careful mapping of the tank for the anchor points was performed to assure that the liner could be assembled after the bricking had been completed. Dimensional checks were also made to assure correct installation of the liner.

6.10.6 Electrical

Electrical checks were made during the system build up. As electrical circuits were completed they were checked for electrical resistance and the wiring insulation was checked by a 500 volt ac megaohm meter. Correct motor rotation was checked by a quick current surge.

6.11 LINER FABRICATION

The liner material was fabricated by Glitsch Field Services, Inc. in Dallas, Texas under license from Technigaz. The internal liner assembly was made from the following components:

a) 56 membrane wall sheets. These sheets were formed from Incoloy 800 material. The sheets were first formed to a configuration that is part of the standard Technigaz design, and then crimped in several places to achieve the correct liner I.D.

b) 70 flat floor panels. The panels were formed in various sizes from Incoloy 800 material, using a standard Technigaz forming configuration.

c) 40 Light Angles. These 90° angles were formed to a standard Technigaz configuration using Incoloy 800 material. The angles provide a transition between the floor and the walls.

d) 40 Accordion pieces. These parts were specially designed for this application. A standard Technigaz corrugation made from Incoloy 800 was crimped in numerous places to provide a curved transition part between the walls and the flat roof deck.

e) 210 Miscellaneous parts including "end caps" and "dog legs". These parts were made from Incoloy 800 to Technigaz drawings, The end caps were used to seal open large and small corrugations. The dog legs were used as transition pieces from sheet to sheet in the floor.

f) 40 Heavy Corners. The heavy corners were made from T-316 stainless steel material to Technigaz drawings, The corners are embedded flush with the refractory brick and provide support for the membrane in the floor to wall area.

g) 238 Anchor points. The anchors were made from T-316 stainless steel and assure an intimate contact between the membrane sheets and the wall or floor respectively. These parts were made by a multi stage punching operation to Technigaz drawings.

h) Suspended Roof deck. The top of the liner was made of welded standard structural components and sheet stock seal welded, to form the configuration per Technigaz drawings.

The forming of the liner pieces was preceded by inspection of the material. Proper identification and mil test reports were first performed. Cutting sketches were established to optimize material savings. Each sheet was visually inspected for deleterious indications. Any major marking of the material was avoided and minor scratches were positioned so that they would be in a flat, no stress, area rather than in a high stress area as a knot (crossing of two corrugations).

6.11.1 Wall Sheet Formation

The sheets were sheared to size as seen in Figure 6.11.1-1. The GO's (large corrugations) were formed with 3 GO's per sheet as seen in Figure 6.11.1-2. Figure 6.11.1-3 shows and end view of the forming die during GO formation. The metal was clamped on each side of the intended corrugation. As the punch was lowered the two clamps moved inward; thus a folded corrugation resulted with no thinning of the material. The spacing of the GO's were equal and were controlled by positive stops in the press.

The small corrugations (POs), were folded into the metal sheet by a similar process but with a more complicated die. The POs equal spacing were controlled by positive stops within the press.

Figures 6.11.1-4 and 6.11.1-5 show POs being formed. The perpendicular POs and GOs form what is called a "knot" at their crossing. The sheets shown in the figures are approximately twice the size used in this program. In the SRE tank the POs were vertical and the GOs were horizontal.

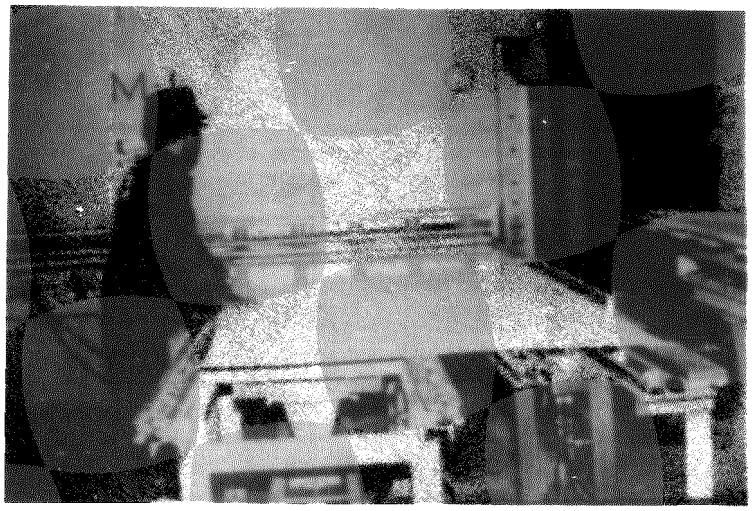

Figure 6.11.1-1 Shearing Liner Sheets

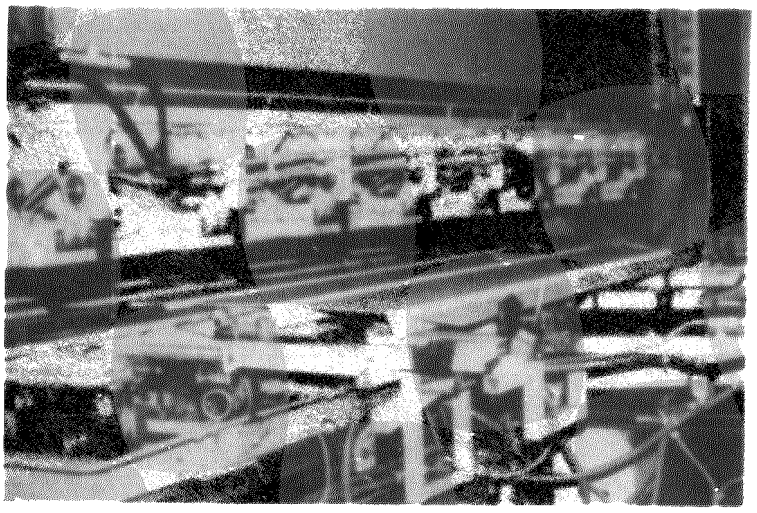

Figure 6.11.1-2 Large Corrugation Forming

The shape of the GOs at initial forming had a shape with straight sides such as a "U". These were rounded to produce a shape like a "V to reduce stresses within the corrugation. Figure 6.11.1-6 shows this step being performed. Some edges were joggles as seen in Figure 6.11.1-7 so that sheet could overlap other sheets. Sheets were trimmed to exact size and any needed special notching or chamfering was performed. Because of the shape of the hot tank the panels were curved. It was necessary to form a dimple on the GOs on each side of the knot to allow this curvature. The sheets were inspected, as seen in Figure 6.11.1-8, for scratches, nicks and dimensional requirements.

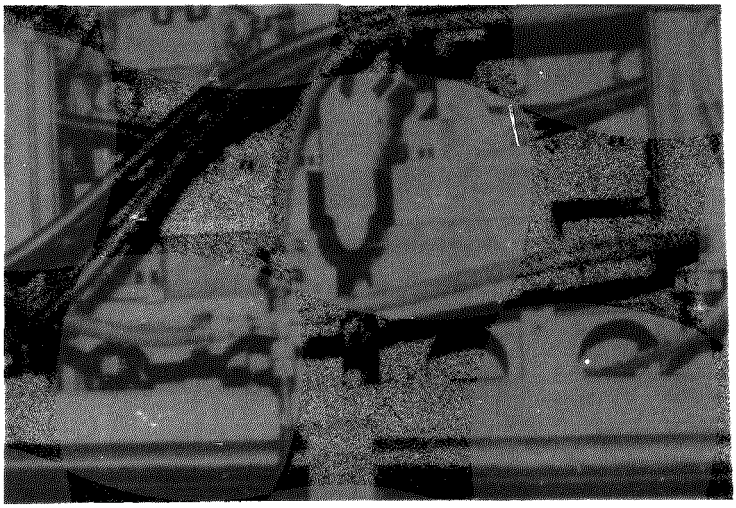

Figure 6.11.1-3 End View of Large Corrugation--Forming Die

Figure 6.11.1-4 Small Corrugation Forming

6.11.2 Light Angle Forming

The light angle material was covered by a poly film for the forming process to assure surface protection. Figure 6.11.2-1 shows the forming of the angle and Figure 6.11.2-2 shows additional dimpling of the angle. Shearing the piece to size is shown in Figure 6.11.2-3 and joggling of the edges, is shown in Figure 6.11.2-4. At completion of the operation the angles were given a visual inspection and dimensional inspections were performed on a special inspection fixture.

Figure 6.11.1-5 Formed Small Corrugation

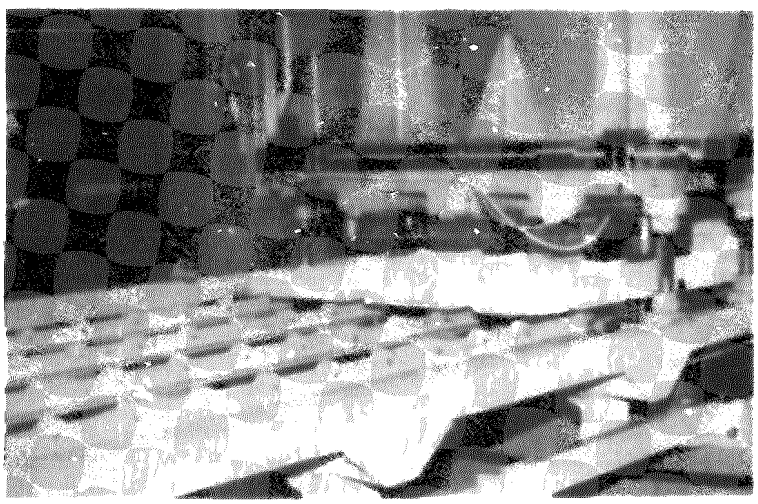

Figure 6.11.1-6 Corrugation "Rounding" Operation

6.11.3 Accordion Pieces

The accordion piece material was protected by a poly film during forming. The single GO per piece was crimped on equal spacing to obtain the correct radius. The end of the accordion was necked down to match the PO corrugation on the tank wall. This necking caused rippling of the accordion pieces which required slots to be cut parallel to the GO at the end of the piece. These slots were covered by separate pieces during liner assembly (refer to Fig. 6.2-15).

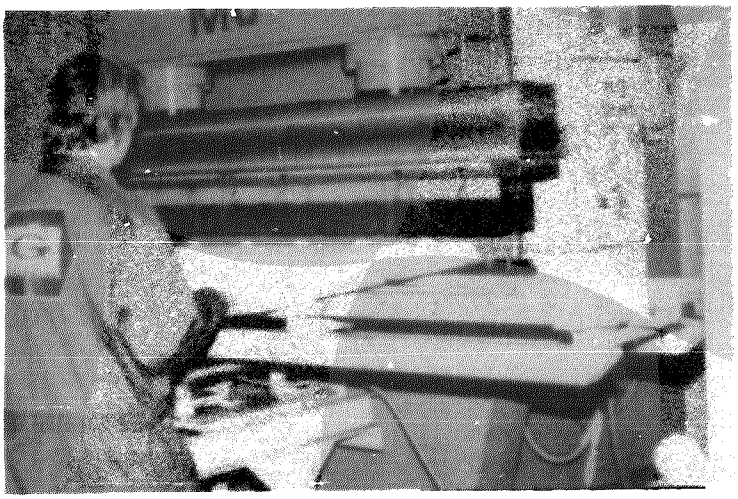

Figure 6.11.1-7 Joggling Process

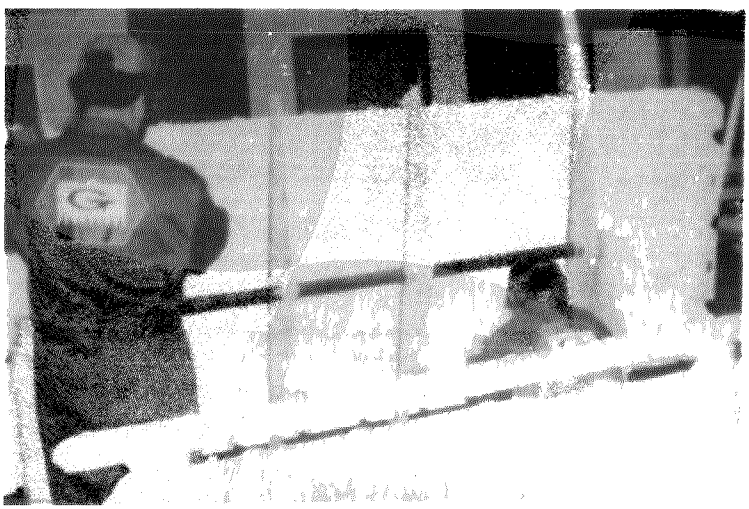

Figure 6.11.1-8 Liner Inspection

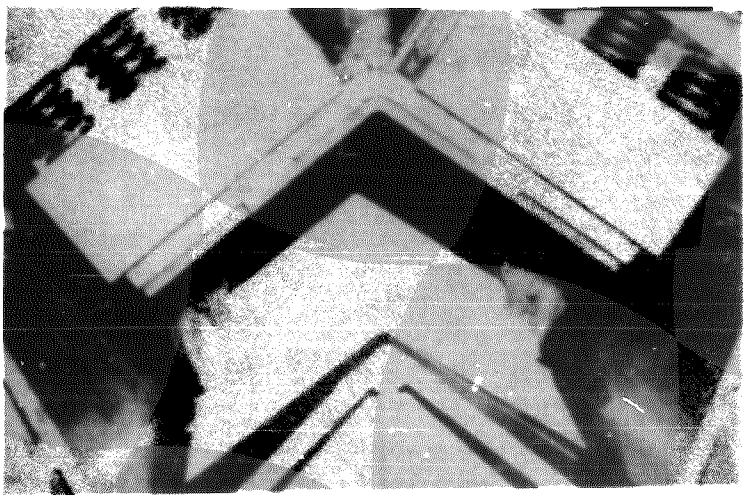

Figure 6.11.2-1 Forming of the Angle

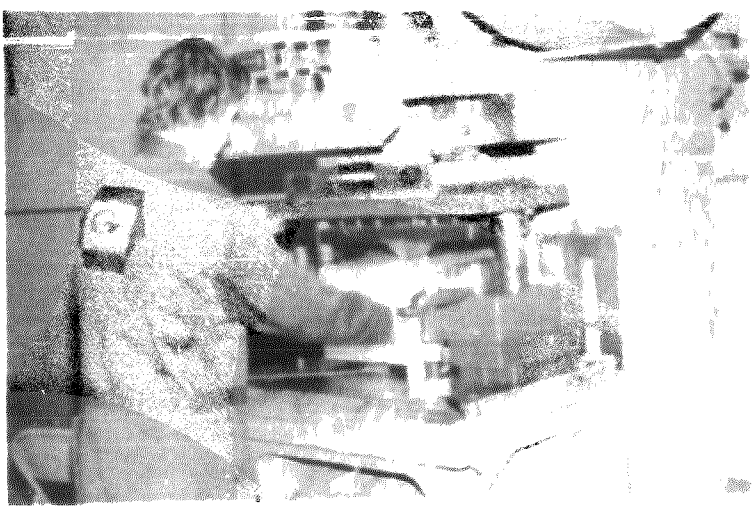

Figure 6.11.2-2 Angle-Piece Dimpling Operation

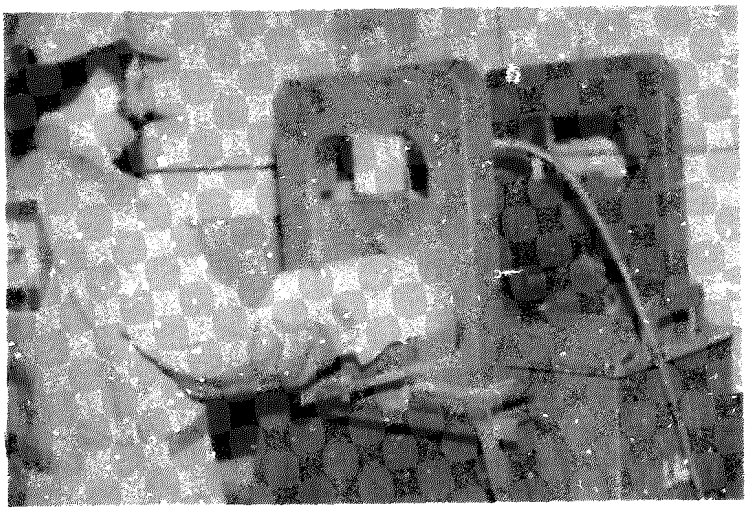

Figure 6.11.2-3 Shearing Angle Piece to Size

Figure 6.11.2-4 Joggling Angle-Piece Edge

6.11.4 Heavy Corners

These pieces were fabricated parts made from formed plate and welded in fixtures. Inspection requirements included dimensional check and visual surface inspection for burrs and weld spatter.

6.11.5 Suspended Deck

The deck was fabricated from standard structural pieces welded and inspected. The panel pieces inserted into the structural frame were the last item of the liner welded during construction.

6.11.6 Dimensional Tolerances

The tolerances of the liner pieces listed in Table 6.11.4-1.

Table 6.11.5-1

PART NAMES	CHARACTERISTICS	TOLERANCE
Flat Sheets (before shaping)	Length + Width	± 1 mm (reference only)
Flat Panels	Edge to Corrugations	± 2 mm
Flat Panels	Overall length	± 6 mm (12 PO/sheet)
Light Angles	Angle	± 1°
Light Angles	Position of Corrugation	± 2 mm
Light Angles	Length and Width	± 2 mm
Heavy Corners	Length and Width	± 1 mm
Heavy Corners	Angle	± 1°

7.0 SRE Test and Analysis

7.0 SRE TEST AND ANALYSIS

7.1 TEST PLAN

The objective of the test program was to demonstrate the operation and performance of a molten salt thermal energy storage subsystem using an internally insulated hot storage tank.

The specific objectives of the test program are listed below:

1) Measure tank heat loss under both steady state and transient conditions.

2) Determine storage system efficiency and salt temperatures under simulated solar plant operating conditions.

3) Demonstrate system cold startup techniques.

4) Demonstrate normal diurnal startup.

5) Demonstrate charging and discharging of system at anywhere between maximum and minimum rates.

6) Demonstrate hold at full and partial charge in both hot and cold tanks.

7) Demonstrate normal diurnal shutdown.

8) Demonstrate emergency shutdown.

9) Perform inspection and maintenance exercises.

The tests were performed at the CRTF. The testing sequence began with loading 79,314 kg (174,000 lb.) of molten salt into the cold tank. This was done at a nominal temperature of 315°C (600°F). The molten salt was then circulated through the entire system at 315°C (600°F) until all components were brought up to temperature. Then the propane heater and air cooler were operated and the hot tank and sump temperatures were brought up in steps. The system was then checked-out and operated.

The startup and checkout phase was followed by the performance test. These performance tests were to include: 1) daily cyclic test of charge and discharge, 2) steady-state conditions for the tank, and 3) transient cooldown of the tanks. A list of the tests performed is in Table 7.1-1.

Table 7.1-1 SRE Tests Performed

Test No.	Title
	Startup & Checkout Tests
1	Salt Loading
2	Functional Flow
3	Heat Up Hot Tank
4	System Operation Checkout
5	Emergency Shutdown Checkout
	Thermal Performance Tests
6	Steady State Heat Loss - Full Hot Tank
7	Steady State Heat Loss - Empty Hot Tank
8	Daily Charge/Discharge
9	Transient Cooldown - Full Hot Tank

The description of the actual test will be detailed later in this section. The complete test plan which was developed prior to the test is in Appendix D.

7.2 TEST PROCEDURES

Test procedures were generated for each of the tests planned. Each procedure was a step by step detailed operational manual. The procedures listed the sequence of each step to be performed in the test so the test operator had no decisions to make during operation assuming no abnormality existed. Any results to be checked during the test were noted. Where caution needed to be exercised in system operation, it was noted prior to execution of the function. Thus an operator familiar with the system could operate any test by following the step by step procedure.

Prior to testing, the procedures were developed by a design engineer familiar with all aspects of the equipment. A Failure Mode and effect Analysis (FMEA) was developed for the system and was used in combination with the test objectives to produce a procedure to safely operate the system. The FMEA is in Appendix E. All safety requirements and equipment were specified in the procedures.

The general outline for the procedure is listed in Table 7.2-1.

Table 7.2-1 Procedure Outline

1. Purpose
2. Experiment checkout a. General inspection b. Electrical checks c. Pneumatic checks d. Equipment checks - Air cooler - Pumps - Foundation cooling - Support equipment - Tank and sump vents e. Propane supply and evaporators
3. Control room checkout a. Verify safety equipment b. Heater circuit checks c. Data system checks d. System temperature verification e. Valve operation checks f. Salt level checks g. Control panel check and operation set up
4. Test a. Step by step operational sequence for - Pump usage - Air cooler operation - Propane heater operation - Temperature set points - Valve positions - Flow rates - Tank and sump heights - Trace heater control

As the system was operated the procedures were updated to reflect refinement in the operation. An example procedure for System Operation (Checkout - Test #4) is included in Appendix F.

Although the procedures are detailed they are not adequate to permit a novice to operate the system. The method of checkout is not detailed as to "how" or "where" (i.e., electrical amperage check of the trace heaters does not define the circuits or where they are located). An operator totally familiar with the system is necessary for system operation, especially in case of equipment abnormalities.

7.3 TEST DESCRIPTION

The following paragraphs describe testing of the SRE and the various problems experienced with equipment and the testing scenario. It should be noted however that although several equipment problems occurred during the test, the overall test objectives were met and the system performance was considered very satisfactory. The SRE system operation and tank cyclic charge/discharge verified the feasibility of the molten salt thermal storage system.

The major testing of the SRE occurred between January and April 1982. Construction of the SRE at the CRTF in Albuquerque, N.M. began in May 1981. The foundation and earth work was accomplished in June. The manufacture of the cold and hot tanks was started in July 1981 and completed in November 1981 and January 1982, respectively. The remaining portion of the test items were assembled and installed during the tank construction span time. The completion and checkout of the data system was accomplished several weeks after the hot tank completion. A more detailed schedule of the construction effort is given in Table 6.9-1. The checkout of the electrical system, trace heaters, pneumatic system and coolant system occurred before the system was filled with salt. The thermal performance of the lines, air cooler, and sumps had also been verified when salt loading was initiated on January 27. The only subsystem not fully checked out at that time was the data system.

Salt pumping into the cold tank began on January 27. Melting and loading the 79,250 kg (174,700 pounds) of salt took three days. The salt melting was done in batches, with up to 18,180 kg (40,000 lb) of salt in the melter. It was not possible to melt small batches of salt. The salt height achieved in filling the cold tank was within a fraction of an inch of the calculated level. The cold sump had also been filled during this time. During the fill, large amounts of steam emerged from the cold tank foundation. Although the concrete and the insulating castable had been poured the previous summer and were assumed cured, increasing the foundation temperature to the boiling point of water liberated large quantities of water vapor. The salt temperature from the melter was increased to approximately 316°C (600°F) to aid in drying out the foundation.

The heat loss from the cold tank was greater than expected and additional trace heating elements were added to the inside of the tank as immersion heaters. The power of the original trace heaters was 8.6 kW and the power required for the additional immersion heaters was 8.1 kW. The total power was maintained on the tank for several months and eventually the inlet salt temperature during charge/discharge was raised to 343°C (650°F) in an effort to dry out the foundation. Eventually 24 kW of heater power was added to the coolant loop in order to heat the water to 119°C (246°F). It was apparent that good thermal performance and good energy balance could not be achieved until all of the insulating castable material was dry. This was true for both tanks, since similar results were experienced with the hot tank when it was filled with molten salt.

Although the top of the castable insulation dried out quickly, the bottom portion did not become dry until the final week of the test and consequently the cold tank temperature was not reduced to 288°C (550°F) until that time.

As the water boiled out of the foundation much of it condensed in the exterior fibrous insulation. Some of the insulation became saturated; however the water did not appear to cause a degradation or collapse of the insulation. A check of the insulation at the end of the test revealed very little water.

The first cycle of the cold tank outlet valve (Valve #3) resulted in salt leakage past the plug. This leakage remained until a new valve seat was installed when the valve was rebuilt on February 24.

The salt was transferred to the hot tank and stored for one night. The transfer of the salt back to the cold tank resulted in two foreign articles being caught in the hot tank drain valve, (Valve #1). A piece of brick and a combined nut and bolt lodged between the plug and the seat. Cycling the valve would not dislodge them. When the hot pump was turned on, to transfer the salt leaking past the valve into the cold tank, the motor failed. This failure was due to a faulty motor and not to poor design or construction. The leakage of the valve caused salt to pour from the sump vent and from the salt pump between the pump mounting plate and main housing. The sump vent had a 0.64 cm (1/4 inch) diameter hole to limit the salt loss for this type of failure. Without this precaution the total salt of the hot tank would have been lost. To stop the salt loss an attempt was made to freeze the salt in the tank outlet line (Line #1) by removing its insulation. Freezing was not achieved until the salt flow through the hot sump vent was stopped and water was hosed over the bare line for several hours. The total salt loss was estimated at 12,700 kg (28,000 pounds). The salt leakage was stopped 7 1/2 hours after the valve and motor failure. Two thirds of the salt had leaked through the hot pump, poured over the hot sump insulation and frozen on the floor of the sump building. The remaining salt froze on the ground within the area of the berm surrounding the SRE. While rebuilding the valve it was found that the valve body had cracked. The valve had been closed with the hand wheel as tight as possible. Spraying the valve body with water caused stresses which may have cracked the valve. The crack was partially ground out and the body was welded. This failure occurred January 31, 1981.

Between February 12 and February 23, four cycles of salt transfer were made between the two tanks. The last cycle included dual transfer simultaneous charge and discharge. The hot tank temperature was raised to 504°C (940°F). System operation and checkout occurred during this period. Minor problems continued to occur. Both Valve #1 and Valve #2 continued to have small leaks. Valve #4, which was the control valve for the flow through the propane heater, severely chattered and resulted in the valve stem guide unscrewing and limiting its ability to fully open. All the valves experienced chatter, (vibration) at some portion of their operational travel.

Valve #3 was rebuilt with a new valve seat which stopped its leakage. A failure of the trace heater on Line #1 caused the line to freeze. Two of the three parallel heaters on the line were on one circuit which electrically opened. The third heater burned out. The heater which burned out was probably caused by rough physical usage it had experienced when Valve #1 was taken apart and rebuilt. The cause of the failure of the two parallel heater circuits was never determined. When all the electrical checks were made the heaters were operational. They operated without problems for the remainder of the test. After Line #1 froze, Valve #1 was cut out and sent back to Denver. The valve body was rewelded and seat threads were remachined. The portion of the stem which had been bent was cut off and a new section was added. The plug was machined and a new valve seat was installed. The rebuilt valve was sent back to Albuquerque and no leaks were experienced thereafter.

The first time Line #1 froze it was thawed out using welding torches. The line insulation had been removed and, as the line was heated from the valve toward the tank, the insulation was reinstalled over the thawed area. The trace heaters were left on so that, in combination with insulation, the line would remain above the salt freezing temperature. The second time Line #1 froze it was thawed by turning on the trace heaters with the line fully insulated. A portion of the line next to the valve had been heated and drained, such that a void volume of pipe existed. The vertical section of pipe penetrating the hot tank foundation required heating with the welding torch to thaw the salt. No trace heaters were installed in this section.

Subsequently, the salt was stored in the hot tank overnight and weekends. In the event of extended power loss the tank outlet lines would freeze. It was considered safer to have salt freeze in the hot tank outlet line since stainless steel is more ductile than mild steel.

Three discharge - charge cycles of the hot tank were performed between March 10 and March 12. The hot tank was discharged to a residual level of 0.4 m (16 inches) and then the salt was pumped back to the hot tank at a temperature of 566°C (1050°F). All the salt possible was drained from the cold tank. This completed the Heat Up Hot Tank - procedure #3.

From March 15 through March 17 the three discharge - charge cycles of the System Operation Checkout procedure #4 were accomplished. During this time Valve #4 was repaired twice. This first repair was to tighten the stem guide. The second time was to replace the valve stem/bellows which had failed.

Two simultaneous charge/discharge cycles were performed over the next two days. The cycle consisted of discharging the hot tank to its residual level and then, charging and discharging the hot tank at approximately equal rates for one hour. Following this the discharge was terminated and the hot tank was charged until the cold tank was empty. During the second cycle the plug of valve number four sheared off the valve stem and leakage developed through the bellows. Draining of the salt from the propane heater after shut down took 12 hours as contrasted to the normal 20 minutes because the plug fell into place on the valve seat. Approximately two thousand pounds of salt flowed out through the stem on to the ground during this time because of the failed bellows.

It was decided that Valve #4 would not withstand the flow dynamics and should be replaced with an orifice. The valve was modified so that the stem and plug could be removed and the valve seat was modified to hold an orifice. Another charge/discharge cycle was run with simultaneous charge and discharge. This completed procedure number four, System Operation Checkout.

Evaluation of the value failure lead to the conclusion that the plug should have a lateral constraint. This was based on the following facts:

a) Four failures had occurred on valves on this and the previous test.

b) The vibration mode was heard when the valves were approximately 25 to 40 percent open.

c) Valve chatter was worse when the valves were downstream of a pump but chatter also occurred in the tank outlet valves.

d) Valves chattered without vertical movement of the stem.

e) Chattered resulted with flow over or under the plug.

f) When valve #4 had a rigid stem constraint the plug was fractured off of the stem.

Between March 24 and March 31 the five cyclic charge/discharge cycles were performed. The hot tank was discharged to approximately 0.4 m (16 inches) salt height. Then dual transfer was performed for one hour. Charging the hot tank at 566°C (1050°F) until the cold tank had a salt residual of 0.4 m (16 inches) completed the cycle. Both charge and discharge rates were approximately 3 MW. This completed procedure # 8, Daily Charge/Discharge.

Three cooldown transient tests of the hot tank were preformed in succession. Their durations were 5 days, 3 days and 5 days, respectively.

Although the initial salt temperature of the tests were different, the first two cooldown rates were the same. The third cooldown had a slower cooldown rate due to the dried foundation. Heating the foundation coolant to 119°C (246°F) had finally forced the foundation temperature above the boiling point of water. Thus, the objectives of procedure # 9, Transient Cooldown - Full Hot Tank, was achieved.

It was necessary to use the cooldown data to determine the heat loss from the hot tank. Three of the seven heater circuits in the hot tanks had failed before installation and the other four had failed just prior to the transient test. Insertion of a new heater inside the hot tank was not considered due to the time, difficulty and cost.

During the cooldown test of the hot tank, steady-state tests were being performed on the cold tank. The foundation of the cold tank was being dried out during the first two tests. During the second steady-state test temporary insulation was added to the exterior of the storage tank foundations to expedite drying of the castable insulation. The foundation insulation was covered with a plastic film. The temporary insulation soon became impregnated with water.

During the first two steady state tests there was a large drop in the tank temperature during windy periods. Probable causes were; 1) air infiltration through the tank sheathing and insulation and 2) air infiltration through the temporary insulation and evaporation of entrapped water. Some of the large gaps in the cold tank sheathing were caulked prior to the third test. The third steady-state test showed improved thermal performance of the cold tank. The windiest day of the steady-state test occurred during this third test but the large tank temperature drop experienced at high winds during the first two tests was not seen. Both the caulking and the drying of the temporary insulation were considered responsible for the better performance.

The last test performed was a second cyclic test. With the foundations dry, better thermal performance of the test was possible. Three days of the test had the following scenario:

- Discharge of hot tank to 0.4 m (16 inch) salt height
- Dual charge and discharge for 1 hour
- Charge of hot tank until cold tank salt residual was 0.4 m (16 inch)

After the last test all the salt possible was placed in the cold tank. Salt remained in the cold and hot sumps but the hot tank had been emptied. The power into the cold tank was reduced to 8.6 kW and the heating of the foundation coolant system was stopped. The outlet line from the cold tank was the only line filled with salt. The last test day was April 16, 1982.

A summary of the test log is given in Appendix G. The occurrences of each day of testing is described including salt transfer and equipment problems.

7.4 THERMAL PERFORMANCE

The thermal performance (heat loss) of the system included the following:

1) Hot tank
2) Cold tank
3) Cyclic test with comparison to analytical model
4) Thermal siphon heat transfer in lines

The thermal performance of all the support equipment (sumps, lines, air cooler) was as predicted. The temperatures required for the support equipment was provided with trace heating.

7.4.1 Hot Tank

Steady state testing was not possible due to the failure of the internal electrical heaters. Three cooldown tests were performed. The temperature history for the tests are shown in Figure 7.4.1-1. By the third test the castable insulation of the foundation appeared to have dried out, which accounts for the slightly better thermal performance. The point taken for the analysis should be as hot as possible and still allow consistent thermal gradients through the insulation. The heat loss from the hot tank was analyzed at a time approximately two days after the start of the third cooldown. The heat loss from the tank was based on the temperature rate of change and heat capacity. The temperature change of 0.86°C/h (1.54°F/h) was derived by averaging the salt temperature data at times of $\pm$ 4 hr around the time used for the thermal analysis. The salt weight was 53,365 kg (117,403 lb) and the heat capacity of the salt was taken as 1.53 joules/g-°C (.366 Btu/lb-°F). The salt temperature was 514°C (957°F) with a heat loss of 19.40 kW. A corresponding heat loss of 21.36 kW would exist at 566°C (1050°F). The thermocouples on the liner, shell and sheathing were placed in a radial line. The temperatures at the analyzed condition shown in Figure 7.4.1-2 are placed in their corresponding vertical height of the tank and sequentially in order of north, east, south, and west. Some temperature variation due to insulation performance was seen but in general the temperatures in each area were consistent.

Figure 7.4.1-3 shows a temperature profile at the liner, shell and sheathing. The liner had a nearly constant temperature vertically within the salt. The ullage section of the liner was approximately 8°C (14°F) cooler than the liner contacting the salt. The wall temperature of the shell was 268°C (514°F) adjacent to the liner. The shell temperature within the attic area was 160 °C (320°F).

The calculated shell temperature at this condition should have been 240°C (465°F). This data indicates that the performance of the brick was not as good as expected. In comparing the brick and the fibrous insulation, the fibrous insulation performed closer to expected thermal conductance. The shell temperature within the attic space was 160°C (320°F) which was cooler than desired. This was due to the fact that the analysis did not take into account the correct area of the attic in the heat transfer from the top of the tank. It was desired to maintain the shell at a constant temperature to reduce stresses. The maximum temperature difference allowed between the roof and the wall was 80°C (176°F). In this test however, the temperature gradient was within the wall and not at the wall/roof junction. It was concluded that the effect of the attic on the thermal performance is much greater in this small tank than in a larger tank.

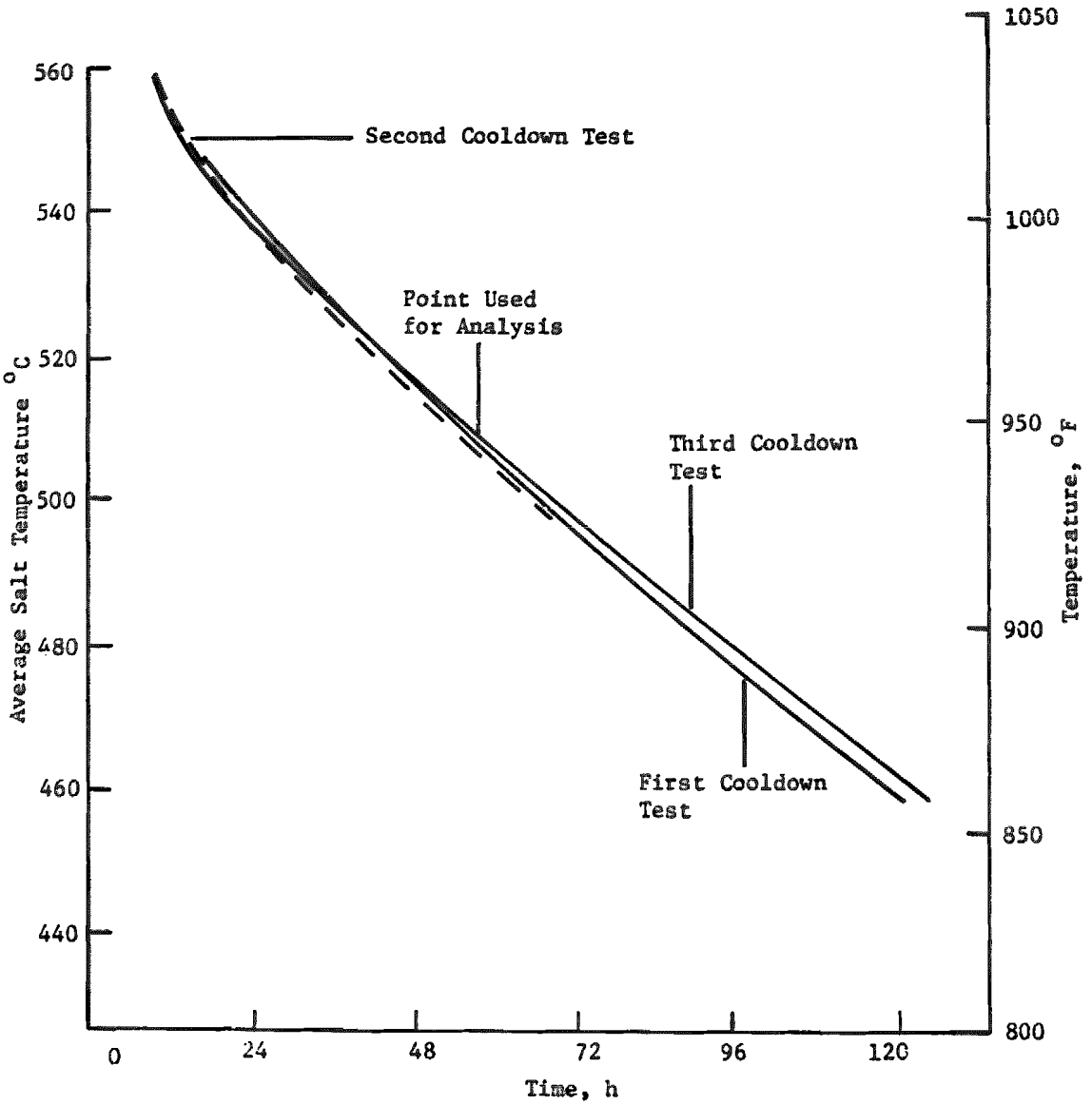

Figure 7.4.1-1 Transient Cooldown of Hot Tank

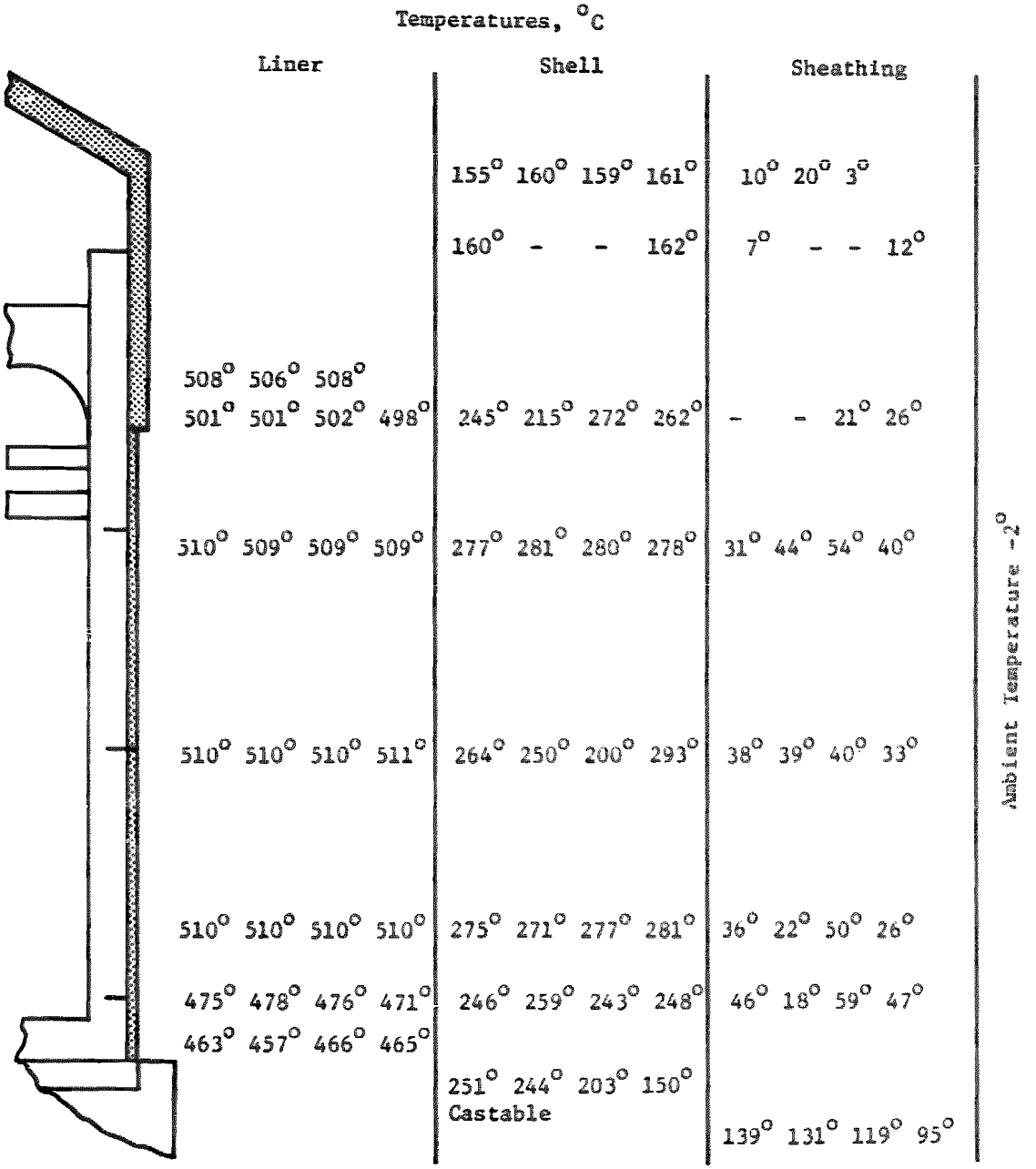

Figure 7.4.1-2 Hot Tank Temperature Profile at Analyzed Condition

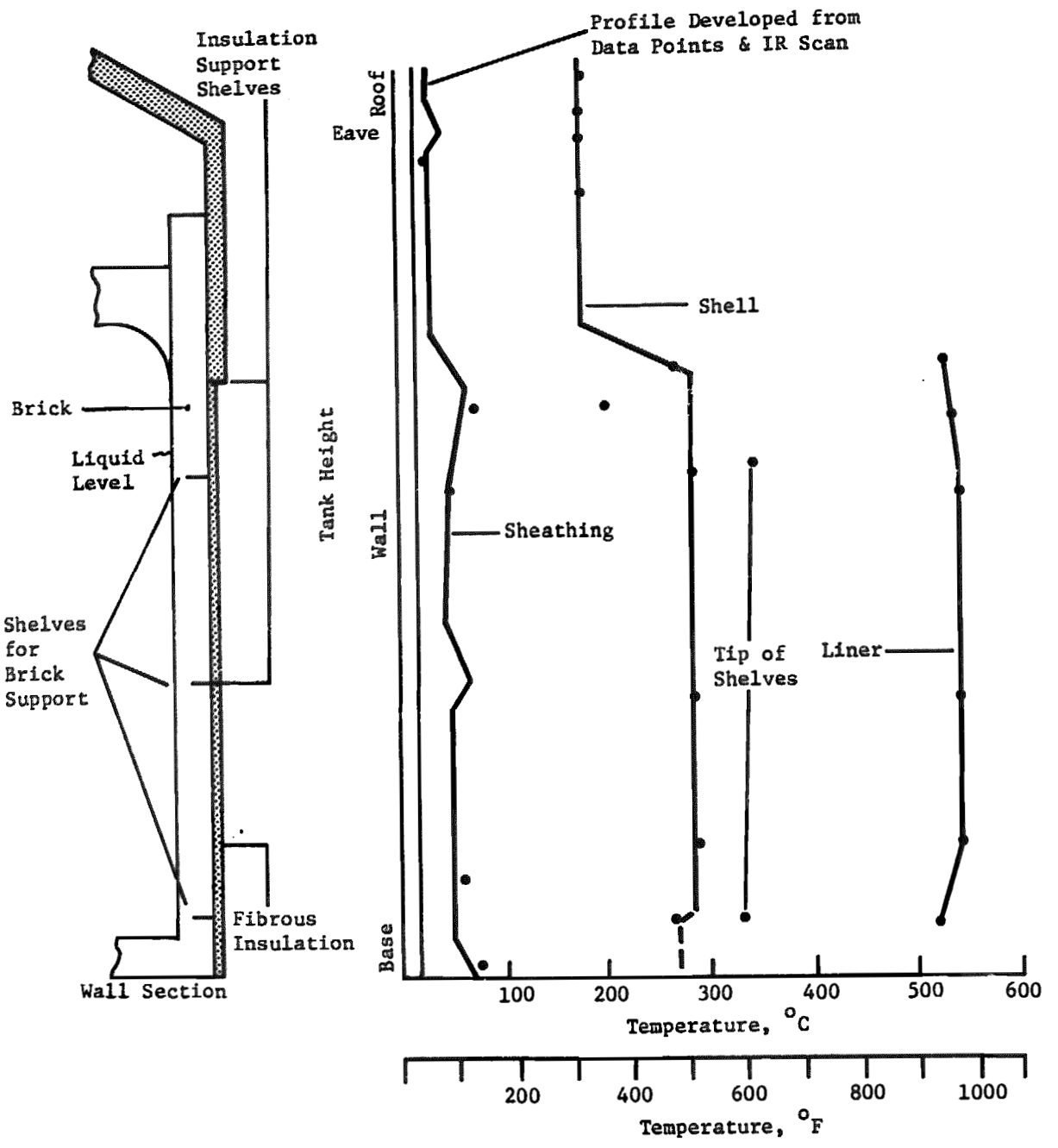

Figure 7.4.1-3 Hot Tank Temperature Profile--North Side

The sheathing temperature profile in Figure 7.4.1-3 included both thermocouple data and data obtained using an infrared optical scanner. Figures 7.4.1-4 shows the pictures taken of the tank which are overlaid with their associated temperature profiles. The surface of the tank scanned is located by the line at the right. The relative temperature scale is 30°C (54°F). As the scan line (a series of red dots) moves to the left, the temperature of the surface scanned was increasing in temperature. The infrared scanner had a floating lower temperature which was the lowest temperature it detects and indicates only relative temperatures. The infrared scanner used was a ThermAtrace by Barnes Engineering Company. These infrared results were plotted along with the thermocouple data (taken at the same time) as seen in Figure 7.4.1-5 and Figure 7.4.1-6. The infrared scan was overlaid on the thermocouple data to obtain the best correlation of the two. Generally there was good agreement. The discrepancies could have been caused by inaccuracy of the thermocouple location definitions. At the period of time that the infrared scans were taken the system was not at the design condition. However; the relative temperature profiles should remain constant for other time periods. The use of this infrared scan was considered very helpful in the analysis of the tank thermal performance.

Evaluation of the tank thermal performance was made by comparing the total tank heat loss with that of the computer model. The input to the thermal model described in section 5.0 was updated to include the correct areas of the tank and to account for penetration. The tank model which was developed to analyze various materials and thicknesses of insulation was a simple model to minimize computer cost. Where the model did not account for various heat losses the input was modified rather than change the model. To account for penetrations, such as brick shelves and insulation support ring, the thermal conductivity of the appropriate insulation was increased. To account for the large shell area associated with the attic the conductivity of the exterior insulation was increased appropriately to result in the correct total heat loss. The derived external film coefficient (both radiation and convection) with the air was entered into the program and the correct ambient and foundation temperature were used. With the above corrections the model predicted 18.1 kW of heat loss with the salt at 508°C (957°F). This value is less than the actual loss of 19.40 kW by about 7 percent which is very good for heat transfer calculators.

To determine which portions of the tank contributed to the increased heat loss, the tank was further analyzed. Using the temperature profile of the tank, potential heat losses were calculated by two methods. The first method was to calculate heat loss through the tank insulation and supports using their advertised thermal properties and the measured temperatures. This analysis was more detailed than the computer model and was more accurate. This calculated heat loss was 17.48 kW and will be referred to as the calculated heat loss. The second method was to use the actual heat loss of 19.4 kW and appropriate it to the various tank areas by using the temperature gradient from the sheathing to the ambient. This heat loss is called the actual heat loss. The heat loss was divided into various sections as shown in Figure 7.4.1-7. In order to define the heat loss from each area it is necessary to have know values of temperature and thermal resistance.

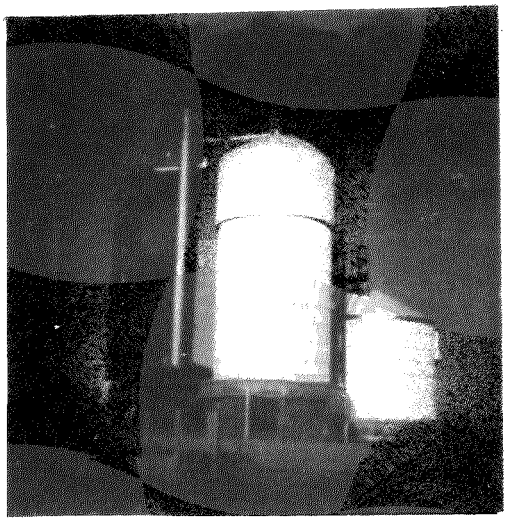

(a) Eastside 7:15 a.m. 16 April

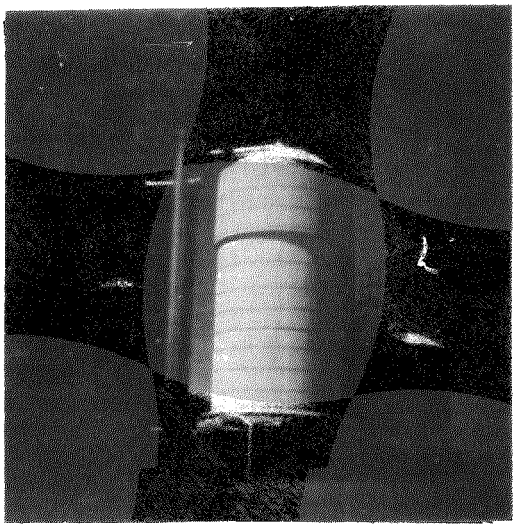

(b) Eastside 10:45 a.m. 16 April

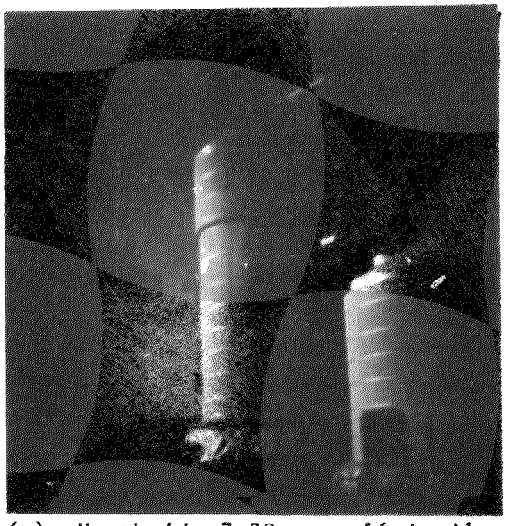

(c) Northside 7:30 a.m. 16 April

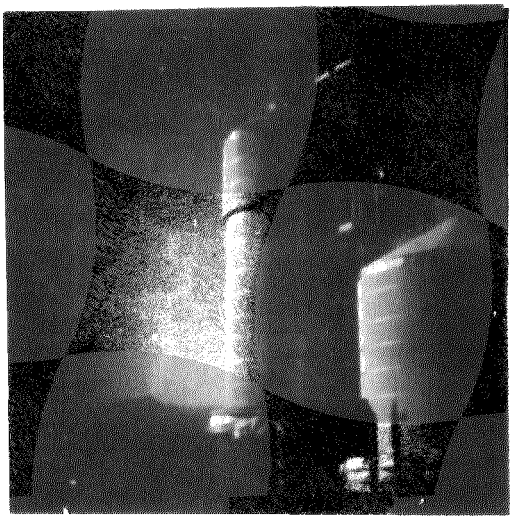

(d) Northside 7:30 a.m. 16 April

The line at the right shows which portion of the picture is scanned. The temperature at the scan line represents the coldest temperature "seen". The line at the left is 30°C (54°F) hotter than the right line. A linear scale of 30°C results.

Figure 7.4.1-4 Temperature IR Scan of Hot Tank

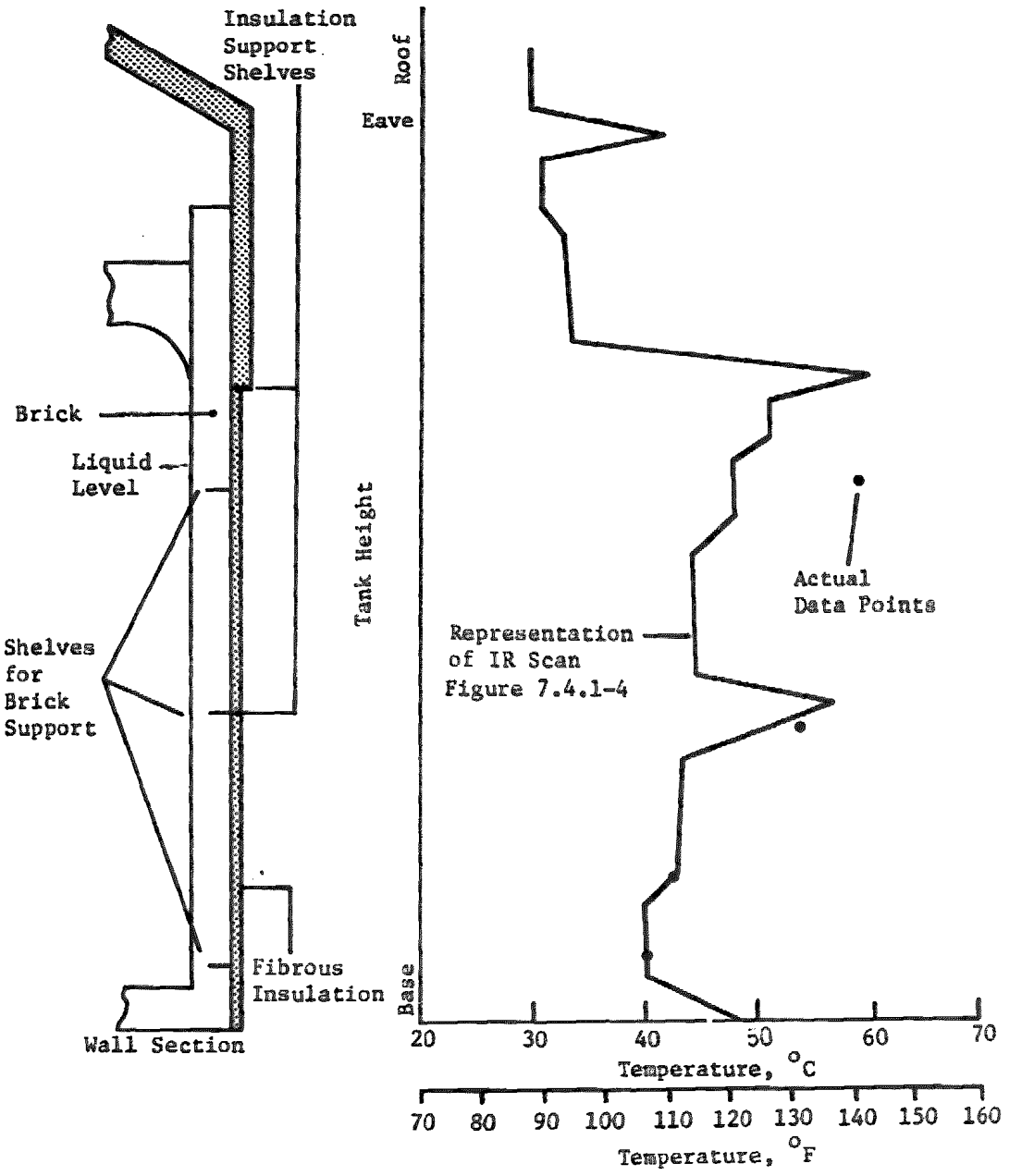

Figure 7.4.1-5 Hot Tank Sheathing Temperature Profile--East Side

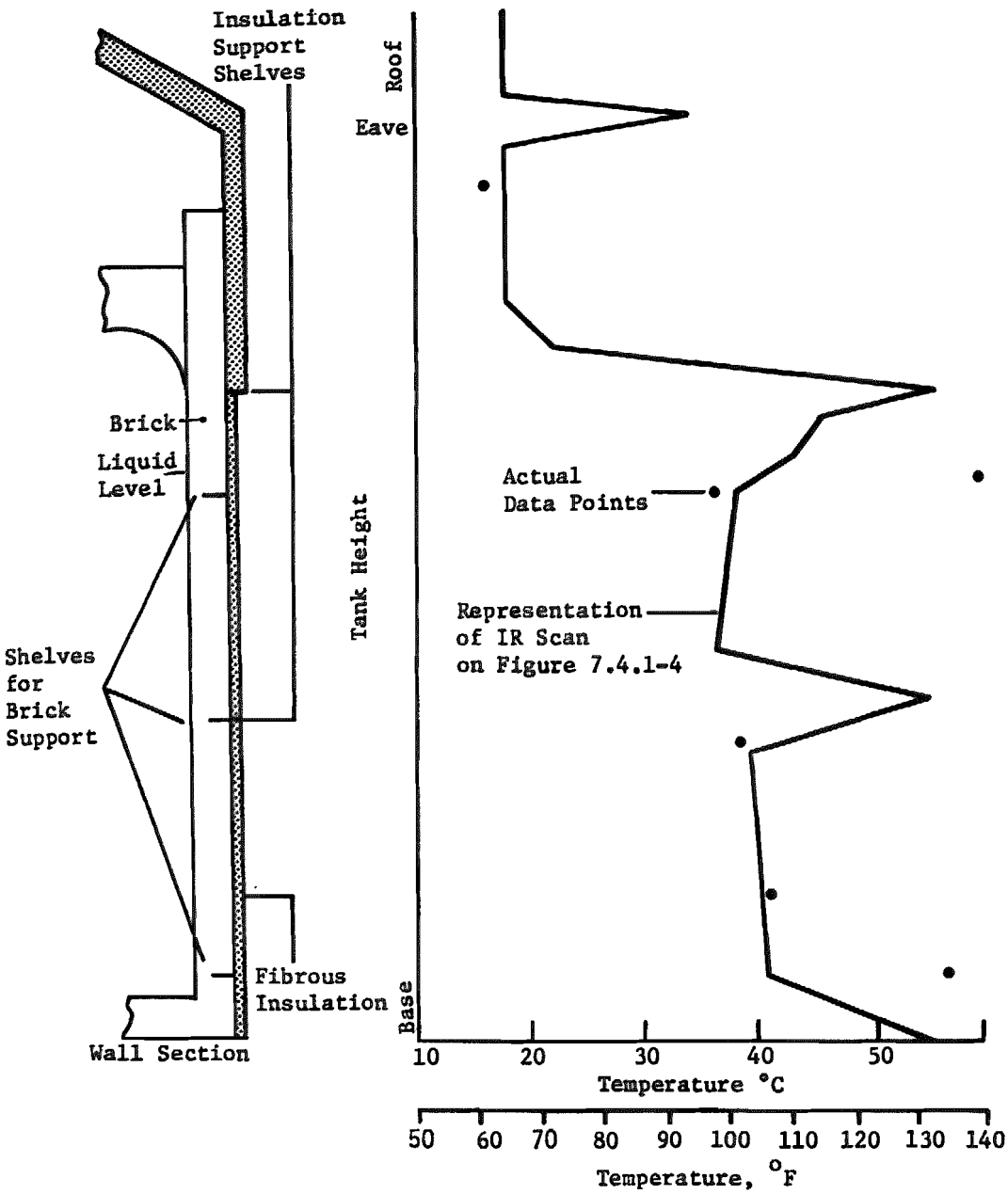

Figure 7.4.1-6 Hot Tank Sheathing Temperature Profile--North Side

Since the effective thermal conductance of the separate areas was to be determined, the heat loss from those areas was estimated by using convection and radiation from the sheathing. The summation of losses from the sheathing can be adjusted to match the total tank heat loss. This accounts for variation in the film coefficient and the surface radiation. The detailed analysis is in Appendix H.

During the test the foundation coolant loop was being heated to 119°C (246°F) by thermostatically controlled heaters. Thus the heat loss from foundation was not determined by the heat rise of the coolant as originally intended. The temperature gradient across the brick and the insulating castable material were consistent with analysis, including edge effects. It was concluded that the heat loss through the foundation was close to the predicted value.

The heat loss through the foundation was added to the initial calculated convective losses from the sheathing. This total was slightly greater than the known loss. The convective losses were then proportionally adjusted so that agreement with the actual loss was made. This was considered reasonable because of the uncertainty of the convective film coefficient, and the variation in the sheathing emittance. These adjusted convective losses were considered to be the actual heat losses and are compared with the calculated loss through the insulation in Table 7.4.1-1. The greater the difference the poorer the insulation performance. The heat loss from the hot tank is shown in Figure 7.4.1-7. The support ring, penetrations (vents, heat trace, instrumentation), lower ring and the foundation are small compared to the total tank heat loss. The difference of eleven percent was considered reasonable. Some of this variation can be reduced as discussed below.

Table 7.4.1-1 Hot Tank Heat Loss

	Calculated Loss		Actual Loss	
	Watts	Btu/h	Watts	Btu/h
Attic	578	1974	1156	3948
Upper INS. Support Ring	91	312	133	454
Penetrations	47	160	47	160
Upper wall	920	3139	787	2685
Wall	13877	47363	15338	52349
Lower Ring & Edge	352	1200	427	1459
Foundation	1573	5367	1519	5169
Total	17438	59515	19402	66229

$$\frac{\text{Actual}}{\text{Calculated}} = 1.11$$

The salt temperature was 508°C (947°F)
Penetration losses were taken as calculated values

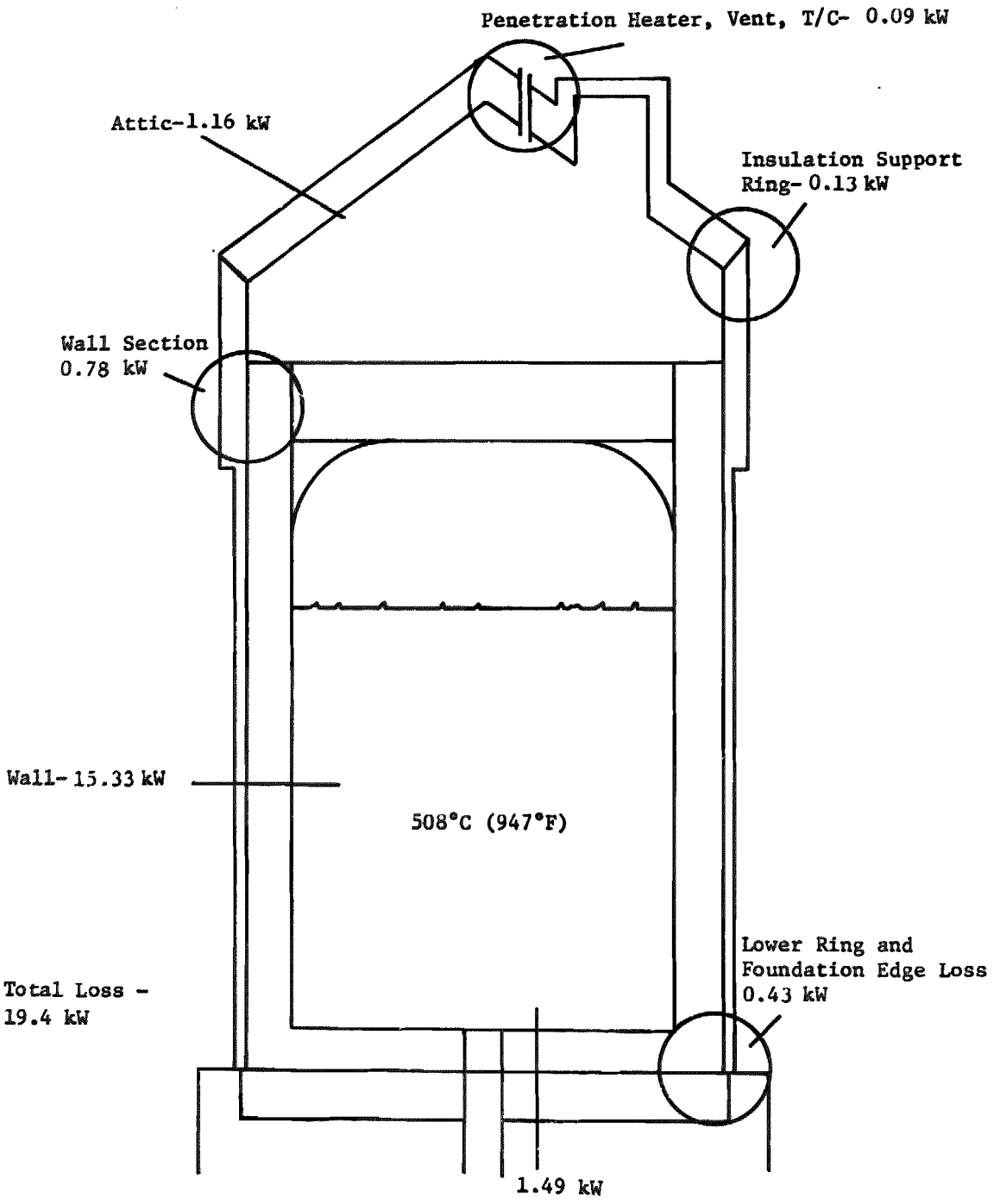

Figure 7.4.1-7 Hot Tank Heat Loss--Actual

The heat loss through the tank wall was greater than calculated by 5 percent. The shell temperature was 268°C (514°F) which was greater than the calculated shell temperature of 238°C (462°F). The small increase of the effective thermal conductance of the brick may have been caused by some cracks between bricks, insufficient fibroue insulation in expansions joints, convection around holes for the anchors, and/or brick thermal conductivity being different than advertised.

The attic shell temperature was 160°C (320°F). It was desired to maintain the shell (roof, wall, floor) at a constant temperature. The maximum temperature difference allowed between the roof and the wall was 80°C (176°F). In this test however the temperature gradient was with the wall and not at the roof/wall junction. The thermal analysis for sizing the tank insulation thickness did not consider the portion of the tank side wall which was in the attic area. This resulted in the lower shell temperature and the increase heat loss. The increased heat loss through the roof was probably due to flat block insulation being installed on a conical roof which made it difficult to achieve a good tight convection free installation. On a large tanks the roof curvature is much smaller thus minimizing this problem.

The heat loss through the attic has increased which also inferred a greater heat loss through the insulation area of the liner top. This increased heat loss was considered to be largely due to convection in and around the vertical corrugation of the liner. This convection increased the temperature of the inner surface of the wall bricks above the liner, which in turn increased the heat loss into the attic and the radial heat loss through the upper wall. The upper wall was defined as the wall area with internal brick which was above the suspended deck. In future applications this convection can be reduced either by eliminating the upper wall by having the brick stop at the suspended deck or by installing insulation in the vertical corrugations to eliminate convection.

In large tanks the shell attic area will be similar to the suspended deck area. Corner losses will be less significant that those in the SRE. Consequently, the unit area heat loss of a large tank will be improved. Heat loss variance from predicted values have been defined, thus the heat loss from the tank can be defined. Future prediction should be quite accurate. The tank attic heat loss can be improved by eliminating problem seen in the SRE.

One phenomenon observed in the hot tank was the lack of stratification of the molten salt. Figure 7.4.1-8 shows the vertical temperature of the salt measured by the temperature rakes. This was data taken from the first cooldown test which is typical for all three cooldown tests. The temperature profile at the rake in the center of the tank showed some lower temperatures at the bottom as the days progressed, but the rake thermocouples near the wall show almost a constant vertically temperature at any given time.

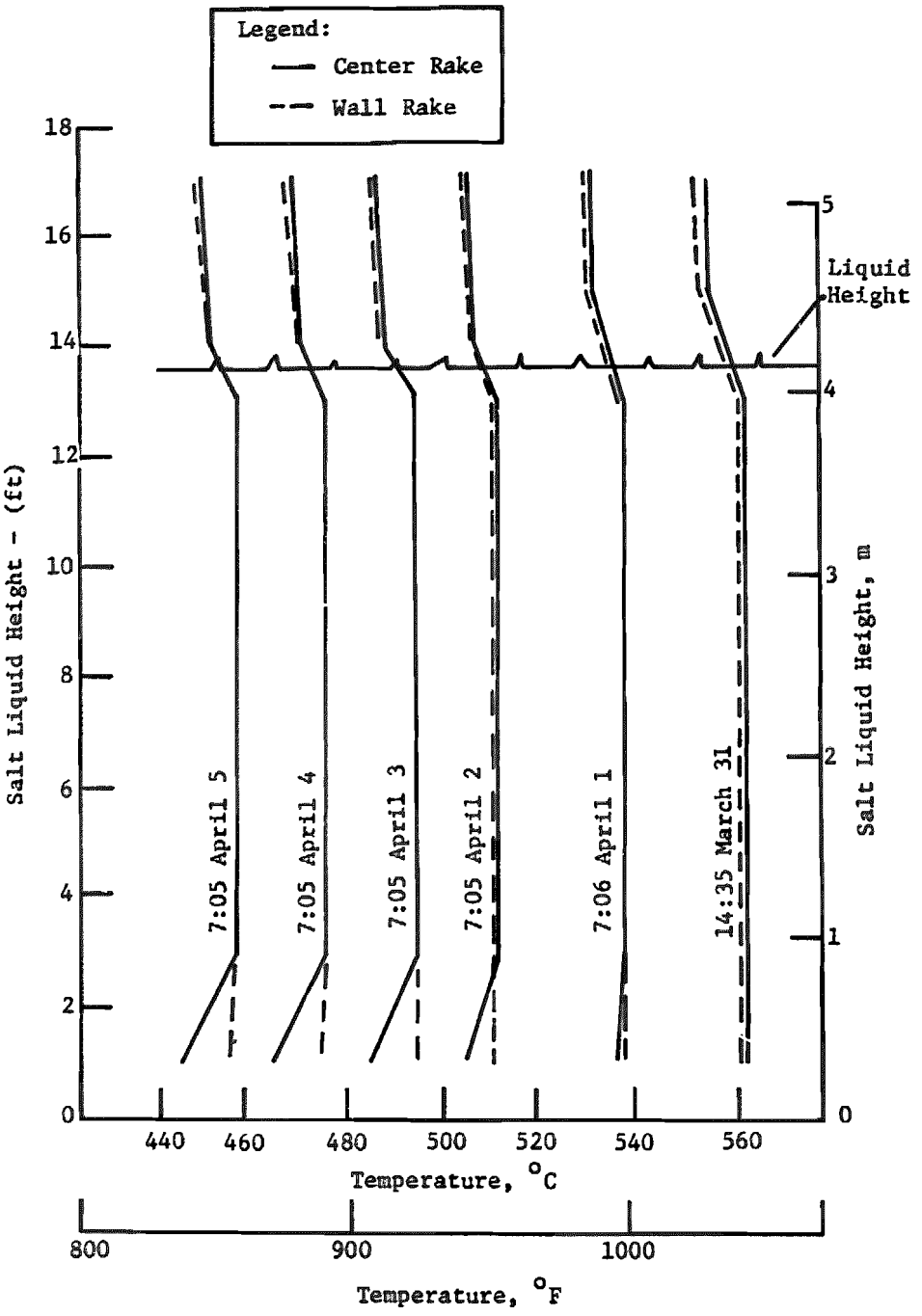

Figure 7.4.1-8 Hot-Tank Salt Temperature History--First Cooldown

7.4.2 Cold Tank

The performance data of the cold tank was taken four days after the start of the third steady state test. Figure 7.4.2-1 shows the temperature history of the tank during the test. During the fourth day a very strong wind occurred which caused a decrease in tank temperature. Figure 7.4.2-2 shows the tank temperatures for the previous two steady state tests. High wind days occurred during both periods with very obvious tank responses. Between the second and third steady state test the tank foundation was thought to have dried out, some of the sheathing cracks were caulked, and to some degree the temporary insulation on the outside of the foundation dried out. The salt in the tank was at a minimum height of 0.14 m (5.5 in.) which allowed a fast thermal response time.

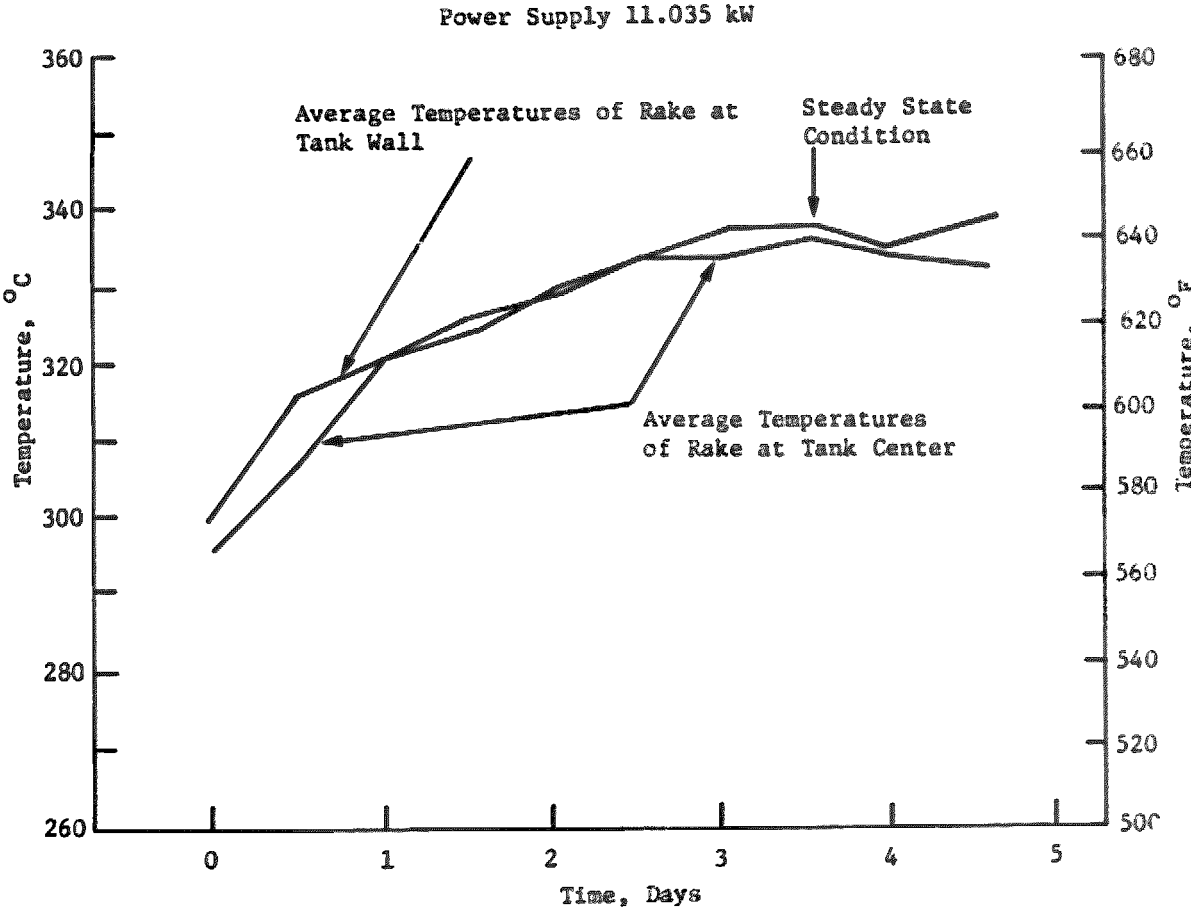

Figure 7.4.2-1 Cold Tank Temperature History--Steady State

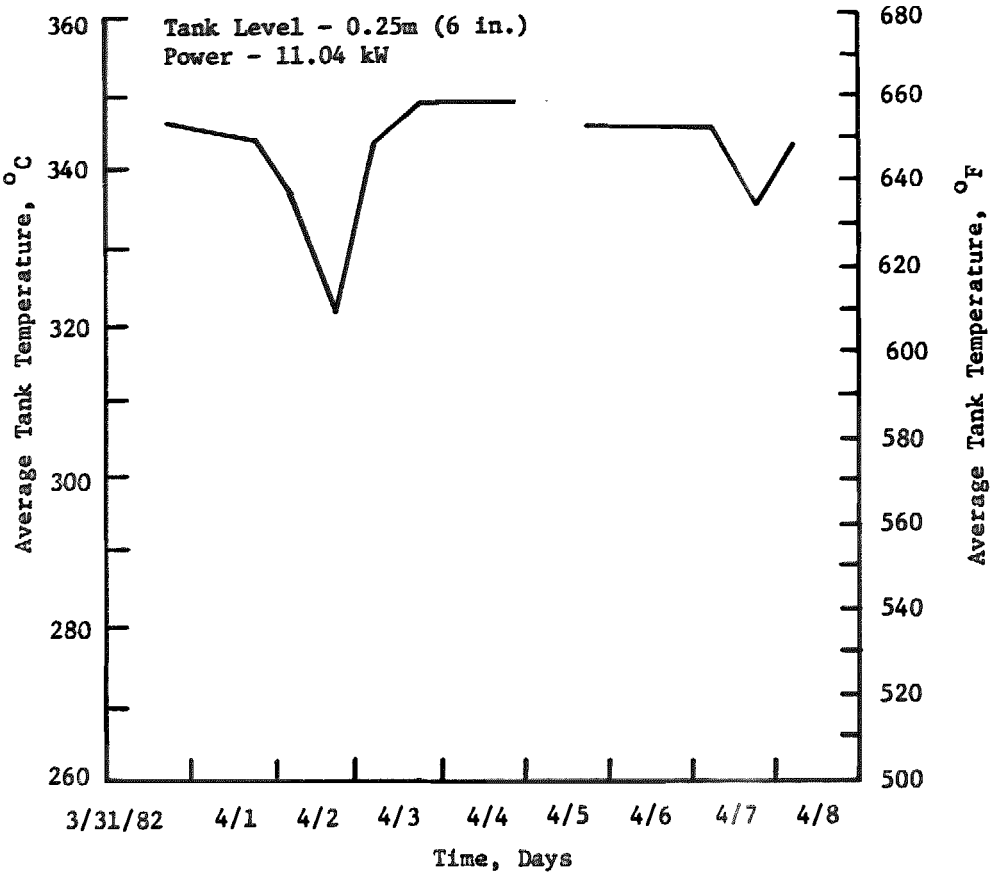

Figure 7.4.2-2 Cold Tank Temperature History--Wind Effect

Figure 7.4.2-3 shows the temperatures of the tank at the design condition. The temperatures are shown for the roof, foundation and the four quadrants of the shell and sheathing of the tank wall.

The infrared scans of the cold tank are shown in Figure 7.4.2-4. These scans were taken at a different time than the reading used in the analysis of the tank heat loss. The temperature gradients measured also existed at the time of the design analysis, so they were considered useful for the heat loss determination. Comparison of the infrared scans with the sheathing thermocouple data is seen in Figures 7.4.2-5 and 7.4.2-6. The infrared scans were utilized in establishing the correct sheathing temperature profile, which was used in the heat loss determination.

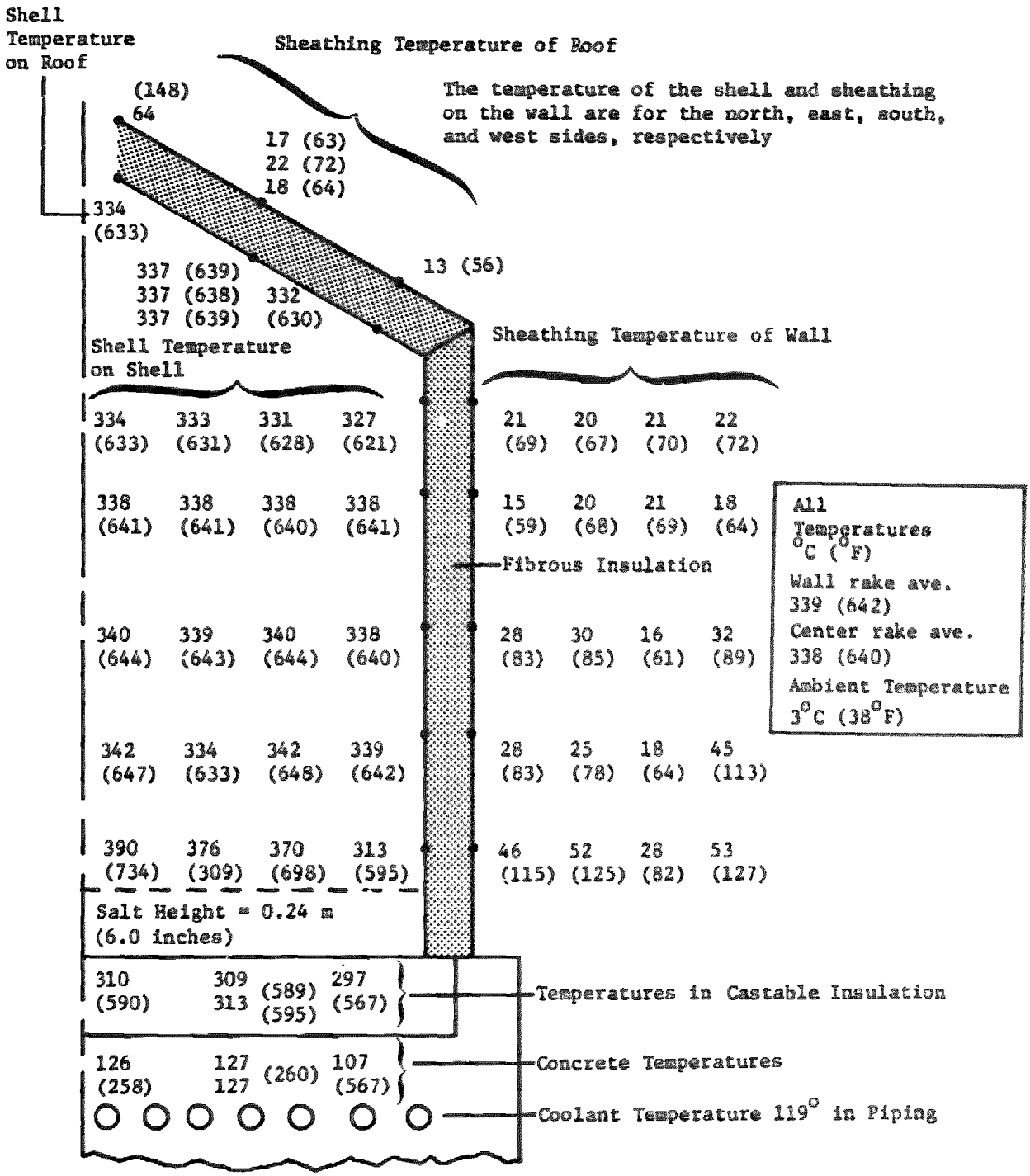

Figure 7.4.2-3 Cold Tank Temperature Profile at Steady State

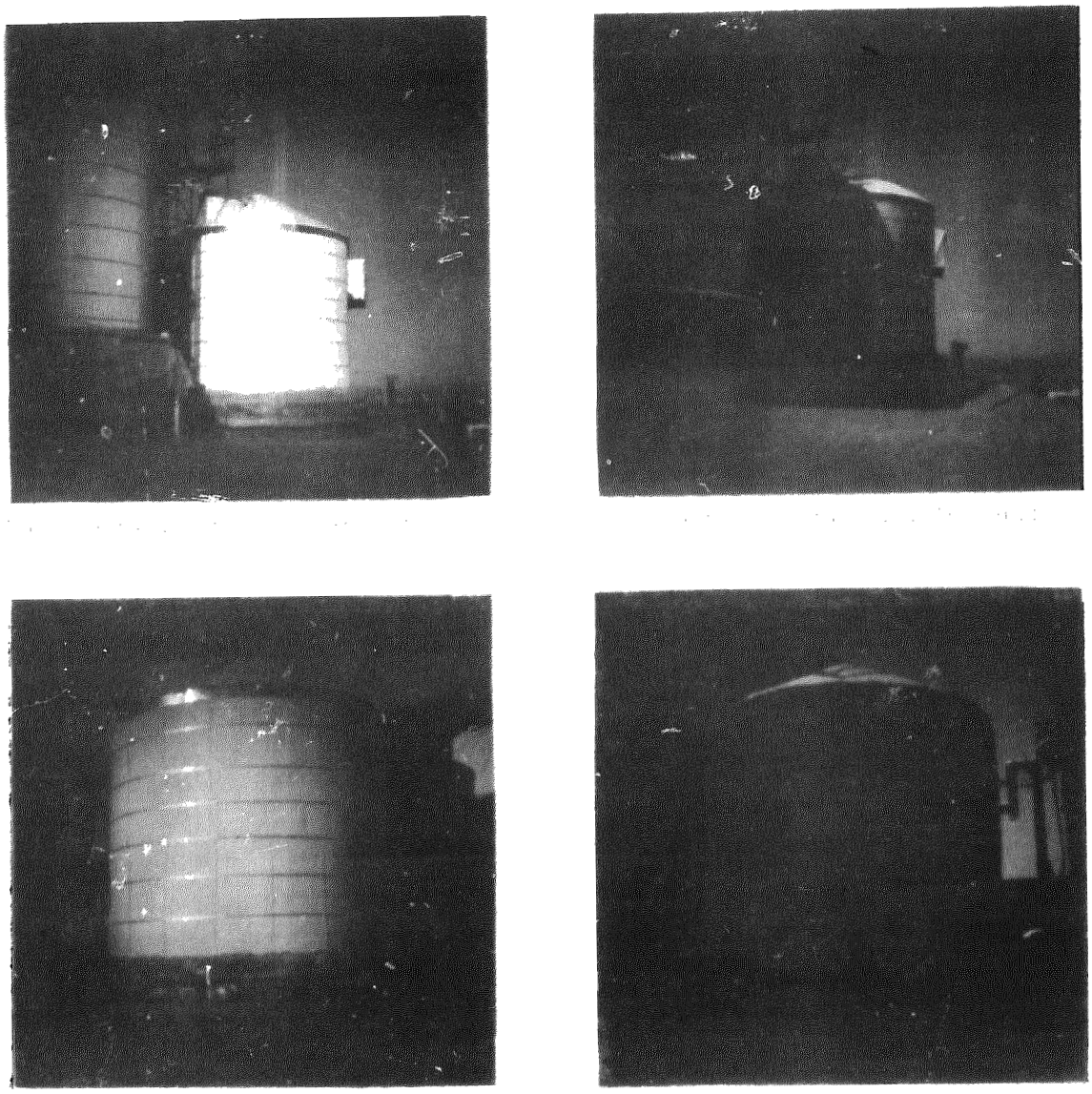

The time at the right shows which portion of the picture is scanned. The temperature at scan line represents the coldest temperature "seen". The line at the left is 30°C (54°F) hotter than the right line. A linear scale of 30°C results.

Figure 7.4.2-4 Temperature IR Scan of Cold Tank

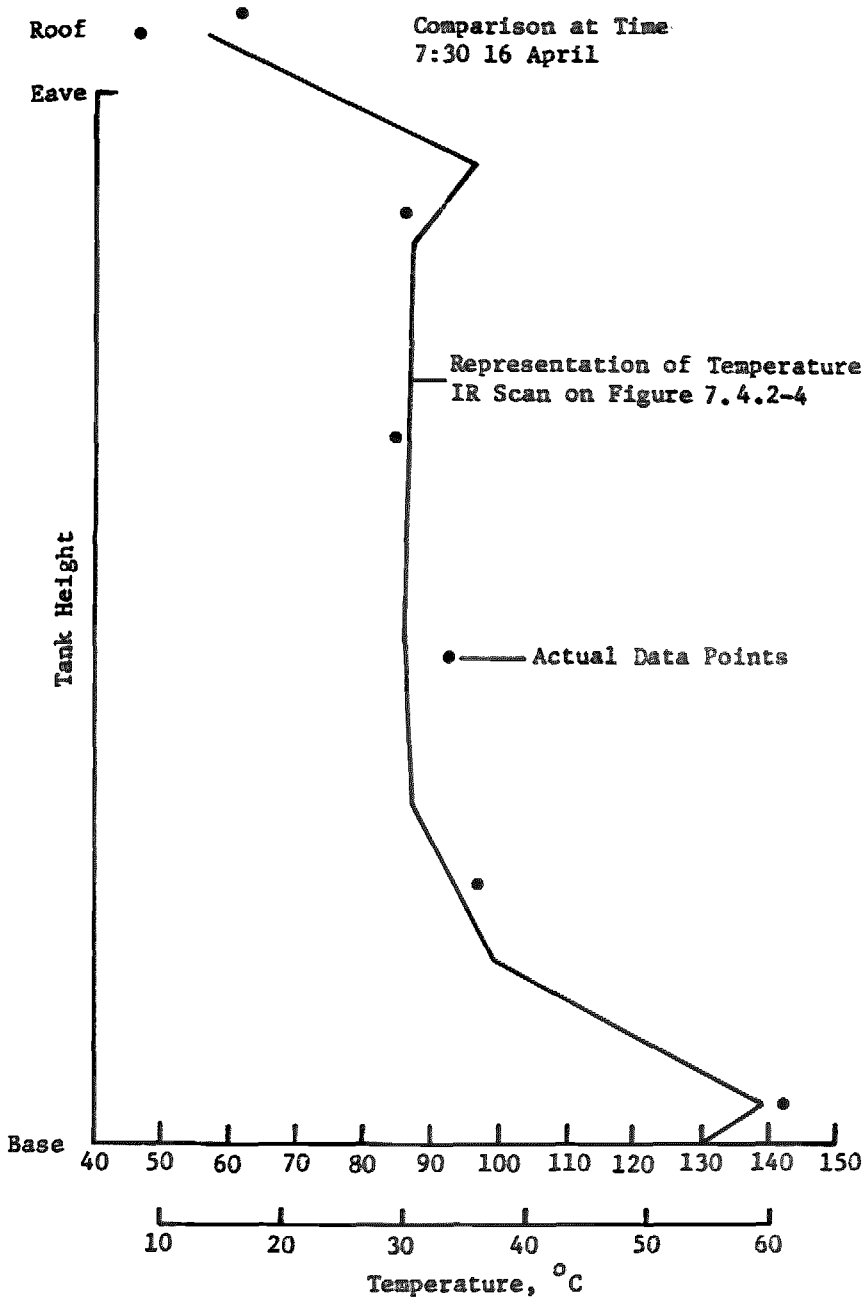

Figure 7.4.2-5 Cold Tank Sheathing Temperature Profile--East Side

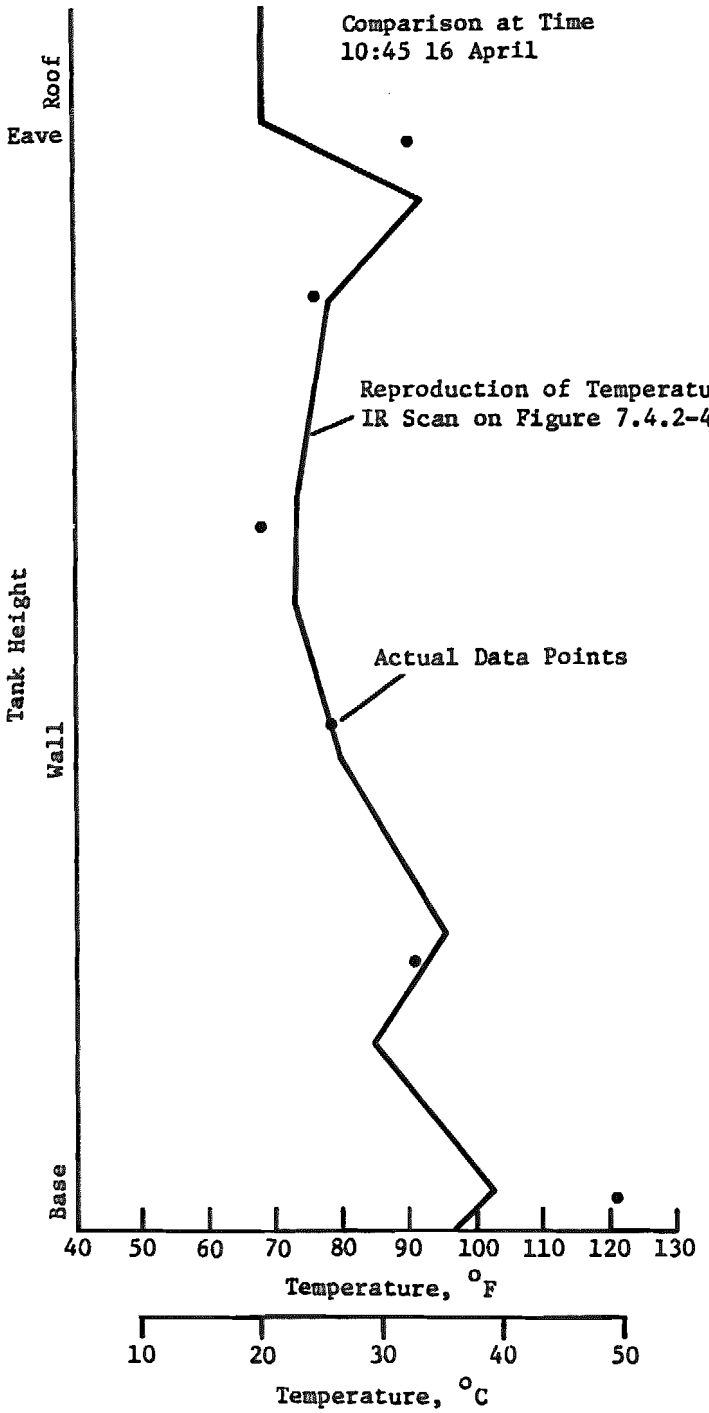

Figure 7.4.2-6 Cold Tank Sheathing Temperature Profile--North Side

The heat input to the tank was determined from the electrical power to the heaters. The resistance of the heaters was measured while they were operational. The voltage was 277 V. Measurement of the voltage was taken at various times but did not show any consistent bias. Voltages higher and lower than 277 V were measured. The total error in power could be $\pm$ 3.6 % with a $\pm$ 10 volt variation. Since several days were involved in the steady state condition, use of a near normal voltage value was deemed reasonable. Thus a small error in the actual power exists. The power into the tank was 11.035 kW.

Calculation of the heat loss was determined in the same manner as used for the hot tank. Appendix H contains the detailed analysis. The actual energy lost from the sheathing (radiation and convection) was compared with the calculated energy transferred through the insulation. The energy losses through the insulation were calculated by using the known temperatures and advertised conductivity of material. The convective heat losses from the sheathing were balanced to agree with the known loss of 11.035 kW. The tank was divided into various areas. The walls roof and floor are obvious areas. A fourth area was the upper ring at the tank eve and a fifth area for the foundation edge and lower ring. From the sheathing temperature profile the areas associated with the upper and lower rings are approximately 97 square feet. The increased temperature and heat loss of these two areas was due to the structural penetrations in the insulation. The calculated heat losses from these sheathing areas are taken as the actual heat losses and are shown in Figure 7.4.2-7. Table 7.4.2-1 compares the calculated heat losses with the actual heat losses. The heat loss of the penetrations and heaters were taken as calculated since no instrumentation has been installed in the test to determine this loss.

The difficulty of insulating tightly against the upper ring is considered the reason for the increased heat loss there. Flat block insulation installed on the conical roof resulted in a poor fit which allowed some convection paths. The 47% increase in heat loss was very similar to the results seen in the hot tank exterior roof insulation.

The major heat loss difference between actual and calculated was in the wall insulation which increase by 123 percent. The insulation which was 0.38 m (15 in.) was installed in three layers, with overlapping joints. The large uniform surface of this wall should provide good insulation performance. One possible explanation for the increased thermal conductance was the presence of water. When the foundation was being dried out large amounts of water condensed in the fibrous wall insulation. Drying of the insulation occurred over the test period and a visual inspection of the insulation at the end of the test gave indication of very little water. However, a small amount of water can transport large amounts of heat by an evaporation-condensation mechanism. The fibrous insulation can act as a wick and, through capillary action, pump the water into the hot portion of the insulation. This heat pipe action could greatly increase the heat loss through the insulations' but it is not considered representative of future tank performance.

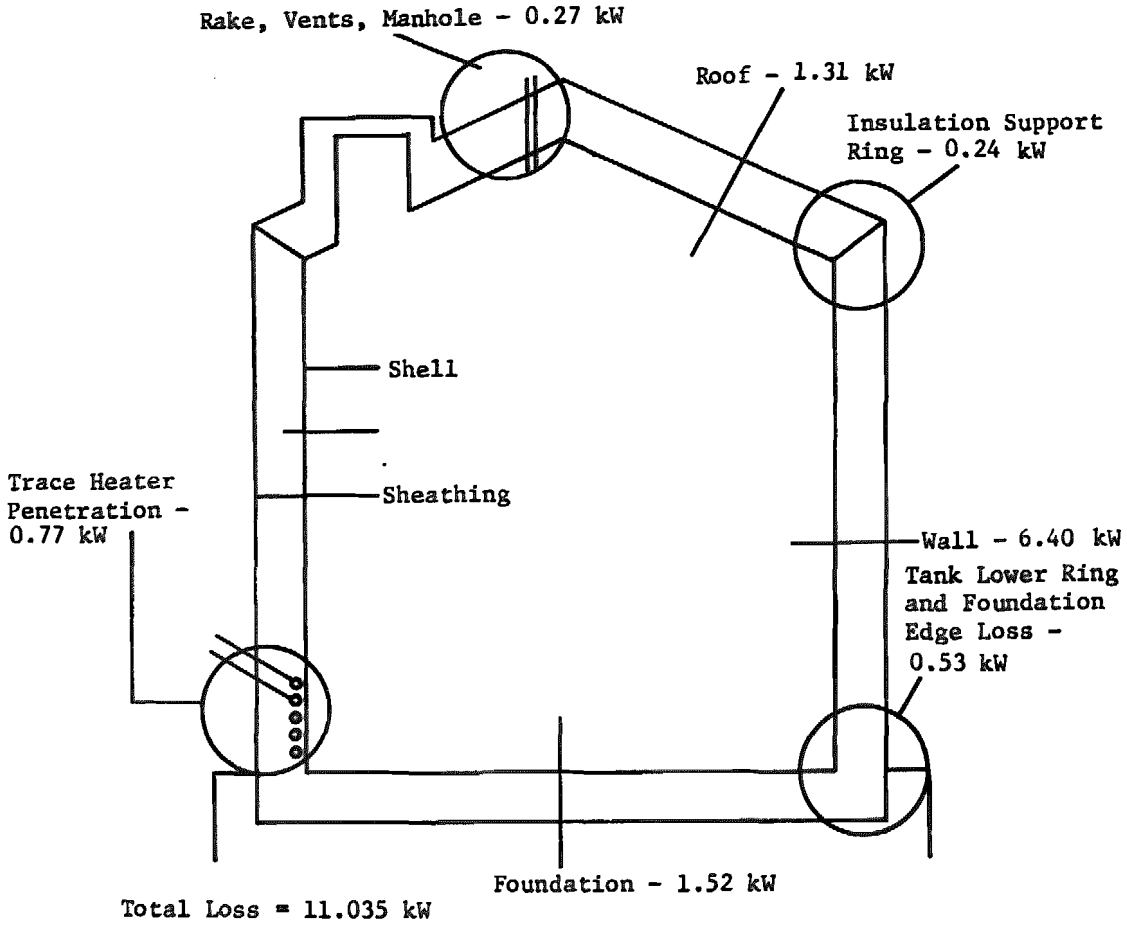

Figure 7.4.2-7 Cold Tank Actual Heat Loss--Steady State Condition

Table 7.4.2-1 Cold Tank Heat Loss

	Calculated Loss		Actual Loss	
	Watts	Btu/H	Watts	Btu/H
Penetrations	177	605	177	605
Heaters	766	2614	766	2614
Upper Ring	74	252	245	838
Tank Top	875	2986	1321	4509
Lower Ring	480	1638	534	1822
Foundation	1478	5046	1520	5190
Wall	2835	9675	6472	22084
Total	6084	22816	11035	37662

$\frac{\text{Actual}}{\text{Calculated}} = 1.63$

The salt temperature was 338°C (641°F)
Penetration and heater losses were taken as calculated values

7.4.3 Cyclic Tests

The cyclic charge/discharge of the storage tanks will be part of the normal operation of a solar plant. The analytical model was developed not only to determine the heat loss from the tank, but also to determine the salt temperature profile during operation and the efficiency of the storage system.

Two cyclic tests were performed with the SRE. The first test was five days in duration and the second test was three days. The second cycles was performed after the foundation had dried out. There was one discharge/charge cycle per day. Figure 7.4.3-1 shows the salt height of the hot tanks as a function of time. The SRE flow parameters were used as input to the analytical model. From the analysis of the SRE various tank insulation were modified to yield the actual heat loss from the SRE.

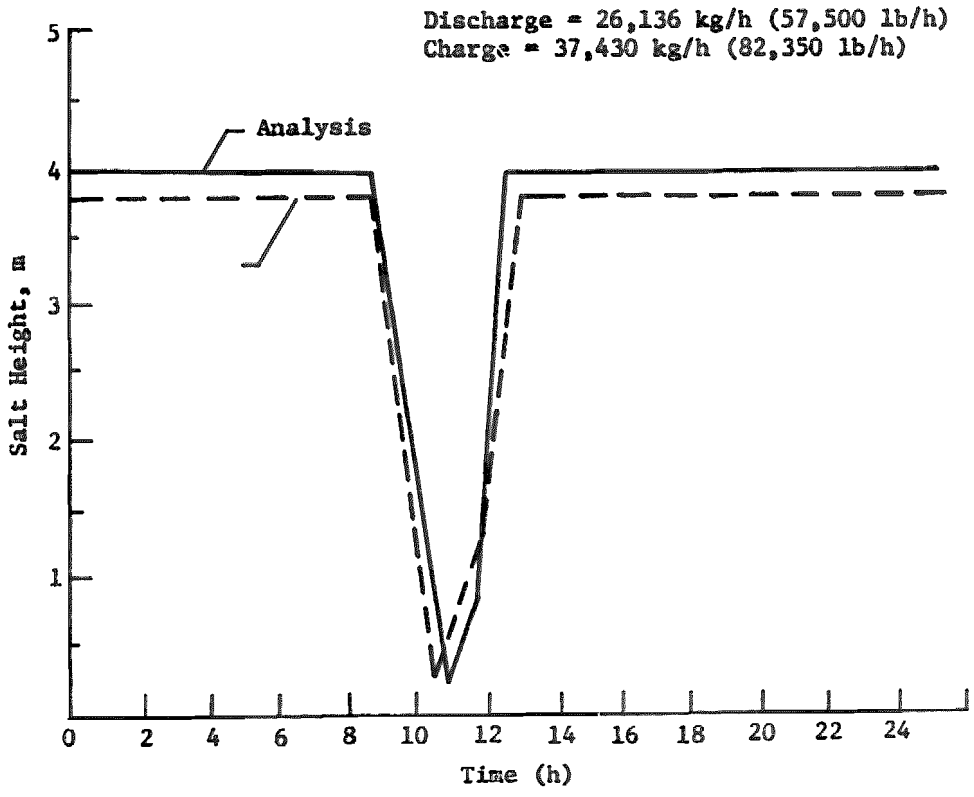

Figure 7.4.3-1 Salt Height Profile--Cyclic Test

Figure 7.4.3-2 gives a comparison of the analysis and the actual SRE results. The temperature of the salt decreased with time during the early morning because of heat loss. The discharge of the salt was initiated at 8:30 am and was terminated at 11:30. There was concurrent charging and discharging for one hour as charging was started at 10:30 am. The bulk salt temperature increased during charge/discharge, but not as rapidly as with a single charge. Due to temperature limitations of the propane heater, the resulting initial temperature of the hot salt into the tank was 400°C (750°F). Increasing the salt to 566°C (1050°F) took 15 minutes. During this time the stored salt decreased slightly in temperature. This was not predicted analytically since only a single inlet temperature of the salt was provided for in the program. This also results in the total temperature profile being lower than predicted. The analytical program does not account for the heat capacity of the insulation, which results in a very small variation of the salt temperature after charge. The analytical program predicted the salt temperature quite accurately and should prove to be a very useful tool in future analysis.

7.4.4 Thermal Siphon in Salt Transfer Lines

Thermal siphon is a term defined by Sandia Laboratories for convective heat transfer from the tank into connecting lines. Figure 7.4.4-1 show the temperature profile of the outlet from the cold tank after the electrical trace heater was turned off. The expected cooldown is represented by the dashed line. The temperature profiles of points #1 and #2 were also the profile of the tank temperature as it was being filled. The analysis shows that the total heat transferred from the tank into the lines over the four hours was 5920 W/h (20,200 Btu). The temperature decreased as the distance from the tank increased. The line 7.3 m (24 ft) away from the tank came to a thermal steady state condition. This phenomenon will average out variations in temperature of lines that are trace heated and may be used to eliminate trace heat as on some lines.

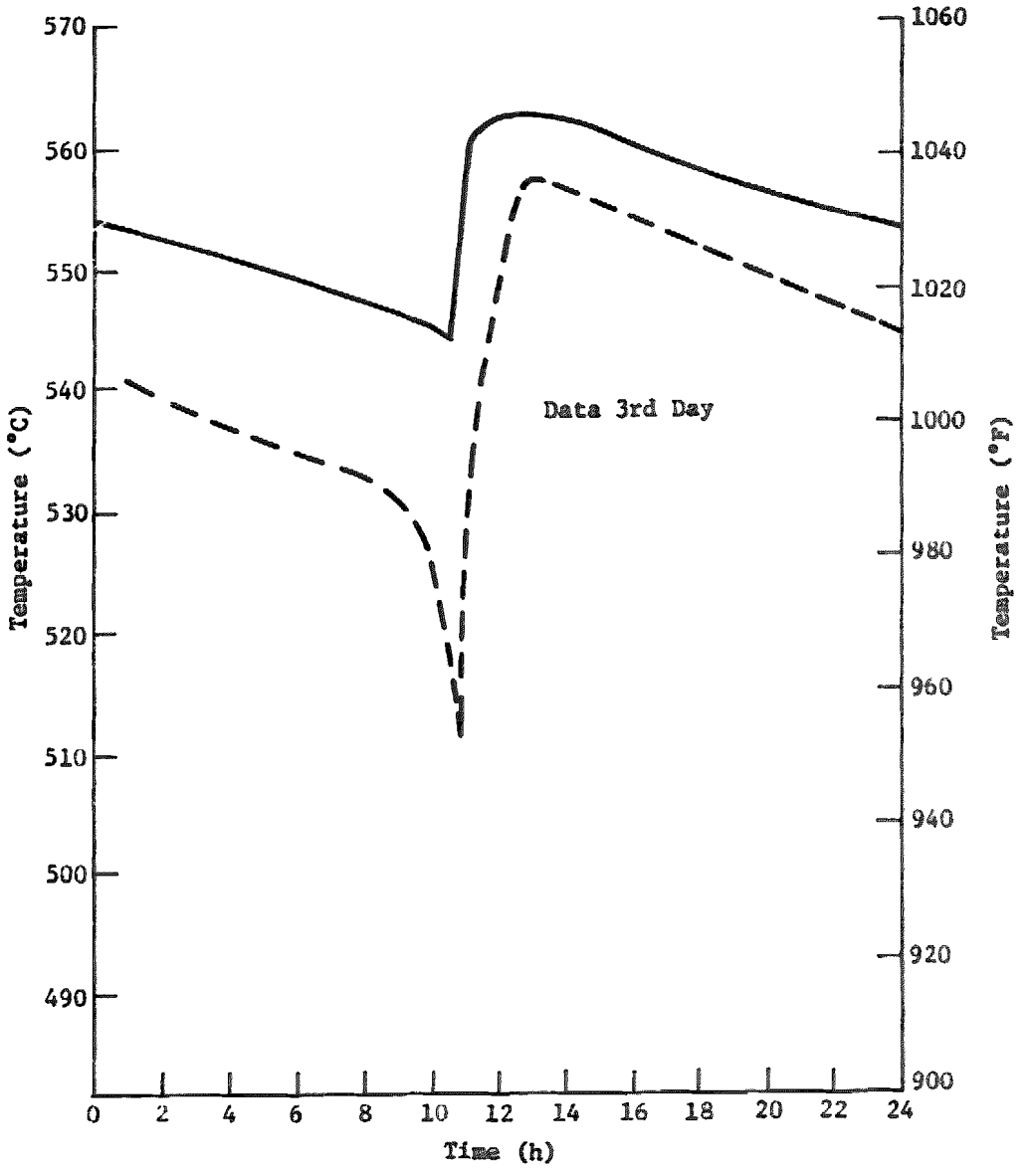

Figure 7.4.3-2 Salt Temperature Profile--Cyclic Test

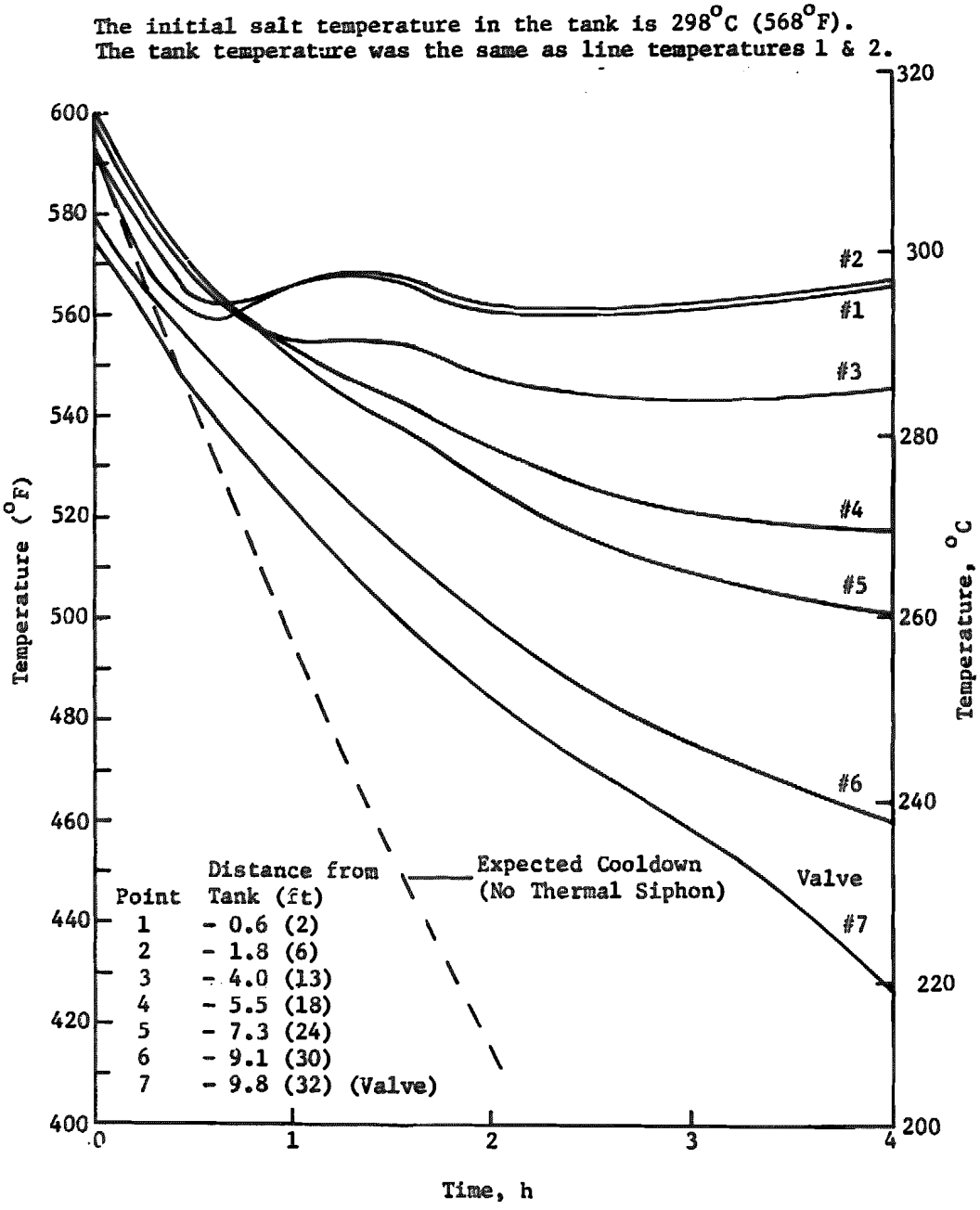

Figure 7.4.4-1 Line 4 Transient Cooldown

8.0 Conclusions and Recommendations

8.0 CONCLUSIONS AND RECOMMENDATIONS

The basic conclusion of the Molten Salt Storage program is that a Thermal energy Storage subsystem is both technically and economically feasible. The program has demonstrated that a commercial version of an internally insulated storage tank for molten salt can be designed and built.

8.1 HOT TANK

a) Pressure cycling of the one cubic meter test item has demonstrated that the Technigaz liner has an excellent fatigue strength margin when compared to the 30-year operational life criteria. This is in a molten salt environment at 566°C (1050°F). The large margin of fatigue life above a 30-year usage gives confidence that creep-fatigue should not produce a failure. It is desirable however to do further testing in the creep-fatigue area.

b) The thermal performance of the hot tank was good. The actual heat loss was only 11 percent greater than the predicted amount.

c) The pressure limitation of the corrugated Incoloy 800 liner permits a molten salt height in excess of that allowed based on typical soil bearing strengths.

d) The ammonia leak test procedure provides an excellent method of producing a totally leak free liner for molten salt containment. The possibility of corrosion resulting from residual ammonia needs to be evaluated.

e) The development and testing done on the liner, internal insulation, and attachments used for the SRE sized hot tanks applies to tanks of any size because these elements do not change as the tank size increases.

f) The one cubic meter test successfully demonstrated the removal and repair of a liner segment in the unlikely event of a leak developing in the liner.

g) A hot tank shell designed to API standards, incorporating internal firebrick insulation with a corrugated Incoloy 800 liner to maintain the steel shell temperature close to 288°C (550°F), has been demonstrated for storage of hot molten salt.

h) No specialized fabrication techniques are required for the shell. Standard commercial practices may be utilized in fabrication of the steel shell and in installation of the insulating firebrick and other tank insulating materials.

i) Johns Manville JM C22ZSL proved, through extensive testing, to be the best internal insulating firebrick for high temperature application in a molten salt environment and under cyclical compressive loading.

j) Improved thermal performance can be achieved by terminating the internal firebrick at the height of the suspended deck. This possibility should be evaluated.

k) Knowledge gained from the SRE test will enable improvements to be made in the analytical model and provide very accurate estimates for future tank builds.

l) The use of anchor pins rather than support rings should be evaluated for future use in supporting external insulation in order to reduce the heat loss.

m) SRE test experience has shown that water is driven from storage tank castable insulation. Future molten salt storage tank designs should consider dehydration of the castable insulation prior to shell fabrication, a water vapor venting method or a different insulating material.

n) The difficulty of achieving a flat bottom of the shell increases difficulty of installing brick. Bowing of the bottom can lead to buckling under load thus fracturing the brick. Eliminating the shell bottom and using structure to support the anchor points should be evaluated on future tanks.

8.2 COLD TANK

a) A steel cold tank shell built to API standards has been demonstrated for molten salt storage at temperatures of 288°C (550°F) with only external insulation.

b) The external insulation support rings should be replaced by anchor studs to further reduce heat loss.

c) Thermal performance of the SRE cold tank was 63 percent worse than analytically predicted. It is thought that the absorption of the water vapor emitted from the castable insulation into the external fibrous insulation may have caused the problem. Steps should be taken in future tanks builds to eliminate this problem such as: change of material, predry blocks of castable material, predry, or install vapor barrier.

d) It is recommended that during the summer the SRE sheathing should be opened to allow any water to evaporate from the insulation. The thermal performance should then be reevaluated.

8.3 SYSTEM HARDWARE

a) Cantilevered vertical pumps performed very well in transporting molten salt.

b) Test experience with the control valves indicates that future system should demand very rigid plug support in the valve design.

c) Very good performance was provided by electrical trace heaters cables composed of a single heater wire surrounded with mineral insulation.

d) A very functional piping design was produced using standard ANSI piping layout and stress analysis.

e) Standard insulation materials and installation techniques provided good thermal performance.

f) Cleanliness and interim inspections during salt transfer line fabrication is mandatory to prevent valve contamination. Dual valves and/or traps should be considered in the piping design.

8.4 TES DESIGN

a) The estimated cost of a 480 MWhe (1200 MWht) storage is 13 million dollars. This results in a cost of 27.1 $/kWhe (10.8 $/kWht).

b) The heat loss of a 480 MWhe storage subsystem on a daily charge/discharge cycle results in storage efficiency of 99.0 percent. The efficiency of the hot and cold tank is 99.3% and 99.7% respectively.

8.5 ADDITIONAL RECOMMENDATIONS

a) Leakage of salt into the internal insulation (brick) should be tested to evaluate detection and repairability.

b) Less expensive sources of salt should be sought.

c) A detailed cost comparison of internally insulated tanks and stainless steel tanks with external insulation should be made.

Appendix

APPENDIX A

APPENDIX A

TES SUBSYSTEM DEFINITION AND SPECIFICATION

A. General Discussion

The present program is directed toward developing a TES subsystem which utilizes the previously described "dual" or "hot/cold" strategy for containing molten draw salt. Typical components which make up the storage subsystem may include:

1. Hot and cold storage tanks
2. Drain tanks for maintenance
3. Ullage gas system
4. Insulation
5. Storage related salt pumps
6. Piping in storage area
7. Tank foundations and diking
8. Cooling systems
9. Trace heating
10. Storage instrumentation and control
11. Salt mixing and meltdown equipment
12. Molten draw salt inventory
    a. Working salt
    b. Hot tank residual salt
    c. Cold tank residual salt
    d. Storage area piping salt

The storage/EPGS heat exchanger, is not considered part of the storage subystem and, as a result, should not be considered in estimating subsystem cost. Normally receiver/storage heat exchangers are credited to the storage subsystem but in the present development it should be assumed that storage is coupled to a molten salt receiver and, as a result, requires no receiver/storage heat exchanger. Any other heat exchangers required in the proposed storage concept should be included in the subsystem cost.

The storage subsystem shall be capable of functioning in the following operational modes:

1. Cold start-up, including loading and meltdown of solid salt.
2. Diurnal start-up.
3. Charging and discharging at the maximum and minimum rates as specified in this section.
4. Cycling between charge and discharge.
5. Hold at full and partial charge.
6. Normal diurnal shutdown.
7. Emergency shutdown.
8. Maintenance exercises (insulation, inspection, tank drainage, etc.).

The contractor shall provide an estimate for a molten salt TES subsystem for use in a 120 MWe solar thermal central receiver plant for electric power generation. Such a plant is similar in size to concepts currently being evaluated. The subsystem shall have a storage capacity of four hours. Four hours of storage is equivalent to the amount of thermal energy which, upon discharge from the TES subsystem through the EPGS, could produce the rated plant capacity (120 MWe) for four hours. It may be assumed that the net EPGS cycle efficiency is 40%. Hence, the storage capacity in MWht is 1,200 (120 MW times 4 divided by an assumed EPGS efficiency of 40%).

The storage subsystem accepts hot molten draw salt at 1,050 degrees Fahrenheit from the receiver at a maximum charge rate of 480 MWt. The maximum discharge rate from storage is 300 MWt which is sufficient to produce 120 MWE assuming the 40% EPGS efficiency. The subsystem shall be capable of variable charge/discharge rates between 10 and 100% of the maximum values.

The temperature of salt returning from the storage/EPGS heat exchanger is 550 degrees Fahrenheit. Hence, the storage capacity of the TES subsystem based on useful energy stored is given by:

$$\text{Subsystem Storage Capacity} = M_s \int_{550\ F}^{1050\ F} c\ dT \qquad = \text{MWht}$$

where M_s is the working mass of salt in the subsystem and c its specific heat. Based on a constant specific heat value of $\bar{c} = .371$ Btu/lbm - ^{o}F equation (1) predicts that 22.1×10^{6} lbm of salt is required to store 1,200 MWht. Depending on the subsystem design, additional salt may be required for tank residuals.

The hot tanks shall be insulated in such a way as to prevent the average temperature of salt in a fully charged tank from reaching 1,035 degrees Fahrenheit (i.e., 15 degrees Fahrenheit drop from 1,050 degrees Fahrenheit) over a 24 hour period. Similarly, the cold tanks shall be insulated to prevent the salt in a full tank from reaching an average temperature of 535 degrees Fahrenheit (i.e., 15 degrees Fahrenheit drop from 550 degrees Fahrenheit) over a 24 hour period. For both the hot and the cold tanks, these specifications imply a maximum heat loss of 36 MWht over a 24 hour period.

The thermal energy storage subsystem specifications described above are summarized in Table II. The specification for internal tank insulation should be regarded as a recommendation rather than a requirement for the subsystem. Other methods which advance the state-of-the-art in molten salt high temperature containment may be substituted, providing they can be shown to be competitive with internal insulation on a cost effectiveness/design risk basis.

TABLE II
SUMMARY OF TEST SUBSYSTEM SPECIFICATIONS

Description	Specifications
Storage Media	Molten Salt (60% $NaNO_3$ 40-% KNO_3)
Tankage Configuration	Dual Tanks
Hot Tank Insulation	Combination of internal* and external
Cold Tank Insulation	External
Power Plant Rating	120 MWe
Storage Capacity	4 Hours 120 MWe (480 MWht)
Maximum Charge Rate	480 MWt
Minimum Charge Rate	48 MWt
Maximum Discharge Rate	300 MWt
Minimum Discharge Rate	30 MWt
Maximum Heat Loss Rate-Hot Tank	1.5 MWt
Maximum Heat Loss Rate-Cold Tank	1.5 MWt

* See Text

B. Applicable Documents

The equipment, materials, design and construction of the storage subsystem shall comply with all Federal, state local, and user standards, regulations, codes, laws, and ordinances currently applicable for the specific site and the user. These shall include but not be limited to the government and nongovernment documents listed below. If there is an overlap in, or conflict between the requirements of these documents and the applicable Federal, state, county, or municipal codes, laws, or ordinances, that applicable requirement which is the most stringent shall take precedence.

The following documents of the issue in effect or the date of request for quotation form a part of this specificaion to the extent specified herein. In the event of conflict between the documents referred to herein and the contents of this specification, the contents of this specification shall be considered a superceding requirement.

1. Government Documents

a. Specifications

- Regulations of the Occupational Safety and Health Administration (OSHA)

b. Standards

- Standards of the AISC
- Nation Electric Code
- American Welding Society Standards
- Applicable Human Engineering Design Criteria

c. Other Publications

- National Environmental Policy Act (NEPA)
- Compliance with the National Environmental Policy Act, 10CFR1021.

2. Non-Government Documents

a. Standards and Codes

- Uniform Building Code --- 1976 Edition by International Conference of Building Officials
  ANSI B31.1 --- 1977 Power Piping
- Institute of Electrical and Electronic Engineering (IEEE) codes, as applicable
- National fire Protection Association (NFPA) National Fire Design, Construction and Fabrication Standards
  Standards of AISC (American Concrete Institute)
  Standards of TEMA (Tub. Exchanger Manufacturer's Ass'n.)
  Standard 650 of API (American Petroleum Institute) Welded Steel Tanks for Oil Storage

APPENDIX B

A P P E N D I X B

BRICK TESTING CONTENTS

S U M M A R Y

Results of tests performed on the C22.Z of JOHNS-MANVILLE may be summarized as follows :

- No variation of the compressive strength between ambient temperature and 560°C :
  - . R_c at ambient temperature : 2.5 MPa (st.dev: 0.7)
  - . R_c at 560°C : 2.4 MPa (st.dev.: 0.4)
- The compressive strength is identical in the three directions.
- The compressive strength is not affected by thermal cycles between ambient and 560°C.
- Specimens are not damaged after 150000 compressive cycles at 560°C between 0 and 0.3 MPa. (one specimen broke at 147 000 cycles) neither after 150 000 cycles, between 0 and 0.45 MPa.
- Flexion tests are in progress.

1. PURPOSE

The purpose of the test program was to verify the capability of the selected brick to be used as load bearing insulation for the corrugated membrane.

2. IDENTIFICATION OF THE TESTED MATERIAL

Type of material : Insulating Firebrick
Supplier : JOHNS MANVILLE
Reference : C.22.Z.

Specimens have been cut in the 50 brick provided by MARTIN MARIETTA and which dimensions were 227 x 115 x 64 mm.
8.94" 4.53" 2.52"

The reference axis system has been marked as follows :

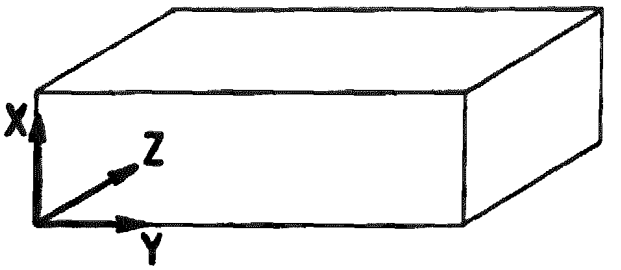

figure 1

For all the tests 20 brick, marked 1 to 20 have been choiced at random.

On the sample mark, the first number indicates the brick number, the second number is the sample number (exemple : 18-4 is the sample n°4 of the brick n°18).

This caution allows to compare the results of the different tests in particular to see the evolution of strength at high temperature.

3. TEST PROGRAM

The test program included the following tests :

- compressive test at ambiant and 560°C,
- effect of thermal cycles on the compressive strength,
- flexion test at ambiant and 560°C,
- compression fatigue test at 560°C.

4. COMPRESSIVE TESTS

4.1. Specimens

1,57"

- Specimens are 40 x 40 x 40mm. cubes,picked up in brick number 1 to brick number 10,
- In each brick,6 specimens were cut :
  - . 3 were tested at the ambiant, load being applied on each of the 3 axis for 1 specimen,
  - . 3 were tested at +560°C, load being applied on each of the 3 axis for 1 specimen.

4.2. Test proceeding

Ambiant tests are carried out on a Houndsfield Laboratory machine,and high temperature tests on an Instron Machine with an oven adapted between the plates as seen on figures 2 and 3.

The rate of the crosshead motion was : 0.01 cm/min.

The stress strain curve is recorded and the strength is determined as the first slide in the curve. As seen on the figure 4 , this slide corresponds to a slope change of the stress-strain curve.

4.3. Results

Results of tests carried out at ambient temperature are given table 1 hereafter.

In addition we have given table 2 the results obtained with preliminary tests carried out with 50 x 50 x 50 specimens cut in 2 brick marked 19 and 20.

Results of tests carried out at 560°C are given table 3.

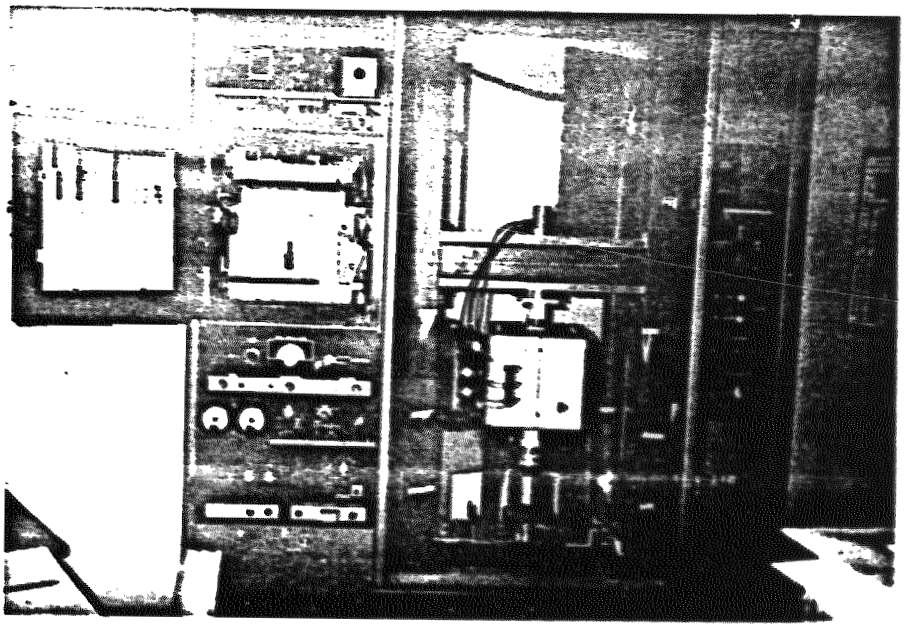

figure 2

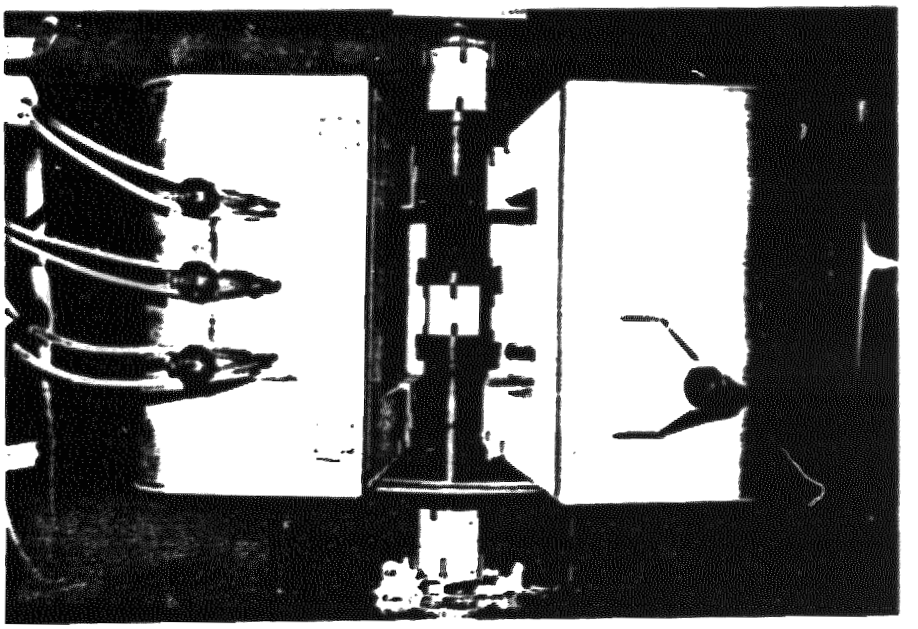

figure 3

Compression machine and specimen in the oven for compressive static tests at high temperature

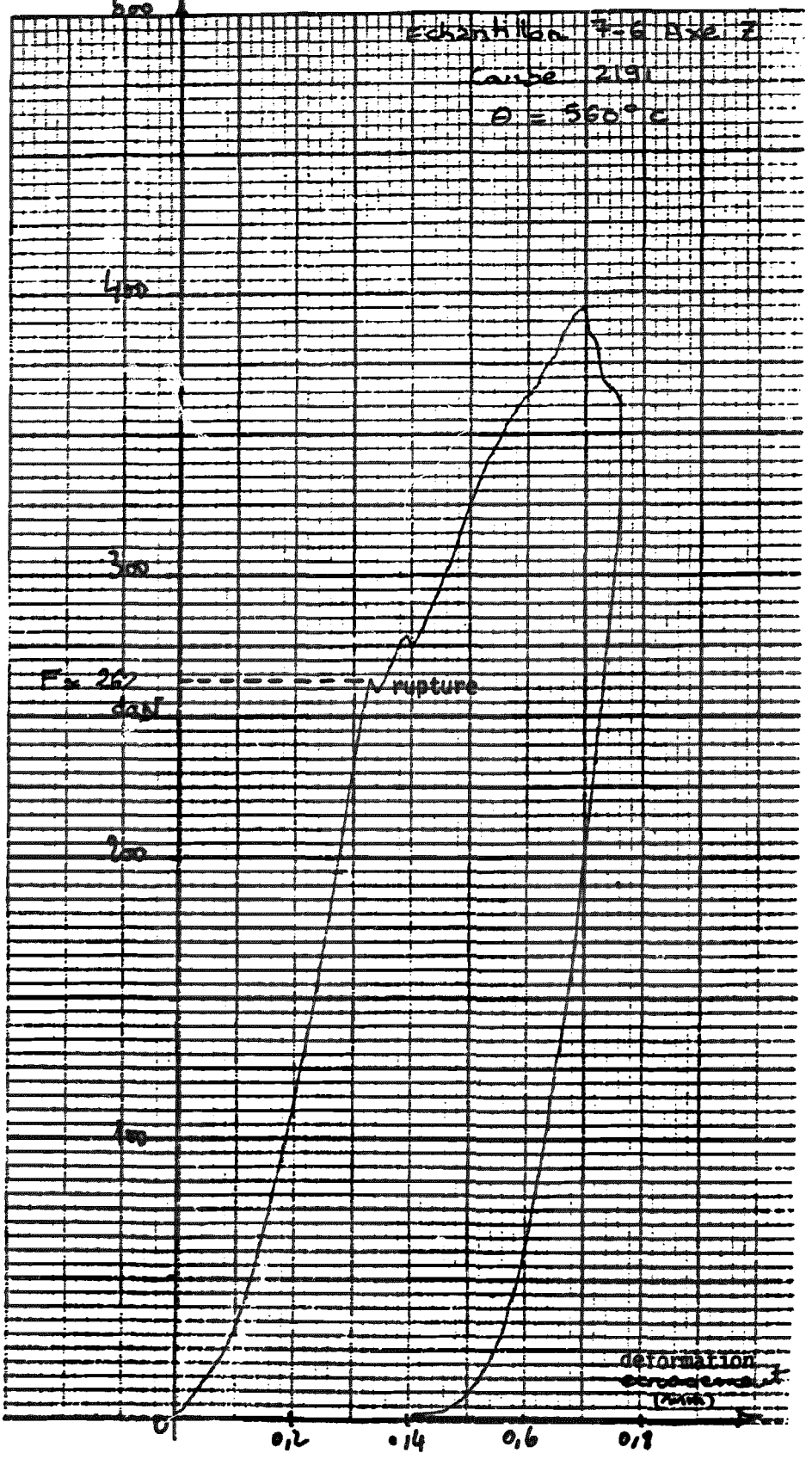
No 104 F(daN)
INSTRON LTD., HIGH WYCOMBE, BUCKS.
Echantillon 7-6 Axe Z
Courbe 2191
θ = 560° C
500
400
300
200
100
0
F = 267 daN
rupture
déformation
0,2
0,4
0,6
0,8

TABLE 1

RESULTS OF COMPRESSIVE TESTS AT AMBIENT TEMPERATURE

40 x 40 x 40 mm. CUBES

rick and specimen reference	direction of the load application	density kg/m3	strength MPa	remarks
1.1.	X	722	1.6 232	fissure in the specimen along X axis
1.2.	Y	725	2.0 290	
1.3.	Z	741	2.4 348	fissure along X
2.1.	X	741	1.6 232	fissure along Y
2.2.	Y	715	2.1 305	
2.3.	Z	742	2.7 392	
3.1.	X	757	2.3 334	
3.2.	Y	755	3.6 522	
3.3.	Z	758	3.2 464	
4.1.	X	684	1.4 203	
4.2.	Y	711	2.8 406	
4.3.	Z	704	2.3 334	
5.1.	X	704	1.6 232	
5.2.	Y	702	2.9 421	
5.3.	Z	722	2.6 377	
6.1.	X	703	2.2 319	
6.2.	Y	705	3.0 435	
6.3.	Z	725	2.3 334	
7.1.	X	713	1.9 276	
7.2.	Y	692	2.3 334	fissure along Z
7.3.	Z	724	2.3 334	
8.1.	X	757	3.2 464	
8.2.	Y	765	4.3 624	
8.3.	Z	757	2.8 406	fissure along Y

TABLE 1

(suite)

brick and specimen reference	direction of the load application	density kg/m3	strength MPa psi	remarks
9.1.	X	774	3.5 508	
9.2.	Y	777	3.4 493	
9.3.	Z	756	2.7 392	fissure along Z
10.1.	X	699	1.8 261	
10.2.	Y	708	2.8 406	
10.3	Z	715	2.2 319	

Note : Fissures were noted before the test.

TABLE 2

RESULTS OF PRELIMINARY COMPRESSIVE TESTS AT AMBIANT TEMPERATURE

50 x 50 x 50 mm. CUBES

brick and specimen reference	direction of the load application	strength MPa psi
19.1	Z	2.9 421
19.2	Z	3.2 464
19.3	Z	3.5 508
19.4	Z	3.0 435
19.5	Z	3.2 464
19.6	Z	3.7 537
19.7	Z	3.1 450
20.9	Z	2.1 305
20.10	Z	1.9 276

TABLE 3

RESULTS OF COMPRESSIVE TESTS AT 550°C

40 x 40 x 40mm. CUBES

brick and specimen reference	direction of the load application	strength MPa psi
1.4	X	2.9 421
1.5	Y	3.2 464
1.6	Z	2.6 377
2.4	X	1.8 261
2.5	Y	2.2 319
2.6	Z	2.5 363
3.4	X	2.7 392
3.5	Y	2.6 377
3.6	Z	2.8 406
4.4	X	2.5 363
4.5	Y	1.7 247
4.6	Z	2.6 377
5.4	X	2.3 334
5.5	Y	2.3 334
5.6	Z	2.3 334
6.4	X	2.2 319
6.5	Y	2.3 334
6.6	Z	2.3 334
7.4	X	2.4 348
7.5	Y	2.0 290
7.6	Z	1.6 232
8.4	X	2.0 290
8.5	Y	2.8 406
8.6	Z	1.9 276

TABLE 3

(~~suite~~) CONT.

brick and specimen reference	direction of the load application	strength MPa psi
9.4.	X	2.5 363
9.5	Y	1.9 276
9.6	Z	2.5 362
10.4	X	2.8 406
10.5	Y	2.1 305
10.6	Z	2.3 334

4.5. Analysis of results

In order to determine if there was a variation of the compressive strength with the load application direction we have plotted results versus axis direction at each temperature. See table 4 below.

TABLE 4

temperature	axis direction	compressive strength MPa	standard deviation MPa
ambiant	X	2.1 305	0.7 102
	Y	2.9 421	0.7 102
	Z	2.5 363	0.3 44
general average		2.5 363	0.7 102
+560°C	X	2.4 348	0.4 58
	Y	2.3 334	0.5 73
	Z	2.4 348	0.4 58
general average		2.4 348	0.4 58

In conclusion the compressive strength does not vary with the axis direction and is in the same range at ambiant and 560°C.

5. THERMAL CYCLE TEST

5.1. Specimens

Specimens are 40 x 40 x 40 mm. cubes cut in brick number 11, 12, 13, 16, 17, 18.

5.2. Test proceeding

In each brick one specimen is kept as reference specimens. The other specimens are submitted to thermal cycles as defined hereafter :

Definition of 1 cycle

Duration 24 hours including :

- temperature rise : 250°C/hour up to 560°C,
- keeping 2 hours at 560°C,
- cooling at ambient.

The compressive strength of the specimens is then checked at ambiant temperature after 3, 6, 9 ..cycles in order to compare to the compressive strength of the reference specimens. Load is applied in the X direction.

5.3. Results

Results are given table 5 here after.

TABLE 5

EFFECT OF THERMAL CYCLES ON COMPRESSIVE STRENGTH

brick and specimen reference	number of thermal cycles	compressive strength MPa	average and standard deviation MPa
11.1 12.1 13.1 16.1 17.1 18.1	reference specimens 0 cycle	2.0 290 2.3 334 2.7 392 2.1 305 2.7 392 3.0 435	2.5 (σ = 0.4
11.3 12.3 13.3 16.3 17.3 18.3	3 cycles	2.0 290 1.7 247 3.0 435 3.0 435 2.7 392 2.5 363	2.3 334
16.4 17.4 18.4	6 cycles	2.1 305 2.5 363 2.9 421	2.5 363
16.5 17.5 18.5	9 cycles	2.2 319 3.2 464 2.5 363	2.6 377
16.6 17.6 18.6	12 cycles	2.2 319 2.5 363 2.3 334	2.3 334

5.3. Analysis of results

No evolution of the compressive strength is noted after 12 cycles. Then we decided to stop the test.

6. FLEXION TEST

6.1. Specimens

Specimens are parallelepiped stroped section 25 x 25 mm, length : 225 mm. cut in brick number 11 to number 18.

6.2. Test proceeding

The device is a "4 points" type flexion device as below.

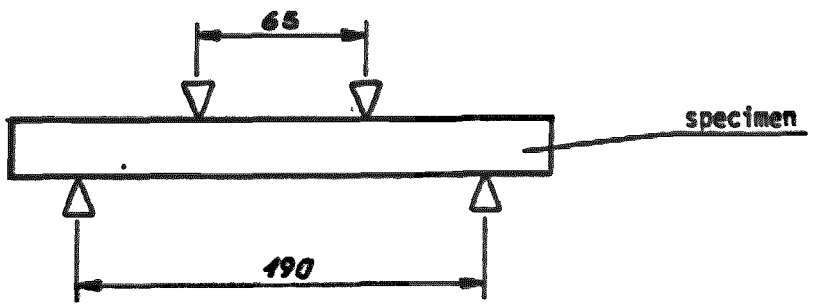

figure 5

Half of the specimens of each brick are tested at ambiant temperature, the others are tested at 560°C, an oven being adapted to the flexion device. (see figures 6 and 7 hereafter).

6.3. Results

These tests are in progress.

7. CYCLIC COMPRESSIVE TEST

7.1. Specimens

Specimens are 50 x 50 x 50 mm.cubes cut in brick number 1 to brick number 10 on which static tests had already been carried out.

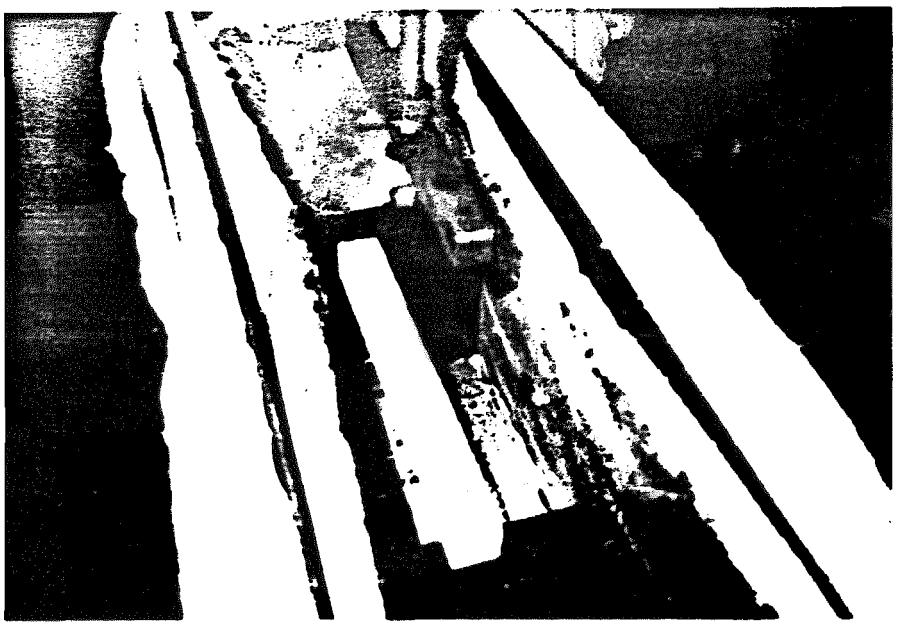

figure 6

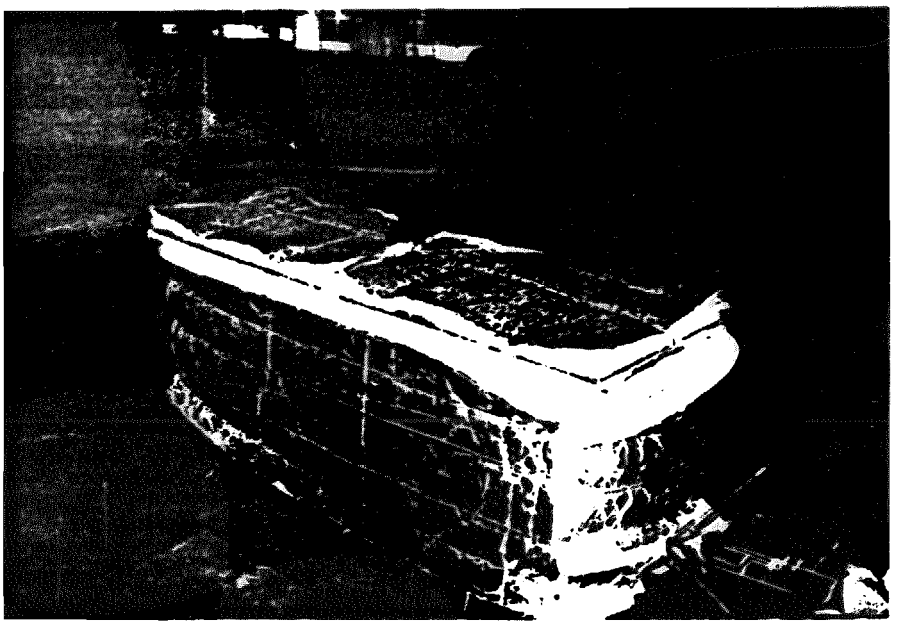

figure 7

Device and oven for flexion test

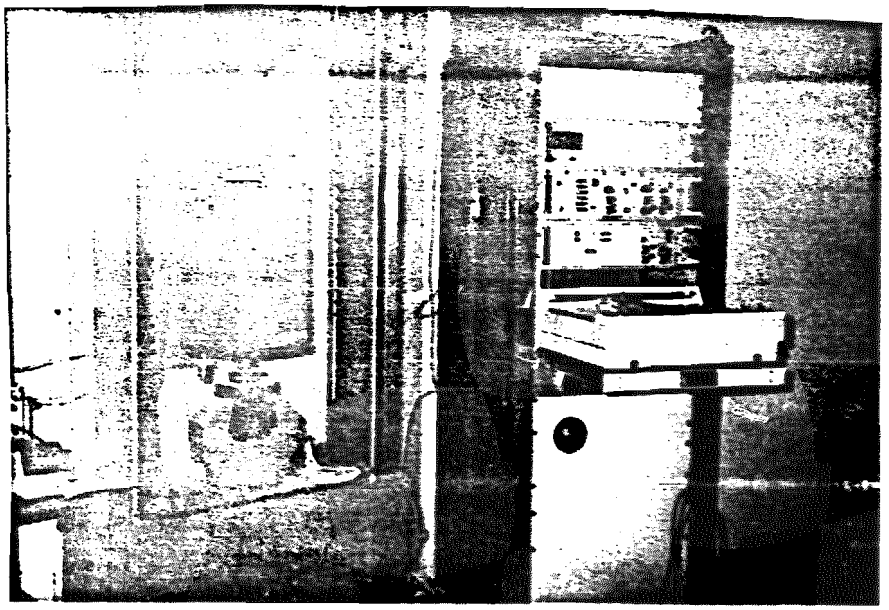

figure 8

General vue of the cyclic compression test arrangement

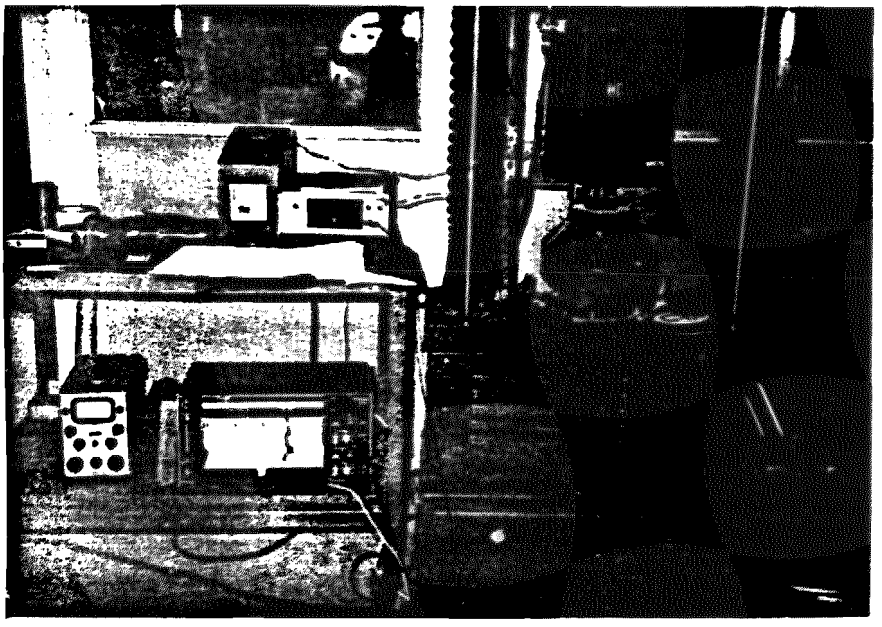

figure 9

Continuous recording of the deformation

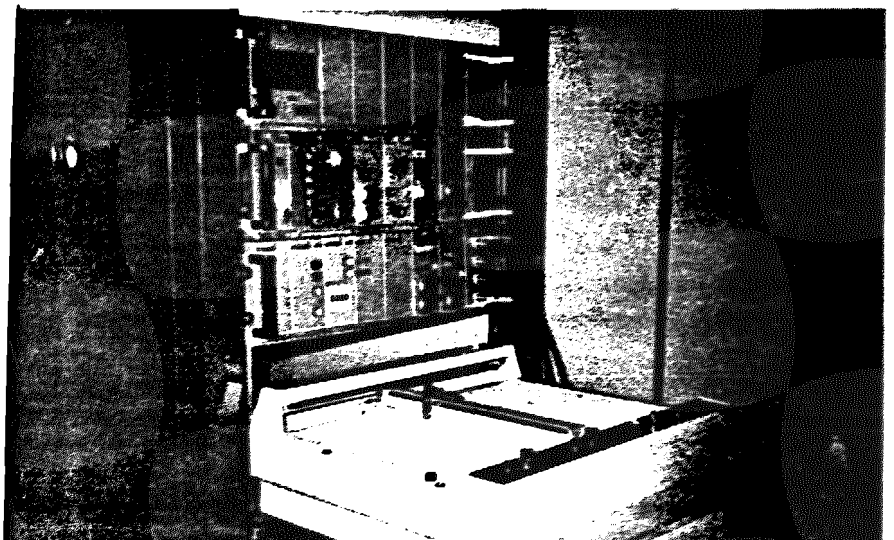

figure 10

Checking of the stress-strain curve

The tested specimens have been selected in brick having the lower compressive strength.

7.2. Test proceeding

Tests are performed on a SHENCK TREBEL Machine type RM 50. on which an oven is adapted. (see fig.8, 9 and 10 the test arrangement).
Temperature test is 560°C.

The monitoring (sinusoïdal shape) is realized on the stress. During the test the deformation is continuously recorded and on regular time interval the stress-strain curve between 0 and the selected maximum pressure test is checked in order to verify that the specimen is not damage.

The cyclic frequency was then 3 Hz.

7.3. Results

Results obtained with the two maximum load level : 0.3 MPa and 0.45 MPa (3 specimens for each level are given hereafter).

TABLE 6
CYCLIC COMPRESSION TEST

brick and specimen reference	direction of the load	stress levels (MPa) mini	stress levels (MPa) maxi	frequency and duration of the test	number of cycles reached
5.8	X	0	0.3	2 Hz 21 hours	151 000 no rupture
6.8	Y	0	0.3	2 Hz 21 hours 25'	rupture at 147 000 cycles
7.8	Z	0	0.3	3 Hz 16 hours 30'	178 000 no rupture
10.8	X	0	0.45	3 Hz 16 hours	173 000 no rupture
1.7	Y	0	0.45	3 Hz 15 hours 10'	164 000 no rupture
2.7	Z	0	0.45	3 Hz 14 hours 30'	156 500 no rupture

Previously another level of stress had to be selected and tested. But as no specimen (except one specimen) had broken at 150 000 cycles and more. It has been decided to proceed with the specimens already tested in order to try to determine the number of cycles at rupture. These tests are in progress.

APPENDIX C

APPENDIX C

LIST OF ANALYTICAL TASKS AND TESTS PERFORMED

American Technigaz, Inc.

- Leak Detection of Molten Salts
- Internal Load Bearing Insulation Tests
- Salt Storage Membrane Stress Calculations
- Liner Development - Element Fatigue Test
- Liner Development - Definition of Membrane Geometry
- Strain Gage Test of Membrane Knot
- Formability of Liner Material and Fabrication of Liner Elements
- Cold Tank Stress Analysis
- One Cubic Meter Tank Cyclic Pressure Test
- Hot Tank Stress Analysis
- Buckling Test of Membrane

Stearns-Roger

- Piping Thermal Analysis
- Piping Hangar Analysis
- Piping Weights Analysis
- Containment Volume Analysis
- Pump and Sump Building Foundation Analysis
- Heater Foundation Analysis
- Cooler Foundation Analysis
- Hot Tank Foundation Analysis
- Cold Tank Foundation Analysis
- Ladder Tower Analysis

- Pipe Support Foundations Analysis
- Required Pressure Delta Across Hot Sump Control Valve
- Hot Tank Foundation Heat Transfer
- Cold Tank Foundation Heat Transfer
- Hot Tank Foundation Coolant Flow Requirement
- Cold Tank Foundation Coolant Flow Requirement
- Heat Rejected By Hot and Cold Sump Pumps
- Heat Loss From Air Compressor
- Heat Loss From Salt Sumps
- Air Flow Required to Remove Equipment Heat From Sump/Pump Building

Martin Marietta Corporation

- SRE System Sizing
- SRE Hot and Cold Tank Sizing
- Control Valve Sizing
- Trace Heating Requirements
- Hot Tank Insulation Requirements
- Cold Tank Insulation Requirements
- Salt Transfer Line Insulation Requirements
- Salt Propane Heater Sizing
- Sump Level Control Analysis
- Salt Cooler Sizing
- Electrical Wire Sizing
- Hot Tank Heat Loss Analysis
- Cold Tank Heat Loss Analysis
- Cyclic Heat Loss Analysis
- Thermal Syphon Heat Transfer in Lines

APPENDIX D

MOLTEN SALT THERMAL ENERGY STORAGE

SUBSYSTEM RESEARCH EXPERIMENT

TEST PLAN

TABLE OF CONTENTS

1.0 INTRODUCTION

This document describes the tests that will be performed with a Thermal Energy Storage Subsystem Research Experiment (SRE). The storage medium used by this SRE is a molten nitrate salt, 60% $NaNO_3$/40% KNO_3 by weight. These tests will be performed at the Central Receiver Test Facility (CRTF) at Albuquerque, New Mexico.

The major elements of this SRE include a hot storage tank, a cold storage tank, a propane heater, an air cooler, a hot sump and pump, a cold sump and pump, and a control system. The nominal salt temperature in the hot tank is 566°C (1050°F) and is 288°C (550°F) in the cold tank. The system is capable of storing up to 7 MWht of thermal energy.

1.1 TEST OBJECTIVES

The overall objective is to demonstrate that a solar thermal energy storage system using molten nitrate salt as the storage medium can operate efficiently, reliably and safely in both steady state and transient modes representative of what would be experienced in a large solar power plant.

The specific objectives of this test program are listed below:

1) Measure tank heat loss under both steady state and transient conditions.

2) Determine storage system efficiency and salt temperatures under simulated solar plant operating conditions.

3) Demonstrate system cold startup techniques.

4) Demonstrate normal diurnal startup.

5) Demonstrate charging and discharging of system at anywhere between maximum and minimum rates.

6) Demonstrate holding at full and partial charge.

7) Demonstrate normal diurnal shutdown.

8) Demonstrate emergency shutdown.

9) Perform inspection and maintenance exercises.

1.2 SCOPE

The purpose of this experiment is to demonstrate the performance of a molten salt thermal energy storage subsystem. Other elements of a commercial system such as the heliostats, tower, etc, are not part of this demonstration. However, molten salt pumps, heat tracing, sumps, piping, instrumentation, and controls will be demonstrated.

1.3 BACKGROUND

Martin Marietta has performed a number of studies of molten salt central receiver systems for the Department of Energy. The first was entitled Conceptual Design of Advanced Central Receiver Power System, Phase I Contract EG-77-C-03-1724. The final report for this activity was released in September 1978. The second study was entitled Solar Central Receiver Hybrid Power System, Contract DE-AC03-7SET21038. The work performed under this contract is documented in a final report dated September 1979. Both of these studies were concerned with commercial-size systems although both of these studies contributed a significant amount of information that was useful in the design of this test.

We have recently completed the Advanced Central Receiver System, Phase II program (Sandia Contract No. 18-6879C). This program involved the design, fabrication, erection and testing of a 5 MWt molten salt receiver at the CRTF. This program provides us with a wealth of relevant experience in molten salt testing at the CRTF.

1.4 TEST PROGRAM SUMMARY

Table 1-1 lists the tests that will be performed during this program. All of these tests will be performed at the CRTF. The testing sequence will begin with loading of approximately 81,720 kg (180,000 lb) of salt into the cold tank. This will be done at a nominal temperature of 288°C (550°F). The molten salt will then be slowly circulated through the entire system at 288°C (550°F) until all components are brought up to temperature. Then, the propane heater and air cooler will be turned on and the hot tank and sump will slowly be brought up to 566°C (1050°F). Once the entire system is at operating temperature, we will check out all the emergency shutdown procedures so as to ensure safe operation of the SRE.

The startup and checkout phase will be followed by the performance test phase. A series of steady state heat loss tests will be conducted at various salt levels in each tank. This will be followed by some transient cooldown tests and some cyclic charge and discharge tests. These tests will measure the thermal performance of the tanks (e.g., heat loss rate, storage efficiency, salt temperature, shell temperature, etc) under realistic operating conditions.

Table 1-1 Summary of Storage SRE Tests

Test No.	Title
Startup & Checkout Tests	
1	Salt Loading
2	Functional Flow
3	Heat Up Hot Tank
4	System Operation Checkout
5	Emergency Shutdown Checkout
Thermal Performance Tests	
6	Steady State Heat Loss - Full Hot Tank
7	Steady State Heat Loss - Empty Hot Tank
8	Daily Charge/Discharge
9	Transient Cooldown - Full Hot Tank

1.5 INTERFACE DEFINITION

Although this storage SRE is being built on site at the CRTF, it requires very little interfacing with the rest of the CRTF once construction is completed and testing is underway. This is because it is designed to be operated as a standalone facility, separate and independent of the tower and heliostat field. The storage SRE is located south and a little west of the tower.

During SRE testing, the only items that the SRE will require from the CRTF are:

1) Elecricity

   - o 480V three phase
   - o 277V single phase
   - o 110V single phase
   - o 145 kW maximum

2) Propane

   - o Supply at 172 - 689 kPa (25 - 100 psig) to 3 MWt salt heater

3) Cooling Water for Foundations

2.0 SRE DESCRIPTION

2.1 SYSTEM OVERVIEW

The major components of this Thermal Energy Storage SRE are:

- o Hot storage tank
- o Cold storage tank
- o Propane fired salt heater
- o Fan driven air cooler
- o Hot sump and pump
- o Cold sump and pump

A flow schematic is shown in Figure 2-1. Hot salt will leave the hot storage tank and flow by gravity to the hot sump. From there, the salt is pumped through the air cooler which reduces its temperature from 566°C (1050°F) to 288°C (550°F). This simulates the action of a salt-to-water/steam heat exchanger in a large solar plant. The cooled salt then flows into the cold storage tank. From there, the salt flows by gravity to the cold sump where it is pumped through the propane heater. The heater simulates the action of a solar receiver in a large plant. The pumps, valves and controls are set up so that simultaneous charge and discharge of each storage tank is possible. The general arrangement of this equipment at the SRE site is shown in Figure 2-2. The system has a storage capacity of 7.0 MWht.

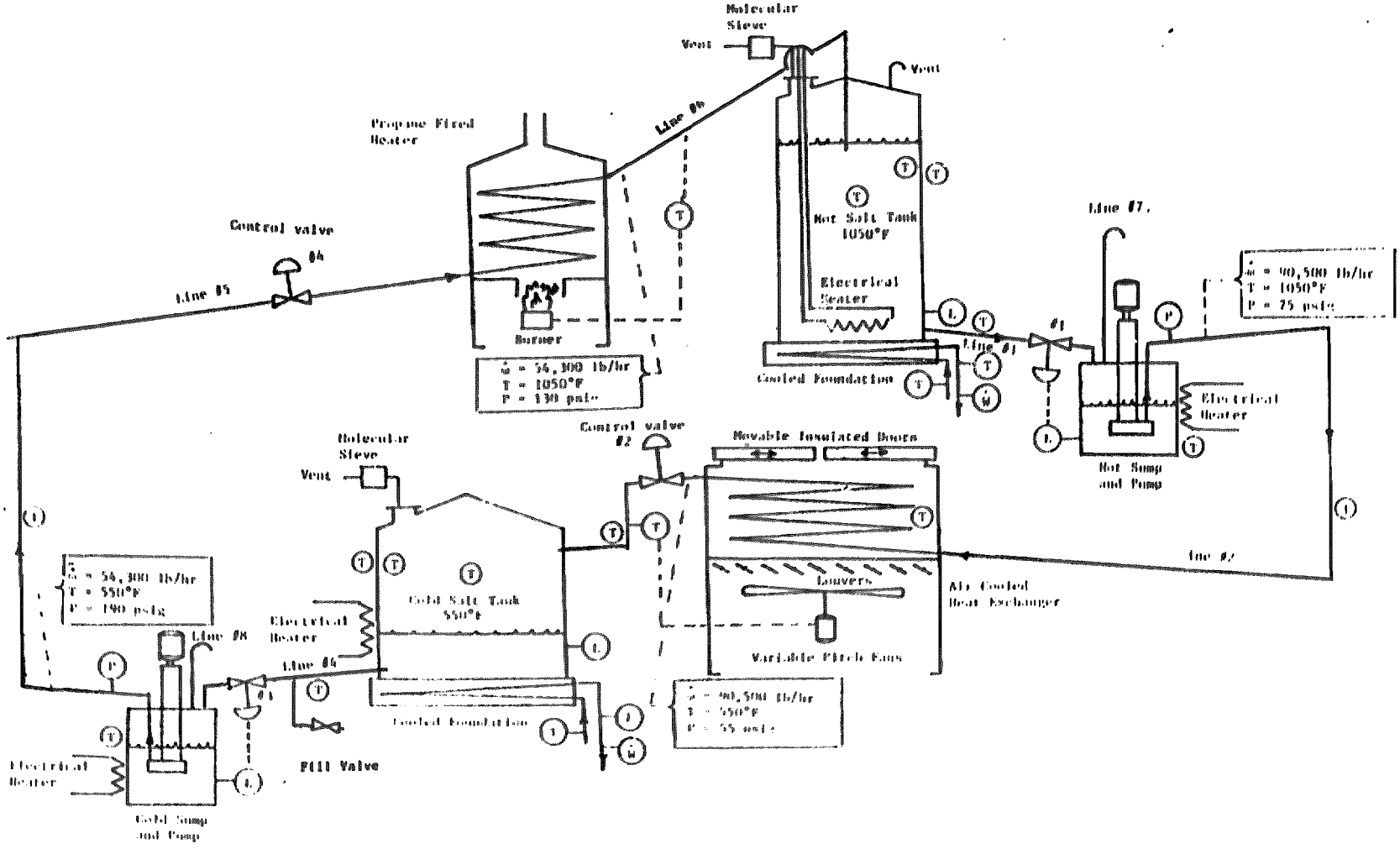

Figure 2-1 SRE Flow Schematic

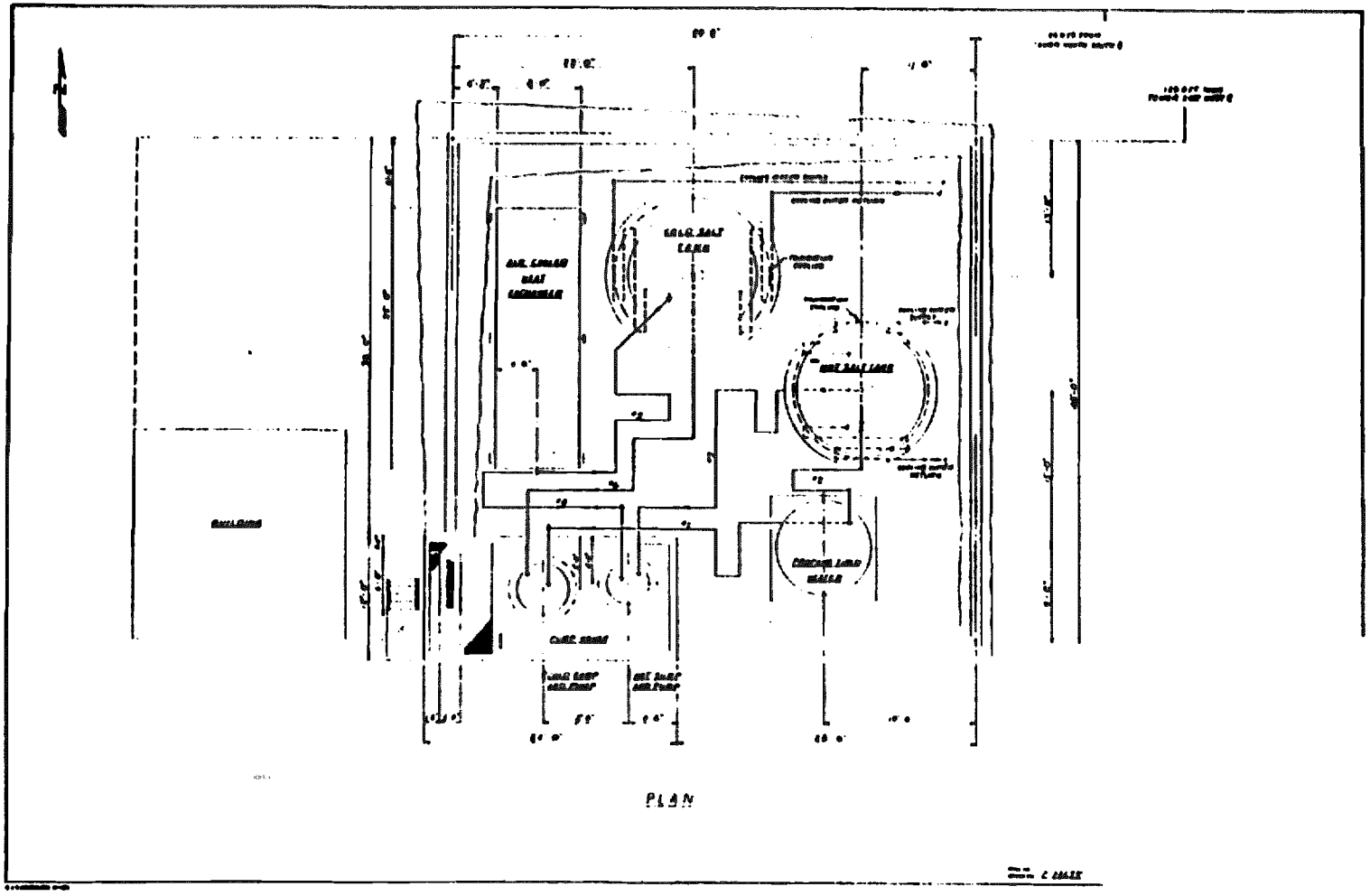

Figure 2-2 SRE Site Layout

2.2 MAJOR COMPOMENTS

2.2.1 Hot Storage Tank

The hot storage tank is a vertical cylinder internally insulated with low density insulating firebrick on the walls and floor, and with fibrous insulation on the top. The internal insulation is protected from the hot (566°C [1050°F]) molten salt by a thin metal liner made of Incoloy 800. The internal insulation reduces the shell temperature so that the shell can be constructed of common carbon steel (A516 Grade 70). The hot tank is also externally insulated. The inside liner dimensions are 3.05 m (10.02 ft) diameter and 5.54 m (18.17 ft) height.

A sketch of the hot tank is shown in Figure 2-3. Note that there will be electric immersion heaters inside this tank located at the bottom in the residual salt. These heaters have a total power of 28 kWt. There will be 7 circuits, and the individual circuits are controlled with on-off switches. The salt heights in the tank are as follows:

Residual salt height	0.41 m (16 in.)
Working salt height	4.57 m (15 ft 0 in.)
Normal maximum salt height	4.98 m (16 ft 4 in.)

Note that the tank sits on a water cooled foundation.

2.2.2 Cold Storage Tank

The cold storage tank is a simple vertical cylinder made of plain carbon steel. The tank is externally insulated with block insulation on the top, fibrous insulation on the side and castable on the bottom. The nominal salt storage temperature is 288°C (550°F) in the cold tank. A sketch of the cold tank is shown in Figure 2-4. The salt heights are:

Residual salt height	0.41 m (16 in.)
Working salt height	2.74 m (9 ft 0 in.)
Normal maximum salt height	3.15 m (10 ft 4 in.)

Note that there will be electric band heaters located on the outside of the steel shell, and that the entire tank will sit on a water cooled foundation.

2.2.3 Fossil Fired Salt Heater

The heater uses propane as a fuel. It has a single vertical helicoil tube which is convectively heated from the exhaust of a forced air burner below the coil. The unit will heat 24,493 kg (54,000 lb) of salt from 288°C (550°F) to 566°C (1050°F) every hour. The burner unit can be "turned down" by a ratio of 20:1. The outlet temperature

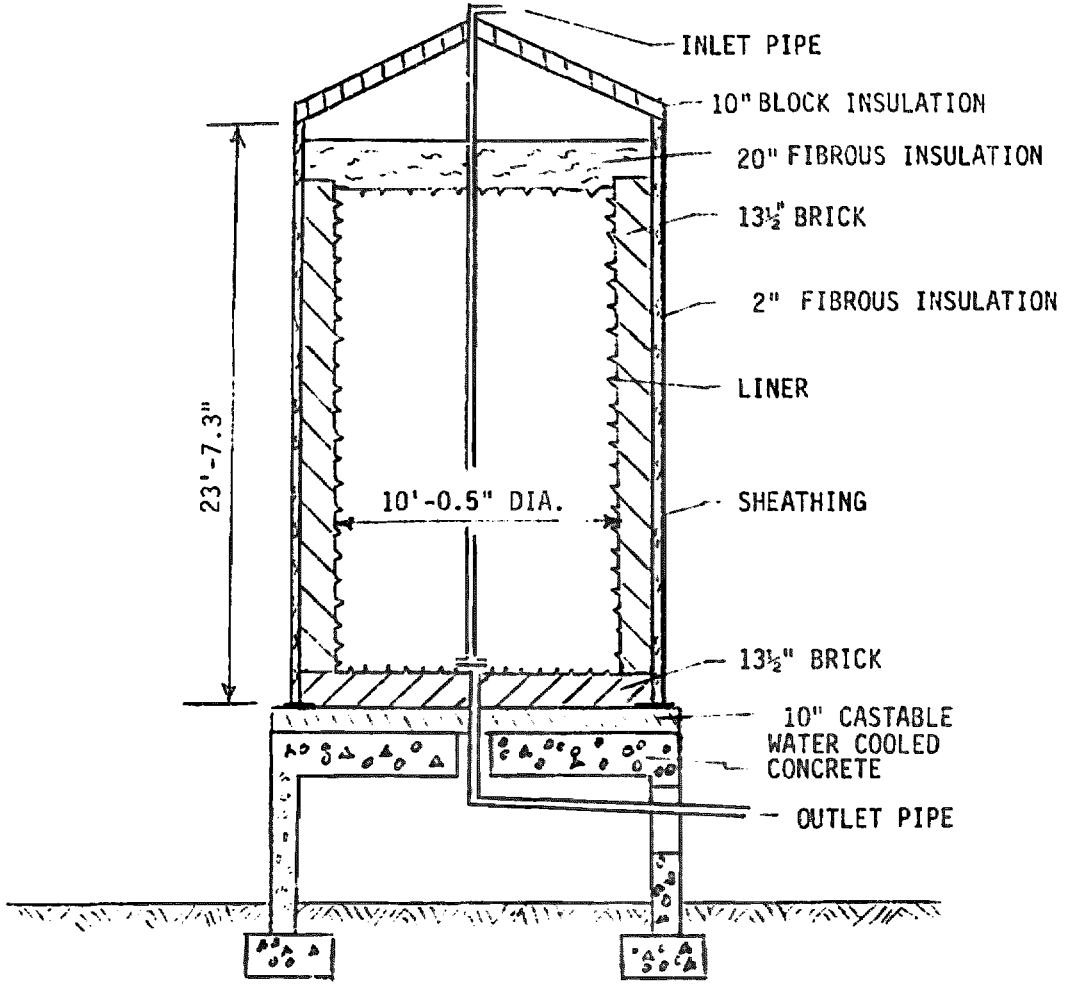

Figure 2-3 SRE Hot Tank

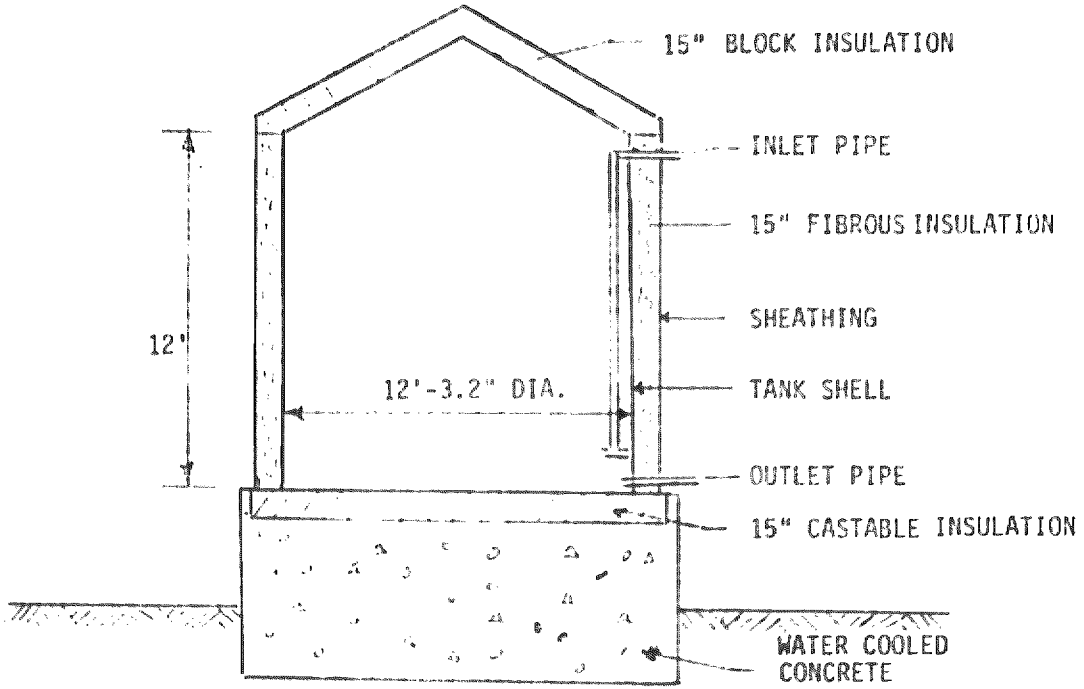

Figure 5-4 GRE Cold Trap

can also be selected below the 566°C. The unit is internally insulated with fibrous insulation which allows rapid heat-up. This design also reduces thermal stresses and insulation breakage which could result from cyclic usage. The unit will be preheated before salt introduction by firing the burner.

The basic heater size is 2.7 m (9 ft) diameter and 7.3 m (24 ft) high. The weight of the heater is 10,910 kg (24,000 lb). The weight of the salt in the heater is 3,310 kg (7,300 lb), thus the total weight is 14,220 kg (31,300 lb). A blower fan for the burner has a 14.9 kW (20 HP) 480 volt 3ϕ motor. Remote start by 110V circuit is possible from the control console. Panel operation and valve interlock power of 110V is necessary at the control console and at the burner.

Control of the salt temperature shall be by a controller which monitors the stack gas temperature. The control for the burner shall be mounted on the console. The fuel is propane at a supply pressure from 689 kPa (100 psig) to 172 kPa (25 psig). The efficiency of the heater is 67 percent. The approximate fuel usage is 6,500 SCFH of 2316 Btu/SCF propane. The usage for one heat cycle is 16,000 SCF of propane.

2.2.4 Air Cooler

The cooler is capable of cooling 11.43 kg/s (90,500 lb/h) of molten salt from 566°C (1050°F) to 288°C (550°F). The unit has a seven pass tubular heat exchanger cooled with two fans. It is insulated to allow preheating the tubes and headers. Beneath the finned cooling coils is a louver and above the coils is a movable insulated door. Electrical trace heaters on the inside of the insulation are used to heat the tubes and headers to 232°C (450°F). The cooler and its fan enclosure are shown in Figures 2-5 and 2-6.

Fans, louvers and the movable insulation door can be operated remotely. Fluid outlet temperature is controlled by varying the fan pitch either by manual control setting or an analog feedback controller. The air cooled heat exchanger weighs 9980 kg (23,000 lb). An additional 700 kg (1540 lb) of salt will be present during usage.

Each of the two fans are driven with a 14.9 kW (20 HP) 48 volt 3 phase motor. The weatherproof electrical start boxes are mounted on the lower structure. Each start box can be operated locally or remotely through a 110 volt supply. The louvers and movable insulated door are air operated. The louvers are operated with a variable pressure dome motor controlled with a 3-15 ma signal. The maximum pressure of 137 kPa (20 psig) is controlled by a regulator. The insulation door is operated by cable cylinders at 413 kPa (60 psig) with 24 volt control signals. Two regulators are used.

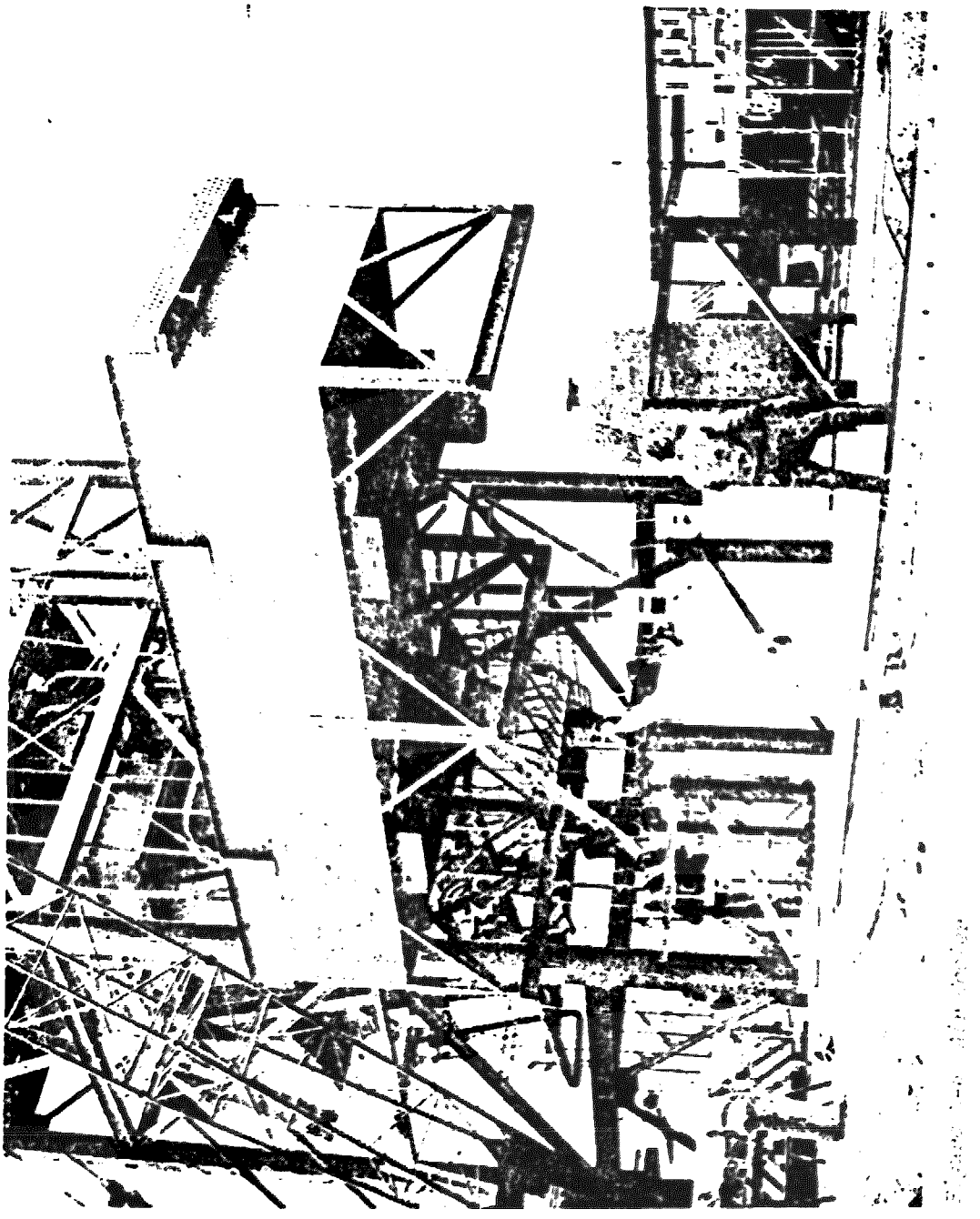

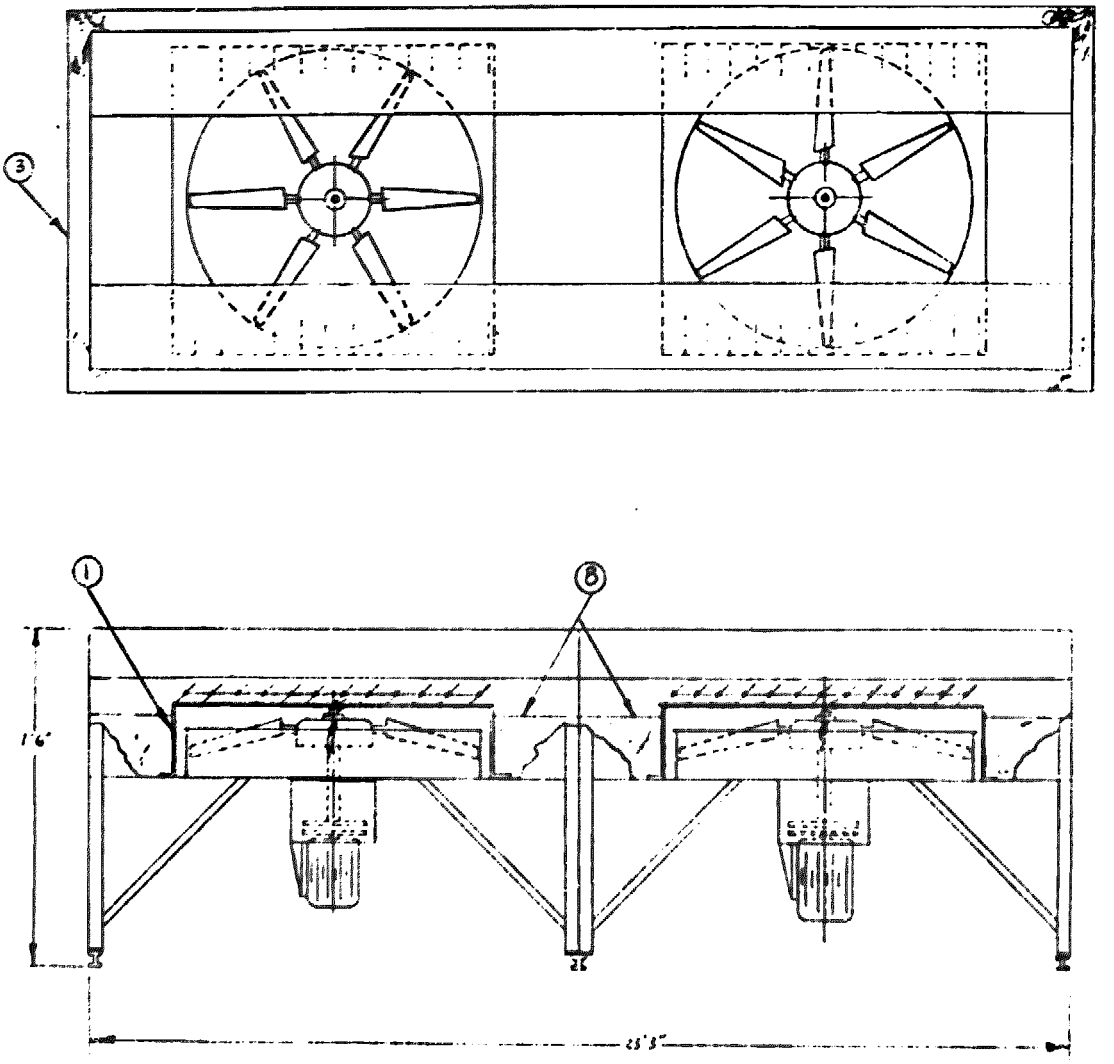

Figure 2-8 Air Cooler Fan Enclosure

2.2.5 Hot Sump and Pump

The sump has a flat bottom and top. It is 1.2 m (4 ft) in diameter and 1.2 m (4 ft) high. The tank rests on 0.19 m (7½ in.) of block insulation. The pump is a vertical cantilever pump capable of 0.0067 m^3/s (106 GPM) at 21 m (68 ft) head rise. The pump lower bearing is water cooled. The pump has a 5.6 kW (7.5 HP) 480 volt 3ϕ motor.

The tank has 6.8 kW of electrical heaters. Instrumentation will include thermocouples and a level sensor. The total tank and pump weight is 1110 kg (2450 lb). The salt load is 2270 kg (5000 lb) making the total weight 3380 kg (7450 lb).

2.2.6 Cold Sump and Pump

The cold sump and pump was used on another molten salt system. The sump is a flat bottom cylindrical tank of 1.5 m (5 ft) high. The tank stands on four legs and is insulated with approximately 0.2 m (8 in.) of fiberglass which is covered with sheathing. The domed top of the tank has a flanged opening for mounting the pump. A vent pipe will allow breathing but limit salt loss in a sump overfill situation. The tank rests on a base structure which includes insulation for the tank leg.

Electrical heaters are wrapped around the tank walls. A level sensor will be added to the tank. The pump is a vertical cantilevered pump manufactured by Lawrence Pump Inc. It has a 44.8 kW (60 HP) motor and delivers 0.076 m^3/s (120 GPM) with a headrise of 1172 kPa (170 psi). The pump lower bearing and packing are air cooled. Two regulators are presently used to supply 68 kPa (10 psig) for the bearing and the packing. Usage rate for each is .0047 m^3/s (10 SCFM). An electrical start box is also used which can be operated locally or remotely via 110 volt signal.

The total weight of the pump, motor and tank is 2360 kg (5200 lb). The operating salt load is 5080 kg (11,200 lb) making a total weight of 7440 kg (16,400 lb). The pump has a 44.8 kW (60 HP) 480 volt 3ϕ motor.

2.2.7 Piping

All hot salt piping will be made of 316 stainless steel, while all cold piping will be made from A516 grade 70 carbon steel. All piping will be insulated and electrically trace heated. The pipes will be sloped to drain all components and lines back to their respective sumps. Expansion loops are used wherever necessary to keep pipe stresses at acceptable levels.

2.2.8 Instrumentation

The storage SRE will be heavily instrumented with thermocouples in order to determine tank thermal performance and to prevent salt freezing anywhere in the system. The thermocouples will all be of the chromel-alumel type. All thermocouples will be connected to an automatic data logger; in addition, a few key readings will be displayed on the control console. A summary of the thermocouples on each component is given in Table 2-1.

In addition, two flowmeters will be used to measure foundation cooling water flow rate, and four level gages will be used to measure salt level in both tanks and both sumps. Also, the power to the tank heaters will be measured to determine steady state heat loss.

2.2.9 Controls

The monitoring and control of the SRE will be accomplished from the control console. This includes the following:

1. Stop/start of all motors
2. Start of heater pilot light sequence
3. Heater stop
4. Cooler fan pitch
5. Louver position
6. Open/close of cooler insulated door
7. Control of valves No. 1 through No. 4
8. Salt level in sumps and tanks
9. Temperature of hardware

Interlocks will be used to provide control and prevent hardware damage. Alarms will be used to warn of conditions which are out of desired limits. Automatic control of the valves No. 1 and No. 3 will be used to maintain specified heights of salt in the sumps. Automatic control of the cooler outlet temperature will be accomplished by the variable pitched fans. Manual control of all automatic controls will be possible. The heater will have automatic control of the outlet temperature by adjusting the burner. The instrumentation displayed on the control console is listed in Table 2-2.

1. Hot Sump Level Control

   The level sensor will indicate the tank salt height from 0.15 m (6 in.) to 1.22 m (4 ft). The level sensor will be used to provide automatic control of valve #1 (hot sump inlet valve) so that the sump is maintained at 0.58 m (23 in.) $\pm$0.10 m ($\pm$4 in.). Valve 1 has a head pressure variation in the hot tank which varies from 84.3 kPa (12.24 psi) to 6.8 kPa (1.00 psi). Flow through the valve varies from 11.43 kg/s (90,500 lb/h) to 1.14 kg/s (9,050 lb/h). An audible alarm will sound when the salt exceeds 1.12 m (3 ft-8 in.). Manual/automatic control of the valve is provided. Sump level, valve position, and open/close lights are available on the control console.

Table 2-1 Thermocouple Summary

Component	No. of Thermocouples	
Hot Tank		
Salt TC rakes	34	
Liner	29	
Shell	35	
Sheathing	31	
Foundation	10	
Cooling Water	3	(one ΔT)
	142	Subtotal
Cold Tank		
Salt TC rakes	25	
Shell	25	
Sheathing	24	
Foundation	8	
Cooling Water	3	(one ΔT)
	85	Subtotal
Propane Heater	4	
Air Cooler	18	
Hot Sump and Pump	7	
Cold Sump and Pump	6	
Piping	48	
	83	Subtotal
	310	Total SRE

Table 2-2 Measurements Displayed on Console

1. Air Cooler
   - A. Pitch Control (GFE)
   - B. Louver (GFE)
   - C. Open/Close Ins. Door - Switch
   - D. Door - Open/Close Lights
   - E. Outlet Temperature
   - F. Over temperature alarm
   - G. Under temperature alarm

2. Heater
   - A. Start/Stop Switch
   - B. Temperature Controller (supplied) Bartlow Series 76
     Stack Temperature (on Controller)
   - C. Overtemperature Kill-Controller Stack Temperature (on Controller)
   - D. Burner Override - Switch
   - E. Outlet Temperature
   - F. Indicator Lights - Timer, Pilot, Burner
   - G. Overtemperature alarm

3. Hot Tank
   - A. Temperature
   - B. Level Gage

4. Cold Tank
   - A. Temperature
   - B. Level Gage

5. Hot Sump and Valve
   - A. Level - (Control of Sump Inlet Valve)
   - B. Valve Control (with Manual Override)
   - C. Valve Stem Position (0-10V, Bailey)
   - D. Overheight Alarm
   - E. Open/Close Lights on Valve Travel

6. Cold Sump and Valve
   - A. Level - (Control of Sump Inlet Valve)
   - B. Valve Control (with Manual Override)
   - C. Valve Stem Position (GFE)
   - D. Over Height Alarm
   - E. Open/Close Lights

7. Cooler Flow Valve
   - A. Manual Valve Control
   - B. Open/Close Lights

8. Heater Flow Valve
   - A. Manual Valve Control
   - B. Open/Close Lights

Table 2-2 Measurements Displayed on Console (continued)

9. Pneumatic Indicator
   A. Loss of pressure
10. Pressure
   A. Cold pump outlet
   B. Hot pump outlet

2. Cold Sump Level Control

The level sensor will indicate the tank salt height from 0.15 m (6 in.) to 1.78 m (5 ft - 10 in.). The level sensor will be used to provide automatic control of valve #3 (cold sump inlet valve) so that the sump level is maintained at 0.38 m (15 in.) ±0.08 (3 in.). The head pressure in the cold tank varies from 61.9 kPa (8.99 psi) to 7.63 kPa (1.11 psi). Flow through the valve varies from 6.86 kg/s (54,300 lb/h) to 0.69 kg/s (5430 lb/h). An audible alarm will sound when the salt level exceeds 1.5 m (4 ft 11 in.). Manual/automatic control of the valve is provided. Valve position and sump level are indicated at the console.

3. Control Valve for the Hot Pump

Valve #2 controls the flow from the hot pump through the cooler to the cold tank. This flow will be set manually with no automatic feedback. A valve position indicator is necessary so that the flow can be set to previously determined values. Open and closed indicator lights will be used.

4. Control Valve for the Cold Pump

Valve #4 controls the flow rate from the cold pump through the heater to the hot tank. This flow will be set manually and no automatic feedback is necessary. A valve position indicator will be used to set the flow rate. Open and closed indicator lights will be provided.

5. Fossil Fired Heater Control

The heater will be supplied with its own control panel which will include burner safety features and start sequence. Several functional items will be available at the console: a start button will start the pilot light sequence, proper pilot lighting will be indicated by a light. The salt temperature outlet will be controlled by the controller (Partlow 76) which is set in the console. Initial preheat of the heater will be accomplished by setting the controller to 550°F. The controller will monitor flue gas exit temperature. A stop button will be available at the console to turn off the burner. A main burner switch in the control console is provided to lock out the main burner until flow is establihsed through the heater.

6. Air Cooler

The controls for the air cooler are GFE and will be identical to the ACR usage. A manual/automatic control will be provided for the variable pitched fans to control the salt outlet temperature. Both fans can be stopped and started from the console.

The louver pitch is controlled by a dial unit on the console. Insulated movable covers on the air cooler are pneumatically operated with switches from the console. Position indicator lights for open and closed will be provided.

7. Foundation Coolant Flow

   The valves for controlling the coolant flow through the tank foundation will be manual. Coolant flow through the foundations will be parallel flow with a valve at each foundation. Each flow will be measured locally.

8. Electrical Trace Heaters

   The controls for the majority of trace heaters will be an off/on switch with the temperature being controlled by a passive design. The heater power is designed to obtain the correct temperature without cycling. The heater switches on the console will operate the heater relays.

9. The fill valve to initially fill salt into the system will be manual.

3.0 TEST PROGRAM

This storage SRE test program will have two main phases:

I. System startup and checkout tests

II. Tank thermal performance tests

In the first phase, the system will be loaded, functioned with molten salt and checked out. In the second phase, we will measure the thermal performance of both the hot tank and the cold tank.

Since the storage SRE is being constructed as a stand-alone facility, this testing will be conducted with very little interfacing with the CRTF. All that is required from CRTF is the propane, electricity and cooling water previously described in Section 1.5. The storage SRE will nominally be operated on a one shift (8 hr) per day, five days a week basis. When left unattended overnight, or on weekends and holidays, the only equipment that may be operating will be electric heaters, the foundation cooling water, and the data logger. All pumps will be off, all valves will be closed and there will be no salt flow.

Each tank will always be left with a small amount of residual salt so as to avoid freezing problems and to reduce thermal cycling. Thus, even when a tank is described as "empty" in this report it still has salt in it. The definitions used herein are listed below:

	Actual Salt Level	
Short Title	Hot Tank	Cold Tank
Full	4.98 m (16' 4")	3.15 m (10' 4")
Half-full	2.49 m (8' 2")	1.57 m (5' 2")
Empty	0.41 (1' 4")	0.41 m (1' 4")

Two other terms that are used herein are "charge" and "discharge." Charge means that hot salt is flowing into the hot tank, while discharge means hot salt is flowing out of the hot tank. The SRE is capable of simultaneous charge and discharge.

Each tank shall also be closely monitored for any salt leaks as a routine matter of practice throughout the test program. This will be accomplished by:

a) Looking for any abnormal rise in shell temperature (hot tank only), foundation cooling water temperature, or external sheath temperatures as measured by the thermocouples.

b) Using an i.r. scanner ΔT gage to observe the outer surface sheathing of each tank to look for any hot spots.

c) Visual observation of all tanks, valves, pipes and sumps.

This monitoring shall be conducted at least daily during the early part of the test program, and at least twice weekly thereafter.

3.1 SYSTEM STARTUP AND CHECKOUT TESTS

The overall objective of this series of tests is to demonstrate how a commercial system would be started up, and how to get the SRE in a state of readiness for subsequent tests.

3.1.1 Salt Loading (Test #1)

The nitrate salt will be stored at the site in the form of a dry granular aggregate. The salt will be heated to the melting point and above (288°C [550°F]), and then pumped into the cold tank. It is planned that this operation will be conducted by an experienced subcontractor who will provide all his own equipment. This will be a 24 hour a day operation until the salt is fully loaded (approximately 79,200 kg [176,000 lb]). The test sequence is as follows:

1) Close all valves in the system, except open the fill valve.

2) Attach external fill pipe to the fill valve.

3) Turn on trace heating on line #4 and turn on the cold tank heater. Monitor the temperatures on these components, and allow them to slowly warm up to as close to 288°C (550°F) as practical. Turn on the foundation cooling water flow.

4) Activate the subcontractor's loading equipment:

   a) Load the dry granular sodium nitrate and potassium nitrate into the hopper; the mixture is to be 60% by weight sodium nitrate and 40% by weight potassium nitrate.

   b) Heat the salt in the hopper until it is all melted, and then heat to 288°C (550°F).

   c) Pump this hopper load into the cold tank.

   d) Adjust the cold tank heater and the line #4 trace heaters to maintain as close to 288°C (550°F) as practical.

   e) Monitor the cold tank salt level gage to ensure that the tank is not overfilled.

   f) Repeat steps a) - e) as many times as necessary to load approximately one-half the salt into the cold tank.

5) When the cold tank is approximately half-full, turn on the trace heating for the cold sump and allow it to reach as close to 288°C (550°F) as practical. Then open valve #3 and allow cold salt to flow into cold sump until the sump is full; then close valve #3.

6) Repeat steps 4.a) - 4.e) as many times as necessary to fill the cold tank to approximately 3.52 m (11.56 ft).

7) When all the salt is loaded, close the fill valve and disconnect the external fill pipe.

8) During the loading process, and for sometime thereafter, closely examine the cold tank for leaks using both visual inspection and i.r. scanner inspection.

3.1.2 Functional Flow Test (Test #2)

A functional flow test with cold salt will be conducted following the salt loading operation (i.e., Test #1). The purpose of this test is to bring all elements of the system up to 288°C (550°F), to checkout the functioning of all pumps, valves and controls with molten salt, and to check the system for leaks. At the beginning of this test, i.e., after the completion of Test #1, the following conditions will exist:

a) Both pumps will be off and all valves will be closed.

b) All trace heaters (except line #4) will be off, and the entire system (except the cold tank and the cold sump) will be at ambient temperature.

c) The cold tank will be extra full of salt (i.e., it will contain its normal full load plus all the salt from the hot sump, all pipes, and the hot tank residual) at 288°C (550°F).

The test sequence is:

1) Turn on trace heating for line #1, #5, & #6, valve #1, #3 & #4, and hot tank; turn on pre-heat on propane heater; slowly bring all these components up to as close to 288°C (550°F) as practical.

2) Open valve #3 and #4, turn on cold pump, and slowly pump cold salt into the hot tank until it is full. Take at least 24 hours to do this.

3) When hot tank is full of cold salt, shut off cold pump and close valve #3. Let lines #5 and #6 and propane heater drain back into cold sump and then close valve #4. Turn off propane heater.

4) Allow the full hot tank to reach thermal equilibrium (or hold at least 24 hours). Closely monitor salt temperature in each tank, and adjust tank heaters so as to maintain as close to 288°C (550°F) as practical. Carefully check hot tank for any leaks, and check all components for proper functioning.

5) Turn on trace heating on line #2, valve #2, hot sump and the air cooler and bring up to as close to 288°C (550°F) as possible.

6) Open valve #1 and slowly fill hot sump.

7) Open valve #2, turn on hot pump, and slowly pump cold salt from hot tank into cold tank.

8) When cold tank is full of cold salt, shut off hot pump, and close valve #1. Let lines #2 and #3 and the air cooler drain back to the hot sump, and then close valve #2.

9) Closely monitor the salt temperature in both tanks and both sumps, and adjust heaters to keep as close to 288°C (550°F) as practical.

3.1.3 Heatup Hot Tank (Test #3)

The purpose of this test is to bring the hot tank up to its final operating temperature, 566°C (1050°F). At the outset of this test the SRE will be in the following condition:

a) The cold tank will be full of salt at 288°C (550°F), and the hot tank will be "empty" (i.e., with only residual salt) at 288°C (550°F); both sumps will have cold salt in them.

b) All electrical heaters will be on.

c) Both pumps will be off and all valves will be closed.

The test sequence is:

1) Assure all components except the propane heater are greater than 288°C (550°F).

2) Open valves #3 and #4, start cold pump, start propane heater with outlet temperature set at 427°C (800°F), and proceed to fill hot tank with warm salt; take at least 24 hours to fill the tank.

3) When tank is full, shut off cold pump, close valve #3, shut off propane heater and allow lines to drain back to cold sump.

4) Allow full hot tank to sit until it reaches thermal equilibrium (or for at least 24 hours). Monitor salt temperature and adjust tank heater to maintain as close to 427°C (800°F) as practical.

5) Open valves #1 and #2, start air cooler, and start hot pump; slowly pump warm salt at 427°C (800°F) from hot tank through air cooler exiting at 288°C (550°F) and flowing into cold tank; stop pumping when hot tank is empty.

6) Repeat steps 1) - 5) only with propane heater set to heat salt to 566°C (1050°F); this will leave the SRE storage system in an uncharged state at fully operational temperatures.

7) At each step of the way, carefully inspect hot tank for any leaks.

3.1.4 System Operation Checkout (Test #4)

The objective of this test is to checkout the fundamental steps involved in operating the SRE on a normal daily basis. Operations to be performed during this test are:

- Charge only
- Discharge only
- Simultaneous charge and discharge

This test will not only allow "bugs" that remain in the system to be corrected but will also provide valuable experience for the operators. It should be noted that during the performance of this test, portions of test #5 will be conducted by simulating various emergency situations that might arise during normal operations.

The scenario for the first part of this test (Part I) is defined below. Note that this will be repeated on each of three days before going on to Part B:

- Charge at 3 MWt until hot tank is full (2.33 hr)
- Hold at full charge for 1 hour
- Discharge at 3 MWt until hot tank is empty (2.33 hr)
- Hold storage system in an uncharged condition for overnight

Part II of this test will have the following scenario (also to be repeated three times):

- Charge at 3 MWt until hot tank is half full (1.17 hr)
- Simultaneously charge at 3 MWt and discharge at 3 MWt for 4 hr holding salt levels constant in each tank
- Discharge at 3 MWt until hot tank is empty (1.17 hr)
- Hold storage system in an uncharged condition for overnight

Note that at the beginning of this test, the SRE is in an "uncharged" state typical of overnight conditions, i.e., the hot tank is empty, the cold tank is full, both sumps are full and the salt is at its proper operating temperature in all places.

The test sequence for Part I is:

I-1 Turn on the preheat on the propane heater, and set it to achieve temperature of 566°C (1050°) salt outlet temperature.

I-2 Open valves #3 & #4, turn on the cold pump and start the main burner. Adjust salt flow rate so that the thermal flow rate into the hot tank is 3 MWt (this requires 6.96 kg/s [55,200 lb/hr] of salt).

I-3 After approximately 2.33 hr, the hot tank will be full; then shut off the cold pump, close valve #3 and allow line #5 to drain back into cold sump.

I-4 Hold in this fully charged condition for 1 hour.

I-5 Assure lines #1, #2, and the air cooler are above 288°C (550°F).

I-6 Open valves #1 and #2, start the hot pump and pump salt out of the hot tank and through the cooler at a rate of 3 MWt (6.96 kg/s [55,200 lb/hr] salt flow rate).

I-7 After approximately 2.33 hr the hot tank will be empty; then shut off the hot pump, close valve #1 and allow lines to drain back into the hot sump.

I-8 Adjust tank and sump heaters to maintain normal operating temperatures for overnight storage.

I-9 At each step of the way, carefully check the whole system for any leaks and for proper function of equipment.

The test sequence for Part II of Test #5 is:

II-1 Turn on the preheat on the propane heater, and allow it to come up to temperature.

II-2 Open valves #3 & #4, turn on the cold pump. Adjust salt flow rate so that the thermal flow rate into the hot tank is 3 MWt.

II-3 After approximately 1.17 hr, the hot tank will be half full; at this time, assure the correct temperature of lines #1, #2, and the air cooler. Open valves #1 and #2, start the hot pump and pump salt out of the hot tank and through the cooler at salt mass flow rate equal to the inlet flowrate.

II-4 Maintain this condition of equal (and simultaneous) charge and discharge for 4 hrs; closely monitor both hot and cold tank salt levels to ensure approximately constant half-full levels in each tank.

II-5 After the 4 hrs, shut off the cold pump, close valve #3 and allow lines to drain back into the cold sump.

II-6 After approximately 1.17 hr, the hot tank will be empty; then shut off the hot pump, close valve #1 and allow lines to drain back into the hot sump.

II-7 Adjust tank and sump heaters to maintain normal operating temperatures for overnight storage.

II-8 At each step of the way, carefully check the whole system for any leaks and for proper function of equipment.

3.1.5 Emergency Shutdown Checkout (Test #5)

The purpose of these tests is to check out the ability of the SRE to be shut down rapidly in the event an emergency should occur (e.g., a fire, earthquake, etc). A corollary objective is to give the operators practice in handling such situations, and to refine (if necessary) the emergency shutdown procedures.

The test sequence is:

1. Shut off both pumps.
2. Shut off heater and cooler.
3. Close valves #1 and #3.
4. Shut off all electrical trace heaters on lines, valves, sumps, and tanks.
5. Evacuate the control room immediately.

This testing sequence is to be performed at least twice during the conduct of Test #4.

3.2 THERMAL PERFORMANCE TESTS

The basic objective of these tests is to measure the thermal performance of the hot storage tank and the cold storage tank under transient and steady state conditions. Specific parameters of interest are:

1. Total tank heat loss rate
2. Distribution of heat loss rate amongst walls, top and bottom
3. Salt temperature
4. Liner temperature

5. Shell temperature
6. Sheath temperature
7. Foundation and cooling water temperature and cooling water flow rate

Referring to Table 1-1, it is seen that these tests will be conducted as follows:

- Steady state heat loss
- Cyclic charge and discharge
- Transient cooldown

3.2.1 Steady State Heat Loss - Full Hot Tank (Test #6)

The specific objective of this steady state test is to measure items 1-7 listed in section 3.2 for each tank at steady state conditions and a constant salt level. Steady state thermal conditions will be established and maintained by the use of the tank heaters. No salt flow will be permitted into or out of either tank during a steady state test.

Since a true steady state test of such a large mass of equipment can take a very long time (e.g., 3 or 4 weeks), it is planned to use a slightly modified procedure. This may be called a "high-low bounding" method. In the first part of the test, the tank heaters will be set at a level approximately 10% above the predicted heat loss rate. If after a few days all salt, liner and shell thermocouple readings are still increasing with time, the tank heater setting ($\dot{Q}_{high}$) is known to be greater than the actual heat loss rate. The heater setting will then be reduced by approximately 20%. After a few days if all the salt, liner and shell temperature are decreasing, then this tank heater setting ($\dot{Q}_{low}$) is known to be less than the true heat loss rate. The true heat loss rate can then be accurately estimated by correcting each heater setting for salt and tank heat capacity effects, and averaging the two values:

$$\dot{Q}_{tank_1} = \dot{Q}_{high} - (W\ C_p)_{total} \left(\frac{dT}{dt}\right)_{\substack{salt \\ high}}$$

$$\dot{Q}_{tank_2} = \dot{Q}_{low} + (W\ C_p)_{total} \left(\frac{dT}{dt}\right)_{\substack{salt \\ low}}$$

$$Q_{tank} = \frac{\dot{Q}_{tank_1} + \dot{Q}_{tank_2}}{2}$$

Where:

$$(W\ C_p)_{total} = W_{salt}\ C_{p_{salt}} + W_{tank}\ \overline{C_{p_{tank}}}$$

The heat capacity corrections are calculated theoretically from our STS computer code, and the time rate of change of salt temperature will be calculated from the thermocouple data. In theory, the two tests ought to give identical values of the heat loss rate.

In practice, the above procedure may require several iterations. The goal is to achieve two tests wherein $\dot{Q}_{tank_1}$ and $\dot{Q}_{tank_2}$ do not differ by more than 10%.

The test sequence is listed below:

1. Turn on the propane heater at preheat condition and allow it to come up to temperature.

2. Open valves #3 and #4, turn on cold pump, turn on main burner and proceed to fill hot tank with 566°C (1050°F) salt.

3. When tank is full, shut off cold pump and propane heater, close valve #3 and allow lines to drain back into sump.

4. Set hot tank heater to a power level approximately 10% above the best estimate of the actual tank heat loss rate (currently predicted to be 21.5 kWt, but use latest available estimate at test time).

5. Leave the heater at this constant setting for at least 48 continuous hours.

6. If during the last 24 hours of this period the salt and shell thermocouples have been increasing with time (or have remained constant), go on to step #7. If not, increase the tank heater setting and repeat steps #5 and #6 until a setting is found which satisfies this criteria.

NOTES: a) In no case is a test to be continued if the hot salt temperature reaches (or exceeds) 593°C (1100°F)--if this should occur, reduce the heater setting at once.

b) Perform steps 4 - 6 for the cold tank at the same time as the hot tank tests are being performed. Current best prediction of heat loss rate is 4.8 kWt.

7. Once a bounding high value has been found ($\dot{Q}_{high}$) by this procedure, reduce the hot tank heater setting by approximately 20%.

8. Leave the heater at this constant setting for at least 48 hours.

9. If during the last 24 hours of this period the salt and shell thermocouples have been decreasing with time (or remaining constant) go on to step #10. If not, reduce the heater setting and repeat steps #8 and #9 until a setting is found which satisfies this criteria.

NOTE: Also perform steps 7 - 9 for cold tank.

10. Correct the two heater settings for heat capacity effects by the methods explained above and thus obtain two estimates of the true tank heat loss rate. It is a goal of this program that the high and low heat rate loss tests should not differ by more than 10%; some iteration may be required to achieve this goal.

3.2.2 Steady-State Heat Loss - Empty Hot Tank (Test #7)

The objective of this test is identical to that of Test #6 except that the salt level in the hot tank is empty and that in the cold tank is, of course, full.

The test sequence is:

1. Verify the air cooler and lines #1 and #2 are at the correct temperature.

2. Open valves #1 and #2, turn on hot pump, turn on air cooler and proceed to fill cold tank with 288°C (550°F) salt.

3. When cold tank is full, shut off hot pump and air cooler, close valve #1 and allow lines to drain back into sump.

4.-10. The remainder of the steps for this test are identical to those for Test #7.

3.2.3 Daily Charge/Discharge (Test #8)

The purpose of these tests is to measure the thermal performance of the storage system under daily cyclic conditions simulating those that would be encountered in a large STCR plant. In particular, we will measure the salt temperature vs time in both tanks and all salt flow rates; these data will be used to calculate heat input and output quantities, and the storage efficiency. The charging scenario selected for this test is as follows:

. Charge at 3 MWt until hot tank is full (2.33 hr)

. Simultaneous charge and discharge for 1 hour

. Discharge at 3 MWt until hot tank is empty (2.33 hr)

. Hold storage system in an uncharged condition for overnight

These tests will be performed without any tank heaters being on, so that the salt temperature in each tank will rise and fall daily according to the natural energetics of the situation.

The test sequence is:

1. Turn on the preheat on the propane heater, and allow it to come up to temperature.

2. Open valves #3 & #4, turn on the cold pump. Adjust salt flow rate so that the thermal flow rate into the hot tank is 3 MWt.

3. After approximately 2.33 hr, the hot tank will be full; at this time, assure the correct temperature of lines #1, #2, and the air cooler. Open valves #1 and #2, start the hot pump and pump salt out of the hot tank and through the cooler at salt mass flow rate equal to the inlet flowrate.

4. Maintain this condition of equal (and simultaneous) charge and discharge for 1 hr; closely monitor both hot and cold tank salt levels to ensure approximately constant full levels in each tank.

5. After the 1 hr, shut off the cold pump, close valve #3 and allow lines to drain back into the cold sump.

6. After approximately 2.33 hr, the hot tank will be empty; then shut off the hot pump, close valve #1 and allow lines to drain back into the hot sump.

7. Let SRE stand overnight with no tank heaters on.

8. Repeat this sequence for five consecutive calendar days.

3.2.4 Transient Cooldown - Full Hot Tank (Test #9)

The objective of this test is to measure the thermal performance of the hot tank under transient cooldown conditions. In particular, under those conditions wherein the tank is brought up to a full salt level and a 566°C (1050°F) salt temperature, and then allowed to cool naturally (i.e., with no electric heaters on or any salt flow into or out of the tank) for two weeks. This will provide several important pieces of experimental data. First, the overall heat loss coefficient U under transient, variable temperature conditions will be measured and compared to the steady state, constant temperature value. Second, the transient thermal lag between the shell and the salt will be measured. Thirdly, the data can be extrapolated to provide estimates of the time it would take to reach the freezing temperature.

The test sequence is:

1-3. Fill hot tank using procedure identical to steps 1-3 in Test #6.

4. Turn off hot tank heaters and allow tank to sit for two weeks.

NOTE: During this test, monitor salt temperature in hot tank frequently, and be sure there is no danger of freezing.

4.0 TEST SCHEDULE

The schedule for this test program is shown in Figure 4-1. The total test period covers nine calendar weeks, with 4 weeks devoted to loading the system with salt, bringing it up to temperature and checking it out, followed by 5 weeks of performance testing. The first five tests must be performed in the exact order specified; it is preferred that the last five tests be done in the order indicated, but it is not mandatory.

The elapsed times indicated on Figure 4-1 are our best estimates of how long it should take to perform each test. These times include a "learning factor" in the beginning, i.e., for Tests 1, 2 and 3. These estimates are based on the test crew working a normal 8 hours per day, 5 days per week work schedule, and of course on the "success orientated" assumption that there will be no major hardware problems. Additional basis for estimates is given below.

As noted previously, the salt loading will be done by an experienced subcontractor. Once the actual loading begins, they will load on a round-the-clock basis until all the salt is loaded. The whole process is nominally estimated to require 2 or 3 days, but we have added several days as a margin. The functional flow and heating up the hot tank tests are estimated at 4 and 5 days respectively, which includes several days to allow thermal soak out to occur all the way through the hot tank. Tests 4 and 5 should require 6 working days, and it is assumed by this time that the test crew is well along the "learning curve" and therefore requires no unusual margin.

The steady state heat loss tests should take approximately 1 week to complete each, 2 days for the "high bound" part, 2 days for the "low bound" part, and 1 day for some iteration on tank heater settings. The charge/discharge tests will be done on a one-per-day basis for a total of 5 times, and so should only require 1 week. Finally, it is calculated that without any tank heaters on in a full hot tank, it will take about 14 days for the salt to cool down to the desired temperature.

Figure 4-1 Test Schedule

Storage SRE Test Matrix

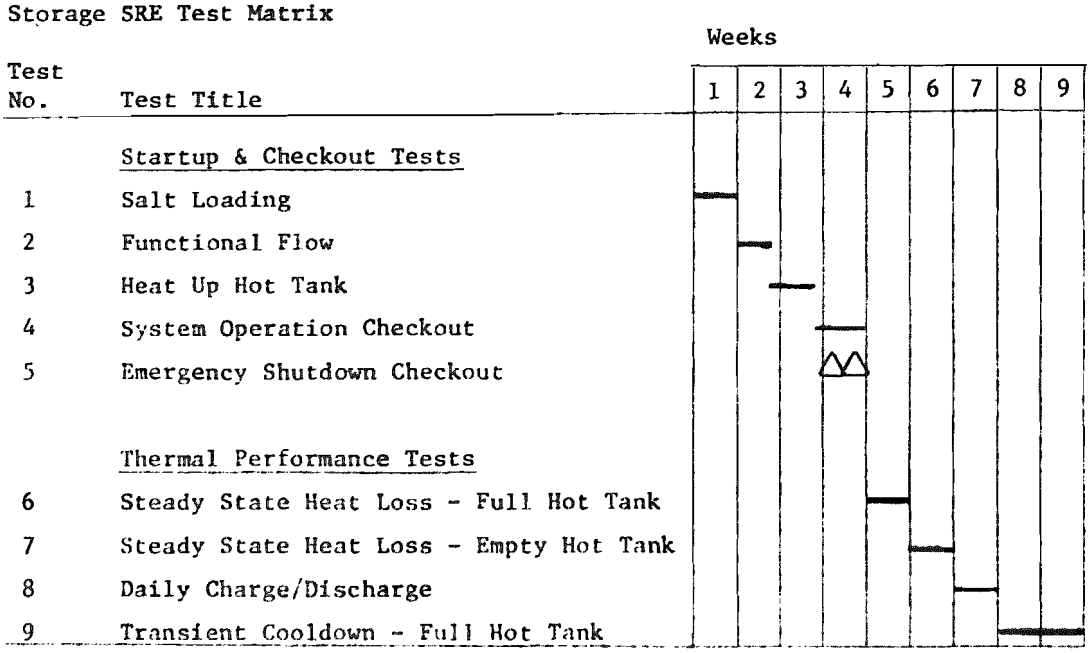

APPENDIX E

FAILURE MODES AND EFFECTS ANALYSIS

SUBSYSTEM/ COMPONENT	FAILURE MODE	EFFECTS		DETECTION	PREVENTIVE MEASURES OR CORRECTIVE ACTION	COMMENTS
		OPS SEQUENCE	CONSEQUENCES			
TANKS	Structure failure	All	Salt loss	Inspection	Design to code and dike area with equipment up off the ground.	
	Leakage	All	Insulation damage. Increased heat loss.	Temp. measurements and inspection.	Leak tests prior to tank usage.	
	Vent plugged with salt	Charge/discharge	Tank deformation or rupture due to pressure.	Tank pressure by level sensor.	Vent line insulation and routine pretest checkout.	
LINES	Leakage	All	Damaged insulation. Possible hot spots or cold spots.	Temp. measurements.	Proof and leak testing.	
	Burst due to volumetric change of salt due to thawing	Warmup after freeze	System inoperative due to excessive leakage or loss of salt from storage tanks.	Visual inspection.	Prevent system freezing by trace heating. Drain lines (where possible) after usage.	
FLOW CONTROL VALVES						
#1 Hot Sump Inlet	Fail open	No salt flow	Drain hot tank into hot sump	Level sensor. Salt out through sump vent. Enunciator alarm of overheight of sump.	Vent on sump limited to small hole and sump designed to withstand total head of hot tank.	This is a fail close valve.
		Salt flow	Improper level of hot sump.	Level sensor. Enunciator alarm for overheight of sump.	Manual closing of valve.	

SUBSYSTEM/ COMPONENT	FAILURE MODE	EFFECTS		DETECTION	PREVENTIVE MEASURES OR CORRECTIVE ACTION	COMMENTS
		OPS SEQUENCE	CONSEQUENCES			
#1 Hot Sump Inlet (cont.)	Valve stuck in semi-open position	Transients	Loss of flow control may result in improper level in the sump. Low level results in loss of fluid to pump, thus possible freezing of air cooler. High level does not allow sufficient volume for line drainage.	Level sensor. Temperature measurements. Enunciator alarm of air cooler under temperature. Enunciator alarm of sump overheight.	Manual override of valve; shutdown and repair.	
	Fail Closed	Salt flow	Decrease sump level and loss of flow through air cooler thus freezing salt.	Level sensor. Temperature measurements. Enunciator alarm of air cooler under temperature.	Shutdown and repair.	
#2 Air Cooler Outlet	Fail open	Salt flow	Increased flow and possible increased cooler outlet temp.	Temp. measurements. Enunciator alarm for air cooler overtemp.	Shutdown and repair.	This is a fail close valve.
	Valve stuck in semi-open position	Salt flow	Loss of flow control may result in temperatures out of limits	Temp. measurements. Enunciator alarm air cooler over or under temp.	Shutdown and repair.	
	Fail closed	Salt flow	Loss of flow possible salt freezing in air cooler.	Temp. measurements. Enunciator alarm air cooler under temperature.	Shutdown and repair	
		Shut down	Will not allow line to drain thus possible salt freezing in air cooler.	Level sensor. Temp. measurements.	Manual open valve.	

SUBSYSTEM/ COMPONENT	FAILURE MODE	EFFECTS		DETECTION	PREVENTIVE MEASURES OR CORRECTIVE ACTION	COMMENTS
		OPS SEQUENCE	CONSEQUENCES			
Control Valve #3 Cold Sump Inlet	Fail open.	No salt flow	Drain cold tank into cold sump.	Level sensor. Salt out through sump vent. Enunciator alarm sump over-height.	Vent of sump limited to small hole and sump designed to withstand total head of cold tank.	This is a fail close valve.
		Salt flow	Increased level of cold sump.	Level sensor. Enunciator alarm sump overheight.	Manual closing of valve	
	Valve stuck in open position	Transients	Loss of flow control may result in improper level in the sump. Low level results in fluid loss to pump, thus overheating salt. High level does not allow sufficient volume for line drainage at shutdown.	Level sensor. Temp. measurements. Enunciator on salt overheight.	Manual override of valve shutdown & repair. Overtemperature kill on salt heater.	
	Fail closed	Salt flow	Decrease sump level and loss of flow through heater. Overheating of salt.	Level sensor. Temp. measurements.	Overtemperature kill on salt heater. Shutdown and repair.	
#4 Heater Inlet	Fail open	Salt flow	Possible decrease of salt outlet temp from heater.	Temp. measurements. Level sensor.	Shutdown and repair.	This is a fail close valve.
	Valve stuck in semi-open position	Salt flow	Loss of control may result in temperatures out of limits.	Temp. measurements.	Shutdown and repair.	
	Fail closed	Salt flow	Loss of flow possible over limit of salt in heater.	Temp. measurements. Level sensor.	Shutdown and repair. Overtemp kill on heater outlet.	

SUBSYSTEM/ COMPONENT	FAILURE MODE	EFFECTS		DETECTION	PREVENTIVE MEASURES OR CORRECTIVE ACTION	COMMENTS
		OPS SEQUENCE	CONSEQUENCES			
#4 Heater Inlet (cont.)	Fail closed	Shutdown	Will not allow line to drain, eventual freezing of salt in heater.	Level sensors. Temp. measurements.	Manual open valve.	
SRE AIR COOLER						
Top Insulation Cover	Stuck in closed position	Salt flow	Salt over-temperature	Door position switch Temp. sensor. Enunciator alarm overtemp air cooler.	Shutdown or manual override.	
	Stuck in open	Pre-fill warmup	Cold spots below freezing point of salt may impair filling operation	Door position switch By inspection prior to start. Temp. instrumentation.	Shutdown and repair.	
Tubes/Headers	Leakage	All sequences involving flow	Salt leakage may create frozen salt stalactites or stalagmites which may impair louver or fan performance. Large leakage may cause excessive loss of salt from system.	Pre/Post-test inspection. Low pressure at PT-3	Pretest/posttest C/O and maintenance.	
Louvers	Fail Closed	Salt Flow	Cooler outlet over-temperature.	Temp sensor. Enunciator alarm. Pre-test inspection.	Shutdown and repair.	"Fail close" design.
	Fail open	Salt flow	Cooler outlet temp. Control range minimized.	Temp. monitoring.	Pretest/Posttest C/O & maintenance.	
Fans	Loss of power	Salt flow	Cooler outlet temperature--too hot.	Temp. Sensor. Enunciator alarm.	Shutdown.	

SUBSYSTEM/ COMPONENT	FAILURE MODE	EFFECTS		DETECTION	PREVENTIVE MEASURES OR CORRECTIVE ACTION	COMMENTS
		OPS SEQUENCE	CONSEQUENCES			
Bladder	Leak in bladder	Salt flow	No pitch control of fans. Decreased salt outlet temp.	Temp. measurements.	Shutdown; replace bladder with spare.	
COLD SUMP/PUMP SUBSYSTEM						
Pump	Loss of power	Salt flow	Loss of flow resulting in possible over limit of salt in heater.	Temp. measurements.	Shutdown. Overtemp kill of heater outlet.	
	Loss of air cooling to bearing	Salt flow	Bearing overheating and eventual failure	T/C on bearing	Verification of pneumatic valve positions during pretest C/O (routine checklist).	
	Vent plugged W/frozen salt	Startup	Possible tank collapse	Salt leak No flow	Routine pretest check-out. Insulate line to keep above freeze point of salt.	
		Shutdown	Increase tank pressure	Inspection	Routine pretest check-out. Insulate line to keep above freeze point of salt.	
HOT SUMP/PUMP SUBSYSTEM						
Pump	Loss of power	Salt flow	Loss of flow resulting in salt freezing in cooler.	Temp. measurements.	Shutdown.	
	Loss of water cooling bearing	Salt flow	Bearing overheating and eventual failure	T/C on bearing and system	Shutdown	

SUBSYSTEM/ COMPONENT	FAILURE MODE	OPS SEQUENCE	CONSEQUENCES	DETECTION	PREVENTIVE MEASURES OR CORRECTIVE ACTION	COMMENTS
HOT SUMP/PUMP SUBSYSTEM (cont.)						
Pump		No flow	High bearing temperature	T/C on bearing and coolant system	Establish coolant flow and cool bearing prior to pump operation.	
	Vent plugged W/frozen salt	Startup	Possible tank collapse	Salt leak, no flow	Routine pretest checkout. Insulate line to prevent freezing.	
		Shutdown	Increased tank pressure.	Inspection	Routine pretest checkout. Insulate line to prevent freezing.	
TRACE HEATERS & CONTROLS	Loss of power	Salt flow	None	None	-	Heater loss due to commercial power loss will be restored with commercial power.
		Nonoperational	Loss of temperatures and eventual salt freezing	Temp. measurements.	Inspection	
		START OF FREEZING				
		Items with salt				
		Cold tank outlet	2.6 hrs			
		Hot tank outlet	14.3 hrs			
		Cold sump	10.8 days			
		Hot sump	8.5 days			
		Residual cold tank	3.8 days			
		Residual hot tank	3.8 days			
		Full cold tank	29.4 days			
		NOTE: At test completion, salt drained from hot tank and hot tank outlet and placed in cold tank.				

SUBSYSTEM/ COMPONENT	FAILURE MODE	EFFECTS		DETECTION	PREVENTIVE MEASURES OR CORRECTIVE ACTION	COMMENTS
		OPS SEQUENCE	CONSEQUENCES			
INSTRUMENTATION						
Level Sensors Hot & Cold Tanks	Fails	All sequences	Height of salt in tanks not known	Consistency of data. Level of other tank.	Repair	Indicators only.
Level Sensors Hot & Cold Sumps	Fails	Salt flow	Improper feedback for control of sump level by inlet valve	Loss of salt flow seen by temp measurements or salt out through vent seen by temp measurements.	Manual control of inlet valves	
Fan Indicator/ Controller	Fails	Salt flow	Low air flow. High cooler outlet temps.	Fan position reads "0"	Shutdown repair	
Fan I/P	Fails electronic pneumatic	Salt flow	Low air flow. High cooler outlet temps.	Fan position reads "0"	Shutdown repair	
Propane Heater Controller	Fails	Salt flow	Reduce temperatures in heater. Low salt outlet temp.	Temp. measurements.	Shutdown repair.	
Temperature Sensor Air Cooler	Fails open	Salt flow	Increases pitch. Cooling of salt outlet temperature.	Temp. measurements.	Manual control shutdown.	
Temperature Sensor Heater Stack Temp.	Fails open	Salt flow	Lower burner temp. Cooling of salt outlet temp.	Temp. measurements.	Shutdown repair.	
Thermocouples	Fails open	All sequences	Loss of data	Data recorder system	Sufficient similar data.	
SRE AUXILIARY SYSTEMS						
Commercial Power	Loss of power	Non operation	Loss of coolant system (see below). Loss of trace heaters results in eventual salt freezing.	Panel lights, instrumentation, coolant flow.	Trace heater will be powered when commercial power is reestablished. Restart coolant system.	

SUBSYSTEM/ COMPONENT	FAILURE MODE	EFFECTS		DETECTION	PREVENTIVE MEASURES OR CORRECTIVE ACTION	COMMENTS
		OPS SEQUENCE	CONSEQUENCES			
Commercial Power (cont.)		Salt flow	Loss of pump, compressed air, trace heaters, air cooler and heater.	Panel lights.	Open valves 2 & 4 to allow line drainage to sumps. Close air cooler insulated doors manually.	
PNEUMATIC SYSTEM						
Compressor	Stoppage	Salt flow	Loss of valve control Loss of cold pump bearing cooling. Loss of insulated door movement. Louver close.	Enunciator	Shutdown	
Pressure Regulators	Pressure out of range	Salt flow	Possible loss of remote and automatic control functions	Inspection of control panel	Use of manual overrides or initiate shutdown.	
PROPANE SYSTEM						
Storage	Loss of propane	Heater on	Loss of heat.	Temp. measurements.	Inspection of propane volume on routine pre-test checkout.	
Evaporator or Pressure Regulators	Malfunction	Heater on	Loss of propane and heat.	Temp. measurements.	Shutdown and repair.	
COOLANT SUPPLY	Loss of flow	No salt flow	Hot pump bearing overheated. Foundation eventually overheated (4 days)	Temp. measurements.	Reestablish flow and allow bearing to cool.	
		Salt flow	Overheating of hot pump bearing	Temp. measurements.	Shutdown and repair.	

APPENDIX F

MOLTEN SALT STORAGE SRE
TEST PROCEDURE
TEST #4

SYSTEM OPERATION CHECKOUT

Revision Two

Test Description Summary

Purpose: This test is to checkout the fundamental steps involved in operating the SRE on a normal daily basis. Operations to be performed during this test are:

Charge only
Discharge only
Simultaneous charge and discharge

Description: The test will start with the hot tank empty, the cold tank full, and the system in its normal filled condition. The following test scenario will be performed three times:

Charge hot tank at 3MWt until full
Hold charge for 1 hour
Discharge hot tank at 3MWt until empty
Hold discharge over night

The second portion of this test shall have the following scenario performed three times.

Charge hot tank at 3MWt until it is 1/2 full
Simultaneously charge and discharge at 3MWt
for 4 hours holding salt level constant in
each tank
Discharge at 3MWt until hot tank is empty (1.17 hours)
Hold discharge overnight

Pre-Test Checklist

NOTE

Pretest checklist should be performed every morning prior to a test or continuing a test.

Experiment Setup

1. Inspect system for evidence of leaks, insulation damage and repair as required.

2. Check for visual evidence of blown fusses or burned relays in power control J-Box.

3. Verify the amperage on the active heat trace circuits.

1,CS-1 Coldsump	11A	21 L-4 Line #4	5.0A
2,CS-2	11A	22 L4-3	2.4A
3 CS-3	16.6A	23 L5 Line #5	8.7A
4 CS-4	16.0A	24 L6 Line #6	4.0A
5 HS-1 Hotsump	9.5A	25 L1-5 Line to sumps	3.9A
6 CT-1 Cold tank	15.2A	26 C1 Air Cooler	13.5A
7 CT-2	6.2A	27 C2	11.3A
8 CT-3	6.2A	28 C3	17.2A
9 CT-4	3.1A	29 C4	17.2A
10 L1-2,L1-4 Line #1	13.5A	30 C5	14.4A
11 L1-1	6.7A	31 C6	14.4A
12 L2 Line#2	6.3A	32 C7	18.9A
13 HT-1 Hot tank	16.9A	33 C8, C9, C10 480,30	19.5A ea,
14 HT-2	16.9A	HS-2	4.3A
15 HT-3	16.9A	C4-4 Line #4	3.7A
16 HT-4	13.5A		
17 HT-5	13.5A		
18 HT-6	13.5A		
19 HT-7	6.8A		
20 L-3 Line #3	7.5A		

4. Start air compressor and verify 80 psig tank pressure.

5. Verify air flow through pump bearing.

6. Verify the air dryer is operating.

7. Verify/adjust pneumatic regulator to valves and controls.

Valve #1, #3	20 psig
Valve #2, #4	20 psig
Louvers	20 psig
Air Cooler doors cylinder	90 psig
Air cooler door tensioner	48 psig (53% of cylinder)
Fan pitch control	20 psig

8. Check zero adjust on Valves #1 and #3 I/P transducers.

9. Verify that fan pitch control operates from 0 to 100%.

10. Verify operation of both fans.

11. Verify operation of louvers.

12. Verify both tanks and both sump vents are free of frozen salt.

CAUTION

A plugged vent can cause a severe pressure difference on the tanks and sumps. The tanks are critical because of their size. Adding salt with no venting can cause an overpressure condition. Removal of salt with no vent will cuase a reduced pressure. The negative allowable pressure of the hot tank is 5 mb. A greater pressure difference will pull the lines away from the insulation.

13. Check level of propane tank and verify sufficient propane for the present test -900 gallons minimum (15%).

14. Check/ignited pilot lights for propane evaporators.

15. Inspect fan and louvers in pump house for proper operation. Set fan thermostat to 70oF.

16. Check coolant pump and radiator for leak and proper operation. Record coolant flow.

Cold tank _____
Hot tank _____

17. Verify coolant flow through pump bearing.

18. Pressure transducer checkout:

Check the zero point of the pressure transducers PT-1 and 2. At each transaducer disconnect one lead and put a digital ammeter in series. The reading with zero pressure should be 4 ma. If not, there is an adjusting screw located on the outside of the transducer that will allow adjustment to 4 ma.

19. Turn both pump breakers "on".

20. Clear all personnel from the test area.

21. Verify both pump shafts are free to rotate.

Control Room Setup

1. Verify trace heater circuits are on.

2. Verify control console data system and CRT are on. Verify printer is operating.

3. Verify system salt temperatures are 450oF minimum.

4. Verify all controllers are in manual position.

5. Verify all valves are in their failed position.

NOTE

If any console light is out that should be illuminated PRESS TO TEST bulb first to verify light functions properly. Replace bulb if necessary.

Valve lights are Red - Closed
Green - Full open

Trace heat lights are Red - Off
Green - On

CAUTION

Opening valves #1 and #3 without system operation will cause overfilling the sumps.

CAUTION

Operating valves when they are colder than 430oF can result in bellow damage.

6. Cycle valves #2 and #4, between full open and full closed. Observe operation of limit lights.

7. Verify the two control console recorders are on and verify charts are inking. Record date, time and test number on charts.

8. Verify data printer has adequate paper supply.

9. Record tank and sump levels and compare with previous data.

	Present (in.)	Previous (in.)	Delta
Hot tank	_____	_____	_____
Cold tank	_____	_____	_____
Hot sump	_____	_____	_____
Cold sump	_____	_____	_____

CAUTION

Leakage of valves #1 and #3 can overfill the sump resulting in salt loss.

10. Verify safety equipment in place.

Protective gloves
Fire retardent coveralls
Approved fire extinguishers
Safety belts

11. Annunciator panel checkout:

Depress the TEST switch. The following channels should show a flashing light and the horn alarm should be on; air cooler over and under temperature, heater outlet over temperature, sumps overheight alarms and loss of pneumatic pressure.

NOTE

The pretest checklists of Experiment Setup and Control Room Setup shall be performed every morning prior to a start of a test on throughout a test.

Test Operation

1. Verify all valves from propane tank to heater are open, the evaporator pilot lights are on, and the pressure at the heater inlet is 55 psig ± 5 psi.

2. Verify hot sump is greater than 700°F.

3. Verify Line #1 is greater than 700°F.

4. Place burner switch on the control console to PILOT.

5. Set burner temperature controller to 700°F.

6. Start propane heater. The ON light and TIMER light should be on. The fan motor will purge the system for 110 seconds prior to introduction of pilot flame gas. If IR scanner does not detect a pilot flame within 6 seconds after pilot gas the start sequence will be stopped. When the pilot flame is acheived the PILOT LIGHT will be on. Switch to MAIN FUEL after PILOT LIGHT is on.

CAUTION

No thermocouples are upon the heating coil inside the heater cabin. Temperature of coil will have to be determined by experience.

7. Unlock valve #4 and open to 100% open.

8. Unlock valve #3 and place in neutral position.

9. Start the cold pump 15 minutes after MAIN FUEL was turned on.

10. Monitor cold sump height and line #6 temperature. Open valve #3 when sump level is 12 inches and salt is flowing through line #6. It will take 4-8 minutes to flow through the propane heater.

11. Adjust heater for 1050°F outlet temperature.

12. Turn off trace heater to line #6.

13. Fill the hot tank at a rate of 3MW. This will be a level change in the cold tank of 47 inches per hour. Time will be approximately 2.33 hours. Record valve #4 setting _____.

14. Switch control of valve #3, inlet to cold sump, to automatic. Monitor the salt level of sump to maintain 12± 3 inches.

15. Turn propane heater to 600°F when hot tank is within 10" of the desired level. (6" of desired height of cold tank).

16. Stop filling the hot tank when the cold tank level is less than 7.0 inches. Stop the pump after sump level reaches 6 inches and pump pressure drops.

17. Switch valve #3 to manual mode and open. Use handwheel to secure valve open so that complete drainage of the cold tank can occur.

18. Turn on trace heaters line #6.

19. Turn off propane heater 20 minutes after pump shutdown.

20. Open valve #4 and allow the salt to drain from the heater. Level increase should be approximately 40 inches. Lock valve #4 open to allow complete drainage of line #5 and heater.

21. Record levels.

Hot tank	_____
Cold tank	_____
Hot sump	_____
Cold sump	_____

22. Monitor system for salt leaks.

23. Hold condition for one hour.

24. Verify the air cooler doors and louvers are closed.

25. Verify air cooler has temperature between 450 and 650°F.

26. Unlock valve #1 and place in neutral position.

27. Open valve #2 to 100%.

28. Start hot pump. Verify flow by monitoring air cooler outlet temperature

29. Turn off trace heaters on lines #2 and air cooler.

30. Slowly open valve #2 to achieve a flow rate of 3MW which will be a level change in the cold tank of 47 inches per hour. Record setting of valve #2 ____.

31. Switch control of valve #1 inlet to hot sump to automatic. Monitor the salt level of sump to maintain 23 ± 4 inches.

32. Adjust the air cooler outlet temperature to 550°F as follows:

    a) Open insulation cover and verify open.
    b) Open louvers in 10% increments and note outlet temperature at each increment.
    c) Start fan #1 at minimum pitch.
    d) Increase fan pitch to control temperature.
    e) Start fan #2 at minimum pitch.
    f) Increase fan pitch to control temperature.
    g) When outlet temperature is 550°F, set the fan set point to the equivalent setting and switch Fan #1 and Fan #2 to automatic.

NOTE

If power setting allows Fan #1 to control outlet temperature, Fan #1 only may be used.

33. Turn off fans when salt level in hot tank is 18 inches.

34. Stop pump, when hot tank level is 16 inches.

35. Close louvers and insulation cover.

CAUTION

Overtorquing valve handwheel can bend valve stem and crack valve housing. Close valve handwheel until valve stem stops moving, then an additional 1/2 turn.

36. Switch valve #1 to manual and close. Use handwheel to secure valve.

37. Turn on trace heater for line #2 and air cooler.

38. With valve #2 open allow cooler to drain into sump. Sump level should increase approximately 12 inches.

39. Record levels.

    Hot tank _____
    Cold tank _____
    Hot sump _____
    Cold sump _____

40. Maintain line and air cooler temperature with the trace heaters.

41. Hold conditions over night.

NOTE

Repeat the above procedure including Experiment Setup, and Control Room Setup for two additional cycles. Thus a total of three cycles shall be performed.

42. Place burner switch on the control console to PILOT.

43. Set burner temperature controller to 450°F.

44. Start propane heater. The ON light and TIMER light should be on. The fan motor will purge the system for 110 seconds prior to introduction of pilot flame gas. If IR scanner does not detect a pilot flame within 6 seconds after pilot gas the start sequence will be stopped. When the pilot flame is acheived the PILOT LIGHT will be on. Switch to MAIN FUEL after PILOT LIGHT is on.

CAUTION

No thermocouples are upon the heating coil inside the heater cabin. Temperature of coil will have to be determined by experience.

45. Unlock valve #4 and open to 100% open.

46. Unlock valve #3 and place in neutral position.

47. Start the cold pump 15 minutes after MAIN FUEL was turned on.

48. Turn off trace heater to line #6.

49. Monitor cold sump height and line #6 temperature. Open valve #3 when sump level is 12 inches and salt is flowing through line #6. It will take 4-8 minutes for salt to flow through the heater. Get valve #4 to setting established in step #13.

50. Adjust propane heater for outlet temperature of 1050°F.

51. Transfer one half of the salt from the cold tank to the hot tank. Rate should be 47 inches/hour for the cold tank. Height in the cold tank should be 70 inches.

52. Switch control of valve #3, inlet to cold sump, to automatic. Monitor the salt level of sump to maintain 18 $\pm$ 3 inches.

53. Verify air cooler has temperature between 450 to 650°F.

54. Unlock valve #1 and place in neutral position.

55. Open valve #2.

56. Start hot pump.

57. Turn off trace heaters on line #2 and air cooler.

58. Slowly open valve #2 to setting acheived in step #30. Adjust valve #2 to achieve constant tank levels.

59. Adjust the air cooler outlet temperature to 550°F as follows:

    a) Open insulation cover and verify open.
    b) Open louvers in 10% increments and note outlet temperature at each increment.
    c) Start fan #1 at minimum pitch.
    d) Increase fan pitch to control temperature.
    e) Start fan #2 at minimum pitch.
    f) Increase fan pitch to control temperature.
    g) When outlet temperature is 550°F, set the fan set point to the equivalent setting and switch Fan #1 and Fan #2 to automatic.

NOTE

If power setting allows Fan #1 to control outlet temperature, Fan #1 only may be used.

60. Switch control of valve #1 inlet to hot sump to automatic. Monitor the salt level of sump to maintain 23 $\pm$ 4 inches.

61. Maintain the charge discharge mode for four hours.

62. Switch propane heater to pilot.

63. Stop the cold pump when salt outlet temperature reaches 700°F.

CAUTION

Overtorquing valve handwheel can bend valve stem and crack valve housing. Close valve handwheel until valve stem stops moving, then an additional 1/2 turn.

64. Switch valve #3 to manual mode and close. Use handwheel to secure valve.

65. Turn off propane heater 20 minutes after cold pump shut down.

66. Turn on trace heaters line #6 and air cooler.

67. Open valve #4 and allow the salt to drain from the heater. Level increase should be approximately 40 inches.

68. Stop fans when hot tank level is 18 inches.

69. Stop hot pump when salt level in hot tank is 16 inches.

70. Close louvers and insulation cover.

CAUTION

Overtorquing valve handwheel can bend valve stem and crack valve housing. Close valve handwheel until valve stem stops moving, then an additional 1/2 turn.

71. Switch valve #1 to manual mode and close. Use handwheel to secure valve.

72. Turn on trace heater for line #2 and air cooler.

73. With valve #2 open allow cooler to drain into sump. Sump level should increase approximately 12 inches.

74. Record levels

Hot tank	_____
Cold tank	_____
Hot sump	_____
Cold sump	_____

75. Maintain system temperature with trace heaters.

76. Monitor the sytem for leaks.

NOTE

Repeat this proceedure from step 42 through step 76 including Experiment Setup and Control Room Setup two additional times.

77. Take IR scan of tanks and record with temperature data.

APPENDIX G

APPENDIX G

Daily Test Log

25 Jan Salt melting/load equipment was set up on site. Salt was loaded into melter and heating was started. Equipment problems with new salt melting equipment were worked out in two days.

27 Jan The first batch of molten salt was pumped into the cold tank. Large amounts of water vapor emitted from cold tank foundation.

29 Jan The cold sump was filled. Leakage of valve #3 occurred after it was cycled. Salt leakage, past the valve was arrested by installing the sight glass on the cold sump and maintaining the bubbling system (liquid level gage). The reason why this worked is not known. Salt loading of 79,314 kg (174,000 lbs) was completed. Salt melting/loading equipment was removed from the test site.

30 Jan The system was brought to temperature so that molten salt could be transfered to the hot tank. Pipe hangars were adjusted to the hot settings. A large temperature spike of the initial salt through the propane heater was seen. Chattering of Valves #3 and #4 resulted with salt flow. Valve chatter occurred at the half open position. Water vapor continued to exit from the cold tank foundation. Large amounts of stean and ammonia issued from the open manhole of the hot tank.

31 Jan Incorrect readings of the hot tank liner thermocouples were observed. It was thought that the metals, brick and ammonia created some millivolt potential but this was not proven. Electrical trace heaters inside the hot tank were turned on. Three circuits were bad.

The hot sump was filled from the hot tank in preparation to cycle the salt back into the cold tank. Valve #1 was again cycled but this time stuck open. The hot pump was started but the motor failed in less than two minutes. It was determined that the motor was faulty. Valve #1 was closed as tightly as possible with its hand wheel. Salt continued to flow into the sump and out of the vent, which had a gap between a mating surface of the cover plate and the pump main frame. Bolts of the pump were checked but found to be tight. Insulation was torn from Line #1 (the line between the hot tank and the sump) and an effort to freeze the salt was made by spraying the outside of the line with water. The leakage could not be stopped. efforts to stop the leakage from the vent were eventually successful when a tapered plug was placed into the hole and the salt was frozen by spraying the line with water. Hours of again spraying Line #1 with water finally froze the salt and stopped the leak. A total time of 7 1/2 hours had elasped with a loss of approximately 12,700 kg (28,000 lb.) of salt. Approximately 96,000 kg (21,000 lbs.) of salt covered the sump building floor to a height of .17 m (8 inches).

1 Feb Disassembly of Valve #1 showed a nut and bolt and a piece of insulating brick as the cause of being unable to close the valve.

2 Feb A new motor for the hot pump was installed. A crack in the body of Valve #1 was discovered.

3 Feb The crack in Valve #1 was welded close. Welding was difficult due to salt in the crack. The salt was pumped from the hot sump into the cold tank. The mating surface area of the hot pump which had leaked salt was welded closed.

The plug and seat of Valve #1 were lapped. Thawing of Line #1 was started from the valve location. The trace heaters were turned on and welded torches were used to heat the bottom of the line. As the line was thawed it was insulated and heating continued toward the hot tank.

4 Feb The heating of Line #1 continued.

5 Feb The system was heated to allow transfer of cold tank residual salt into the hot tank. Flow through the heater could not be achieved. It appeared that there was a blockage at the outlet of the propane heater or in the line from the heater to the hot tank (Line #6).

9 Feb Two test ports were welded into Line #6 but no blockage could be found. It was later determined that there were some instrumentation problems which might have given an indication of blockage. This condition did not occur again and was not explained.

10 Feb The cold tank residual salt was pumped into the hot tank.

11 Feb Valve #3 was taken apart and lapped. This valve appeared to have tis seat and plug battered. This valve had been used on the salt receiver test.

12 Feb Salt melting was completed on line #1 and the salt was transferred into the cold tank. The hot tank was totally drained.

15 Feb Valve #3 leaked which caused some salt to leak out of the cold sump. Salt froze in the vent. Valve #1 was lapped. Efforts to remove its seat were unsuccessful.

16 Feb Salt was transferred to the hot tank at about 371°C (700°F).

17 Feb Valve #3 was still leaking. Salt was frozen in the sump vent. Effort to transfer salt back into the hot tank was stopped because of what appeared to be blockage in the heater. However, it was found that the sump level readout was sticking midscale and that the zero point on the pump outlet pressure measurement had shifted. Salt was transfered into the hot tank at about 371°C (700°F).

18 Feb Salt in the cold sump was pumped to the hot tank without any line blockage of insturmentation problems. Salt was transferred to the cold tank. Temperature of salt into cold tank had not been cooled since hot tnak temperatures were approximately 315°C (600°F). Cold tank temperatures were raised in order to dry the foundation. Salt was transferred to the hot tank at approximately 400°C (750°F). The cold tank was reduced to minimum level. Valve #4 did not fully open. Valve #1 was leaking.

19 Feb The salt in the hot sump was pumped to the cold tank to allow room for the salt leaking past Valve #1. System repairs were peformed.

20 Feb Salt in the hot sump was pumped to the cold tank.

21 Feb Salt in the hot sump was pumped to the cold tank.

22 Feb The salt in the hot sump was pumped to the cold tank. Salt from the cold sump was pumped into the hot tank. The hot tank was discharged and after one hour, charging of the hot tank was started. The inlet temperature to the hot tank was raised to 426°C (800°F). Valve #4 developed an extreme leak so the dual transfer was stopped. The belllows of Valve #4 had cracked. The plug stem and bellows assembly was replaced with a used one taken from the molten salt receiver. Valve #4 had a severe chatter at midrange and operating the valve at reduced or high flows was necessary to eliminate the chatter. Salt was transferred from the cold tank to the hot tank with the temperature reaching 504°C (940°F).

24 Feb Valve #3 was rebuilt with new seat.

25 Feb Failure of Line #1 trace heaters occurred early in the morning. Salt at the valve and an adjacent portion of the line had frozen. One circuit which had two of the three heating elements became electrically open. Heating of the line with the welding torches failed to establish flow before the line froze. The second circuit failed because salt penetrated a crack in the sheathing of the heater. Reason for failure of the first circuit was never determined, since after all electrical checks were performed it was found normal. It did not fail for the remainder for the test. Valve #1 was cut out of the system and sent to Denver for rebuilding.

8 March Two trace heaters circuits on the air cooler failed open.

9 March Valve #1 was welded back into the line. The heat trace circuits on Line #1 were turned on.

10 March The vertical leg of Line #1 leading out of the hot tank remained frozen. Heating this line section with a torch was necessary to thaw the salt.

Salt was transferred into the cold tank and then back to the hot tank at a maximum temperature of 566°C (1040°F). The temperature of salt into the cold tank was 316°C (600°F).

12 March Salt was again cycled from the hot tank into the cold tank and back to the hot tank. An effort to control the salt temperature by the flow rate resulted in a salt peak temperature of 593°C (100°F).

15 March The orifice in the burner was increased to allow full capacity of the heater which allowed the design flow rate to be achieved. The salt was cycled from the hot tank to the cold tank and back to the hot tank. This was considered the first transfer of procedure #4. Valve #4 would not fully open.

16 March It was necessary to take Valve #4 apart and tighten the stem guide. Draining the hot tank and refilling the hot tank accomplished the second cycle of procedure #3. Control of the burner allowed for a rapid increase of the salt outlet temperature to 566°C (1050°F).

17 March The salt was transferred from the hot tank into the cold tank. Charging the hot tank was tried but there was blockage through the heater which appeared to be at the heater inlet. Heating this area with the welding torch did not indicate any frozen salt. Salt flow through the heater was achieved. Severe leakage at Valve #4 required stopping the charge of the hot tank. The bellows were broken on Valve #4. New bellows and stem were added and the valve guide was reassembled and the completion of charging the hot tank was accomplished. This was the third cycle of procedure #4.

18 March The first simultaneous charge/discharge cycle of procedure #4 was accomplished. Salt again was stored in the hot tank. Salt inlet temperature to the cold tank was raised to 343°C (650°F) to dry the foundation.

19 March A discharge/charge cycle was stopped when a freeze occured at the propane heater inlet. Heating the inlet section of pipe with a welding trouch was necessary to thaw the frozen salt. Dual transfer was established. The outlet temperature of the salt from the heater had a temperature spike of 621°C (1150°F) due to a very low flow rate through the heater, which was expected. Charging of the hot tank was completed at a low flow rate (1/2 of normal). The drain back from the heater was unusually slow. The normal time was approximately 20 minutes but this time it took 12 hours. A loss of approximately 2,000 pounds of salt occurred through the valve stem. The power into the cold tank was reduced to 11.035 kW. A 9 kW heater was added to the foundaion coolant water. Water flow was established. Prior to this time water was not pumped through the foundation.

20 March The cause of the low flow through the heater and the long drain back time was due to a failure of Valve #4. The valve stem broke allowing the valve plug to be detached. Due to all the failures of Valve #4 and the consistent chatter which occurred (especially at starting conditions) it was decided to place an orifice plate in the valve and eliminated the stem and bellows.

22 March Valve #4 was modified with an orifice plate. One fuse of the 480 V 3 phase trace heaters burned out over the weekend. The cause could not be determined.

23 March The same fuse again burned out and still the cause could not be determined. The hot tank discharge was started and then dual discharge was initiated. The pumps were stopped because the charge flow rate was too large. A smaller orifice plate was made and installed at Valve #4. Charging of the hot tank was completed. The fuse replace that morning again blew and again the cause could not be determined. Three of the nine trance heaters circuits were removed and two of them added back over the following week, with no more failures. It was assumed that the third circuit had caused the problems.

24 March The hot tank was discharged for one hour and twenty minutes. Dual transfer was inititiated but it was found that blockage again occurred at the heater inlet. After this area was heated with a welding torch flow was established. The charge/discharge of the hot tank was performed for one hour. The hot tank charge took one hour 23 minutes. This was the first cycle of procedure #8. The history of the hot tank heater was that 3 of the 7 heater circuits were always faulty. The other 4 circuits had now failed.

25 March The hot tank discharged for one hour. Dual transfer was run for one hour. The hot tank charge took 1 hour, 43 minutes. This accomplished the second cycle of procedure #8. A trace heater was added to the inlet secion of the propane heater to eliminate the freezing problem.

26 March The hot tank was discharged for 1 hour and 26 minutes. Dual transfer was run for one hour. The hot tank was charged until the cold tank was empty. This test accomplished the third cycle of procedure #8.

30 March The hot tank was discharged for 1 hour and 10 minutes. Dual transfer was run for one hour. The hot tank was charged for 1 hour and 46 minutes. Due to high wind the pilot lights of the propane evaporators were blown out. This resulted in a drop of the salt oulet temperature of the heater to 500°C (930°F). This was the fourth cycle of procedure #8.

31 March The hot tank was discharged for 1 hour and 32 minutes. Dual transfer was operated for one hour. The hot tank was charged until the cold tank was empty. This was the fifth cycle of procedure #8. The first transient was started at the end of the cycle test.

1 April A 15 kW heater was added to the foundation coolant loop. This made a total of 24 kW. The temperature set point of the loop was 199°C (246°F). Initially the power was on constantly. Eventually the heater duty cycle dropped to approximately fifty percent.

2 April It was a windy afternoon, resuling in higher than normal tank heat losses.

5 April End of transient cooldown test #1 resulted with transfer of salt to the cold tank and back to the hot tank. This was done to heat the hot tank which started the second transient cooldown.

7 April It was very windy afternoon. Temporary fibrous insulation was added to the exterior of the tank foundation to reduce the heat loss. The insulation was covered with a plastic film. The bottom surface of the hot tank was also insulated. The end of cooldown test #2 resulted when the salt was cycled and reheated. The start of the third cooldown started at the end of the heating cycle. The salt inlet to the cold tank was lowered to 288°C (550°F). The foundation was drying out.

12 April A very windy afternoon occurred again, producing excessive heat loss.

13 April The third cooldown transient was ended with the initiatiion of the second set of cycling tests. The hot tank was discharged for 1 hour and 43 minutes. Charge/discharge occurred for 1 hour and 6 minutes. The hot tank was charged for 1 hour and 27 minutes.

14 April The hot tank was discharged for 1 hour and 39 minutes. Charge/discharge lasted for one hour. The hot tank was then charged for one and one half hours. This was the second cycle of the second cyclic test. two trace heaters in the air cooler failed.

15 April The hot tank was discharged for one hour and 40 minutes. Dual transfer lasted for one hour. The hot tank charge took one hour and 20 minutes. This was the start of the third cycle of the second cyclic test.

16 April The cyclic test ended with the transfer of all the hot tank salt into the cold tank at 288°C (550°F). The hot sump was pumped down such that the salt was below the pump housing. The cold pump was full.

APPENDIX H

THERMAL ANALYSIS OF TANKS

A COLD TANK

I. The power into the cold tank was by the following electrical circuits.

Internal Heater Resistances	17.9, 44.7, 44.5 and 87.2 ohms
External Heater Resistances	31.4 ohms

Nominal voltage 277 Vac, Measured voltage of 279 to 274 was seen over weeks of testing. No bias was seen in the voltage from the ideal value.

Power	External Heaters	8595 Watts
	Internal Heater	2440 Watts
	Total	11035 Watts

II. Thermal resistance at sheathing with the environment convection and radiation resistance per square foot.

A. $\bar{h}_{Radiation} = \sigma \varepsilon \left(\frac{T^4 - T^4}{\Delta T}\right)$

$= 0.1714 \times 10^{-8} \times 0.83 \times \left(\frac{525^4 - 515^4}{525 - 515}\right) = 0.80$ Btu/hr-ft^2-°F

B. $\bar{h}_{Convection}$ (Btu/h-ft^2-°F)

Gr for L = 12 $\Delta T = 20$ Air Film = 68°F

Gr = 5.665×10^{10} Film is turbulent

Vertical Turbulent Physical Properties for Air

$\bar{h}_c = \frac{K}{L} * 0.13 (GrPr)^{1/3}$

$= 0.51$

Horizontal Heated Plate Facing Up

$\bar{h}_c = \frac{K}{L} \times 0.14 (GrPr)^{1/3}$

$= 0.54$

C. Combined Radiation Convection (Btu/h-ft^2-°F)

$\bar{h}$ = 1.31 Vertical

1.34 Horizontal

III. Heat loss through foundation was evaluated radially due to temperature gradient within the foundation. Heat losses to the castable and the concrete were evaluated separately to determine possible edge effect. It was realized that the calculated heat loss to the castable can be questioned due to the known placement of the thermocouple. The placement of the thermocouples in the concrete are not as critical because of the greater thermal resistance to the molten salt.

A. Resistance salt to castable T/C (unit area)

Salt Film $h = \frac{K}{L}\ 0.27\,(GrPr)^{1/4}$ (Horizontal - Hot Plate Facing Down)

$= 1.3$ Btu/h-ft^2-°F

$$\bar{K}_{Castable} = \frac{KA}{L} = \frac{0.14x1}{0.625/12} = 2.688 \text{ Btu/h-ft}^2\text{°F}$$

$$\bar{K}_{Steel\ Bottom} = \frac{KA}{L} = \frac{25}{0.25/12} = 1200 \text{ Btu/h-ft}^2\text{°F}$$

$$\bar{K}_{Gap} = 500 \text{ (Radiation + Conduction)}$$

$$U_{Salt\text{-}Castable} = \frac{1}{\Sigma \frac{1}{\bar{K}}} = 0.872 \text{ Btu/h-ft}^2\text{-°F}$$

B. Resistance salt to concrete T/C (unit area)

Modify above by

$$\bar{K}_{Castable} = \frac{KA}{L} = \frac{0.14x1}{15/12} = 0.112 \text{ Btu/h-ft}^2\text{°F}$$

$$\bar{K}_{Concrete} = \frac{KA}{L} = \frac{0.54}{0.625/12} = 10.3 \text{ Btu/h-ft}^2\text{°F}$$

$$U_{Salt\text{-}Concrete} = \frac{1}{\Sigma \left(\frac{1}{\bar{K}}\right)} = 0.102 \text{ Btu/h-ft}^2\text{-°F}$$

C. Calculated heat loss through bottom.

	Center	3 ft Radius	6 ft Radius
T_{Salt} (°F)	640.8	640.8	640.8
$T_{Castable}$ (°F)	590.1	591.8	567.0
$T_{Concrete}$ (°F)	257.9	260.2	224.1
Q to Castable (Btu/h-ft^2)	44.5	42.7	64.5
Q to Concrete (Btu/h-ft^2)	39.1	38.9	42.5

Increased loss at 6 ft radius is due to the edge effect.

Approximating the heat loss profile from the tank bottom was as follows:

Q_{Loss} = 39 Btu/h-ft^2 for 11.02 dia

plus 60 Btu/h-ft^2 for 11.02 to 13.02 dia

$Q = 3720 + 2266 = 5986$ Btu/h

Without Edge Effect

$$Q = 39 \times 13.02^2 \frac{\pi}{4} = 5192 \text{ Btu/h}$$

Edge Effect is Difference of Last Two Heat Losses

$$Q_{Edge} = 5986 - 5192 = 794 \text{ Btu/h}$$

Percent Increase of Edge $= \frac{794}{5192} = 15\%$

D. Analytical evaluation of edge loss.

Edge conduction shape factor. For two-plane section and edge section (Principles of Heat Transfer, Frank Kreith, Jan 1962, pg 83)
$Q = SK(\Delta T)$

$$S = \frac{a\ell}{\Delta X} + \frac{b\ell}{\Delta X} + 0.54\ell$$

An approximate shape factor was derived by modifying the above equation to a disk to

$$S = \frac{\text{Area Disk}}{\Delta X} + 0.54\,\pi D \text{ (Effective area/thickness)}$$

thus;

dia Base ℄ 13.02 ft (Area = 133.1 ft^2)

$$S = \frac{\pi/4\ 13.02^2}{15/12} + 0.54\,\pi\ 13.02 = 133.1 + 22.1 = 155.2$$

Effective Area = S x thickness = 160.8

$$\text{Percent Increase} = \frac{160.8 - 133.1}{133.1} = 21\%$$

Since some of the concrete exterior is insulated the edge loss of by the data is less than analyzed by a reasonable value. An edge loss of 15 percent was used. Thus the foundation heat loss is taken as 5192 with the 794 being a portion of the lower ring loss. There was no way to directly confirm the loss from the tank bottom. Evaluation of the hot tank foundation added confidence to the foundation effective conductivity.

E. Penetration Losses

1. Electrical heating elements

Since the heater penetrations through the insulation are surrounded by an open cavity their heat generation is lost from the system.

External heaters; 20 penetrations - 15 in. long each; 10 heaters - 38 ft long

$$\text{Percent Loss} = \frac{20 \times 15/12}{38 \times 10} \times 100 = 6.6\%$$

$$Q = 0.066 \times 8595 \times 3.413 = 1907 \text{ Btu/h}$$

Internal heaters; 6 penetrations - 2 ft long each; 3 heaters - 47 ft long

$$\text{Percent Loss} = \frac{6 \times 2}{47 \times 3} = 8.5\%$$

$$Q = 0.085 \times 2440 \times 3.413 = 707 \text{ Btu/h}$$

2. Rakes

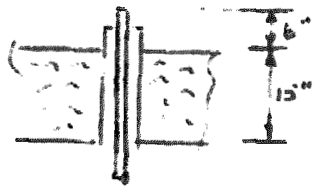

Conduction up to 1¼ in. ϕ pipe and 1 in. ϕ tube then convection from surface

$$\bar{K}_{pipe} * KA/L = \frac{K \pi Dt}{L} = \frac{25 \pi \frac{1.75}{12} \frac{0.145}{12}}{18/12}$$

$$= 0.092 \text{ Btu/h-°F}$$

$$\bar{K}_{tube} = \frac{K \pi Dt}{L} = \frac{25 \pi \frac{1.0}{12} \frac{0.065}{12}}{18/12}$$

$$= 0.024 \text{ Btu/h-°F}$$

These in Parallel

$$hA = h\pi DL = 1.3 \pi 1.9/12 \times 6/12 = 0.35 \text{ Btu/h-°F}$$

$$U = 1/\left(\frac{1}{hA} + \frac{1}{\Sigma K}\right) = 0.087 \text{ Btu/h-°F}$$

Heat Loss

$$Q = U\Delta T = 0.087 (634 - 37.8)$$

$$= 53 \text{ Btu/h each}$$

3. Vent

Conduction up 1½" ϕ pipe then convection from 8" long surface.

$$\bar{K}_{pipe} = \frac{K\pi Dt}{L} = 25\pi\frac{1.75}{12}\frac{0.145}{12} \Big/ 18/12$$

$$= 0.092 \text{ Btu/h}$$

$$hA = h\pi DL = 1.3\pi\frac{1.9}{12} \times \frac{8}{12}$$

$$= 0.43 \text{ Btu/h}$$

$$U = 1/\left(\frac{1}{hA} + \frac{1}{K}\right) = 0.077 \text{ Btu/h-°F}$$

$$Q = U\Delta T = 0.077\ (641 - 37.8)$$

$$= 46 \text{ Btu/h}$$

4. Manhole

The insulation on the manhole was less than 15 in.

$$Q = \frac{KA}{L}\Delta T \ ; \ \left(A = \frac{D^2}{4} + \pi Dh\right)$$

$$= \frac{0.042}{4/12}\left(\pi\left(\frac{20}{12}\right)^2\frac{1}{4} + \pi\frac{20}{12}\frac{4}{12}\right)(641 - 37.8)$$

$$= 298 \text{ Btu/h}$$

5. Internal heater penetration

Conduction up 1½ in. ϕ pipe through 4 in. insulation in the 2-ft convection area.

$$K_{cond} = \frac{KA}{L} = \frac{K\pi Dt}{L}$$

$$= 25\ \pi\ \frac{1.75}{12} \times \frac{0.145}{12} \Big/ \frac{4}{12}$$

$$= 0.415 \text{ Btu/h-°F}$$

Fin $\bar{K}$ finite length no end loss

$$\bar{K} = \sqrt{Ph\ KA}\ \tanh\left(\frac{hP}{KA}L\right)$$

$$= \sqrt{\pi\frac{1.9}{12}\ 1.3 \times 25\pi\frac{1.75}{12} \times \frac{0.145}{12}}\ \tanh\left(\frac{1.3\pi 1.9/12}{2\pi 1.75/12\ 0.145/12}\right)^{1/2}$$

$$= 0.31$$

$$U = 1/\Sigma\frac{1}{K}$$

$$= 0.178 \text{ Btu/h-°F}$$

$$Q = U\Delta T$$
$$= 0.178\ (641 - 37.8)$$
$$= 107\ \text{Btu/h}$$

6. Increase loss of rakes, vent, and heater penetration by 20% to account for internal convection in pipes.

F. Using the sheathing temperatures, atmosphere temperature, and the calculated film coefficient, the heat loss from the exterior of the tank can be calculated. The tank was divided into the following areas, due to temperature difference.

Lower 18 in. of the wall: $A = \pi D\ell = \pi 15 \frac{18}{12} = 70.7\ \text{ft}^2$

Wall: $A = \pi D\ell = \pi 15\ (12.74 - 1.5 - 1.0)$
$= 482.5\ \text{ft}^2$

Upper 12 in. of wall + outer 12 in. of roof: $A = \pi D\ell + \pi/4\ (D^2 - D^2)\ 1/\cos\theta$
$= \pi 15 \times 1 + \pi/4\ (15^2 - 13^2)/0.866$
$= 47.1 + 50.8 = 97.9\ \text{ft}^2$

Roof: $A = \pi/4\ (D^2)\ 1/\cos\theta = \pi/4\ (13)^2/.865$
$= 153.3\ \text{ft}^2$

The tank diameter of approximately 15 ft is greater than the theoretical diameter and probably is due to gaps in the insulation. The average temperatures associated with these areas was a collection of the T/C data and the IR scan data.

Lower Wall	112.4 (T/C ave) - 12 (IR Scan) = 100.4°F
Wall	74.6 (T/C ave) °F
Upper Wall	69.6 (T/C ave) + 5.5 (IR Scan) = 75.1°F
Roof Outer Edge	Same as upper wall from IR Scan = 75.1°F
Roof	59.4°F (T/C ave)

Sheathing heat loss by convection and radiation:

Lower Wall	$Q = hA\Delta T = 1.31\ (70.7)(100.4 - 37.8)$	= 5,798
Wall	$Q = hA\Delta T = 1.31\ (482.5)(74.6 - 37.8)$	= 23,260
Upper Wall	$Q = hA\Delta T = 1.31\ (47.1)(75.1 - 37.8)$	= 2,301
Roof Edge	$Q = hA\Delta T = 1.34\ (50.8)(75.1 - 37.8)$	= 2,539
Roof	$Q = hA\Delta T = 1.34\ (153.3)(59.4 - 37.8)$	= 4,437
		38,335

G. Adjustment of film coefficient achieved the total loss of 37663 Btu/h. Error can exist in surface emittance and the fact that the design point was at the coldest atmosphere temperature whereas the heat loss was based over eight hours. Adjusted losses were:
Heat loss of foundations, heaters, and penetrations remain as calculated.

Lower wall	4,424
Wall	17,750
Upper wall	1,755
Roof edge	1,937
Roof	3,387

H. The energy loss from the lower wall was divided into the wall loss which is consistent with the loss of the remaining wall and the heat loss attributed to the lower tank ring and foundation edge. Thus 4424 Btu/h becomes 2602 Btu/h for the wall loss and 1822 Btu/h for the lower ring and foundation edge.

Taking the upper wall and roof edge heat losses and dividing them similarly as the above the result is a heat of 1732 Btu/h for the wall, 1122 Btu/h for the roof, and 838 Btu/h for the upper ring.

I. The heat loss for the cold tank is:

Area	Btu/h
Foundation	5,190
Heaters	2,614
Penetrations	605
Wall	22,084
Upper Ring	838
Lower Ring & Foundation Edge	1,822
Roof	4,509

B HOT TANK

I. Heat loss was calculated by the heat capacity change.

Salt Mass	117,403 lb
Heat Capacity	0.366 Btu/lb-°F
Temp Rate of Change	1.54°F/h Avg of All T/C on Rakes in Salt.
Heat Loss	66,226 Btu/h

II. Thermal resistance at the sheathing to the environment was taken at the same values as derived for the cold tank.

$\bar{h}$ = 1.31 Btu/h-°F-ft^2 (vertical)
1.34 Btu/h-°F-ft^2 (horizontal)

III. Heat Loss Through Foundation

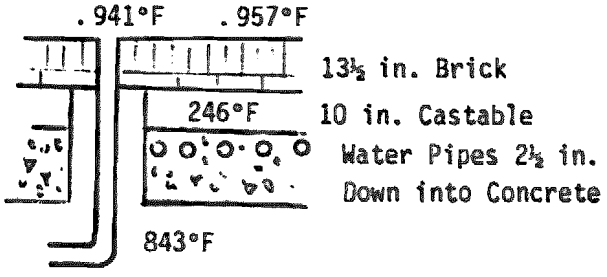

A. Heat Loss Down the Pipe

$$\bar{K}_{Pipe} = \frac{KA}{L} = \frac{10\ 4.5/12\ \pi.12/12}{(13.5+10+10)/12} = 0.04 \text{ Btu/h-°F}$$

$$\bar{K}_{Salt} = \frac{KA}{L} = \frac{0.30\ (\frac{4.25}{12})^2\ \pi/4}{33.5/12} = 0.01 \text{ Btu/h-°F}$$

$U = \Sigma K = 0.05$ Btu/h-°F

$Q = U\Delta T = 0.05\ (941 - 843) = 5$ Btu/h

The heat loss down the outlet pipe is insignificant. Experience from the test would indicate that no significant convection occurs.

B. Thermal Resistance of Foundation (Unit Area)

$$\bar{K}_{Brick} = \frac{KA}{L} = \frac{0.125}{13.5/12} = 0.111 \text{ Btu/h-ft}^2\text{-°F}$$

$$\bar{K}_{Castable\ T/C} = \frac{KA}{L} = \frac{1.68/12}{0.625/12} = 2.69 \text{ Btu/h-ft}^2\text{-°F}$$

$$\bar{U}_{Salt\ to\ castable\ T/C}\ 1/\Sigma\ \frac{1}{K} = 0.106 \text{ Btu/h-ft}^2\text{-°F}$$

$$\bar{K}_{Castable} = \frac{KA}{L} = \frac{1.68/12}{10/12} = 0.168 \text{ Btu/h-ft}^2\text{-°F}$$

$$\bar{K}_{\text{Concrete T/C}} = \frac{KA}{L} = \frac{0.54}{0.625/12} = 10.37 \text{ Btu/h-ft}^2\text{-°F}$$

$$\bar{U}_{\text{Salt to concrete T/C}} = 1/\Sigma \frac{1}{K} = 0.066 \text{ Btu/h-ft}^2\text{-°F}$$

$$\bar{K}_{\text{T/C Castable}} = \frac{KA}{L} = \frac{1.68/12}{(10-0.625)/12} = 0.1792 \text{ Btu/h-ft}^2\text{-°F}$$

$$\bar{U}_{\text{T/C Castable-Concrete}} = 1/\Sigma \frac{1}{K} = 0.1762/\text{h-ft}^2\text{-°F}$$

C. Heat loss through the foundation

Section - Radius (in.)	0-20	20-45	45-60	60-75
Area (ft)	8.73	35.4	34.4	44.2
$\Delta T_{\text{Salt-Castable T/C}}$ (°F)	460	488	557	
$Q_{\text{into Castable}}$ (Btu/h)	428	1841	2040	
$\Delta T_{\text{Salt-Concrete T/C}}$ (°F)	658	688	710	
$Q_{\text{into Concrete}}$ (Btu/h)	379	1610	1610	
$\Delta T_{\text{Castable-Concrete}}$(°F)	199	203	151	98
$Q_{\text{Castable-Concrete}}$ (Btu/h)	707	3050	3372	5109

Summation
$Q_{\text{into Castable}}$ = 4309 Btu/h
$Q_{\text{into Concrete}}$ = 3599 Btu/h
$Q_{\text{Castable-Concrete}}$ = 3248 Btu/h

To make the heat loss consistent throughout the foundation, the conductance of the castable insulation has to be increased. The heat loss through the foundation was based on the heat loss into the castable insulation.

Edge effect same formula as on page 3.

A = 78.5 ft^2 (10 ft dia)
S = 86.78
Effective Area = 97.63
Percent Increase = 24%

Due to the insulation on the exterior of the concrete foundation, the edge loss was assumed at 20 percent, (860 Btu/h). Thus, the total loss from the foundation was 5169 Btu/h.

D. Penetration Losses

1. Manhole

The manhole was similar to the cold tank except for temperature difference.

Thus $Q = Q \frac{\Delta T_{hot}}{\Delta T_{cold}} = 298 = \frac{318-35}{641-37.8} = 140$ Btu/h

2. Vent

Ratio the vent loss from the cold tank by the same temperature difference thus loss is 20 Btu/h.

Total penetration loss is 160 Btu/h.

E. Convection Areas

Lower Ring $A = \pi D\ell = \pi \frac{151.6}{12} \times 1 = = 39.7$ ft^2

Wall $A = \pi D\ell = \pi \frac{151.6}{12} \times (16.95 - 1) = 633.0$ ft^2

Upper Wall $A = \pi D\ell = \pi \frac{159.6}{12} \times 3.64 = 152.1$ ft^2

Upper Ring $A = \pi D\ell = \pi \frac{159.6}{12} \times 10/12 = 34.8$ ft^2

Attic Wall $A = \pi D\ell + = \pi \frac{159.6}{12} \times 2.19 = 91.5$ ft^2

Attic Roff $A = \frac{\pi D^2}{4 \cos \theta} = \pi(\frac{159.6}{12})^2 \frac{1}{4 \cos 30^\circ} = 160.5$ ft^2

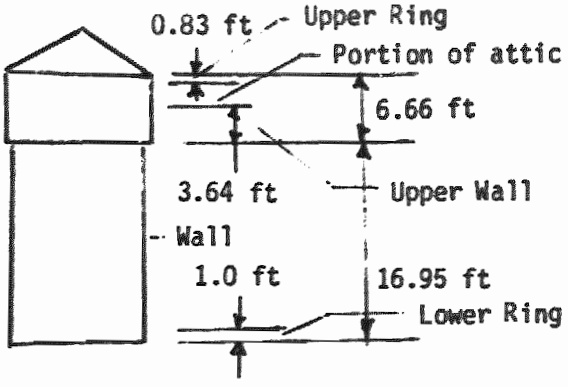

The upper section of the tank wall has 6 in. external insulation and the 13.5 in. of brick, which is above the suspended deck.

F. Temperature of Area

Location	T/C Average	IR Scan Adj	Temp
Lower Ring	123		123
Wall	104.9	-10	94.9
Upper Wall	48.9		48.9
Upper Ring	48.9	+10	59.9
Attic Wall	48.9		48.9
Attic Roof	43.4		43.4

G. Convection Heat Loss (Btu/h)

Lower Ring	$Q = hA\Delta T = 1.31\ (39.7)\ (123 - 35.4)$	= 4,556
Wall	$Q = hA\Delta T = 1.31\ (633.2)\ (104.9 - 10 - 35.4)$	= 49,342
Upper Wall	$Q = hA\Delta T = 1.31\ (152.1)\ (48.9 - 35.4)$	= 2,690
Upper Ring	$Q = hA\Delta T = 1.31\ (34.8)\ (48.9 + 10 - 35.4)$	= 1,071
Attic Wall	$Q = hA\Delta T = 1.31\ (91.5)\ (48.9 - 35.4)$	= 1,618
Attic Roof	$+ hA\Delta T = 1.34\ (160.5)\ (43.4 - 35.4)$	= 1,721

Total Convection Loss 60,998

H. Convection loss to agree with the known energy loss of 66,226 minus the foundation and penetrations loss is 60,897

	Adjusted loss
Lower ring	4,548
Wall	49,260
Upper wall	2,685
Upper ring	1,069
Attic wall	1,615
Attic roof	1,718

I. The energy loss from the lower wall was divided into the wall loss which is consistent with the remaining wall and the heat loss attributed to the lower ring and foundation edge loss. Thus 4548 Btu/h becomes 3089 Btu/h for the wall loss and 1459 Btu/h for the lower ring and foundation.

Using the same technique for the upper ring 1069 Btu/h becomes 455 Btu/h for the ring and 615 Btu/h for the attic wall.

J. The heat loss for the hot tank is:

Area	Btu/h
Foundation	5,169
Penetrations	160
Lower Ring	1,459
Wall	52,349
Upper Wall	2,685
Upper Ring	455
Attic	3,948

C SYMBOLS

K - Thermal Conductivity
$\bar{K}$ - Thermal Conductance
σ - Stefan-Boltzmann Constant
ϵ - Emissivity
A - Area
L - Length
Gr - Grashof Number
Pr - Prandtl Number
U - Overall Conductance
ℓ - Length
ΔX - Insulation Thickness
D - Diameter
a - Length
b - Length
t - Thickness
P - Perimeter
ΔT - Temperature Difference
S - Shape Factor
Q - Heat Loss

APPENDIX I

Effect of Material Creep on Fatigue Life of Technigaz I-800 Corrugated Liner Molten Salt Storage

The evaluation of the feasibility of utilizing the Technigaz cross-corrugated liner for the containment of molten nitrate salt mixtures was intended to complement the previous test and analysis work performed by Technigaz to qualify the liner for containment service. Particular emphasis was placed upon those areas that were substantially different from the previous applications.

Liner qualification procedures included:

- Strain and pressure fatigue testing at room and service temperature on liner elements fabricated on industrial tooling from the I-800 alloy.

- Cyclic pressure fatigue testing under molten salt conditions in accordance with recognized fatigue testing codes which accounts for rapid strain and pressure cycling. Great care was taken to duplicate the full structure and simulate actual service conditions and construction tolerances in accomplishing this test program.

As defined in classical material analysis, creep is a plastic deformation of a material caused by stresses existing in a structure over an extended period of time. The rate of creep increases with increasing temperature and material stress. The creep rate of the of the I-800 material at elevated temperatures is quite well documented.

However, classical analysis does not apply for this liner which behaves as an elastoplastic material. The exact level of stress existing in the corrugations and corrugation intersections (called "knots") is not known with sufficient accuracy to lead to any firm analytical predictions. This lack of knowledge is due to the complex geometry of the element, and the dependence upon fabrication techniques and their effect on the metal sheet.

Due to these reasons, evaluation of the liner's performance has been predominately carried out by experimental and empirical methods. For each new application we conduct new tests relying on the previous tests and actual performance to the maximum extent possible. We can therefore make the following observations.

- The creep rate in the maximum loaded areas of the knot is lower than that given by the general documentation for a given level of stress, as these areas receive a greater degree of cold working during liner fabrication and cold working enhances the material's resistance to creep.

- In creep, the material is subjected to a plastic deformation which modifies the shape of the maximum stressed areas slightly. Thus the initial creep lowers the local stress level thereby causing a lower level of creep and so on.

We therefore have compensated for creep effects by ascertaining that we have such large margins of safety in fatigue life that the effects of creep become secondary considerations.

Test Results

Elemental Tests

Elemental liner testing was carried out at levels of pressure (0 to 44 psi) about 1.34 more than that found in the Solar 100 thermal energy storage. Liner elements lasted up to 150,000 cycles before testing was stopped with no leakage and no surface cracking. This affords a large safety factor as compared to the 10,950 cycles which correspond to 30 years of daily fill and drain cycles. These results confirmed that the large factors of safety to which we are accustomed in other applications and materials are present with I-800.

It should be noted that we have another factor of a safety on top of these 15 lifetimes. For testing ease we have adopted the criterion that failure occurs when a crack is detected rather than when a leak is generated. This is contrary to the recognized fatigue testing codes, but it is rather conservative.

Previous testing has shown that ten times the number of cycles found to initiate a surface crack in the liner are required for that crack to propagate through the thickness of the liner and cause a leak. This is in addition to the 15 or more times proven by our recent high temperature tests.

Full Scale Tests

The results of the cyclic pressure fatigue test, conducted in accordance with ASME Pressure Vessel Code, Appendix II, Article II-100, showed no cracks of the tight internal liner. These were conducted at a cyclic pressure level of 1.34 times the maximum service pressure, and with 1.73 times the number of cycles encountered over the 30 years service life.

The ASME procedure defines specific factors to be applied to the design service loads and cycles. These factors are intended to account for accelerated testing or material variables that are not accurately simulated by the test. By making a conservative use of the test procedure to define loads and number of cycles we have accounted for unknowns. This has also been our testing approach in all previous applications.

It should be noted that this test did not establish the structure fatigue life, as no failures had occured before reaching the required number of cycles. From the elementary tests though, we can conclude that structure fatigue life at the higher pressure levels is far beyond the cycles tested.

Thus a considerable margin of safety is present before considering the effects of creep upon element fatigue properties. We are well aware that differences in the liner element geometry can cause a difference in fatigue performance. For example, the first liner elements manufactured for test purposes were formed on wood prototype tools. Fatigue life of elements formed with these prototype tools was nevertheless adequate and within the code procedure. When elements fabricated by industrial tooling were later tested for comparison, an increase in fatigue life of about two was accomplished.

Thus, if substantial creep were to occur in the liner under molten salt service conditions, we may expect a decrease in the fatigue life of the liner. However, the fatigue factors of safety are so great in this application that a reduction in the fatigue life will be of no consequence.

Scenarios of Projected Failure

The consequences of a failure of the tight liner due to material creep or corrosion affecting fatigue properties were also examined. The design concept of the molten salt tight internal liner system is to separate the containment, or tightness function of the system from the mechanical, load bearing function. Thus, the liner is "integrated" to the supporting structure, but the stressed supporting structure

is not subjected to the extreme temperatures of the contained liquid.

If the creep rate of I-800 is such that it will result in a significant distortion of the liner with time, we doubt that any real failure (salt leakage) will occur.

The liner has been subjected to static pressures as high as 390 psi where the corrugations have been substantially deformed. No cracks or leaks were generated by these pressures. But even if we assume that creep will drastically reduce the fatigue life so that not only cracks but leakage will occur we are reasonably certain of the following failure mode.

- The bottom of the tank where the creep-fatigue problem might occur will experience pin hole leaks which will wet the foil protection surface. If these leaks are not detected they will progressively wet the bottom internal brick insulation. Tests have shown that the insulation being compatible with molten salt will not be mechanically affected, but insulation conductivity will increase causing a slight increase in carbon steel shell temperature.

- Even if complete wetting of the bottom occurs, the brick not acting as a barrier to further salt penetration, eventually the lower elements of the outer cylindrical carbon steel sides will reach a temperature beyond the material design limits, at which time remedial action will have to be taken.

This whole failure process cannot occur suddenly and will take weeks, months or years, during which the thermocouples, the leak detection system or regular inspection would have given adequate warning.

There can be no catastrophic failure of the containment system when fitted with the tight corrugated liner and associated internal insulation system.

High Temperature Liner Service Experience

In addition to the recent development program associated with the subsystem research experiment, the Technigaz corrugated liner was used to line a chemical reactor at the Humble Refinery in Baytown, Texas for twelve years. While the process is proprietary to Exxon, we do know that the reactor operated at 650 degrees F with yearly regeneration cycles up to 1000 degrees F. The maximum pressure on the liner was 48.5 psi. Liner material was Inconel 600. No problems attributed to creep were identified by the time the Humble process was modified and the reactor was no longer necessary and taken out of service.

Incipient Failure Inspection Procedures

The internal liner concept lends itself to periodic monitoring of its integrity during its life without affecting the overall economics of the project. A regular internal inspection program can be developed similar to the the one we use in LNG vessel operation.

The hot tank can be emptied and internally inspected during normal plant maintenance shutdown. A special monorail/scaffolding arrangement is installed in the tank for close inspection of the internal walls in addition to the bottom.

Visual inspection every other year for the first 6 years and every four years during the remaining life can provide adequate confidence of the liner performance.

In addition flat and angle piece elements from various key locations in the tank can be easily cut out with new pieces installed. The tank can then be available for refill immediately thereafter.

The removed pieces can then be checked in detail and a chronological record of any material deterioration due to corrosion, fatigue or creep can be maintained which will be a guide to any incipient problems, in addition to the other methods of liner control.

Conclusions

The corrugated liner has been shown to have a fatigue life in excess of that required for the Solar 100 thermal energy storage so that the effect of creep or corrosion on the fatigue life, if any, will not affect the cumulative margins of safety.

Failure analysis has concluded that catastrophic failure of the system is not possible and there are several methods to anticipate any possible problems.

Regular inspection and detail metalographic check of the liner with time can be part of the routine maintenance operation.

In the extreme, preventive replacement of deteriorated parts of the liner can be scheduled within the normal plant maintenance shutdowns.

UNILIMITED RELEASE
INITIAL DISTRIBUTION

U.S. Department of Energy
Forrestal Building, Room 5H021
Code CE-314
1000 Independence Avenue, S.W.
Washington, D.C. 20585
Attn: C. Mangold

Arizona Public Service Company
P.O. Box 21666
Phoenix, AZ 85036
Attn: E. Weber

Babcock and Wilcox (2)
91 Stirling Avenue
Barberton, OH 44203
Attn: R. Dowling
D. Smith

Black & Veatch Consulting Engineers (2)
P.O. Box 8405
Kansas City, MO 64114
Attn: C. Grosskreutz
H. Laverentz

Bechtel Group, Inc.
P.O. Box 3965
San Francisco, CA 94119
Attn: P. DeLaquil

Electric Power Research Institute
P.O. Box 10412
Palo Alto, CA 94303
Attn: E. DeMeo

Foster Wheeler Development Co.
12 Peach Tree Hill Road
Livingston, NJ 07039
Attn: R. Zoschak

Martin Marietta Aerospace
P.O. Box 179, MS L0450
Denver, CO 80201
Attn: T. Tracey

McDonnell Douglas Astronautics Company
5301 Bolsa Avenue
Huntington Beach, CA 92647
Attn: R. Holl

McDonnell Douglas Astronautics Company
c/o SNLA, Division 6222
P.O. Box 5800
Albuquerque, NM 87158
Attn: S. Saloff

Olin Corporation
P.O. Box 2896
Lake Charles, LA 70602
Attn: A. Quakenbush

Pacific Gas and Electric Company
3400 Crow Canyon Road
San Ramon, CA 94583
Attn: T. Hillesland

Public Service Company of New Mexico
Alvarado Square
Albuquerque, NM 87158
Attn: A. Akhil

Southern California Edison
2244 Walnut Grove Road
Rosemead, CA 91770
Attn: P. Skvarna

J. Holmes, 6222
W. Delameter, 8473 (7)
Publications Division 8265, for TIC (30)
Publications Division 8265/Technical Library Processes Division, 3141
Technical Library Processes Division, 3141 (3)
M. A. Pound, 8024, for Central Technical Files (3)